Design and Fabrication of Flexible Tactile Sensing and Feedback Interface for Communication by Deafblind People

Oliver Okwudili Ozioko

Thesis

Submitted in Partial Fulfilment of the Requirements for the Degree of
Doctor of Philosophy

School of Engineering
College of Science and Engineering
University of Glasgow

October, 2018

Abstract

Humans generally interact and communicate using five basic sensory modalities and mainly through vision, touch and audio. However, this does not work for deafblind people as they have both impaired hearing and vision modalities, and hence rely on touch-sensing. This necessitates the development of alternative means that allows them to independently interact and communicate. To do this requires a solution which has the capability for tactile sensing and feedback. Therefore, tactile interface becomes a critical component of any assistive device usable by deafblind people for interaction and communication. Given that existing solutions mainly use rigid and commercial components, there is a need to tap into the advancements in flexible electronics in order develop more effective and conformable solutions. This research involves the development of flexible tactile communication interface usable in assistive communication devices for deafblind people. First, commercial sensors and actuators were utilised as a proof-of-concept and then four novel tactile interfaces were explored which include two similar touch-sensitive electromagnetic actuators, one capacitive tactile sensing array, and a facile flexible inductance-based pressure sensor.

The two fabricated touch-sensitive electromagnetic actuators (Type 1 and 2) are both based on electromagnetic principle and capable of simultaneous tactile sensing and feedback. Each comprises of a tandem combination of two main modules - the touch-sensing and the actuation module, with both modules integrated as a single device in each case. The actuation module employs a flexible planar spiral coil and a Neodymium magnet assembled in a soft Polydimethylsiloxane (PDMS) structure, while the touch-sensing module is a planar capacitive metal- insulator-metal structure of copper. The flexible coil (~17µm thick and with 45 turns) was fabricated on a Polyimide sheet using Lithographie Galvanoformung Abformung (LIGA) process. The results of characterisation of these actuators at frequencies ranging from 10Hz to 200Hz, shows a maximum displacement (~ 190µm) around 40Hz. Evaluation of this by 40 (20 deafblind and 20 sighted and hearing) participants show that they can feel vibration at this range.

Another tactile interface fabricated is an 8 x 8 capacitive tactile sensing array. The sensor was developed on a flexible Polyvinyl Chloride (PVC) sheet with column electrodes deposited on one side and row electrodes on the reverse side. It is intended for use as an

assistive tactile communication interface for deafblind people who communicate using deafblind manual alphabets as well as the English block letters.

An inductance-based pressure sensor was also designed, fabricated and characterised for use as an input interface for finger Braille as well as other tactile communication methods for deafblind people. It was realised with a soft ferromagnetic elastomer and a 17µm-thick coil fabricated on a flexible 50 µm-thick polyimide sheet. The ferromagnetic elastomer acts as the core of the coil, which when pressed, sees the metal particles moving closer to each other, leading to changes in the inductance. The coil, with 75µm conductor and 25µm pitch, was also realised using LIGA micromolding technique. Seven different sensors were fabricated using different ratios (1:1, 1:2, 1:3, 1:5, 2:1, 3:1, and 5:1) of Ecoflex to Iron particles. The performance of each sensor was investigated and generally, sensors with higher Iron particles gave better sensitivity, linear as well as dynamic range. In comparison with all other fabricated sensors, the sensor made with 1:5DD was recommended for application as a tactile interface.

Acknowledgments

This work couldn't have been possible without the wonderful support of great people around me. My profound gratitude goes to my Supervisors - Dr. Marion Hersh and Prof. Ravinder Dahiya for their unquantifiable support and guidance throughout this work. Your great contributions in my life will remain evergreen. I am eternally grateful to Tertiary Education and Trust Fund (TETFund) and Federal Universtiy of Technology Owerri, Imo state Nigeria, for sponsoring me to come to the UK for this program. My earnest gratitude also goes to Gilchrist Educational Trust, The Leche Trust, Deafblind Scotland, Deafblind UK, Sense Scotland - Paul Hart and Jackie Reid, and all those who participated in the user test towards the completion of this program. To all members of Bendable Electronic and Sensing Technology group (past and present), especially William, Shoubhik, Nivasan, Dhayalan, Fengyuan, Tasos, Wenting, Ensieh, Ambarish, Carlos, Kafi, and Libu I say a very big thanks to you for unalloyed support and loving care. Indeed you all were indispensable pillars during this program. I surely cannot repay your support. I cannot forget wonderful family friends like Jean Urquhart who shouldered my burden with patience when I needed it most. I am also very grateful to Tom O'Hara, for all his technical and friendly support. Tom, you are the man. To my friend Waqar Nabi, I say a very big thank you for you are a good friend in all ramifications. To my Parents Chief Tobias Ozioko, Late Mrs. Theresa Ozioko and Mrs Chinedu Ozioko I say a very big thank you for making it all possible. To my siblings, Anthony, Mrs. Nonye Ucheaga (Nee Ozioko), Ukamaka, Uchenna, Onyinye, Sunday, Ebuka, Chinwendu, and Onyedikachi Ozioko – Your prayers have been my anchor.

My whole heart goes to my dearest son Jeremy Chiemela Ozioko and dearest daughter Jessica Chikambinaka Ozioko – you guys are special blessings. To my lovely wife Chinwe, - I say an immeasurable thanks to you for your love and great support. If not for your love I would have given up. Thanks for being my heartbeat and for understanding me when I focus only on research and don't have time for you, and for all the time I failed to live up to expectations. To all my lovely friends, Obinna Unigwe, Jim, James Good Fellow, and many that I have not mentioned, I say thank you for being there for me. Finally and most importantly, I am forever indebted to my God who made me who I am today. He is my only hope, the only perfect mathematician and He who gives rain to my land in its season. Lord, I will worship you forever.

Author's Declaration

I, Oliver Okwudili Ozioko declares that, except where explicit reference is made to the contribution of others, this thesis is the result of my own work and has not been submitted for any other degree at the University of Glasgow or any other institution. In particular, Mobile Apps used in this work for application of the fabricated sensors and MATLAB program for actuator characterisation is a collaborative work with William Taube Navaraj (W.T.N).

Contents

List of Tables

List of Figures

List of Symbols

A	Area
I	Current
ε	Permittivity of dielectric material
F	Force
k	Rubber stiffness
c	Speed of light
μ_r	Relative permeability of the material
μ_o	Permeability of vacuum
Q	Quantity of Electricity
e	Charge
ρ	Density
p	Pitch of spiral coil
N	Number of turns of spiral coil
α	Coil Aspect Ratio (CAR)
r_i	Inner radius of spiral coil
r_o	Outer radius of spiral coil
π	pi
H	Magnetic field
B	Magnetic flux density
E	Electric field
J	Current Density
L	Inductance
C	Capacitance

List of Acronyms

PDMS	Polydimethylsiloxane
B-DMA	British Deafblind Manual Alphabet
A-DMA	American Deafblind Manual Alphabet
PVC	Polyvinyl Chloride
FSR	Force Sensing Resistor
PEDOT: PSS	Poly(3,4-ethylenedioxythiophene) polystyrene sulfonate
LIGA	Lithographie Galvanoformung Abformung
SEM	Scanning Electron Microscope
UV	Ultraiviolet
MEMS	Microelectromechanical System
IZO	Indium Zinc Oxide
EAPs	Electroactive Polymer
CNT	Carbon Nanotube
PVDF	Polyvinylidene Fluoride
DEA	Dielectric Elastomer Actuator
SMA	Shape Memory Alloy
ER	Electrorheological
MR	Magnetorheological
CVD	Chemical Vapour Deposition
PVD	Physical vapour Deposition
POC	Proof of Concept
ADC	Analog to Digital Converter
ERM	Eccentric Rotation Mass
LCD	Liquid Crystal Display
LRA	Linear Resonant Actuator
FPCB	Flexible Printed Circuit
ITO	Indium Tin Oxide
CAD	Computer Aided Design
ABS	Acrylonitrile Butadiene Styrene

Publications

1. O. Ozioko, M. Hersh, and R. Dahiya, "Inductance-based Flexible Pressure Sensor for Assistive Gloves," in IEEE Sensors, New Delhi, India, 2018.
2. O. Ozioko, W. Taube, N. Yogeswaran, M. Hersh, and R. Dahiya, "Tactile Communication System for the Interaction between Deafblind and Robots," presented at the IEEE ROMAN 2018, Nanjing, China, 2018.
3. W. T. Navaraj, O. Ozioko, and R. Dahiya, "Capacitive-Piezoelectric Tandem Architecture for Biomimetic Tactile Sensing in Prosthetic Hand," in IEEE Sensors, New Delhi, India, 2018.
4. O. Ozioko, W. Taube, M. Hersh, and R. Dahiya, "SmartFingerBraille: A tactile sensing and actuation based communication glove for deafblind people," in 2017 IEEE 26th International Symposium on Industrial Electronics (ISIE), 2017.
5. O. Ozioko and M. A. Hersh, "Development of a Portable Two-way Communication and Information Device for Deafblind People," in 13th AAATE International Conference, Budapest, Hungary, pp. 518-525, 2015.

Journal Articles (In Progress)

1. O. Ozioko, Prakash Karipoth and M. A. Hersh, Ravinder Dahiya, "Wearable Assistive Smart Finger Braille Interface using Touch-Sensitive Actuators.
2. O. Ozioko, William Taube, Prakash Karipoth, Marion Hersh, Ravinder Dahiya, Touch-Sensitive Electromagnetic Actuator for Assistive Tactile Display.

Chapter 1

1 Introduction

This Chapter presents the motivation of the work, objectives, main contributions as well as the structure of the thesis.

1.1 Motivation

Human communication and interaction with the real world comes through five basic sensory modalities and mainly through vision, touch and audio. However, this does not work for deafblind people as they have both impaired hearing and vision modalities, and hence rely on touch-sensing. Reports show that majority of deafblind people are with age-related dual impairment, and their number is set to increase with increase in longevity in the developed countries. So, there is a need to develop a tactile communication interface that will enable this important group of people to independently communicate. To do this requires a solution which has the capability for tactile sensing and feedback. A range of technologies have been explored to support deafblind communication including wearable (e.g. smart gloves) and non-wearable (e.g. Braille displays) tactile displays. The smart gloves generally have a set of tactile sensors and actuators, sensors are used to get information about contact feature and the actuators serving as a means of vibrotactile feedback. For improved acceptance of these communication technologies and their effective use, the sensors and actuators integrated in these smart gloves should be flexible, wearable and conformable.

However, most of the assistive deafblind communication devices available today make use of rigid and/or commercial sensors and actuators not specifically made for this purpose. This poses a challenge when it comes to the integration of these separately made devices together to realise a tactile communication interface. The communication methods used by deafblind people requires the use of the same tactile point on the hand for both touch-sensing and tactile feedback. But this is difficult if the available tactile sensors and actuators are made separately as there will always be incompatibility in terms of size, functionality and integration. No wonder why majority of the existing tactile interfaces for deafblind people have had this challenge. This has made it difficult to effectively adopt deafblind communication methods. Interestingly, the rapid advances in flexible electronics provide timely opportunities for the development of flexible and customisable tactile sensors and actuators for use in these assistive tactile interfaces. Tapping into the opportunities provided

by flexible electronics, this thesis presents the Design, fabrication and characterisation of flexible sensors and actuators usable as tactile interfaces for communication by deafblind people. This will facilitate the development of portable two-way assistive communication devices for deafblind people capable of sending and receiving information in the form of vibrotactile feedback. Eventually, assistive communication devices for deafblind people will have flexible and customisable dual-functional tactile interfaces (with integrated tactile sensing and feedback) which are representative of the current communication method used by this important group.

1.2 Hypothesis

- Same touch-point can be used to send and receive message by deafblind people using a tactile interface equipped with a touch-sensitive actuator
- Custom sensors could be developed to improve the integration and flexibility of tactile displays for communication by deafblind people
- Array of tactile sensors will represent the touch points required for deafblind communication using block letters

1.3 Objectives

The objectives of this work are as follows:

- To carry out a requirement-gathering research in order to establish appropriate requirements for the design of a tactile communication device for deafblind people.
- To fabricate and characterise a tactile feedback actuator that supports the provision of tactile-feedback capability (two-way communication) in assistive communication devices for deafblind people
- To fabricate and characterise a flexible touch-sensing interface that supports the development of flexible, customisable and portable communication devices for deafblind people

1.4 Contributions

This thesis makes novel contributions is four areas as summarised in Fig. 1-1.

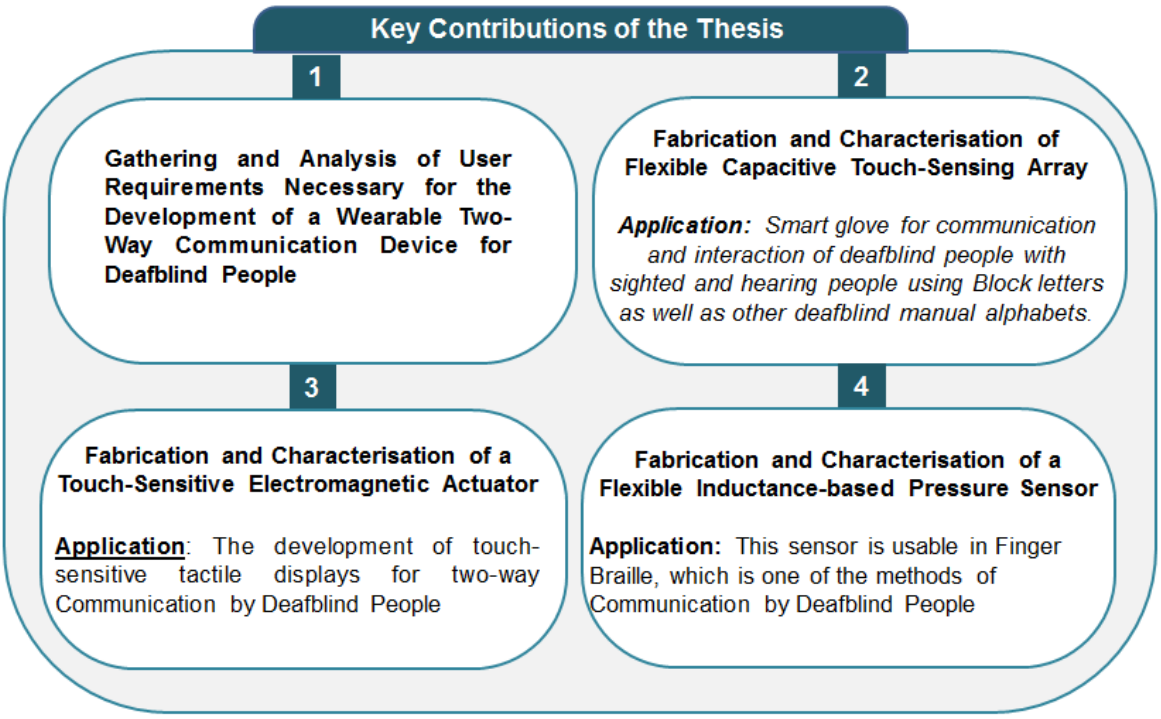

Fig. 1-1 Key Contributions of the Thesis

Firstly, it contributes in the gathering and analysis of user requirements necessary for the development of a wearable two-way communication device for deafblind people. Most times, assistive devices are developed without consulting this important group of people and hence the users adapt themselves to the device rather than the device being developed and customised to suit their needs. This work has made an original contribution in this direction by interviewing staff of two deafblind organisations (deafblind Scotland and Sense Scotland) as well as deafblind people who are the real end-users of the proposed device.

Secondly, it contributes in the fabrication and characterisation of flexible capacitive touch-sensing array usable is a smart glove for communication and interaction of deafblind people with sighted and hearing people using Block letters as well as other deafblind manual alphabets. To date, the existing wearable tactile displays for deafblind communication which are based on deafblind manual alphabets do not employ sensor arrays and hence it is difficult to fully represent all touch points necessary for effective deafblind communication. Also majority of them use rigid and commercial sensors which make customisation and wearability a challenge. The application of the tactile sensing array was demonstrated for the interaction of deafblind person and a virtual Baxter robot via a mobile app that uses convolution neural network capable of character recognition.

Thirdly, it contributes in the fabrication and characterisation of a touch-sensitive electromagnetic actuator which is an original contribution that supports the development of touch-sensitive tactile displays for two-way deafblind communication. The available tactile displays for deafblind communication do not have inherent touch capability, hence are limited in the ability for simultaneous tactile sensing and feedback. This third contribution is a step to overcome this existing limitation.

Fourthly, it contributes in the fabrication and characterisation of a flexible inductance-based pressure sensor. This sensor is usable in Finger Braille. Finger Braille is an effective deafblind communication method for people who understand Braille. It requires the use of separate tactile sensors and actuators which are positioned in the index, middle and ring fingers for communication. Development of an inductance-based pressure sensor makes it possible to use similar technology for both sensor and actuator. This is because the actuator fabricated in this work is an electromagnetic actuator of which a spiral coil is its primary element. An inductance pressure sensor also uses a similar spiral coil for its sensing, so the sensor and the actuator uses same coil which will eventually reduce the fabrication steps required to achieve the entire finger Braille device. Apart from its application in finger Braille, it also finds application in the touch-sensitive tactile actuator mentioned earlier. In this case, the sensor and actuator for the tactile displays will also use the same coil for both sensing and actuation.

Mobile Apps used in this work for application of the fabricated sensors and MATLAB program for actuator characterisation is a collaborative work with (W.T.N).

1.5 Structure of the Thesis

This thesis is structured into following main phases:

- Review of Literature (Chapter Two)
- Tools and Methods (Chapter Three)
- Proof-of-Concept Phase (Chapter Four)
- Component Fabrication and Demonstration Phase (Chapter Five, and Chapter Six)
- Evaluation and User Feedback (Chapter Seven)
- Discussion (Chapter Eight)
- Conclusion (Chapter Nine)

The following are the summary of the motivation for each chapter as well as what it contains:

Review of Literature:

- **Chapter Two,** Review of Literature: This begins with the definition of deafblindness and the description of the various categories of deafblind people. It continues with classification of the methods used for communication by deafblind people, as well as the existing devices developed based on these methods. Next is the description of the human tactile sensing and perception where the mechanoreceptor and its properties were introduced as well as the various threshold of human tactile perception. Finally, existing tactile sensing technologies and tactile displays were described.

Tools and Methods:

- **Chapter Three,** Tools and Methods*:* This chapter presents some relevant tools used in this work, methods followed including the rationale behind them. It started with brief introduction to microfabrication techniques and tools including lithography, Electron Beam Evaporation (EBE), Lithographie Galvanoformung Abformung (LIGA) process, and Electroplating. Then the chapter was concluded with a presentation of the methods used in this work

Poof-of-Concept (POC) Phase:

- **Chapter Four,** Proof-of-Concept (POC): This chapter presents the Proof-of-concept (POC) phase, which contains the implementation of two communication devices for deafblind people using commercial tactile sensors and actuators. This was done to understand their strengths and weaknesses as well as try the proposed two-way communication system and simultaneously show the application of tactile communication interface for deafblind people. First a generic communication system for deafblind people is presented. Then followed by two prototypes implemented with commercial sensors and actuators- (1) A prototype communication glove for user of the British deafblind manual alphabet including the analysis of interview of deafblind people and (2) A finger Braille glove for Braille users. How both of them adopted the generic communication system is also presented.

Component Fabrication and Demonstration Phase:

This phase involves Chapter Five and Six. It contains the fabrication and demonstration of the different tactile sensors and actuators and hence tactile interface for communication by

deafblind people. Here, single element tactile sensors, tactile sensing array as well as actuators were fabricated for adoption and implementation of the methods of communication used by deafblind people as attempted using the commercial components in the POC phase.

- **Chapter Five,** Design and Fabrication: Tactile Feedback Actuators: This workThis chapter presents details of the fabrication of touch-sensitive flexible tactile feedback actuators which is required to give feedback to deafblind people in the form vibration. The actuator is based on electromagnetic principle and hence the chapter started with the description of the design and simulation of the spiral coil used for the actuator including the necessary calculations. This is then followed by the fabrication of the coil, fabrication of the touch-sensitive layer and eventually the realisation of the touch-sensitive actuator. Then the Characterisation of the actuator followed, and finally the application of the fabricated actuator is presented
- **Chapter Six,** Design and Fabrication: Tactile Sensors: This chapter describes the design, fabrication and characterisation of a flexible capacitive tactile sensing array as well as a single element inductance-based pressure sensor. It started with the description of fabrication steps and characterisation of the capacitive tactile sensing array, followed by the presentation of its novel implementation in an application for the interaction between deafblind person and robot. The last part of this chapter describes the fabrication of flexible inductance-based pressure sensor, including its structure, fabrication details as well as characterisation

Evaluation and user Feedback:

- **Chapter Seven,** Evaluation and **User Feedback:** This Chapter presents the methods and results of the evaluation of the tactile interfaces developed in this thesis. Overall, 40 (20 deafblind and 20 sighted and hearing people) participants were involved.

Discussion:

- **Chapter Eight,** Discussion**:** This Chapter provides the discussion of the work carried out in this thesis and how it relates to the literature of the exisiting communication interfaces developed for deafblind people.

Conclusion

- **Chapter Nine,** Conclusion and Future Work: This chapter started with a summary of the research carried out in this thesis, including their limitations. Finally it discusses the possibility for future work in the area of development of assistive deafblind communication devices.

Chapter 2

2 Review of Literature

This chapter presents the review of literature related to the works carried out in this thesis. It starts with the definition of deafblindness and a brief discussion of the different categories of deafblind people, in order to expand the understanding of the user group for whom this work directly applies to. It continued with the discussion of existing tactile communication devices used by deafblind people with a focus on the technologies used for tactile sensing and feedback. Existing popular and related tactile sensing and feedback technologies were then discussed and analysed with a focus on their principles, advantages and disadvantages. In each case a summary of the advantages and disadvantages is given in the last paragraph of the corresponding section. The effort in this chapter facilitated the choice of the technology and methods used in this work and enabled the advancement of the state of the art.

2.1 Deafblindness and Categories

Deafblindness is a dual sensory impairment and presently there is no clear definition of dual sensory impairment which involves the presence of both hearing and vision loss [1]. So there is a lack of consensus on the definition of deafblindness [2, 3]. In [4, 5], deafblindness is defined as a dual sensory impairment, resulting from the combination of (significant) vision and hearing impairments and which leads to significant barriers to communication, accessing information, mobility and participation in society. The history of deafbliness is as old as the era of Helle Keller (1880 – 1968) but the research in this area is still in its early stage [6]. Generally, the two definitions employed are medical and functional definitions. Medical definitions are focused on measurement of hearing and vision whereas functional definitions are particularly based on how the vision and hearing impairment affect the individual's ability to communicate and have active participation in the society [3]. However deafblindness does not only include those who are deaf and blind, but includes those who have residual vision and/or hearing [4] and varies from country to country. As reported in [7], some countries like Haiti, Indonesia, Iran, and Venezuela include only people who are completely deaf and blind in their definition of deafblind people, while others surveyed include additional group which have residual vision and/or hearing.. Although deafblindness is known to affect more of older people [1, 3, 8], the prevalence of severe

deafbliness in children of 5 years and over has been reported to be 0.01% in Cambodia, Haiti, Iran and Venezuela and up to 0.85% in the United States [7].

According to [9] deafblindness is often researched as two separate groups; (1) congenital and (2) Acquired deafblindness. These two groups are sometimes referred to as pre-lingual and post-lingual deafblindness respectively [7]. Congenitally deafblind people are people who were born deaf and blind or become deafblind early in life before the development of language (pre-lingual) [9, 10]. Acquired deafblind people on the other hand are people who become deafblind after development of language (post-lingual) [3]. According to [11] [12], acquired deafblindness can be divided into the following categories:

1. Those who were born deaf or hearing impaired, and then later lost their sight
2. Those who were born blind, then later lost hearing
3. Those who become deafblind as a result of old age, accident or illness

According to a 2018 report by the World Federation of the Deafblind (WFDB), deafblind people represent about 0.2 - 2% of the global population and between 20 -75% of persons with deafblindness have additional impairments [7]. This report by WFDB involved about 22 countries and is the first ever global report on deafblindness. The following are some other key findings:

- Socio-economically, families with deafblind people are more likely to be in the least 40%
- People with deafbliness have low access to mental services but more likely to be depressed
- Deafblind persons over the age of 50 are more likely to be socially isolated than those without the dual impairment
- Communication barrier is a very big concern for deafblind people in many countries and many healthcare staff do not have the requisite communication skills to support these individuals

According to Sense UK, about 222,000 people aged over 70 are with dual sensory loss in the UK, and by 2030, close to half a million people in the UK will have enough dual sight and hearing loss to be considered deafblind; amongst which 418,000 will be people over the age of 70 [13]. More so, for about 2 million people living with sight loss in the UK, over 80 per cent are aged over 60, and 45 per cent are aged over 80 [14], and more than 50 per cent of people over 60 will be affected with hearing loss [15]. As reported in [16] between 11%

and 20% of individuals over 80 years have concurrent hearing and vision impairment in America. Furthermore, with increase in longevity in the developed countries, people in this age group are expected to increase and therefore lead to an increase in the number of deafblind people [17] . These facts clearly show that majority of the deafblind people are people with age-related dual sight and hearing impairment as well as the need to develop an effective solution to support their communication.

2.2 Methods of Deafblind Communication

Human communication and interaction with the environment is mostly governed by vision, touch and audio. Hence communication for deafblind people is a challenge due to the impaired hearing and vision modality. Consequently, deafblind people use several different communication methods, including speech and tactile approaches [11, 18], depending on the extent of their hearing, vision, and personal history of the onset of dual sensory impairment [19]. An individual deafblind person may use different communication approaches in different circumstances or at different times of their life. These communication methods include: Non-verbal, used mainly by people born deaf and blind (congenital), block alphabets, moon, object and symbol-based approach, lip-reading (e.g. Tadoma), imitation, observation, Braille etc. However, the main tactile approaches are deafblind manual alphabets [11] and Braille [20]. Majority of the devices developed to support deafblind communication are mainly inspired by these two tactile communication approaches. This is done particularly to have a user-friendly interface that allows deafblind people to use these methods which they are already familiar with.

The following sections present the existing deafblind communication methods, devices, as well as the technologies used. They are grouped in accordance with the aforementioned tactile approaches as follows:

1. Deafblind Manual Alphabets
    a. One –handed manual alphabets,
    b. Two-handed alphabets
2. Braille
3. Block Letters

2.2.1 Deafblind Manual Alphabets

Deafblind manual alphabet is “an alphabet-based method of spelling out words onto a deafblind person's hand”, in which letters are denoted either by a touch or movement on the

palm, or by a sign with the fingers [11]. Different deafblind manual alphabets or fingerspellings are used in different countries and/or regions, and are classified into (1) One handed (Fingerspelling) and (2) Two-handed alphabets [21]. The major difference between these two is the number of hands used for communication – one is used in the former while two hands are used in the latter.

2.2.1.1 One-handed Deafblind Alphabets and Existing Devices

In one-handed manual alphabets letters are spelt by either opening or closing one or more fingers with the handheld vertically. The listener feels the movement by putting their hand over the top of the speaker's fingers and the back of their hand. A typical example of this is the American deafblind manual alphabet (A-DMA) used in the America.

Table 2-1, summarises the previous research carried out towards the development of deafblind communication devices based on one-handed manual alphabets. Two-way communication means that the device has a means for the deafblind people to send and receive information, whereas one-way means that the deafblind person can receive but cannot send. Majority of the early devices has one-way communication. The first of them all was developed in 1977 and published in 1978 by South-West Research Institute in San Antonio [22, 23]. Its main components are the mechanical hand and the keyboard logically linked to the hand. To send a message to the deafblind person, users typed letters using the keyboard and these letters controls the mechanical hand which moves in accordance with the A-DMA. To read a message, the deafblind person feels this fingerspelling hand to understand the hand position in order to determine the letter that was sent. The device has several limitations which includes improper forming of letters, slow speed and lack of fluid motion[22].

An improved fingerspelling hand called Dexter was later developed in 1985 as presented in [22, 24]. Dexter is a five-fingered mechanical fingerspelling hand developed for deafblind people [25]. It converts ASCII characters into mechanical finger position which represents different letters. The deafblind person touches this hand to feel the position and as such understand the letter. The major goal of Dexter was to develop a system with improved timing and understandable finger position. This was realized which makes it an improvement over the very first fingerspelling hand. Dexter II was later developed as an improvement over Dexter. It was designed with about one-tenth the volume of Dexter, has an improved speed of four letters per second, and higher repeatability of finger positions for all letters.

Table 2-1 Summary of Devices based on one-handed deafblind manual alphabets

Device	DB Communication Strategy	Tactile Sensor Used	Tactile Feedback Actuator used	Type of Communication	Year	Ref.
Mechanical Hand	A-DMA	None	None[a]	One-way	1978	[23]
Dexter & Dexter II	A-DMA	None	None[a]	One-way	1987	[24, 25]
Gallaudet Fingerspelling Hand	A-DMA	None	None	One-way	1993	[26]
Robotic Alphabet (RALPH)	A-DMA	None	None[a]	One-way	1994	[27]
The Talking Glove	A-DMA	None	None (uses LCD for feedback to DB Person)	Two-way	1988	[28]
PARLOMA	A-DMA	None (Depth Sensor used as input)	None	Two-way	2015	[29]

[a]No Feedback to Deafblind Person, A-DMA – American Deafblind Manual Alphabet, DB – Deafblind, LCD – Liquid Crystal Display.

Later in 1992, a fingerspelling hand for Gallaudet was developed at Gallaudet University [26]. Like Dexter II, and other fingerspelling devices, the deafblind person also receives message by feeling the mechanical hand position, but it have improvement in size reduction and speed.

A fourth generation computer-controlled fingerspelling hand called Robotic Alphabet, RALPH was developed at the Rehab R&D Centre [27]. The device offers deaf-blind individuals improved access to computers and communication devices in addition to face-to-face conversations. This particular fingerspelling hand has an improvement over the aforementioned in terms of intelligence, smaller size, and the ability to optimize hand positions. Despite the improvement of the fingerspelling devices over the years, all of them are still considerably big, expensive and requires a computer to work well.

The talking glove is another invention in 1988 by engineers at Stanford [28]. The entire system is made up of a glove, a mechanical hand, braille display, digital display, and a computer. The glove and the mechanical hand have been developed independently for different uses, but they can be used together to enable deafblind people communicate with

one another. To communicate, the deafblind person uses the glove to make gestures which is converted to speech and sent to a hearing person through a speaker. The hearing person replies through a keyboard and this message will be displayed on the braille display which is worn on the left arm. The digital display allows deaf people who do not know how to use braille to be able to communicate. This device is equally not wearable or portable and requires many different components.

The most recent and advanced of all is Parloma [29], a system developed for deafblind people to remotely communicate using one-handed alphabets. It uses a depth sensor as the input and by signing in front of it; a robotic hand located in a remote location is controlled accordingly via the internet. The deafblind person at the remote location feels the shape of the robotic hand to interpret the message. This is an improvement over the others but still requires further reduction in size as well and lacks ability for real time communication.

2.2.1.2 Two-handed Deafblind Alphabets and Existing Devices

In the manual two-handed alphabets, the letters are spelt onto the palm and/or fingers with the other hand (of the speaker). So the palm of the listener is used as a paper with the speaker using a finger to write on it. The following are the popular alphabets:

(a) British deafblind manual alphabet(B-DMA) used in the UK [30]
(b) The Lorm alphabet used in Austria, parts of Germany and Poland [31]
(c) The Malossi alphabet used in Italy [32]

For the purpose of explaining these deafblind manual alphabets, the person sending message will be regarded as the sender while the recipient will be regarded as the listener. An extensive review of these manual alphabets, shows that the English alphabets could be grouped based on the touch points as single touch letters(STL), multi-static touch letters (MSTL) and trace letters (TL) as shown in Table 2-2 . In STL, the speaker's finger touches the corresponding point in the palm (of receiver) just once, In MSTL, more than one finger of the speaker touches or pinches the corresponding part of the palm (of the listener) while in TL, the speaker's finger is used to trace out a pattern on the palm (of the listener) in order to represent a letter as shown in Fig. 2-13.

Table 2-2 Comparison of the different two handed manual alphabets

Deafblind Manual Alphabet	**Single -Touch Letters (STL)**		**Multi-static Touch Letters (MSTL)**		**Trace Letters (TL)**		**Country Popularl y used**
	Letters	No.	Letters	No.	Letters	No.	
[a]B-DMA	A,E,I,K,O ,Q,S,T,U, X	10	B,D,F,G,L, M,N,*P,R, V,W,Z	12	C,H,J,Y	4	UK
[a]Lorm	A,C,E,I,O, U,V,	7	*F,*J,K,M, N,W	6	B,D,G,H,L,P ,Q,R,S,T,X, Y,Z	13	Austria, Germany, Poland,
[b]Malossi	A, B,C, D, E,F,G, H,I,J, K,L, M,N,O	15	(P,Q,R,S,T, U,V,W,X, Y,Z)*	11	None	0	Italy

[a]*Touch points Corresponding to all letters are randomly located in the hand,*
[b]*Touch points Corresponding to all the letters are located in a clockwise order over the fingers*
**The corresponding touch - points for these letters are pinched*

The palm shown in Fig. 2-13 and Fig. 2-2 are the pam of the listener while the touch points represented with letters are the points where the speaker touches to send the corresponding letter.

Fig. 2-13 shows the different touch-points, the letters and how they are signed on the palm of the deafblind for the B-DMA for the different letter categories. Given that some letters overlap, the 26 English letters were represented in two separate figures (Fig. 2-13) for the sake clarity and convenience. Each dot on the palm represents a touch point for the letter labelled and for the letters that require more than one touch-point, of trace, the relative area and/or shape is represented. Detailed description of each letter and how to sign it is given in Appendix 1.

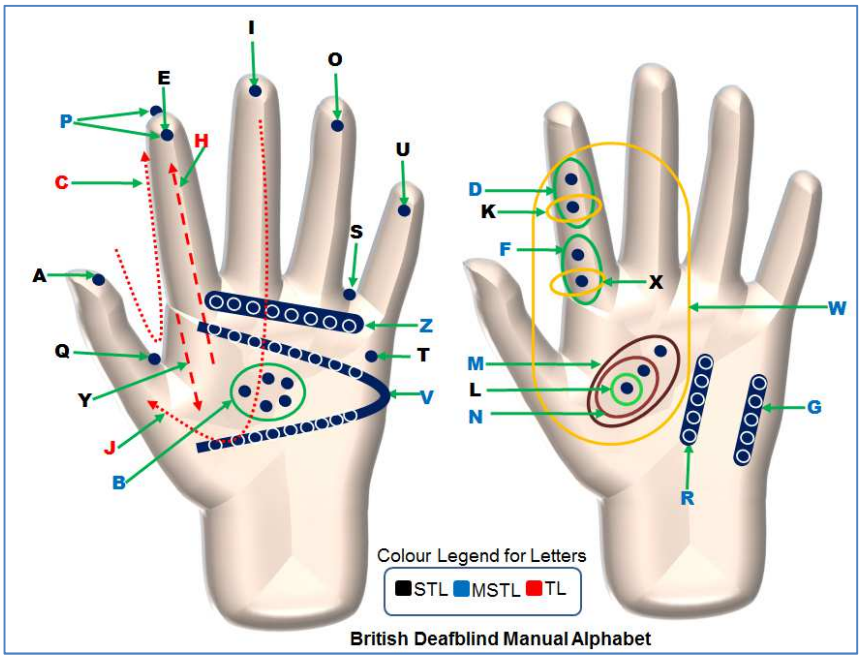

Fig. 2-1 Tactile Points and Letter Representation for the British deafblind manual alphabet

Fig. 2-2 (a) and (b) shows the tactile points and letter representation for Lorm and Malossi deafblind manual alphabet respectively.

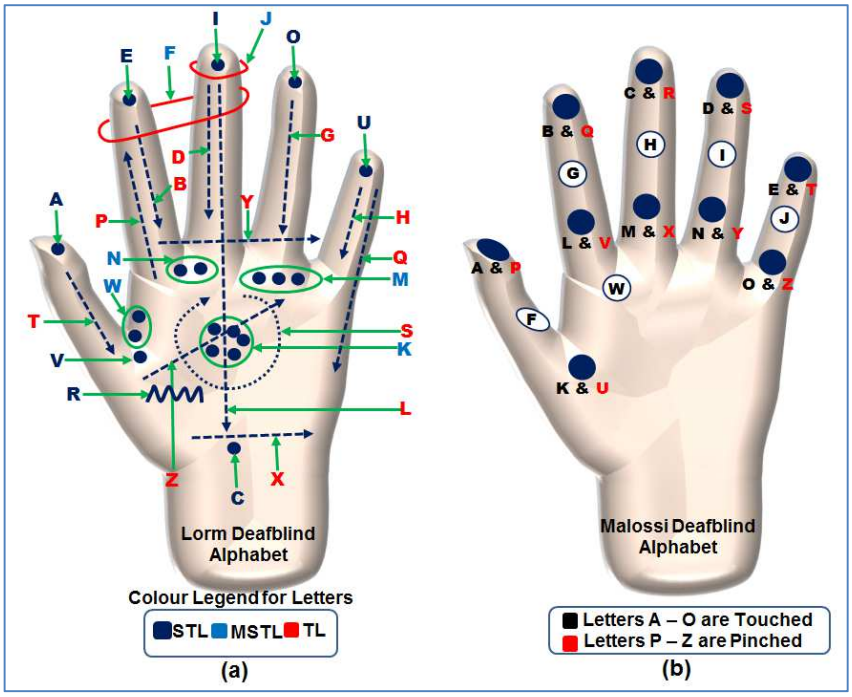

Fig. 2-2 (a) Tactile Points and Letter Representation for the Lorm Deafblind Manual Alphabet (b) Tactile Points and Letter Representation for the Malossi Deafblind Alphabet

While B-DMA and Lorm alphabets have STL, MSTL, and TL, the Malossi alphabet has only STL and MSLT with touch-points in the palm mapped to corresponding letters in a

sequential and clockwise direction as opposed to the former two, whose touch points are randomly mapped [21].

Considering the development of a tactile glove that will have touch-points mapped based on these manual alphabets, the number of TL (see Table 2-2) has an implication in the glove's level of complexity. This is because to trace a particular letter, more than one tactile point is required, meaning that the higher the number of TL, the more the tactile points required to effectively represent them. Equally, this will have implication in the user's ability to distinguish between touch points when they receive tactile feedback. A critical look at Table 2-2 shows that the Lorm alphabet has the highest number (13) of TL, which means it will have more complexity in terms of touch-point to letter mapping as well as user's ability to easily distinguish between touch-points. Fig. 2-3 shows how the trace letters as well as complexity of implementation increases.

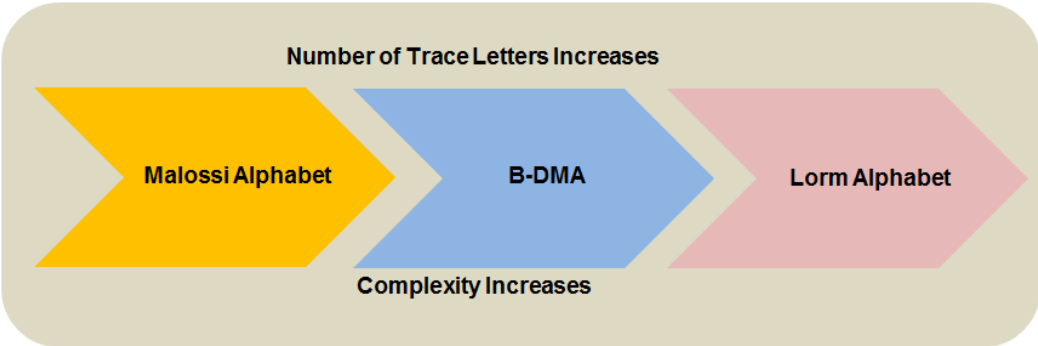

Fig. 2-3 Comparison of the complexity of the three different deafblind alphabets (B-DMA, Lorm and Malossi Alphabets)

Table 2-3 presents a summary of the existing devices based on the two-handed deafblind manual alphabets. Most of these devices are worn like a glove on the hand in order to adequately represent the deafblind manual alphabets which are all signed inside the palm of the hand as described in Section 2.2.1.2. While earlier devices are not portable or efficient; recent devices which are portable/wearable employed mainly rigid and commercial tactile sensors as well as feedback actuators. Hence they are not entirely wearable and/or customisable.

In [30] a device was developed in the UK called handtapper that adopted B-DMA method of deafblind communication, it uses twelve solenoids that are mounted below a hand-shaped base plate. These solenoids produce vibrations which typically correspond to the B-DMA. It also employed a seven-key braille board which allows users to control the flow of material, and to read, review, and re-read a message. Although this has a vibration feedback to the

deafblind person, it's not portable and expensive just like the US fingerspelling devices. Handtapper has some limitations which include insufficient representation of the B-DMA caused by its few tactile points. A complementary device the pattern decoding glove was developed to help remedy this [33]. It uses Force sensitive resistors (FSR) at tactile points to accept input from users. However, both Handtapper and the pattern decoding glove are not portable and both tethered to a computer.

Table 2-3 Existing Devices based on Two-handed manual alphabets

Device	DB Communication Strategy	Tactile Sensor Used	Tactile Feedback Actuator Used	Type of Communication	Year	Ref.
Handtapper	B-DMA	None (uses Standard QWERTY keyboard for input)[a]	14 Movable pins[a,b]	Two-way	1991	[30]
Pattern Decoding Glove	B-DMA	14 Force Sensing Resistors(FSR) [a]	None	One-way	1993	[33]
Glasgow Glove	B-DMA	12 Tactile buttons [a,b]	12 Vibration Motors [a,b]	Two-way	2003	[19]
Lorm Glove	Lorm	Fabric Pressure Sensors	32 Vibration Motors [a,b]	Two-way	2012	[31]
DB-Hand	Malossi	10 Tactile buttons [a,b]	10 Vibration Motors [a,b]	Two-way	2008	[32]

[a]Commercial [b]Rigid, A-DMA – American Deafblind Manual Alphabet, DB – Deafblind

More recent devices based of two-handed alphabets include the Lorm glove presented in [31]. This glove is based on a deafblind manual alphabet called Lorm described previously (See Fig. 2-2) [31]. They tried to make communication easy for deafblind people who can use the Lorm alphabet by bridging the gap between the Lorm users and those who doesn't know how to use Lorm.

This communication device is made up of a glove, worn by the deafblind person, a mobile phone and a control unit. The glove contains fabric pressure sensors which serve as input and are located on the palm at positions corresponding to the Lorm characters, also on the glove are 32 off-the-shelve vibrating motors which are situated at the back of the palm and are equally position so as to correspond to Lorm alphabets. This means that on the glove there are pressure sensors for input and vibrating motors for output all at corresponding

positions for LORM characters. To communicate the deafblind person types characters using the pressure sensors. The typed characters are then transmitted from the glove to the mobile phone of the receiver via a control unit. To reply the message the person types a message using the mobile phone and sends it to the glove via the control unit as well. When the message is received on the glove the motors at the back of the palm vibrates accordingly to interpret the message to the deafblind person. The control unit and the mobile phone communicate via a Bluetooth. Despite the fact that the authors stated that the device was tested and it worked, however it is not without limitations. It uses off-the-shelf vibration motor which means it is rigid and not customisable.

In [32], DB-hand was developed for users of the Malossi alphabet (see Fig. 2-2) [32]. In this device, deafblind people read and write messages based on tactile impulses and the sighted and hearing people view their messages using a display device or hear them through audio speakers (only for those with residual hearing). The glove uses 10 commercial off-the-shelf tactile switches as input for the glove and 10 vibration motors for tactile feedback.

Another deafblind communication glove was developed at The University of Glasgow and this is the only recent portable device reported for deafblind people which is based on the British deafblind manual alphabet [19]. To send information the deafblind person presses the tactile switches on the glove and the receiver views it on a portable handheld display. The glove is only capable of one-way communication and therefore deafblind people can only send messages with it, but cannot receive. It equally uses off-the-shelf on-off switches as input which is not flexible or easy to integrate in a glove.

The following section describes Braille which is another tactile communication method used by deafblind people. It is popularly used by the blind community and a few deafblind people.

2.2.2 Braille and Finger Braille

This is a tactile system of reading and writing found by Louis Braille and used mainly by the blind community and a minority of deafblind people [20]. Letters and numbers are represented by raised dots arranged in six-dot Braille cells as shown in Fig. 2-4a. It is read by moving a finger over a line of Braille cells and shapes outline by raised dots are used to mentally determine the alphabet [21, 34, 35].

As reported in a document from the department for works and pension office of the disabilities UK, approximately 18,000 blind and partially sighted adults in the UK prefers reading with Braille [36]. Generally Braille provides reading and writing opportunity for

people who cannot access print, and is today being also used by some companies for labelling [37]. This shows that today, blind and deafblind community still use Braille as it provides an opportunity for them to read and write independently. Despite this, Braille has several disadvantages which include the fact that Braille books are often bulky, requires acute sense of touch and not easy to learn and more so at an older age [37]. Lack of Braille teachers makes this situation even more challenging.

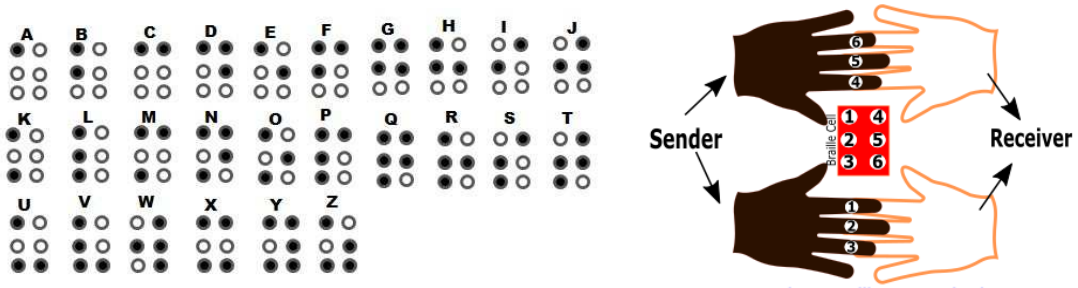

Fig. 2-4 (a) The Braille alphabet (b) Finger Braille

Fig. 2-4 shows the standard Braille alphabets with the black circles representing raised dots and the white one otherwise.

In Japan, there is a type of Braille-based tactile communication method used by deafblind people called Finger Braille. This is a method of deaf and blind communication in which the index, middle and ring fingers of both left and right hand are used to represent the six dots of the Braille cell [38]. To communicate, the sender physically touches these fingers on the recipient's hand in order to pass across information (see Fig. 2-4 (b)).

Finger Braille is simple, easier to learn and use as compared to the standard Braille reading. Hence any device that adopts this method of communication is likely to also to be easier to use due to the simplicity of this method. In comparison to the deafblind manual alphabets, Finger Braille is much more efficient but a few people in the UK are familiar with it. Flexible sensors and actuators as well as a prototype towards this goal is presented later in Chapter 4, 5 and 6.

Table 2-4 shows a summary of existing tactile communication devices which uses Braille method for their tactile interface and particularly developed for deafblind people. Some of the devices make use of standard Braille displays which is expensive and others use commercial sensors and actuators which is not easy to customise.

In [39], a portable two-unit device was developed that allows wireless communication between the deafblind person and a sighted and hearing person. The deafblind person sends message using a Braille terminal and it displays on a display device for a sighted person to read. Messages sent to the deafblind person are read and interpreted using a Braille terminal. The device has no means for remote communication and is very expensive due to the use a Braille display as a tactile interface.

Table 2-4 Summary of Existing Braille-based Deafblind Communication Devices

Device	DB Communication Strategy	Tactile Sensor Used	Tactile Feedback Actuator Used	Type of Communication	Year	Ref.
Portable Communication Aid	Braille (Mandarin Phonetics)	None (uses a Terminal)	None (Uses a Braille Display)	Two-way	2001	[39]
Body Braille	Braille	Braille Keypad	Microvibrators [a,b]	Two-way	2008	[40]
P-brll	Braille	Braille Keypad	Microvibrators [a,b]	Two-way	2012	[41]
Communication Glove	Braille	Capacitive sensors [b]	Vibration Motors [a,b]	Two-way	2015	[42]
SPARSHA	Braille	None (Braille keys)	Movable pins[b]	Two-way	2013	[43]
UbiBraille	Finger Braille	None	Vibration Motors[a]	One-way	2013	[44]
MyVox	Braille	None (uses Keyboard)	Braille Display/Vibration Motor [a,b]	Two-way	2014	[45]
V-Braille	Braille	None (uses Mobile phone screen)	None (uses Mobile Phone Screen)	Two-way	2010	[46]

[a]*Commercial,* [b]*Rigid , DB – Deafblind*

A tele-support and body Braille device was developed in 2008 for deafblind people using body-Braille and mobile phone [40]. Body Braille is a method in which some parts of the body especially the back are used to interpret Braille. The system is made up of a mobile phone and six small commercial vibrators which are placed on any part of the body, and directly mapped to a Braille-based keypad. To get a tele-support, deafblind person snaps objects around them and send to a remote person who interprets and sends the message back. Messages are received by the deafblind person via vibrators won on the body which vibrates

according to the Braille alphabet. Though the technology was able to make remote support possible, it did not remove the high cost inherent in the transmission of video. The micro-vibrators are also tethered to the Braille-based keypad using a wire, and this reduces convenience as the deafblind person will have plenty of wires on their body to contend with.

P-brll" was later developed using body Braille and skype called "P-brll". This system enables a deafblind person to communicate with another deafblind person without any assistance [41]. Its interface consists of body Braille with two micro-vibrators and other components include a Play Station Portable (PSP), a computer and internet connection". Communication from the deafblind person starts from he/she making an internet connection and then talks to the other person using braille by means of Dual Tone Multiple Frequency (DTMF) tone signals which corresponds to points of Braille cells. Two micro-vibrators are driven to interpret messages for the deafblind people. It also employs infrared which is not very good as it uses line-of-sight communication as mentioned earlier. The system is highly dependent on internet connection which means no internet, no connection. In addition it employs a computer system making the users tethered to a computer which remove portability.

In [47] the authors developed a micromechanical SMS-based body braille system that helps deaf and deafblind people to communicate. The system uses a mobile phone, a computer and a digital Braille writer. The deaf or deafblind person wears the body Braille with micro-vibrators positioned at the back of the user. To communicate, the deaf or deafblind person composes messages using a digital braille writer and sent to through a computer to the mobile phone of the non-deafblind person. The non-deafblind person replies by composing message using a mobile phone and then this message is sent to the deafblind person's mobile phone which is connected to a computer, the computer then translates it to its Braille equivalent and through the parallel port stimulates the micro-vibrators according to the message sent. This device is not standalone as it requires a computer for the deaf or deafblind person to receive messages. This makes it hard for the deafblind person to receive messages anywhere and anytime.

Researchers also developed a finger Braille interface for users of finger Braille [48]. They developed two types of finger-Braille devices, the vibration motor type and the solenoid type both connected to a wearable computer. They tested the two on some users and the results shows that majority of the users need an improved version of the solenoid type. The research

mainly geared towards developing an interface to support navigation of deafblind people and use wearable computers and finger Braille based devices. The lacks tactile sensors to be used by deafblind people for sending messages. Furthermore it uses off-the-shelf vibration motors for tactile feedback.

Recently a communication device for deafblind people was developed using ARM-based computer (Raspberry Pi) as the main processing unit. Other units of the system include: a Liquid Crystal Display, speaker, a refreshable braille display, vibrating motor, and a real time clock [45]. The tactile interface for deafblind person is a keyboard used for composing messages, the message is translated to speech through the speaker for hearing people, and displays on an LCD for sighted people. Messages sent to deafblind people are read via a Braille display. The major limitation in the interface used here is that it is not wearable, flexible, or portable. It is also expensive because of the use of a Braille display.

In [35], three interaction methods were designed for reading six-dot Braille characters by embedding a prototype device that has a piezoelectric actuator under the touchscreen. The prototype creates tactile feedback and with three interaction methods, scan, sweep, and rhythm, Braille readers can read characters one at a time either by exploring the characters dot by dot or by sensing a rhythmic pattern presented on the screen. The presented results showed that temporal tactile feedback and Braille coding can be used to transmit single-character information. However, users were not able to read multiple Braille characters consecutively.

In [46], V-Braille was introduced. It is software used to modify the mobile phone screen to function as a Braille cell. This means that it adopts the mobile phone screen as a tactile interface to be used by deafblind people. The screen is divided into six parts with each part representing a Braille dot. When the screen is touched, the raised dots vibrate while the lower dots do not and by so doing the reader can understand the message. This is a potential alternative to the use of the bulky Braille displays and introduction of Braille to the mainstream mobile devices. UbiBraille was also developed in [44] for the purpose of reading Braille, and its tactile interface is based on the concept of Finger Braille. It has six commercial vibration motors on the fingers for reading of the Braille characters. One of the limitations of this device is that it has no tactile sensor in its interface or any means of sending information from deafblind to sighted and hearing person. So the tactile interface used supports only one-way communication.

2.2.3 Block Letter Communication Method

This is a method of communication used by deafblind people in which the English block letters are signed on the palm of the deafblind person who intuitively senses the shape of the letters and then interprets it. It is particularly useful for those categories of deafblind people who have acquired the knowledge of English language before becoming deafblind. Fig. 2-5 shows how to sign the letters including the number of strokes involved in each case. In order to communicate, the letters of the word to be sent by the speaker are signed on palm of the listener who intuitively decodes and puts these letters together mentally to form meaningful words.

This method is usable by people who have the knowledge of English alphabets, and in this case they are deafblind people with acquired deafblindness - which means they must have learnt the English language before they became deafblind. Given that majority of deafblind people are older people with acquired deafblindness; this method is likely to be preferred compared to the deafblind manual alphabets discussed in Section 2.2.1.

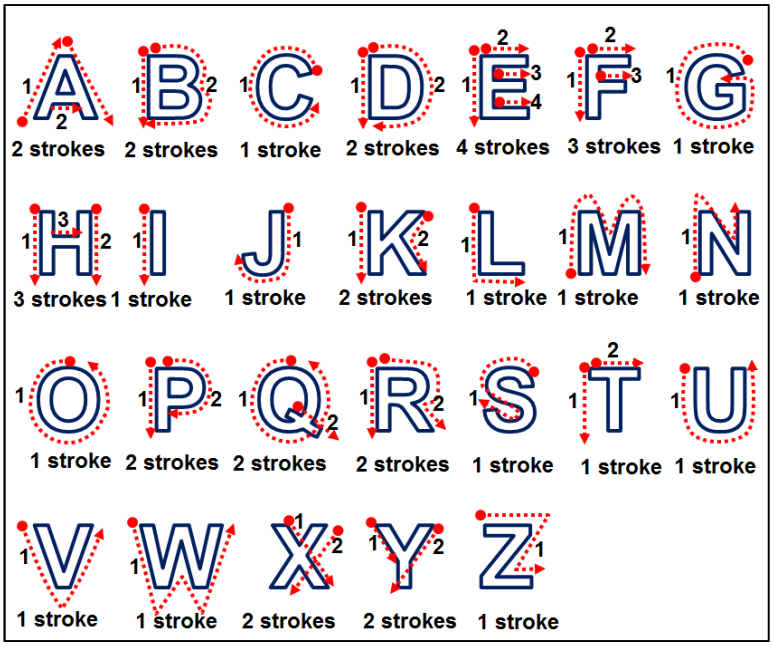

Fig. 2-5 Block Letter Communication Method

2.2.4 Comparison of Tactile deafblind communication methods

The comparison was carried out from reviewed literature and the fact that majority of deafblind people are older people with acquired deafblindness. This means that they must have acquired language before they became deafblind. They were rated 1 to 4 where 1 means poor and 4 means excellent Fig. 2-6

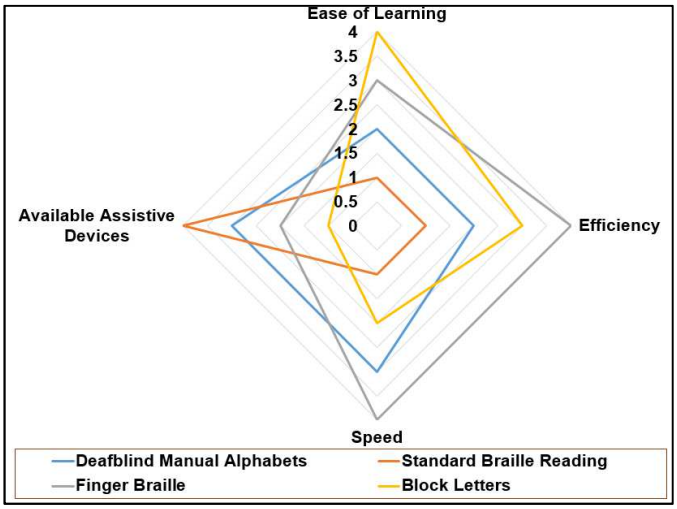

Fig. 2-6 Comparison of Tactile deafblind communication methods

It is clear from the review of existing deafblind communication devices that greater majority of the tactile interfaces used in these devices make use of rigid and commercial tactile sensors and actuators. Devices that are based on Braille are more popular and much more advanced and commercialised while majority of the devices based on deafblind manual alphabets are still prototypes and require further improvement, popularity and increased acceptability. To advance the current state of the art for deafblind communication devices, there is a need to fabricate tactile communication interfaces (using tactile sensor and actuators) that will enable the portability, flexibility and conformability of these devices as well as suit specific communication methods used by deafblind people.

The following sections present the human tactile sensing and perception as well as different existing tactile sensing and feedback technologies.

2.3 Human tactile sensing and perception

The knowledge of the psychophysics of touch is very essential in order to realise an effective tactile interface that gives a realistic feeling. The sense of touch in human are broadly grouped into two sub-modalities based on the site of the sensory input. These are the cutaneous and kinesthetic sense [49]. The cutaneous sense receives sensory input from the receptors embedded in the skin, while the kinesthetic sense receives sensory input from the receptors within muscles, tendons and joints. The following section discusses the human skin and the mechanism of human tactile sensing and perception.

2.3.1 The human skin

The human skin is the single largest human organ with $2m^2$ of surface and 3.6kg of weight in adults [50]. It is the primary entry point for human sense of touch and perception with

countless neural sensors [51]. The skin enables humans to touch, recognise, manipulate objects as well as communicate with one another. It can be broadly categorised as glabrous (hairless) and hairy. The glabrous skin (particularly the hand and feet) gives the most effective detailed tactile information [52], but the hairy skin also have touch-sensitive hair follicles [52, 53]. The human skin is complex from the Neurophysiological perspective; it is innervated by sensory receptors like the nociceptors (for pain), thermoreceptor (for temperature), pruriceptors (convey itch), and the low-threshold mechanoreceptors (LTMR - for non-painful mechanical stimuli) [54, 55]. The sensitivity of these receptors depends on their size, frequency and branching of nerve fibres [52]. These are all part of the cutaneous sense but the major focus will be on the LTMR which is well connected to tactile sensing.

2.3.2 Mechanoreceptors

Mechanoreceptors are part of the several human sensory receptors that translate tactile stimuli for the brain in the form of electric nerve impulses [52, 53, 56, 57]. These electric nerve impulses are information encoded as action potentials (time between voltage spikes) [58] which are then interpreted in the brain as human perception [53]. Mechanoreceptors are particularly concerned with the interpretation of mechanical stimuli like force, vibration or movement at the surface of the skin [52, 53]. The mechanoreceptors measure forces on different time scales and with different receptive fields (area of the skin that was stimulated), and there are about17,000 mechanoreceptor units in the glabrous skin [56].

In the glabrous skin, the mechanoreceptors are divided into two subcategories based on their distinct sensitivities, conduction velocities, and adaptation to sustained mechanical step indentation to the skin. They include the fast adapting (FA) and the slow adapting (SA) touch receptors. The SA touch receptors are indentation detectors that fires continuously during a sustained stimulus, whereas FA touch receptors are velocity detectors that respond only during the onset and offset of stimulus [55, 56, 59]. The SA and FA are each subdivided into two types (Type I and II) based on the properties of their receptive field. The SA type-I (SA I) and FA (FA I) type-I has small and well-defined receptive fields, while the SA type-II (SA II), and FA type-II (FA II) [56]. In [55] SA and FA- types were particularly defined as Aβ SA I (innervate Merkel cells in the basal epidermis and report the static nature of touch stimuli), Aβ SA II (hypothesized to terminate in Ruffini corpuscles in the dermis and are particularly sensitive to skin stretch). Aβ FA I (innervate Meissner's corpuscles in dermal papillae and are sensitive to movement across the skin), and Aβ FA II (terminate in Pacinian corpuscles deep in the dermis and are tuned to high frequency vibration) [60-62](Fig. 2-7a).

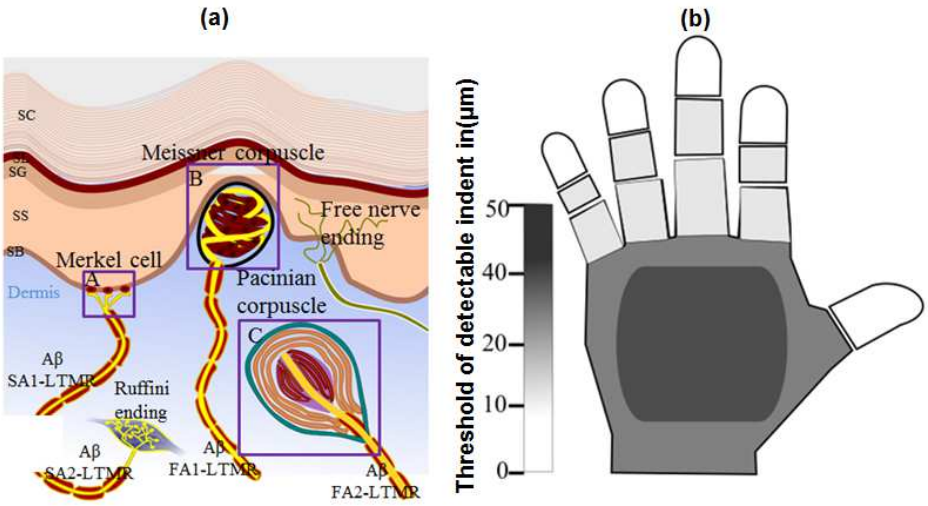

Fig. 2-7 Innervation of the skin: (a) LTMR innervation of the glabrous skin (b) Threshold of detectable indents on the human hand.

Fig. 2-7a was adapted from [55] and shows the LTMR innervation of the glabrous skin, while Fig 2-3b was adapted from [63] and shows the threshold of detectable indents on the human hand. In hairy skin, several LTMRs form specialized terminals associated with hair follicles, allowing the sense of touch to extend beyond the skin surface as shown in Fig. 2-7a.

2.3.3 Tactile perception threshold

In this section the different thresholds for human tactile perception are presented. Generally, studies on the function of the human hand usually consider the threshold of the hand's response to different stimulations like pressure, temperature, spatial acuity, and vibration. The human sense of touch is well developed and there is often a minimal perceived intensity. these stimuli Although there are different mechanoreceptors, tactile reception results from a combination of all the receptors in a particular skin area. The threshold of tactile perception depends on several factors like location, contact area, type of stimulus, duration, age, gender and even hormone levels [52, 64-68]. In [66], it was observed that the most significant age difference in vibrotactile detection threshold was found in the glabrous finger with the difference being less pronounced at lower frequencies (5-10Hz) and more pronounced as the frequency increases to 300Hz. Studies have equally shown that the perceived intensity of stimulation is determined by both the depth of penetration and the rate of skin indentation [53, 69].

Table 2-5 Characteristics of different receptors.

	FA I Meissner	**SA I Merkel**	**FA II Pacinian**	**SA II Ruffini**
Field diameter*	3 - 4mm	3 - 4mm	> 20mm	> 10mm
Mean receptive area*	12.6mm^2	11mm^2	101mm^2	59mm^2
Spatial acuity†	poor 3- 4 mm	0.5 mm	10+	7+
Frequency range	8 - 200 Hz	DC - 200 Hz	50 -1000 Hz	DC -200 Hz
Most excited frequency range*	8 - 64 Hz	2 - 32 Hz	> 64 Hz	< 8 Hz
Indentation threshold†	6µm	30 µm	0.08 µm	300 µm
Response properties‡	Responsive to dynamic skin deformations at relatively low frequency (~5–50 Hz);	Responsive to dynamic skin deformations at low frequency (~<5 Hz);	Extremely responsive to high frequency vibration (~40–400 Hz);	Low responsiveness to dynamic force; responsive to static force;
Density and location *, ‡	70 - 140 /cm^2 in dermal papillae of the fingertip	70 - 140 /cm^2 in fingertip epidermis	20 /cm^2 in dermal and subcutaneous tissue, distributed throughout the hand	50 /cm^2 in dermal and subcutaneous tissue, distributed throughout the hand

Adapted from * [53], †[49], ‡ [62]

Table 2-5 summarises the different receptors, their end organs and characteristics. It shows the different parameters for the different receptors with different reported range at which they respond to various stimuli. Considering indentation which the FA II (Pacinian) has the least indentation threshold of 0.08µm while the SA II (Ruffini) has the highest value (300 µm). For vibrotactile application, the target would be to stimulate the FA II which is extremely responsive to frequency vibration of ~40–400Hz.

When considering the absolute tactile sensitivities, pressure threshold is a common parameter and various studies have been carried out in this direction [70]. Studies have shown that the sensitivity of a specific part of the body to pressure decreases as the pressure increases and the threshold depends on the part being considered [49]. Humans are able to recognise common objects by touch within 1-2s and the skin is very sensitive to light pressure [53]. The sensitivity of pressure was reported in [70] to have a normal mean of

0.158g on the palm and around 0.055g (0.032g and 0.019g for women) the fingertips. In [71], and as shown in Fig. 2-7b human detectable indent corresponding to different areas of the palm is around 10µm to 50µm, and in [72], the pressure exerted by a tactile device should be above 60mN/cm^2 in order to adequately stimulate the finger mechanoreceptor. According to [63], 5mN of force is able to excite 90% of the SA I and FA I mechanoreceptors and a force of 87mN/mm^2 could be applied with a Von frey hair with a diameter of 0.27mm [49]. In [73], it was reported that on the distal part of the index finger, most people can perceive normal and tangential forces in the range of 0.15 – 0.7N without slip. According to [74], more sensitivity is observed at the forearm when stimulated with tangential forces in comparison with the normal forces, while at the finger pad sensitivity to tangential forces is lower than that of normal force. Based on this, the authors provided the following guideline for development of tactile displays: (1) Tangential stimulation should be a superior choice when an actuator is limited primarily in terms of peak displacement (2) Normal stimulation should be a superior choice on finger pad (and tangential on hairy skin) when an actuator is limited primarily in terms of peak force.

Considering surface exploration, 0.85µm has been reported as minimum perceivable height of a static raised feature on a smooth surface while small dots of 40µm in diameter and 8µm in height can be detected 75% of the time with active scanning [53]. In [75], it was shown that human skin is sensitive to spatial differences at the frequency bands of 1-3Hz and 18-32Hz (this corresponds to frequency range of FA I and SA I receptors) and spatial acuities gradually decreased as the frequency of vibration increased over 50Hz. However, it has been known that vibration perception varies with age [76] and vibration is perceived differently at different frequencies. In [77], the effects of vibration frequency, pulse-width duty cycle, number of contactors, on differential thresholds were examined at five different areas of the hand. The reported result shows variation of threshold with the frequency and number of active contactors with highest sensitivity observed at 120 Hz [77]. In [78, 79], it was shown that the vibration range of 20 to 1000Hz are perceivable with maximum sensitivity around 250Hz which corresponds to the frequency range of FA II receptors. For vibrotactile perception of the human finger, the sensitivity is shown to increase as the frequency increases, with the exception of very high frequencies [75].

In order for the hand to effectively read an array of haptic actuators, it is important to consider spatial resolution in case of array of actuators as this will aid effective discrimination of individual stimulation. A spatial resolution of 1mm is recommended for

the fingertips and 5mm for less sensitive areas like palm and shoulders [49]. However, the significant loss of receptors with age affects tactile sensitivity and the ability to discriminate vibrotactile patterns [80, 81]. The experiments carried out in [81, 82] shows that older adults (60 years and above) were only able to reliably identify only simple one-element vibrotactile pattern, while younger subjects mastered even three to four elements. It is therefore important to pay attention to this age-related tactile threshold in the design of tactile aids for deafblind people as majority of them are older people. Tactile aids for deafblind people often involve rapid tactile processing information like reading of Braille. Experienced adult Braille readers can read at the rate of 104 wpm [83]. This means that they are meant to scan 100-300 separate Braille cells with one fingertip in 60 s. A Braille cell is composed of one to six raised dots, which is about 1.5mm diameter at the base, separated by 2.3 mm from each other, and by 4.1 mm from the nearest dots in adjacent cells [84].

2.4 Tactile sensing technologies

In this section, different tactile sensing technologies are discussed including the research and development in this area. This is to make it possible to identify a suitable technology for the development of tactile communication interface for deafblind people. Tactile sensing involves the use of tactile sensors to acquire information through physical touch. So tactile sensors are a category of sensors that acquire information through physical touch and measures properties such as temperature, vibration, pressure, texture, shape, and normal forces [85, 86]. Tactile sensing not only involves the detection and/or measurement of the spatial distribution of forces perpendicular to an area but also on the interpretation of the corresponding information [57, 87].

Generally, the existing strategies for the development of tactile sensing units could be grouped into three [59] – (1) Tactile sensors developed based on various transduction methods (2) development of a structure that generates a signal on touch (3) the use of new materials that intrinsically converts mechanical stimulus on touch into usable signals. The importance of tactile sensing becomes very apparent in cases where other sensing modalities such as vision are not sufficient or completely unavailable – an example is the case of deafblind people.

The following sections, presents the different categories of existing tactile sensing technologies, their working principles, and a summary of their uniqueness, strengths as well as limitations.

2.4.1 Resistive Tactile Sensors

In resistive tactile sensor, contact forces are measured based on the change in the resistance of the sensing material used. Resistive touch sensing can be grouped as discrete and analog resistive touch sensing. In the former, the sensor is made of two-dimensional grid of sensing elements and in the latter the sensor is made of two flexible sheets coated with resistive material placed on top of each other and separated by an insulating material like air, microspheres and so on [49], as shown in Fig. 2-8 .

In analog type of tactile sensing array, the point of touch is determined by scanning through the rows and column at a fast rate. To determine the point on the column (Y axis) that was pressed, voltage is applied to one end of the column and the other end is grounded while the back sheet is left on a high impedance state (Hi-Z, i.e unconnected). So the back plate now acts as the slider of a potentiometer and causes different voltages to be realised for different touch points as shown in Fig. 2-8 (b & c). Fig. 2-8 (d-g) shows that before the membrane is touched, a certain resistance is presented to the sensor (R_x for x and R_y for y-axis), when the membrane is touched at any point, R_x is divided into R_{x1} and R_{x2} while R_y is divided into R_{y1} and R_{y2} The same thing happens in order to determine the contact point on the row (x-axis) with the front sheet now in a high impedance state (Hi-Z) (Fig. 2-8 (b)), and with this the x and y coordinates of the point that was touched will be determined by reading the V_{Xout} and V_{Yout}, and this varies as a proportion of the V_{in} (V_{in-x} and V_{i-y}).

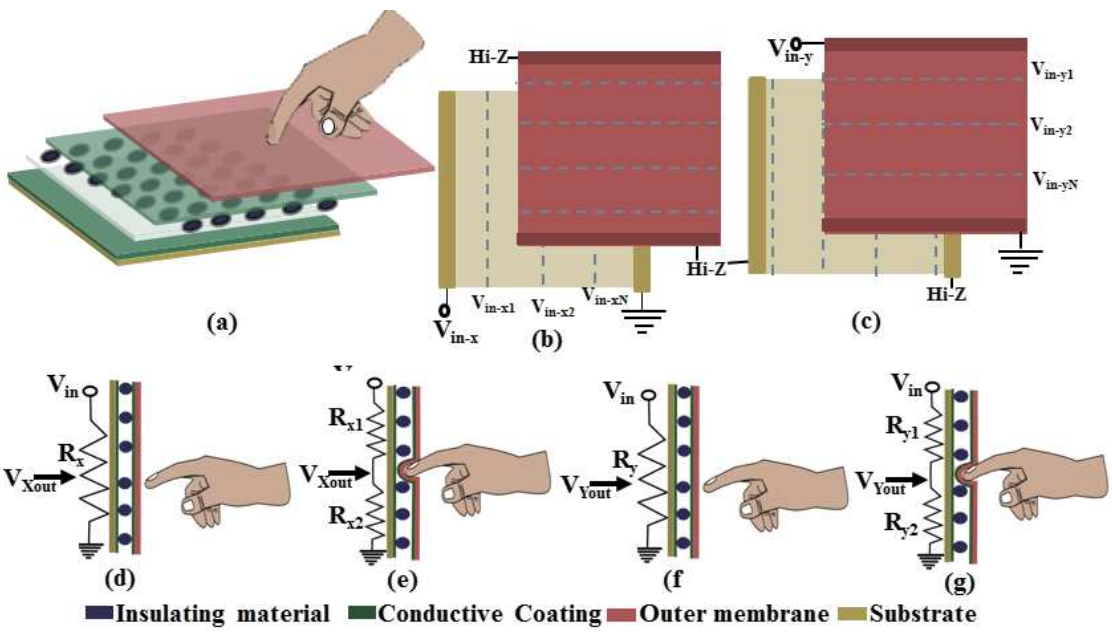

Fig. 2-8 The principle of resistive tactile sensors. Adapted from [49]

So with this configuration, the coordinate of the contact point is determined by the measured output voltage on the y-axis ($V_{in\text{-}y1,2\ldots N}$) and x axis($V_{in\text{-}x1,2\ldots N}$) as shown in Fig. 2-8 b &c where N is the number of the wire configuration. For an N-wire configuration, the contact point on x and y axis could be determined reading the fraction of the input voltage as described in Equation (2-1) and Equation 2-2 with i starting from the point closest to V_{in}. i.e point of highest potential. One common configuration of the analog resistive touch sensors is the 4-wire configuration.

$$V_{out(X\ or\ Y-axis)} = \left(1 - \frac{i}{N}\right) V_{in(Xor\ Y-axis)}\ i = 1,2,3 \ldots N \tag{2-1}$$

Note that $V_{out(X)}$=V_{in-XN}, $while\ V_{out(Y)} = V_{in-yN}$ and this is the output voltage measured at the contact point on the x and y axis respectively. The value of this output voltage is determined by the combination of the different resistances in accordance with voltage divider rule as described in equation 2-2.

$$V_{out(X)} = \left(\frac{R_{x2}}{R_{x1} + R_{x2}}\right) V_{in-x} \tag{2-2}$$

$$V_{out(Y)} = \left(\frac{R_{y2}}{R_{y1} + R_{y2}}\right) V_{in-y} \tag{2-3}$$

So the coordinate of the contact point could literarily be written as$(V_{out(X)}, V_{out(Y)})$.

One of the challenges of analog type is its ability to register multi-touch which makes it unsuitable for applications where multi-touch is required like robotics as well as deafblind communication. One of the remedies to this is the use of hybrid resistive tactile sensing which combines the analog tactile sensing technique and array touch sensing technologies as described in [88].

There are also piezoresistive tactile sensors which are made of materials whose resistance changes with force/pressure [89]. Such materials popularly used include, conductive rubber, conductive yarns, conductive gels, and force sensing resistors (FSR).

Existing resistive tactile sensors include that in [90], a resistive tactile sensor array using commercial force sensing resistor (FSR) embedded in 8mm thick PDMS. The FSR array

was arranged in the form of an equilateral triangle whose sides are 20mm each. The array uses commercially available sensors which means that controllability of the parameters are quite limited. A conductive polymer PEDOT:PSS was used in [91] to develop a 100mm^2 x 100mm^2 resistive tactile sensing array capable of measuring forces of 0.2 – 0.7N. In [92], single layer graphene was used to realise piezoresistive tactile sensing array for surface texture recognition. The sensor was reported to be able to detect a vertical pressure of 24Pa with a response time of approximately 2ms for deformation and 3ms for restoration. Also in [93] an array of 2cm^2 x 2cm^2 having 48 piezoresistive tactile sensors for detecting pressure/force on nonplanar surfaces was presented. The sensor utilises Wheatstone bridge geometry and has an average sensitivity of 1.25 V/N. Also a liquid-based single resistive tactile sensor with a working range of 0.007N to 0.25N was fabricated using graphene oxide Nano-suspension [94]. Although this is just a single sensing element, there is possibility of extending it to an array of sensing elements.

Generally resistive tactile sensing technology is low-cost and simple to fabricate and use. However, one of its limitations is high power consumption and for analog types the inability to register multi-touch.

2.4.2 Capacitive Tactile Sensors

A capacitive tactile sensor is made of two conducting parallel plates separated by a dielectric medium. By touching the sensor, a change in capacitance takes place and this is given by Equation 2-4.

$$C = \frac{\varepsilon A}{d} \tag{2-4}$$

Where A =Area of the plate, ε = permittivity of the dielectric material, d= distance between the plates.

When a force is applied on the plate of the capacitor, the distance d, of the dielectric material changes and this causes a change in capacitance. This gives the sensor its force/pressure-to-capacitance characteristics and has been used to develop capacitive force/pressure sensors (including single element as well as array).

Two categories of capacitive tactile sensors have been reported – self or absolute capacitance type and mutual capacitance type. In the former, a touch on the plate loads the parasitic capacitance $C_{Electrode}$ to ground (Fig. 2-9 a & b), while in the latter, the object alters the mutual

capacitance, C_{Mutual} between two electrodes (Fig. 2-9 c & d) [49]. In case of the mutual capacitance type, there is a transmit electrode (with a capacitance $C_{Tx\text{-}Electrode}$) and a receive electrode (with a capacitance $C_{Rx\text{-}Electrode}$). This type of capacitive tactile sensors are used for tactile sensing arrays in which a voltage is applied to the row or column and the mutual capacitance between transmit and receive electrodes are measured by a proper read-out circuit. This means that an array with n x n elements will have n^2 independent capacitance.

An example of a readout circuit for a capacitive tactile sensing array is the one presented in [95] as shown in Fig. 2-9 . A touch on a particular point on the array is determined by accurately measuring the capacitance at every point. For the example shown in Fig. 2-9 e, one cell is selected by row and column decoders and voltage V_{step} is applied to charge the selected mutual capacitance C_m in that cell. When V_{step} is switched to ground, the stored charge in the capacitor is transferred to the feedback capacitor C_f and this changes the output voltage V_0 as shown in Equation 2-5. This scan is quickly carried out and by so doing the sensor is able to determine which point was touched. In this case, the cell capacitance was read in 100µs (20 frames per second).

$$\Delta V_0 = \Delta V_{Step} \frac{C_m}{C_f} \tag{2-5}$$

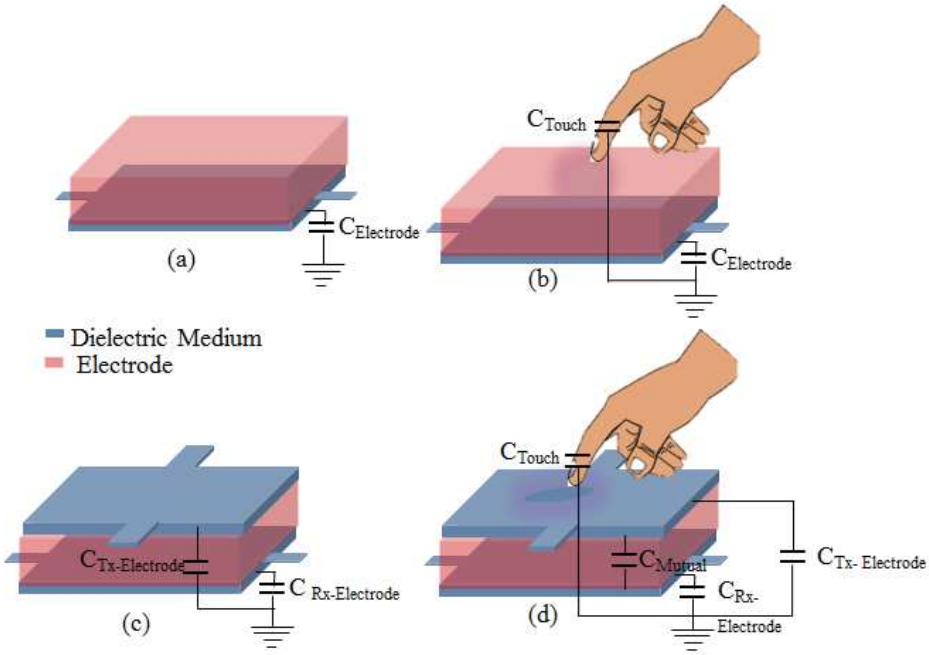

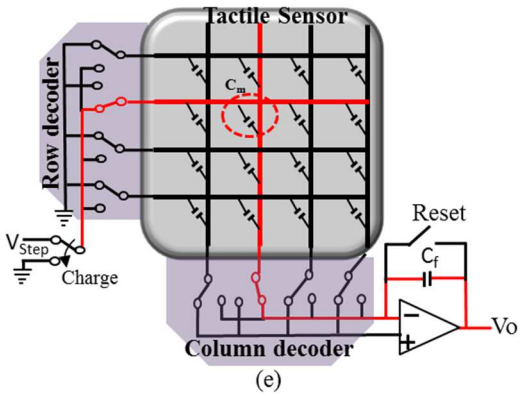

Fig. 2-9 (a) Self or absolute capacitance type without touch (b) Self or absolute capacitance type with touch (c) Mutual capacitance type without touch (d) Mutual capacitance e type with touch (e) Readout circuit of Capacitive Tactile sensor array with mutual capacitance.[49, 95].

In [96], a 20 x 20 transparent tactile sensor array with 2mm spatial resolution and a 6.7% cell-to-cell capacitance variation was designed. They used 120µm polycarbonate (PC) films for top and bottom layer, 13 µm SU-8 as spacers and an insulator, and an Indium Zinc Oxide (IZO) thin film as electrodes. The cell and electrode size were 2mm x 2mm and 1mm x 1mm respectively. The device is able to recognise multi-touch and capable of force sensing which enables it to discriminate different levels of touch. An array of 4 MEMS-based capacitive tactile sensing array measuring 500 µm x 400 µm with a 150 µm separation was demonstrated in [97]. The sensing array was fabricated using a bonded and etched-back silicon-on-insulator (BESOI) wafer as a substrate. The upper layer is a 2 µm thick highly doped single crystal silicon diaphragm and a lower electrode of doped silicon both separated by a 2 µm air cavity The entire device was packaged with a 200 µm thin layer of PDMS and its application is basically for texture recognition and it has an accuracy of 10fF.

In [95], a 16 x 16 capacitive tactile sensor array with a 1mm spatial resolution and a cell size of 600 x 600 μm^2 and a 400 μm^2 x 400 μm^2 copper electrodes embedded in PDMS membrane was presented. Each cell has a capacitance of about 180 fF with a sensitivity of 3%/mN. The array was proposed application on the sensor array is in robotic tactile skin. PDMS was also used to fabricate an 8 x 8 capacitive sensing array in [98]. The capacitive sensing electrodes and the metal interconnect for signal scanning were fabricated on the FPCB, while the floating electrode was patterned on PDMS. To measure the capacitance, a force is applied to the sensor array and the capacitance is measure when the force value reaches a certain level. Tactile images induced by PMMA stamps of different shapes were also demonstrated and the sensitivity of the device is about 2.27%/kPa with a minimum resolvable force of 38mN. A 2 x 2 capacitive sensing array was equally fabricated with FPCB

and PDMS as presented in [99]. The measured maximum sensitivity of this sensing array is 1.67%/mN with a minimum resolvable force of 26 mN.

A multi-sensor array has also been developed as reported in [100]. The sensor has an 8 x 8 capacitive tactile sensor array combined with a thermal sensor with the ability to detect cell capacitance within ±0.01pF. The thermal sensor was obtained by the rows of the capacitive array enabling it to detect the temperature gradient which helps to improve object recognition.

The advantages of capacitive-based tactile sensors include low-cost, high sensitivity, less temperature dependence, and better long-term stability. On the other hand, the readout circuit for measuring the measurements of capacitance changes are complicated. Additionally, capacitive sensors that employ elastic dielectric layers also suffer from non-linearity and hysteresis which is caused by the material property of the elastomer.

2.4.3 Ultrasonic tactile sensors

Researchers have also developed tactile sensor base on the ultrasonic technology. Measurement of tactile stimulus using ultrasonic principle could be in two ways, one is by measurement of the surface while the other one is by measurement of deeper tissue. Polyvinylidene Flouride (PVDF) is generally used for transmitting and receiving ultrasound [101]. The principle of ultrasonic sensors is shown in Fig. 2-10. The sensor comprises of ultrasonic transmitters and receivers covered by an elastomer which correspondingly deforms in accordance with the applied force. The transmitter transmits pulse into the elastomer which is reflected from the exposed surface of the elastomer. The reflected pulse is then received by the receiver and the time for the round-trip is measured. This time is proportional to the thickness of the elastomer and so by measuring the difference in the time (t_1 - t_2) for round trip, the change in thickness (d_2 – d_1) of the elastomer can be determined and hence the applied force (See Equation 2-6 and 2-7).

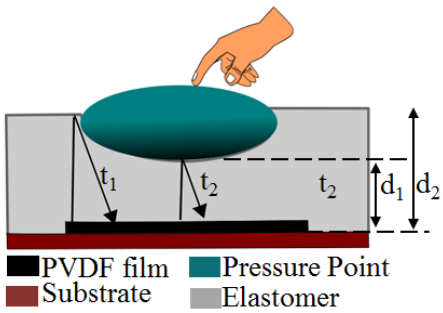

Fig. 2-10 Ultrasonic tactile sensors

$$d_1 - d_2 = \frac{1}{2}c(t_1 - t_2) \tag{2-6}$$

$$F = k(d_1 - d_2) = \frac{1}{2}kc(t_1 - t_2) \tag{2-7}$$

Where F= applied force, k = rubber stiffness, c = speed of light in rubber.

An 8 × 8 ultrasonic tactile sensor array with a special resolution of 1.1mm was developed in [102]. The array measures 8.5mm x 8.5mm x 0.5mm, and the dimension of one element was shown to be 820µm x 820µm x 300µm. Characterisation of the sensor shows it has a resonance frequency of 867 kHz and impedance at resonance of 230Ω. Acoustic load impedance sensing test with droplets of water and isopropyl alcohol (IPA) showed that over a range of 0.1 - 0.3N surface force, there was 11% increase in impedance with IPA and 14% increase with water. The sensor is targeted at surface load detection including surface load of different materials and force loading.

Three tactile arrays (3 × 6, 4 × 9, and 6 × 15 arrays) were fabricated in [103]. The sensor consists of a thin-film transistor (TFT) sandwiched between a PVDF transmitter and receiver. An AC signal is applied to the PVDF transmitting layer to generate ultrasound waves which passes through the sensor components and is detected by the receiver which produces a voltage that is then detected by the TFT layer. The sensor surface is coated with a PDMS layer which is deformed by an applied force and the sensor array is able to detect static forces ranging from 1 to 6N.

2.4.4 Optical tactile sensors

The basic operating principle of optical sensors is that light is passed through usually a soft or deformable material and the pattern or intensity of the light is measured when a force is applied on that material. Optical tactile sensors can be grouped into two depending on how the pattern or amount of light is detected. These are – intrinsic and extrinsic. In intrinsic optical sensors, the change in the light intensity is often utilised for measuring tactile parameters like force/pressure. In extrinsic, there is usually a light emitting source (usually light emitting diode – LED) and a photo detector and between them lies an opaque pin which moves up and down when pressed. The pin is often attached to a flexible membrane which when pressed causes the pin to block the light reaching the photo detector from its emitter as shown in Fig. 2-11 [87]. The amount of light blocked corresponds to how much force/pressure applied.

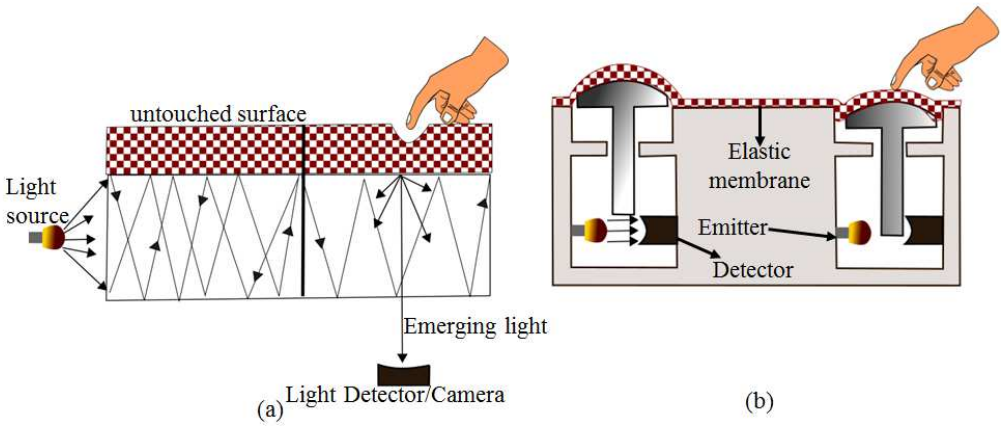

Fig. 2-11 Optical tactile sensors (a) Intrinsic (b) Extrinsic. Adapted from[49, 101].

Examples of intrinsic type of optical sensor were described in [104]. They are optical sensor arrays that utilise the most widely reported principle for intrinsic optical tactile sensors called frustrated total internal reflection as shown in Fig. 2-11. One is a 32 x 32 optical planar sensor array that operate on the with 1mm spacing between taxels. The force range is 0-0.4N per taxel with a frequency response of 0 to 200Hz. The second sensor is a 13mmx13mm finger-shaped sensor with 256 taxels.

Extrinsic optical tactile sensors have also been reported. In [105], the authors presented an optical-based sensor array with an arrangement of an LED-phototransistor laid on a printed circuit board and an 11.4 mm × 11.4 mm deformable top elastic layer. The LED-phototransistor arrangement on the printed circuit board is located on every array element. The LED illuminates each point and the phototransistor measures the amount of light on each point. Pressing the deformable layer on a particular point, changes the amount on light reaching that area and this is used to determine to point that was touched. The maximum power consumption of the sensor is 200mW. The characterisation of the sensor shows it can measure force of up to 3.5N and a torque of up to 10Nmm.

Equally in [106], a two 3 x 3 extrinsic optical tactile sensing arrays that uses fibre Bragg grating sensors was described. One is for a large area tactile sensor that has good sensitivity but low spatial resolution while the other is for a small area tactile sensor that has good sensitivity and spatial resolution. Sensors that work based on fibre Bragg grating injects light to the fibre which is reflected by the grating. A shift in the wavelength of the returned Bragg signal is monitored and related to the tactile parameter like force or pressure. The advantage of fibre Bragg grating is linear response and it can easily be multiplexed.

One of the limitations of optical tactile sensors is hysteresis particularly the extrinsic type and calibration is often needed for each pair of the light emitter and detector. Advantages include high resolution, low-cost, and simplicity.

2.4.5 Magnetic tactile sensors

Magnetic-based tactile sensor works by detecting the magnitude or orientation of magnetic field. Two main types have been reported – Those that use electromagnetic coils, cores and permanent magnets and the ones that use active magneto elastic materials (Fig. 2-12 (a) – (d). In [107], the authors proposed a tactile array based on magnetic induction with an array of inductors and a permanent magnet. Each inductor measures 3.2mm x 2.5 mm x2.2mm. A permanent magnet is attached to an elastic membrane and helps to detect the external force (Fig. 2-12 (a)). The magnitude of the external force is calculated based on displacement of the magnet which is at the centre of the inductors.

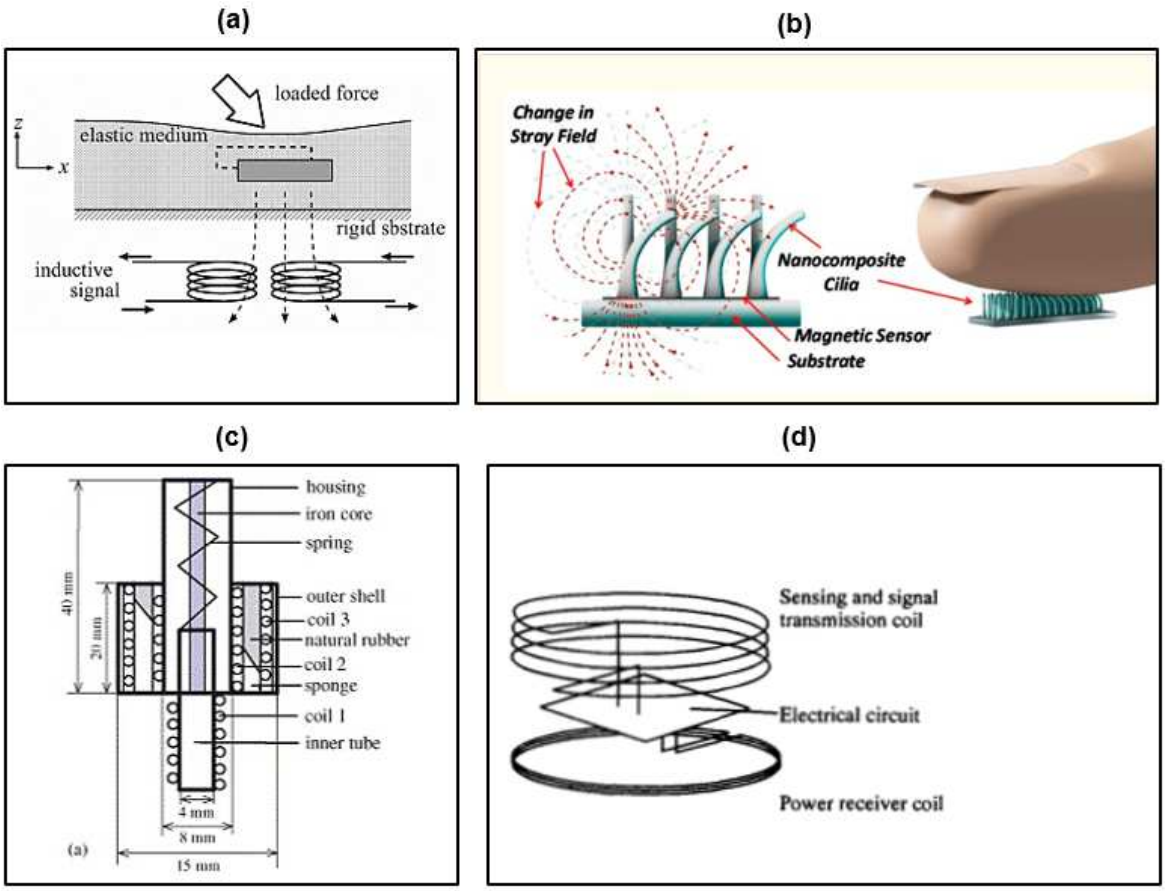

Fig. 2-12 (a) Magnetic Tactile sensor using coil, permanent magnet and elastic medium IEEE 2009 [107] (b) Magnetic tactile sensor with magnetoresistive material, figure copied from Sensors 2016 [108] (c) Magnetic tactile sensor using two coils, figure copied from (a sensing and a transmission coil) Figure copied from IEEE (1999)[109]

A tactile skin with sensors based on magnetic induction was described in [109] Fig. 2-12 (d). The skin has touch-sensitive spots called chips and each chip has a sensing coil, signal

transmission coil, power receiving coil and electrical circuit with some capacitors. The inductance of the sensing coil and the circuit capacitance form a Colpitts oscillator. Tactile sensing is achieved through the fact that a change in the length of the sensing coil induces a frequency change of the Colpitts oscillator which is used to measure the applied force. In [110], a sensor that is able to measure three-dimensional applied force using three coils and a dielectric medium was proposed (Fig. 2-12 (c)). One of the limitations of the sensor is that it is very bulky.

Also reported are sensors with magnetoelastic materials which a change in magnetic field occurs when an external force is applied. This change is often detected using a magnetic sensor whose resistance changes in accordance with changing magnetic field as in [108] (Fig. 2-12 (b)). In [111] an 8 x 8 tactile skin based on magnetoresistive technology was presented. The elements of the sensor array are 2.5mm apart and copper strips to create magnetic fields which vary as a result of some permalloy resistors. The advantages of magneto elastic sensors include wide dynamic range, linear response, low hysteresis and they are easy to fabricate at micro-scale. On the other hand, magneto elastic sensors are susceptible to surrounding magnetic fields and have low output power. Generally, magnetic tactile sensors are simple, have wide dynamic range and the ability to detect large forces.

2.4.6 Piezoelectric tactile sensors

Generally, piezoelectric tactile sensors generate charge or voltage proportional to the force applied to it. It has a similar structure like the capacitive tactile sensors but in this case the dielectric is replaced with a piezoelectric material which produces a charge in the presence of an applied pressure. This charge causes an induced voltage which is proportional to the applied pressure as shown in Fig. 2-13

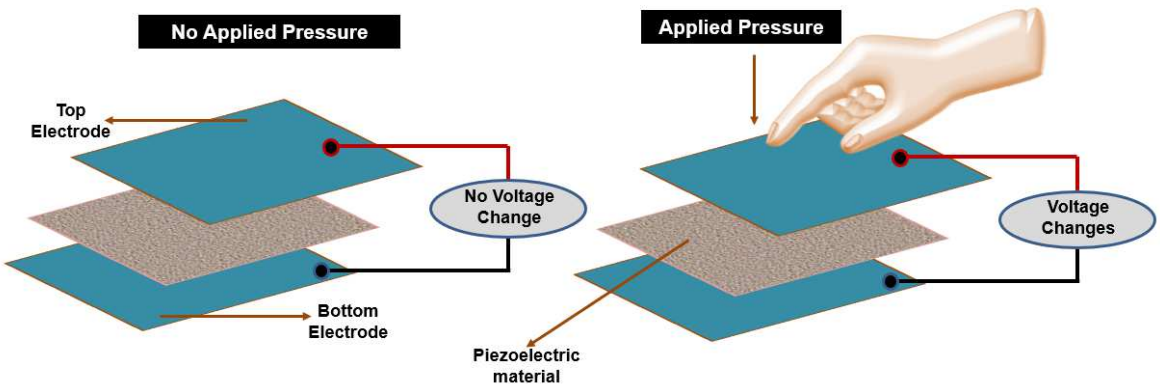

Fig. 2-13 Basic Principle of piezoelectric tactile sensor

In [112], the authors proposed a 3 x 2 piezoelectric tactile sensor array with 8 mm spacing between elements. Each array element measures 1.5 x 1.5 mm^2 and contains a PVDF film sandwiched between four square-shaped upper electrodes and one square-shaped lower electrode to form four piezoelectric capacitors. The results of using forces of 0 to 0.5 N in the x-axis, 0 to 0.5 N in the y-axis, and 0 to 1.5 N in the z-axis shows sensitivities of 14.93, 14.92, and 6.62 pC/N respectively and a frequency response of 5–400 Hz. An approach for large area flexible artificial skin using an array of piezoelectric polymers was proposed in [113] proposed some an. The sensor array consists of PVDF transducers integrated on the flexible PCB substrate with a PDMS coating to protect the sensor. An 8 x 8 tactile sensor array for service robots using 28µm PVDF film was presented in [114]. Each element of the array shows a response of 0.1377N/mV for applied forces of 1.3N to 10N with a time delay of 10ms. Another tactile array based on piezoelectric transduction method is the 5 x 5 tactile sensor array model presented in [115]. This sensor array is based on piezoelectric oxide field effect transistor (POSFET).

Advantages of piezoelectric sensors include high sensitivity, high bandwidth, as well as dynamic response. However, some of the limitations are the fact that piezoelectric sensors are quite sensitive to temperature and often lack robust electrical connections.

Table 2-6 Advantages and Disadvantages of different tactile sensor technologies

	Resistive	**Capacitive**	**Ultrasonic**	**Optical**	**Magnetic**	**Piezoelectric**
Cost	Low	Low	Low	High	Low	Medium
Sensitivity	Sensitive	Sensitive	Sensitive	Sensitive	High Sensitivity	High Sensitivity
Power Consumption	High	Low	Low	Medium	High	Low
Electronics Circuit/ Material	Simple	Complex	Complex Electronics	Complex	Complex	Simple

Ability for Multi-Touch	low	excellent	Good	Good	Good	Very Good
Dynamic range	Low	medium	excellent	Low	High	Medium

Table 2-6 shows a qualitative comparison of the characteristics of different tactile sensing technologies. In relation to the application in the design of a tactile interface, capacitive tactile sensors with excellent multi-touch capability is a good choice.

The following section describes the research and development in the area of tactile feedback actuator technologies including their characteristic, merits and demerits.

2.5 Tactile feedback actuators and technologies

Comparatively, the tactile sensors presented in the previous section are for sensing, while actuators (to be presented here) are used to provide haptic feedback through various forms of stimulation such as skin stretch, vibration, force or painless electric shock [116, 117]. Being able to provide this assistive feedback, they form key components of a tactile interface for deafblind communication.

In [116, 118] haptics was defined as manual interactions with environments through touch, such as exploration for extraction of information about the environment or manipulation for modifying the environment, and stated that the interaction may not be accompanied by vision or audition. In the area of robotics and virtual reality, haptics is defined as real and simulated touch interactions between robots, humans, and real, remote, or simulated environments, in various combinations [119]. This means that these interactions may be accomplished by human, machine or both and the environments can be real or virtual and recently changing the way humans interact with information and communicate ideas [116, 117]. In case of haptic visual aids for deafblind people, the interaction is not accompanied by vision or hearing.

In general, haptic feedback is categorised as kinesthetic (related to forces and positions of muscle and joints) and cutaneous (tactile – relating to skin) feedback [119]. Haptic force feedback systems usually involves measuring the force exerted on the real body and transmitting an equivalent (scaled) resolved force to the user by means of force (kinesthetic) feedback devices; while tactile feedback involves stimulation (vibration, heat, or pressure)

of the mechanoreceptors. Most tactile interfaces developed for deafblind people employ tactile feedback popularly achieve using tactile displays [22, 120].

Tactile displays are devices made using actuators for the purpose of creating tactile feedback to users. As mentioned earlier, this feedback may take different forms such as skin stretch, vibration, force or painless electric shock. They are fabricated using single or array of actuators and have been used over decades to provide feedback. Early research and development in this area were mainly to provide sensory substitution for the blind using Braille devices. Recently, research and application of tactile displays has expanded to fields such as robotics, telepresence, teleoperation, virtual reality, video games, as well as in prosthesis for the restoration of feeling to amputees.

Although all tactile feedback presents certain information to the user, the difference between tactile information for sensory substitution and information for robotic surgery is obvious. So the existing tactile displays could be classified based on the nature of information they can present to the user. These classifications are of two main types – (1) Tactile display for realistic tactile information (TD-RTI) and (2) tactile display for coded tactile information (TD-CTI) (See Fig. 2-14 . In TD-RTI the tactile information like pressure, temperature, roughness, depth, are communicated proportionally via the feedback from the tactile display, which means that with the tactile feedback, a known tactile information can be sent or received. Example is the case of robot-assisted surgery where the force for instance is proportional to the vibration (tactile feedback) on the surgeon's hand which assists the surgeon to carry out accurate surgery.

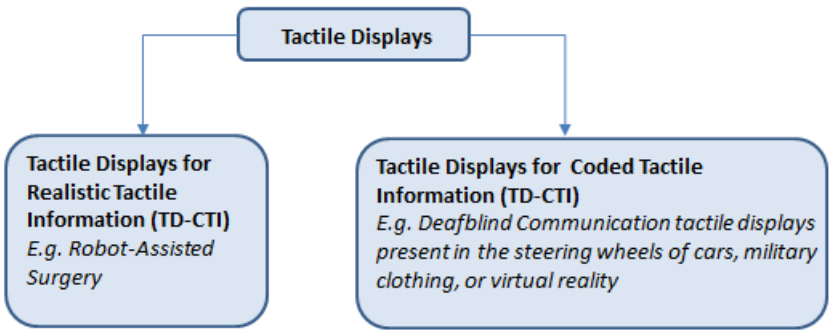

Fig. 2-14 Basic classification of tactile displays

TD-CTI on the other hand is a case where tactile feedback is coded to pass across certain information – either by mimicking already existing methodology or creating a whole new way of coding the information. An example of this is the communication by deafblind people

(see Section 2.1), as well as tactile displays present in the steering wheels of cars, military clothing, even in robot manipulation or virtual reality. The main purpose in this case is to present certain information in a coded form and hence proportionality is not a key factor.

Popularly, the available tactile displays are only able to display tactile information without inherent sense of touch. These existing tactile displays include the ones in which users explore the surface of objects like in Braille displays, or in cases where the actuator is positioned on the palm to exert localised stimulation like vibration – e.g. Lorm glove, DB-Hand, Finger Braille etc. (see Section 2.1).

The following sections present the principle, technologies as well as merits and demerits of existing actuators used in tactile displays.

2.5.1 Electromagnetic

Electromagnetic actuators function by converting magnetic energy into mechanical energy. This often occurs through the interaction of the magnetic field produced by a current carrying coil with a permanent magnet and/or a ferromagnetic material. This interaction produces either a repulsive or attractive force on a membrane or plunger thereby actuating it. Fig. 2-13 shows the different classification of the actuators which depends on how the actuators are actuated. Membrane actuated means an underlying membrane is moved when actuation occurs whereas non-membrane actuated means that a plunger moves through a give hole when actuation occurs. See Fig. 2-16 for the basic arrangement representing each type.

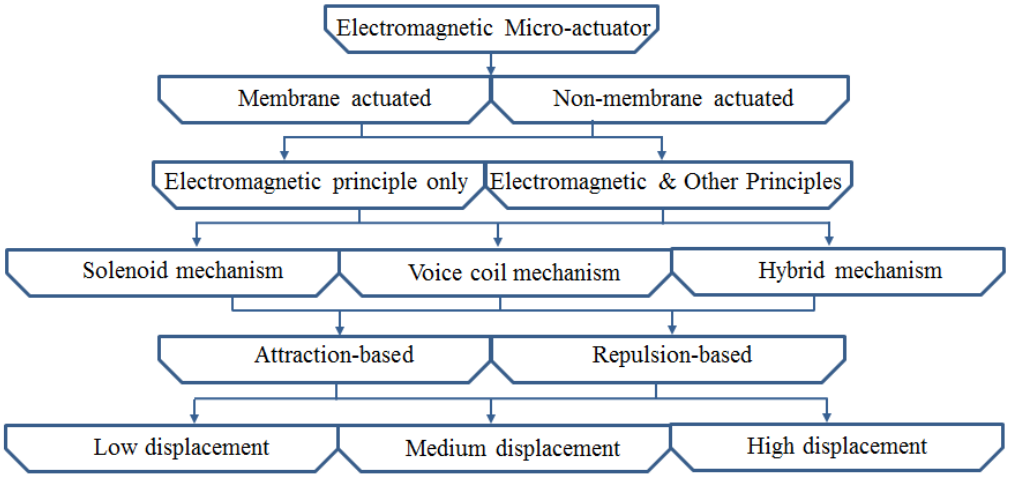

Fig. 2-15 Classification of Electromagnetic Actuators

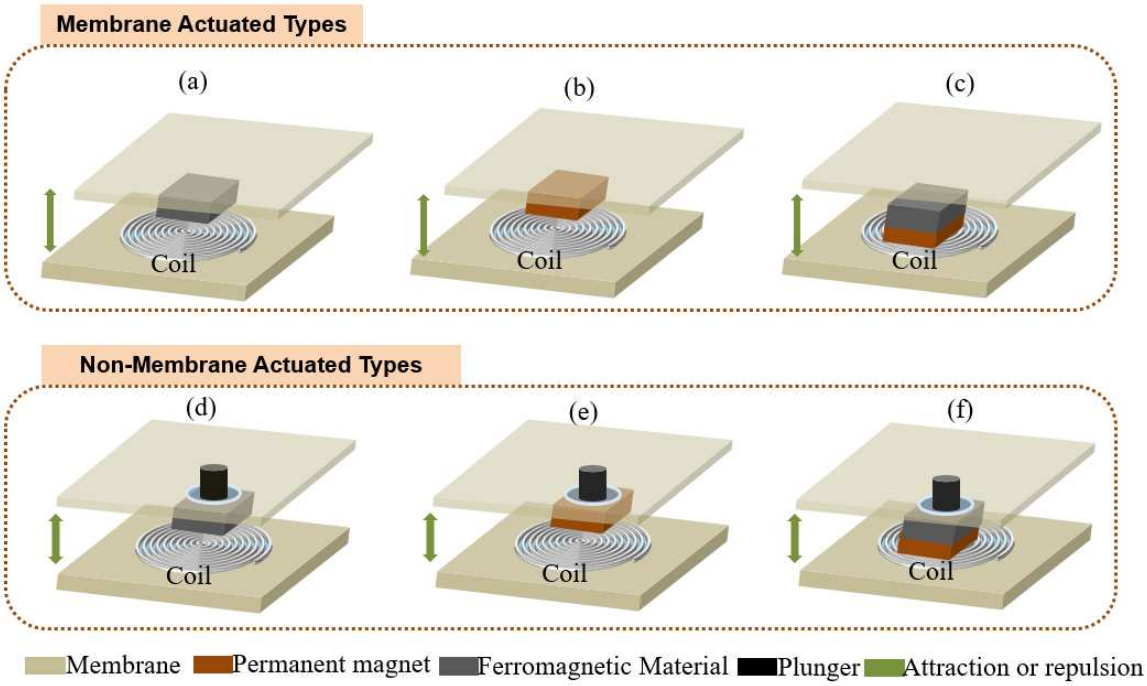

Fig. 2-16 Types of Electromagnetic Actuators (a)- (c) Membrae actuated types (d) – (e) Non-membrane acuated types

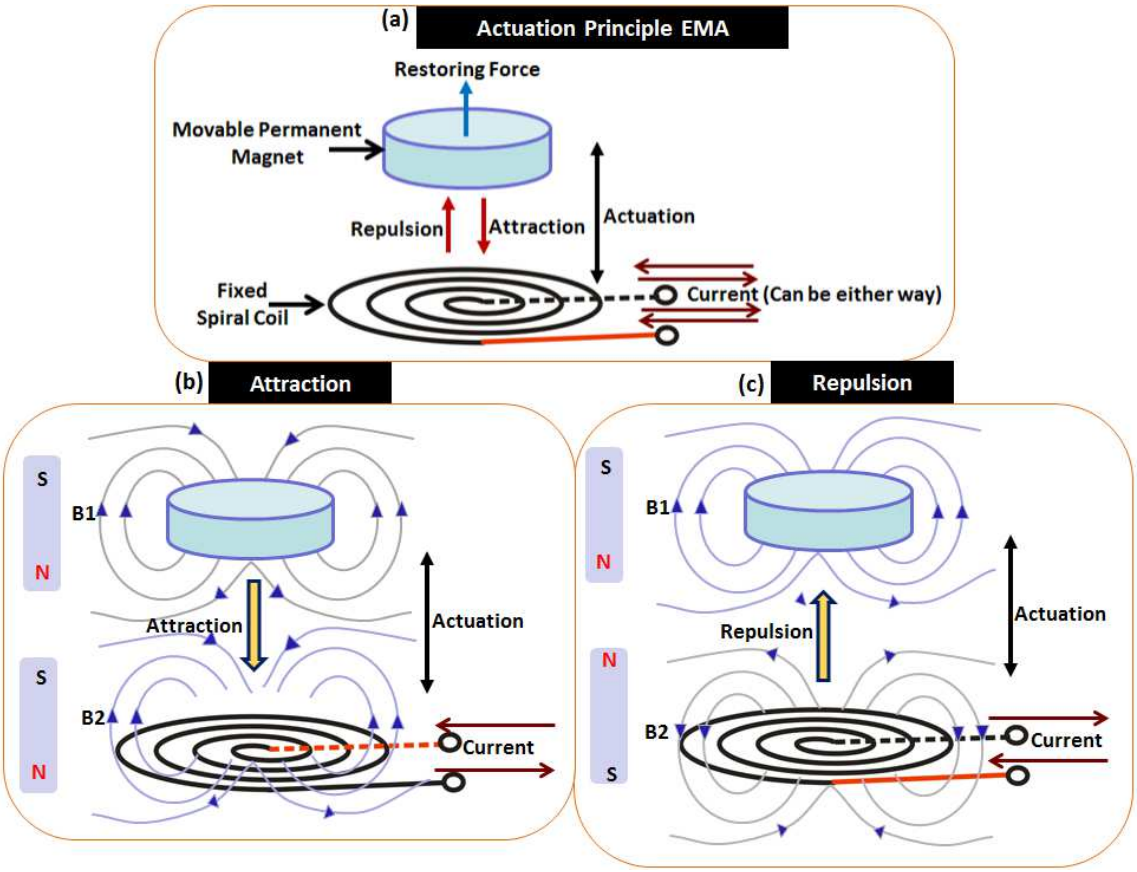

Fig. 2-17 Principle of Electromagnetic Feedback Acutators (a)Electronic principle for electromagnetic actuators (b) Attraction mechanism for electromagnetic actuators (c) Repulsion mechanism for electromagnetic actuators

Fig. 2-17 shows the principle of the electromagnetic feedback actuators. It describes two main principle. The actuation type and the repulsion type. With the coil as a reference for instance, repulsion means that the magnet moves away from the coil when actuated and vice versa for attraction type. This occurs depending on the direction of the current supplied through the spiral coil.

Principally, electromagnetic actuation occurs by means of two main circuits - the electrical circuit which establishes the current and voltages (2) the magnetic circuit which establishes the magnetic field strength and flux. The current I produces the controllable magnetic field $\vec{H}$, while the magnetic field produces the magnetic flux ø and magnetic flux density $\vec{B}$. The magnetic flux B and magnetic field are related as shown in Equation 2-8.

$$\vec{B} = \mu_r \mu_o \vec{H} \tag{2-8}$$

Where μ_r = relative permeability of the material, , μ_o= permeability of vacuum or magnetic constant =$4\pi \times 10^{-7} H$.

Electromagnetic actuators are governed by three main fundamental laws: Lorentz law, Faraday's law, and Biot-Savart law [121].

Lorentz law states that a current I flowing through a conductor of length $\vec{L}$ in the presence of a magnetic flux density $\vec{B}$ produces a force $\vec{F}$ given by Equation 2-9 & 2-10.

$$\vec{F} = I\vec{L} \times \vec{B} \tag{2-9}$$

and if orthogonal, $F = BIL$ (2-10)

Faraday's law states that the voltage in a closed circuit is equal to the time rate of change of the magnetic flux through the circuit. Mathematically

$$v = -\frac{d\emptyset}{dt} \tag{2-11}$$

Biot Savart law (See details in Appendix 5) describes the relationship between current and non-uniform fields, and for uniform fields **Ampere's law** is considered. It can be used to express the magnetic field along the axis of a circular current loop of radius r and steady current I as in [122-125].

In literature, different electromagnetic actuators (including flexible and rigid types) have been developed for tactile display (including array and single element types). In [72], a 4x4 actuator was developed using Polydimethyl Siloxane (PDMS) and electromagnetic interaction of a coil and permanent magnet. It has a resolution of 2mm and the coil is surrounded by a permalloy core and a neodymium permanent magnet that sits above the coil. The power consumption of the actuator was found to be 100mW and its displacement could reach 50µm for a typical 800mA RMS driving current. The actuator worked quite well but the coil was manually fixed during the fabrication process. This could be improved by electroplating the coil and embedding it in the structure. This actuator was further redesigned in [126] with an SmCo micro magnet and a miniature coil to realise an actuator that could be used both in pulse mode and continuous mode with ability to give a displacement of 54 µm for continuous actuation and 80/150µm at 4A pulse actuation. However, this current is quite high for a typical low-current application.

In [127], a 4 x 4 actuator array for vibrotactile stimulation of the human fingertip using a polysilicon cantilever beam was proposed. However, the complete integrated actuator was not fabricated and characterised. The interaction of the attractive forces between periodically arranged magnetic elements in PDMS were proposed in [128] as a means of actuating a cantilever beam structure. Only a large working prototype was developed with this, although the author stated that it will also work well when miniaturized. A single element electromagnetic actuator with planar coil embedded in PDMS was also described in [129]. Here two different structures for embedding the coil were described. One is the fully-embedded coil structure and the other one is the partially-embedded coil structure. This actuator was primarily purposed for pumping applications and it was experimentally shown that the deflection can get up to 55µm.

Furthermore, a polymer-based actuator with magnetic particles embedded in PDMS was presented in [130]. Two different membrane designs were fabricated and characterised - the flat membrane and the embossed membrane. A laser displacement meter was used to test the deformation of the membranes, and this showed that the flat membrane had the highest deflection of 9.16 µm against the embossed that has 8.14 µm under a magnetic flux density of 0.98T. Magnetic pieces made of electroplated permalloy ($Ni_{80}Fe_{20}$) was embedded in flexible membrane of silicone elastomer and was utilised in the fabrication of a high-displacement actuator in [131]. The actuation is based on the torque generated by an external magnetic field and the magnetic particles – this led to the deflection of a PDMS membrane.

The displacement was shown to be >80 µm with $2.85x10^5$A/m. In [132], an electromagnetic actuator with a PDMS diaphragm, small magnet and copper coil was fabricated and characterised. The result shows a diaphragm displacement of 150µm with a current of 0.6A.

In [133], multilayer integration approach was used to realise a vibrotactile display which is made of an 8 x 8 electromagnetic actuator with pin array. Each pin is 2mm in diameter and 5mm space between them. Neodymium permanent magnet of 2mm diameter and 4mm height was used. Each of the pin's amplitude and frequency is controlled independently making it easy to display various haptic patterns. Maximum static force delivered by each actuator is 13mN the coils are 7.5mm high, 3.8mm in external diameter, and 2.6mm in internal diameter. In this case the maximum applied current should not exceed 0.5A and the microactuator has a maximum pin deflection of ±100micrometer. The display can operate at frequencies of up to 800Hz with first resonance frequency of 270Hz. Power dissipation is approximately 64mW. However, the actuator is not flexible.

In [134], micro-machined polymer magnets were used to fabricate an integrated magnetic micro actuator. The polymer magnets consist of strontium ferrite powder embedded in an epoxy matrix and are 4mm in diameter and 90µm in thickness. Static characteristics yielded 17µm deflection at 100mA and for dynamic characteristic a current of 20mA yielded a deflection of 0.3mm at fundamental resonance frequency. In[135], an actuator based on parylene was presented. Two special types of diaphragms were tested- the flat and corrugated. The deflection of the diaphragm is based on the interaction between a spiral coil and a permanent magnet and was measured to be 20 µm for flat diaphragm and 30 µm for the corrugated one using an input current of 100mA at 1Hz.

In [136], a tactile display was proposed using a micro resonator that is driven with a magnetic force in order to vibrate pins. It contains a 3 x 3mm matrix of micro resonators. A fixed beam type (the gimbal tip type) was tested with a one-turn coil and gave a displacement of 2nm at 70Hz and 65mA current. The actuator is particularly suited for micro valves, micro-pumps, and micro-syringes. More recently, an electromagnetic actuator for tactile display was presented in [137], it uses 3 layer stators and is able to give a stroke of 1mm.

2.5.2 Electroactive Polymers (EAP)

Electro active polymers (EAP) are materials that exhibit a change in shape or size when subjected to electrical stimulation [138, 139]. They are classified based on the actuation mechanism used – (1) Electronic EAPs which are driven by electric field or Coulombs

forces) and (2) Ionic EAPs which change shape as a result of the mobility or diffusion of ions and their conjugated substances [139].

Electronic EAPs include piezoelectric, electrostatic, and dielectric EAPs, while ionic EAPs include Ionic Polymer Metal Composites (IPMCs), conducting polymers, ionic polymer gels and carbon nanotubes (CNT) [140]. Electronic EAPs require high activation fields typically above 150V/µm but produce high actuation forces and rapid response time. In contrast, ionic EAPs requires lower voltages of around 1 – 5V but produce very low actuation force, larger response time and must be operated in wet state or in solid electrolytes.

Researchers have previously developed EAP-based actuators for assistive purposes, including Braille displays. The most popular uses piezoelectric polymers and IPMC for Electronic EAPs and ionic EAPs respectively. The latter involves an active polymer sandwiched between two electrodes, and deformation of the layer occurs through ionic exchange when an electric field is applied between these electrodes. In [141], a 5 x 5 controllable tactile bump array was presented. It comprises of a soft and thin PDMS layer realised underneath a 3 mm × 0.8 mm × 0.2 mm IPMC cantilever beams. The actuator gave a maximum moment variation of 1.6 µN m with maximum blocked forces of 0.68 mN and 0.55 mN for the bumps of masses 4.1 mg and 15.5 mg, respectively. An 8mm x 8mm IPMC membrane-shaped actuator was fabricated in [142]. It showed displacement of 14~27µm at the applied voltage ranging from 4Vp-p to 10Vp-p at 0.5Hz. However, this actuator was particularly made for application in micro pumps.

EAPs popularly find application in artificial muscles used in robotics, but gradually finding its way into tactile displays, particularly Braille. However, the greatest limitation with these novel materials is the high voltage required for the electrical stimulation (for the Electronic EAPs) and wet conditions (for the ionic EAPs). This makes it challenging for them to be applied in wearable deafblind communication devices which require (see Section 2.2.1).

2.5.3 Piezoelectric

Piezoelectric actuators achieves actuation through piezoelectric effect, which is the deformation of a material under the influence of an applied electric field [101]. This effect is described in [101, 121], and materials (EAP and electro-active ceramics) with this property have been used for actuator designs. A piezoelectric actuator with only one active piezoelectric layer is a unimorph whereas those with multi-layers are bimorphs (consists of two active layers which deforms when activated) [101].

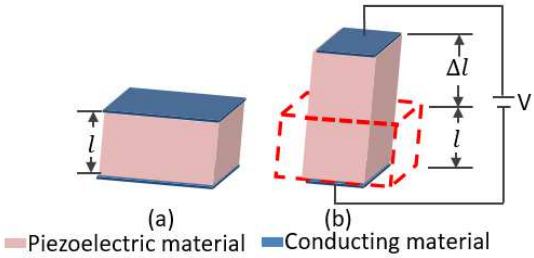

Fig. 2-18 The Piezoelectric effect

In [143], a 6 x 5 pin array tactile display with each pin 1.8mm apart and actuated by 30 piezoelectric bimorphs was presented. The displacement achievable ranges from 0 - 0.7mm. A tactile display that presents sensation via a vibratory pin array driven by a piezoelectric actuator was presented in [144]. It includes 5 x 10 contact piano-wires which is 0.5 mm in diameter and aligned in a 2 mm pitch and a vibration of 250Hz and is able to produce a displacement of about 5µm to 57µm. The design has some limitations such as large voltage of 250V and limited bandwidth due to fixed operating frequency.

A tactile graphic display was presented in [145]. This display is made up of 48 piezoelectric actuators assembled in a movable tactile output unit. It has an active area of 43mm x 16mm and has 12 x 6 active taxels with 3.21mm between taxels in the x-direction and 2.45mm in the y-direction. The possible vertical taxel movement is 0.7mm. It can receive data from camera system and computer with a maximum refresh rate of 20 Hz. Its limitation includes low bandwidth and large control voltage of 200 V. Furthermore the design and fabrication of a cantilever-based piezoelectric actuator was presented in [146]. It was fabricated using Polyvinylidene fluoride (PVDF) with an electroplated layer of nickel-Iron (permalloy) alloy. The actuator achieved a deflection of 35 – 160 µm for applied voltage from 60 - 180V. One of the limitations is the high supply voltage of 60-180V.

2.5.4 Electrostatic

Researchers have also developed actuators based on electrostatic principles. Electrostatic actuators are based on Coulomb's law which gives the Coulomb force in the electric field between two charged parallel plates – this force is given in [101, 121, 147]. Additionally, a number of electrostatic actuators use capacitive principle by exploring the energy stored in the capacitor as given in [121]. Different materials including EAP have been used.

In electrostatic stimulation, the mechanoreceptors are stimulated by applying high voltage between electrodes and ground and when touched, it produces an electric field which causes an electrostatic force [148]. The first investigation of the use of array of electrostatics

actuators for the stimulation of the finger with textural effect produced by an electrostatic stimulator was demonstrated in [149]. The array consists of small electrodes with a diameter of about 1.778mm and 2.54mm centre-to-centre spacing and could be used for Braille display. In [150], a multiply arrayed tactile display device with Dielectric Elastomer Actuator (DEA) was presented. By applying voltage from 0 to 7kV, a displacement of 340µm was observed. The displacement was found to decrease as the frequency increases and for 3 – 10Hz the displacement was about 240 - 120µm correspondingly. Force measurements shows that the device was able to give force of 40mN to the hand.

An electrostatic comb drive was designed in [151]. This actuator is usable in applications that require 150µm displacement at an operating voltage less than 150V. Two designs that relatively differ from conventional comb drives were presented. One design has half the comb and half the suspension with the folded suspension outside the combs which increases stiffness. The second design a bent comb which is meant to delay the onset of electrostatic instability. Although the operating voltage is lower that 150V, it is still very large for low voltage applications. A 7 x 7 electrostatic haptic display was designed in [148]. When touched, the electrostatic forces between the finger skin and the electrodes cause friction and vibration. It has two columns with two-column spacing and the result shows that it can be resolved with 80% accuracy on the small array for a spatial resolution of 5.8mm.

An electrostatic actuator was also presented in [152]. This actuator was designed for large deflection and is based on periodically repeated electrostatic force. It has a 2mm cantilever-based structure with elementary actuator cells and a half-elementary actuator cell with 200nm electrode separation. The elementary actuator cell transforms the electrostatic forces into lateral mechanical forces, which leads to bending of the cantilever. The actuator displacement reached up to 272nm with applied voltage of 45V.

However, the draw backs of electrostatic actuators include limited spatial resolution[153] and the fact that it works well only when the finger is dry [148, 154].

2.5.5 Shape memory alloys (SMA)

Shape memory allows is a group of metallic alloys capable of memorising its original shape and is able to return to this shape when heated [155]. SMAs may be found in two different phases (austenite and martensite) – the austenite structure is stable at high temperature, while the martensite structure is stable at lower temperatures and has two crystalline structures(twinned and detwined martensite) [155-157] (See Fig. 2-19). SMA transforms

from martensite to austenite when heated, and this transformation starts at austenite start-temperature and completes at austenite finish- temperature. During cooling, the transformation will start reverting to martensite, and this starts at martensite start temperature and completes at martensite end temperature [157, 158]. Over the years, researchers have taken advantage of this transformation known as shape memory effect (SME) to design force and displacement actuators.

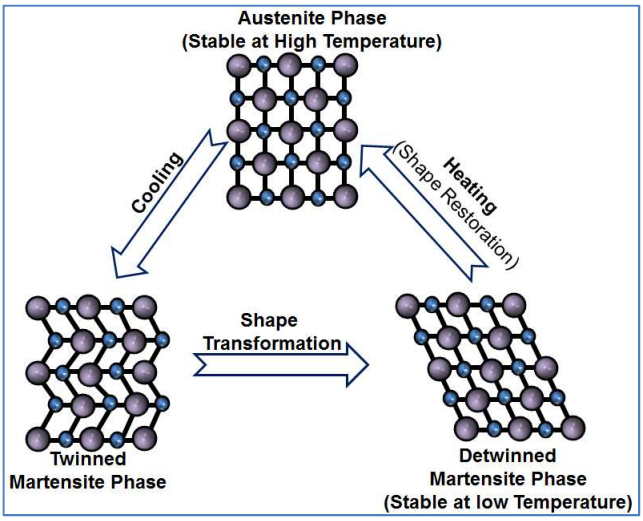

Fig. 2-19 Principle of the Shape memory alloys

In [158], a 10 x 10 tactile display with each pin 2.5mm apart based on shape memory alloy was presented. Each pin has a magnetic tube attached to it and a permanent magnet inside it accurately moves the pins up and down. Actuation is achieved through a shape memory alloy coil which contracts when heated by an applied current of about 120mA for 0.3s. The pins move with a force of 0.1N which produces a displacement of 2mm, thus displaying characters and graphics accordingly.

In [159], the design of a tactile display based on SMA for shape recognition was presented. It has 10 pins which are each 2mm apart and actuated with an SMA wire and has a water cooling system that enables it to achieve a bandwidth of 40Hz. A larger array with sixty-four elements were used to realise a tactile display in [160]. It has a group of eight tactel module interconnected together in a box with each element comprising of a 120 mm length, 0.004 in. diameter with a Nickel Titanium (NiTi) SMA wire crimped to a pin at one end and a fixed connector at the other. Resistive feedback was used to control the height of each tactel, within a PWM and tactel scanning technique using a 12V supply voltage and a maximum of 3.2mm was observed. The authors acknowledged that the display cannot be used in high bandwidth applications. In [161], an 8 x 8 SMA tactile display device with a

2.6 mm spatial resolution and 1 mm vertical displacement. Information is displayed by means of thermally driven actuation of the SMA springs which are triggered once heated. A test with the subjects shows they are able to recognise most of the shapes presented to them on the device. However, the device is not wearable.

2.5.6 Pneumatic

Actuators based on pneumatic principle have also been developed. Actuation is generally achieved by pressures through pneumatic valves. Previous works carried out in this area is presented here and a summary of the advantages and disadvantages given at the end.

In [162], a Braille-base tactile display using a 2 × 3 pneumatic microbubble actuator array made up of a pneumatic actuator layer, a fluidic manifold and valves was presented. The microbubbles represent the six dots of a Braille cell and a combination of the bubbles is actuated to represent Braille characters. The actuator was able to generate a force of 66mN with an applied pressure of 100kPa and a displacement of 0.56mm at a frequency of 0.2Hz. A 5 x 5 pneumatic actuator that uses solenoid valves to control air pressure in a cylinder was presented in [163]. Each element of the array has a cylinder with a movable piston of 800µm diameter and maximum displacement of 3mm. The air pressure in the cylinder amounts to 75psi and is capable of giving a force of 340mN per piston and the solenoid is driven by a 12V square wave. An aluminium-based 4 × 4 pneumatic tactile feedback array with element spacing of 1.75mm was designed in [164]. It measures 15mm x 15mm x10mm and is made up of aluminium array and a movable stainless steel pin within a micro-cylinder of 2.75mm diameter and a pneumatic inflow at the rear of the pins produces the actuation force.

A wearable pneumatic tactile display with air jet nozzle was presented in [165]. The phase of the air jet from each nozzle is controlled by sixteen on-off valves supplied with the compressed air pressure of 0.4 MPa and its frequency response is below 10Hz. In [166], a 5 x 5 pneumatic tactile display for teletaction using silicone rubber was presented. The tactors are spaced by 2.5mm and are each 1mm in diameter. The tactile display uses a pressurized chamber as stimuli rather than pins and has a working frequency of 5Hz. A tactile display based on suction pressure was proposed in [167]. The concept is based on the illusion that skin stimulation could be achieved by pulling the skin with air suction. Two categories of 6mm diameter holes were used – the big holes were for smooth sensation, and small holes for sharp sensation.

Examination of the reviewed pneumatic actuators shows that they have the advantage of conforming to the finger and produces large displacement. On the other hand, their limitations include cumbersomeness, very complex system including so many tubes, as well as low bandwidth.

2.5.7 Electrocutaneous (Electrotactile)

Electrocutaneous or electrotactile actuators stimulate the mechanoreceptors with electric current [168]. An electrotactile display with an array of micro-needle electrodes was presented in [168]. A unit of the display has 7 electrodes each 2mm apart and tactile stimulation is achieved by means of electric current that flows through the electrodes. Different needle diameters were tested and needles with 10, 20 and 30µm diameter were found suitable. A 2D electrotactile display that uses microneedles was also presented in [169]. It consists of a 9 x 9 array of microneedles which are 3mm apart, 600µm in length and 20µm in diameter. A test was carried out on subjects with an applied voltage of 30V for 18-22s with frequency of 50Hz. In [170], SmartTouch – a tactile display system capable of sensing and translating visual images into tactile information and display them through electrical stimulation was developed. The display consists of 4 x 4 stainless steel electrodes each 1mm in diameter with a pitch of 2.5mm and 2mm between row and column elements respectively. Stimulation of the skin is achieved with a controlled current pulse of 100 – 300V, 1-3A for 0.2ms.

Though tactile stimulation of the skin could be achieved by electrocutaneous method, it is a controversial method because current is directly applied to the skin, and subjects have reported things like numbness after a prolonged testing. So, it's not very safe and equally it's difficult to choose a current value that will suit the tolerant level of all. This means that current which is comfortable for one person may be uncomfortable for another which makes this method not a very suitable method for development of an efficient tactile display.

2.5.8 Rheological Fluids

Rheological fluids are fluids that change their rheological behaviour in the presence of an external field [171]. They are typically suspensions of particles (e.g. metals, dielectrics) in suitable non-conducting carrier liquid which are capable of transforming from a free-flowing liquid state into a semi-solid state [172, 173]. This means that in the presence of external field, the flow resistance of these fluids changes dramatically. They can be grouped into two – Magnetorheological (MR) [174] and electrorheological(ER) fluids[171]. The rheological behaviour of MR fluid changes in the presence of a magnetic field and this was first

discovered by Jacob Rabinow [175, 176], while that of ER fluid changes in the presence of an electric field. The effect of ER fluid was first reported in [177].

The change in flow resistance of MR and ER fluids is useful as an actuating force and hence these fluids have been used in many actuators for tactile display applications. A cylindrical-shaped actuator based on MR fluid with a diameter of 10mm and height of 14mm was presented in [178]. The actuator is made up of a solenoid, an elastic spring, plunger and an MR fluid. When pressed, MR fluid flows into the gap where the plunger lies and with a current applied to the solenoid, the MR fluid builds up particle chains in the gap creating a resistive force which causes a button-click sensation on the hand. It is capable of producing a stroke of up to 1mm with a maximum current of about 360mA and has a force range of about 1.5 – 5N. Device is not wearable.

In [179] the design of a 5 x 5 tactile display based on ER fluid was presented. It has a 0.47mm thick conducting rubber layer on top of a 2.5mm thick layer filled with ER fluid which is stiffened upon the application of a high voltage of 1.5kV. One of the drawbacks of this display is that the high voltage used here is a risk to the user.

A 40 x 40 Braille display based on ER fluid had also been fabricated. The actuator has an array of holes made from fabric and copper on the top and bottom of each hole to serve as electrodes [180]. MR fluid was reported to start to stiffen at voltages of about100 - 300V. In [181], a single cell tactile display based on MR fluid was presented. Two different electromagnets were used in the design with an MR fluid housed in an aluminium tray. One is a 2000-turn electromagnet with a magnet of 70mm in width and 10mm in thickness with an open area of 10 x 10mm^2. The second electromagnet is a modified 3W commercial solenoid. The display surface is a 0.24mm thick neoprene rubber. An applied current on the electromagnet creates a magnetic field which stiffens the MR fluid. Magnetic field of about 0.13T for 30s was reported to give more stiffness. Tactile information is displayed in the form of a bump on the display surface which could be felt by dragging a finger over the surface.

Rheological fluids (MR and ER fluids) actuators generally have the advantage of high frequency response but the fact that their output is linearly related to magnetic and electric fields affects the size of the actuators used as well as spatial resolution. In addition, the high currents for MR fluids due to the big solenoids and high voltage for ER fluid is also a drawback.

Table 2-7: Summary of the Characteristics of the Existing Tactile Feedback Actuators

Actuator Technology	Displacement	Current Requirements	Voltage Requirements	Operating Frequency	Response Time	Force/ Stroke
Magnetic	8.14 µm - 700 µm	8mA-30A	5V	270Hz-800Hz	2ms-50s	13mN-8N
Piezoelectric	5 µm-0.7mm	-	60V-250V	20Hz-250Hz	-	-
Pneumatic	0.5mm-3mm		12V	0.32Hz-5Hz	-	334mN-66mN
Electrostatic	120 µm-340 µm	-	45V- 7kV	3Hz-10Hz	1ms	40mN
SMA	1-3.2mm	120mA	12V	-	0.3s	0.1N
Electrocutaneous(Tactile)		1A-3A	30V-300V	-	-	-
Rheological Fluids	1mm	360mA-2.5A	100V-1.5kV	-	0.1s	1.5-5N
EAP	14 -27 µm		150V/µm (Electronic EAPs) 1-5V(Ionic EAPs)	0.5Hz		0.55-0.68mN

2.6 Summary

In this chapter, existing devices for deafblind communication was presented, including the tactile interfaces used as well as existing tactile sensing and feedback technologies. This lead to the expansion of knowledge in this area and enabled the discovery of gaps to be filled in order to develop effective solutions that will advance the state of the art. It is obvious from

the literature that majority of the existing tactile communication devices for deafblind people are rigid and based on commercially available tactile sensors and actuators. Hence, they are not wearable, conformable or customisable. Tactile communication is very important for deafblind people owing to their impaired vision and hearing modalities and hence method of communication. Again, existing tactile displays do not have inherent touch-sensing capability, and for deafblind communication there is a requirement to have both tactile sensing and feedback on same points.

Furthermore, majority of the tactile sensing arrays and actuators (tactile feedback actuators) usable as interface for deafblind assistive communication devices are based on Braille. However, Braille is used only by minority of the deafblind community and difficult to learn especially at older age. Hence, there is a need to develop tactile communication interfaces that will simplify the use of Braille as well as those that will make use of other methods of deafblind communication (e.g. deafblind manual alphabets and block letter) making sure they are wearable and flexible as presented later in this work.

Chapter 3

Tools and Methods

This Chapter presents the tools, techniques and methods used in this work. It started with a general overview of the microfabrication techniques and continued with specific techniques employed in this work. The techniques presented include Photolithography, Lithographie Galvanoformung Abformung (LIGA), electroplating – including the gold plating process and calculation of parameters. The tool(s) used for each of these techniques were described in the corresponding sections. These processes were used in the fabrication of the proposed tactile sensors as well as actuators for application in communication by deafblind people, and the chapter concluded with an overview of the methods employed in this work.

3.1 Microfabrication Tools and Techniques

In this research, different microfabrication tools and techniques were used for the fabrication of the tactile interface. Microfabrication is a process of creating devices in the micrometre scale and smaller, it has been used for over 30 years [182, 183]. Originally it was used in the fabrication of integrated circuits (IC) and the first IC was fabricated by Texas instruments in 1954 using Germanium (Ge) [184]. Miniaturisation has for the past two decades become faster in order to meet the increasing complexity of IC and lots of microfabrication techniques are currently in use.

Today, the same technology that has enabled the fabrication of ICs are now being employed in the development of microelectromechanical systems (MEMS) using lots of available alternative materials [185]. Technically, MEMS is an area of research that involves the creation of micro devices, particularly those that have moving parts, electronic circuits and sensors [186, 187]. Popularly, the MEMS acronym is universally used to represent all devices produced using microfabrication apart from ICs, owing to the diverse and a number of devices being miniaturised. Other similar names include microsystems popularly used in Europe and micromachines in Asia [185]. Example of MEMS devices includes microactuators, switches, motors, tactile sensors, temperature sensors, and PH sensors. These devices are able to sense, control and actuate at micro scales and generate macro-scale effects, and are realised using different microfabrication techniques and tools.

In addition to IC fabrication techniques (like doping, etching, dicing, and growing of films), MEMS fabrication include other unique techniques which are not direct IC fabrication techniques like bulk micromachining, surface micromachining and micromolding techniques [188, 189]. While some methods involve creating a micro-device from a bulk material, others involve the fabrication of these devices on the surface of material and any material used for this carrier-purpose is called a substrate. The variety of techniques and materials leads to a fabrication of a number of devices. Bulk micromachining is a technique that employs etching techniques to mould MEMS structures on silicon or other substrates [190-193]. Surface micromachining involves the fabrication of MEMS structures from deposited thin films. Here the substrate is primarily used for the sake of mechanical support, and after patterning it, the unwanted patterns are chemically removed leaving the wanted patterns. Apart from silicon, other materials used as substrates in the fabrication of micro devices include polyimide, glass, and polyvinyl chloride (PVC).

Micromolding technique involves the use of micromold to create microstructures and one of the most popular micromolding techniques is the LIGA process [194-197]. In this work, the LIGA process was employed and the detail of how it works is described in Section 3.1.2.

3.1.1 Photolithography

Photolithography, involves the transfer of a pattern on to a photosensitive polymer called photoresist by exposing the photoresist to a light source via an optical mask [198]. The mask is usually a glass patterned with Chrome or Iron oxide that allows light to pass through specific defined areas and opaque on the other areas. Photoresist is often applied on the substrate through spin-coating at a controlled speed and time. So through photolithography, the spin-coated photoresist is patterned using the mask by exposing it to light. The exposed photoresist is then developed by appropriate chemical developer to reveal the patterns. The pattern in the photoresist is then further transferred to the underlying substrate by subtractive (etching) or additive (deposition) techniques.

Additive processes like thin film growth or deposition enables materials of interest to be grown or deposited on specific areas respectively, as defined by the patterned photoresist. Two most common thin-film deposition methods are chemical vapour deposition (CVD) and physical vapour deposition (PVD) such as sputtering or evaporation. Another method of deposition employed in microfabrication is electroplating, which is usually used in cases where very thick films are required and was used in this research work.

Etching /lift-off is a subtractive method that involves the removal of unwanted materials from a substrate. Lift-off is carried out using wet chemicals and usually involves removing the unwanted materials deposited on top of an underlying patterned photoresist. Etching which also involves removal of unwanted areas of material could be achieved using two methods- dry etch and wet etch. Dry etch is carried out through gas-phase chemistry unlike wet etch which involves the use of wet chemicals to remove the material.

Photolithography was chosen in this thesis for the fabrication of the tactile sensors and actuators coils. In this thesis, all the photolithography carried out was done using Suss Microtec Mask Aligner 6 (MA6) with a 350 W mercury lamp and the photoresist used was the AZ4562 and an adhesion promoter called hexamethyldisilazane (HMDS).

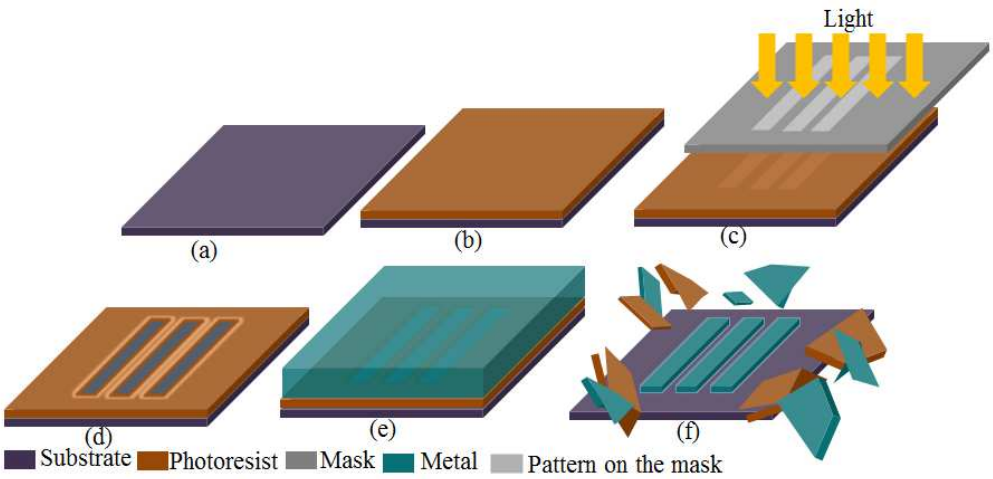

Fig. 3-1 Basic steps of photolithography: (a) substrate preparation (b) spinning of photoresist (c) patterning of photoresist using light (d)development of patterned photoresist (e) deposition of metal (f) Photoresist lift-off

3.1.2 Electron Beam Evaporation (EBE)

Electron Beam Evaporation is a physical vapour deposition technique in which a metal kept inside a crucible is evaporated to coat a substrate with thin layer of the metal, all in a vacuum chamber (typically $<10^{-7}$mBar). In this process, the desired metal in the crucible is bombarded with an electron beam from a heated tungsten filament. The metal melts and undergoes evaporation, and then the evaporated metal moves to coat the attached substrate with the chosen thickness. EBE is a line of sight process; hence, the substrate is tilted during the process to ensure proper deposition of the evaporated metal on the horizontal and vertical sidewalls.

In this thesis, the EBE was carried out using Plassys MEB 550S system. Plassys MEB 550S - it has eight crucibles, main chamber and cryo-pumped load lock, 10kW electron beam source, ability to tilt substrates, fully controlled by computer and can process samples of up to 150mm in addition to onscreen thickness monitor. During this research, the metals evaporated using the MEB 550s include Au, Ti, and Nichrome.

3.1.3 LIGA Process

The acronym LIGA is a German word that stands for lithography (lithographie), electrodeposition (galvanoformung), and molding (abformung) [199]. LIGA is one of the processes used in this work for the fabrication of spiral coils. LIGA process is a micro molding process that enables the creation of micro structures with high aspect ratio. Lithography involves the use of a light source to pattern a photoresist which is now plated and molded to create the desired structure. There are two types of LIGA process depending on the source of light used for the lithography. These are ultraviolet (UV) LIGA where the source of light for photolithography is UV light and X-ray LIGA which involves the use of X-ray to pattern an X-ray sensitive photoresist. UV-LIGA which was employed in this work is generally easier and cheaper that X-ray LIGA.

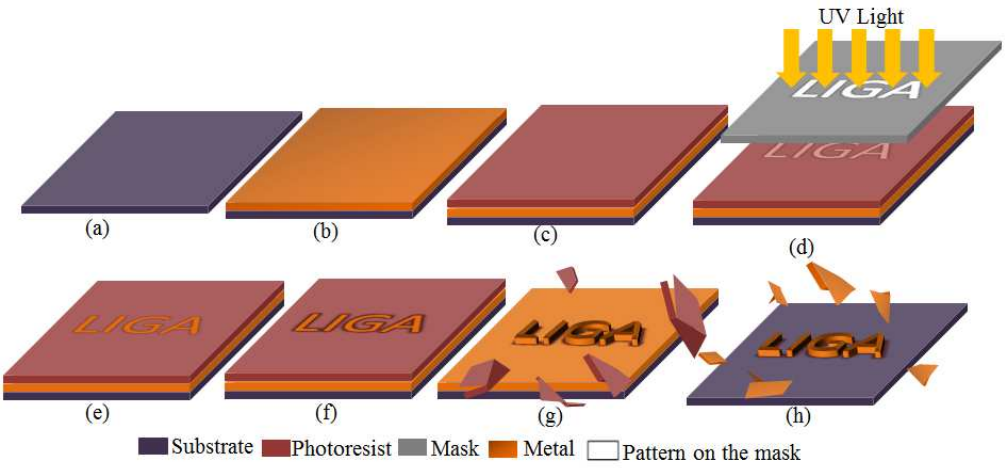

Fig. 3-2 Basic principle of LIGA(a) sample preparation(b) metal seed layer deposition (c) spin coating of photoresist (d) lithography (e) development of the resist (f) electroplating of the seed layer (g) removal of the resist (h) Etching of the seed layer

3.1.4 Electroplating

Electroplating is an electrodeposition process for producing a dense, uniform, and adherent coating, usually of metal or alloys, upon a surface by the act of electric current [200, 201]. It was used in this work to increase the thickness of the fabricated spiral coils. In this process, two electrodes (anode and cathode) connected to source of electricity, and an electrolyte

through which current from the electrodes passes during metal deposition (see Fig. 3-3. The metal to be plated is made the cathode while the anode can be of two types – sacrificial or permanent. Sacrificial or dissolvable anode is made of same material as the metal to be deposited while permanent or inert anode only completes the circuit. This means that unlike inert anode, the dissolvable anode is able to provide a source of fresh metal into the solution as electrodeposition progresses.

During electroplating, the electrodes are connected to a source of electricity and current flows from one electrode to another via the electrolyte. The electrolyte (usually salts of metals to be deposited) contains positively and negatively charged ions which moves as a result of the applied current. Positively charged ions in the electrolyte will move towards the cathode while negatively charged ions will move towards the anode. At the cathode which bears the workpiece, the positive metallic ions from the solution are reduced to metallic atoms thereby depositing the metal on the workpiece. So generally, oxidation and a reduction reaction takes place during electroplating; oxidation takes place at the anode while reduction takes place at the cathode.

At the cathode, the positively-charged metallic ions from the electrolytes will be reduced to metallic form by gaining electrons at the cathode thereby depositing the metallic atom on the workpiece as shown in Equation (3-1), where M is the metal while n is the number of valence electron.

At the Anode, the metallic atom are oxidised metallic ions enters into the electrolyte. This is

$$M^{n+} + ne^{-} \rightarrow M \tag{3-1}$$

particularly for dissolvable anode.

$$M \rightarrow M^{n+} + ne^{-} \tag{3-2}$$

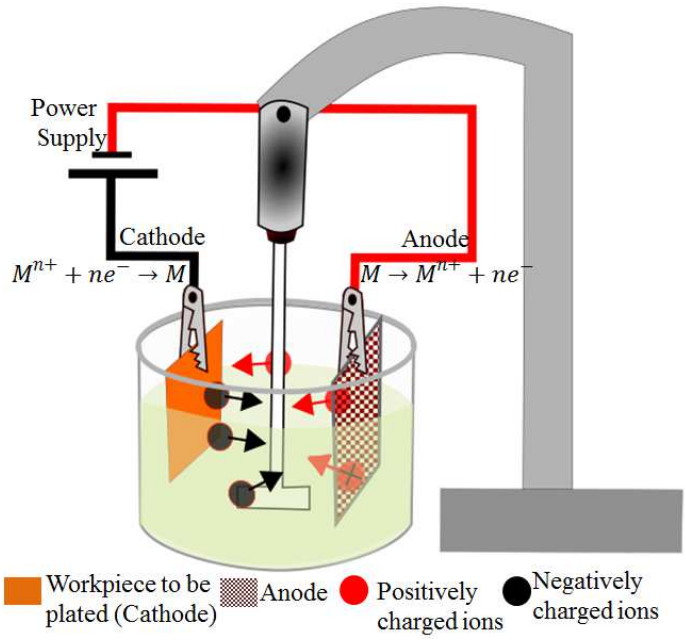

Fig. 3-3 Electroplating process

3.1.5 Calculation of electroplating parameters

Faraday's law is the basic law governing electroplating, and it states that the amount of substance liberated at the electrodes is proportional to the quantity of electricity Q that was used [201]. This means that, the number of atoms deposited is equal to the number of electrons passing through the circuit. This can be determined by measuring the amount of current passing through the circuit as shown in Fig. 3-3.

If I is constant, then

$$I = \frac{dQ}{dt} \tag{3-3}$$

$$Q = It \tag{3-5}$$

$$Q = \int I dt \tag{3-4}$$

$$\text{Number of Electrons} = {}^{Q}/_{e} = {}^{It}/_{e} \tag{3-6}$$

Where $e = 1.6 \times 10^{-19} C$

3.1.5.1 Calculation of Thickness of Metal Deposited

$$Volume = A \times Thickness \tag{3-7}$$

$$Volume(cm^3) = \frac{mass}{\rho} \tag{3-8}$$

Where $\rho = density\ (gcm^{-3}, A = Surface\ Area(cm^2)$

Therefore, combining equation (3-8) and (3-9)

But mass here is equivalent to weight of metal deposited. Considering Avogadro's number,

$$Thickness(cm) = \frac{mass}{A \times \rho} \tag{3-9}$$

Atomic weight of a metal contains $6.02 \times 10^{23}\ atoms$, so number of atoms in the deposited metal will be the ratio of this weight to the atomic weight of the metal multiplied by Avogadro's number.

Where W = weight of metal deposited

$$No.of\ Atoms = \frac{W}{Atomic\ Weight} \times 6.02 \times 10^{23} \tag{3-10}$$

Recall that from Faraday's law, the number of atoms deposited is equivalent to the number of electrons that passed through the circuit. So, n- number of electrons is required to deposit one atom where n is equivalent to the valency of the metal. In case of copper for instance 2 electrons are needed to deposit one atom of copper ($Cu^{2+} + 2e^- \rightarrow Cu$). Which means, n =2 and this is equivalent to the valency of copper.

So if n - number of electrons are required to deposit one atom, Then from equation (3-7) we have that

So equating Equation (3-11) and (3-12) we have

$$Number\ of\ atoms = \frac{It}{n \times e} \tag{3-11}$$

$$W = \frac{Atomic\ Weight \times I \times t}{n \times e \times 6.02 \times 10^{23}} \tag{3-12}$$

and considering that Faraday's constant F is given by $e \times 6.02 \times 10^{23}$ (96,485 $Cmol^{-1}$), then equation (3-13) can be re-written as:

$$W = \frac{Atomic\ Weight \times I \times t}{n \times F} \tag{3-13}$$

Therefore, combining Equation (3-10) and (3-15) and setting $W = mass$ (weight of metal deposited) the thickness of deposited metal becomes:

Rate of deposition is given by:

$$Thickness(cm) = \frac{Atomic\ Weight \times I \times t}{A \times \rho \times n \times F} \tag{3-14}$$

$$Rate = Thickness/t \tag{3-15}$$

And Current Density is given by

$$Current\ density, \qquad J = I/A \tag{3-16}$$

3.1.6 Gold plating

In this work, gold plating was also used in the fabrication of the spiral coil for the actuator as well as tactile sensor. Gold plating was chosen given that gold is a very valuable metal due to its characteristic softness, ductility, and density as well as corrosion resistant. It has very good electrical and thermal conductivity and its use in the electronic industry as electrical conductor is well known. Gold exists in +1 and +3 oxidation states as Au(I) and Au(III). Complexes of Au(I) are commonly used for electroplating due to the stability of Au(I). In gold plating, three main baths are commonly used – alkaline cyanide bath, the acid bath and the non-cyanide bath [201]. The bath is kept at 50-60°C during gold plating.

In cyanide baths, the most important ion being $[Au(CN)_2]^-$. The reaction at the anode and cathode for cyanide baths is as shown:

The reaction at the cathode is given by:

$$[Au(CN)_2]^- + e^- \rightarrow Au + 2CN^-$$

The reaction at the anode is given by:

$$Au + 2CN^- \rightarrow [Au(CN)_2]^- + e^-$$

In acid cyanide bath, the anode used here is often platinised titanium, or gold.

Although $[Au(CN)_2]^-$ is the most important ion in gold deposition, the stability of cyanide baths causes co-reduction of hydrogen ions as a result of negative reduction potential. This causes a reduction in plating efficiency and as a result of this the use of non-cyanide gold plating baths has become a huge interest. Commonly available non-cyanide gold complex includes gold sulfite, and gold thiosulfate. Other gold complexes include mixed sulfite and thiosulfate, thiourea, ascorbic acid, and Au (I) thiomalate bath. In gold thiosulfate bath, gold is found in the form shown in [202]:

$$Au^+ + 2S_2O_3^{2-} \rightarrow [Au(S_2O_3)_2]^{3-}$$

While in gold sulfite bath, gold is found as

$$Au^+ + 2SO_3^{2-} \rightarrow [Au(SO_3)_2]^{3-}$$

Table 3-1: Comparison of the gold plating baths

	Means of replacing ion in solution	**Merits**	**Demerits**
Alkaline cyanide	Gold anodes	90-100% current efficiency	High pH and cyanide concentration degrades photoresists. Toxic. Soft deposits that wears easily
Acid cyanide		Reliable hard gold deposit,	Compatible with photoresists and other polymers
Non-cyanide		High plating efficiency. Very compatible with photoresist. Controllable residual stress of plated gold, non-toxic	Susceptible to disproportionation

Chapter 4

4 Proof-of-Concept (POC)

This chapter presents the Proof-of-concept (POC) phase, and in it, three major tasks were accomplished (1) a generic two-way communication system was designed for assistive communication devices usable by deafblind people. (2) A prototype communication glove for user of the British deafblind manual alphabet was developed using this system (3) A Finger Braille glove for Braille users was also developed. The overall aim of the POC is to use commercially available components to develop some tactile interfaces for communication by deafblind people. This was done to understand their strengths and weaknesses as well as try the proposed two-way communication system and simultaneously show the application of tactile communication interface for deafblind people. In view of these, the prototypes were developed using commercial tactile sensors and actuators by adopting two communication methods (British deafblind manual alphabet and Finger Braille) used by deafblind people as presented in Chapter 2. Hence, these prototypes are pointers to how and where the fabricated tactile sensors and actuators presented in Chapter 5 and 6 could be used.

4.1 Proposed Generic Communication System

In this section, a proposed generic communication system for deafblind people is presented. This system is for independent communication between deafblind-to-deafblind or deafblind-to-hearing and sighted person using a suitable tactile interface. Fig. 4-1 shows the basic block diagram of this system and summarises the modules and communication between deafblind-to-deafblind as well as deafblind with sighted and hearing person.

The system is made up of two main modules, (1) the interface unit, and (2) the control unit. The interface unit is made up of the input and output unit, while the control unit is made up the transmission unit and the processing unit. The input unit is used for sending information while the output unit is used for receiving information. In this work, tactile sensors were used for input while tactile feedback actuators were used for output. The transmission unit is wireless and was achieved using Bluetooth, while a microcontroller serves as the processing unit. As described earlier, commercial sensors and actuators were used for the purpose of proof of concept and the fabrication of novel custom tactile sensors and actuators as well as how they will replace the commercial types are described in subsequent chapters.

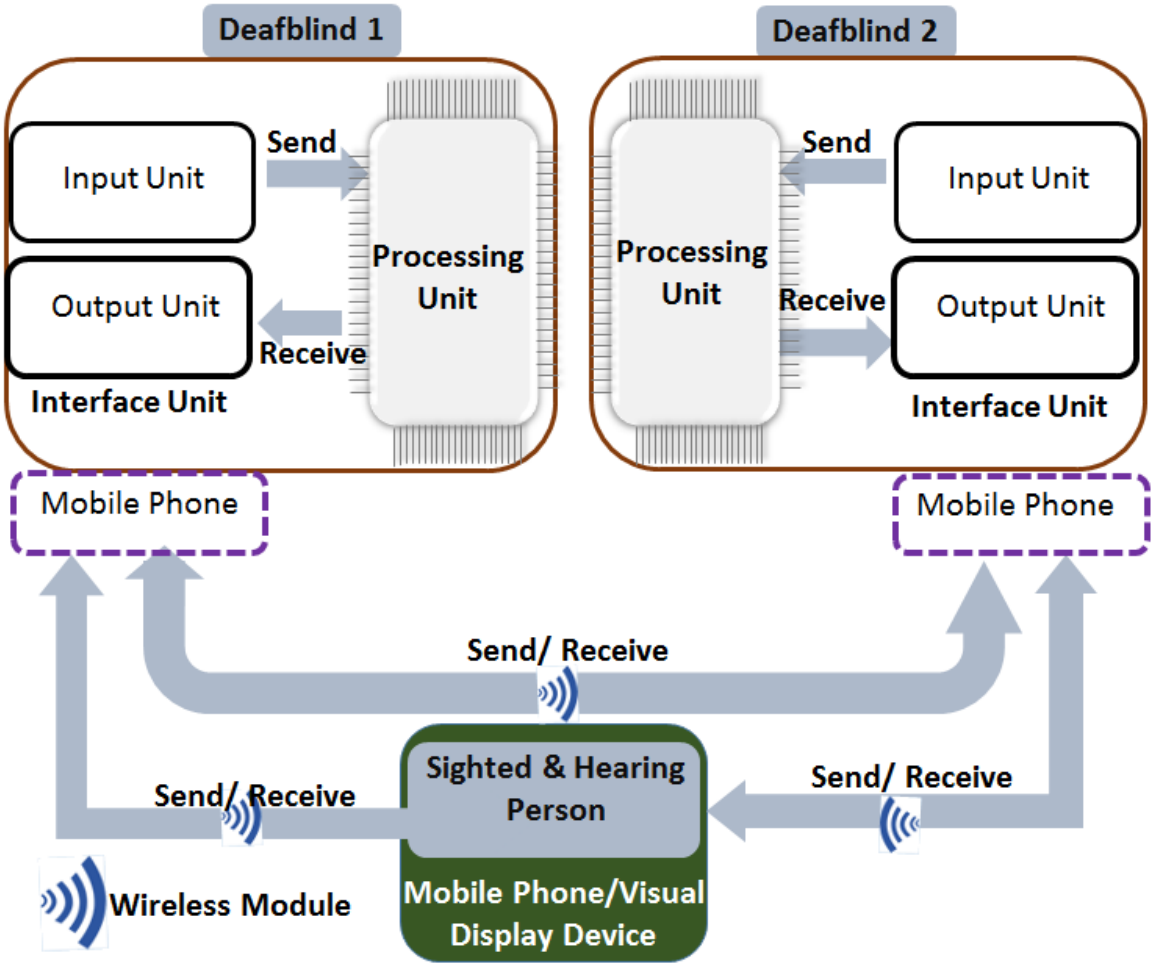

Fig. 4-1 Generic Block Diagram of Deafblind Communication System

Generally, deafblind person (deafblind 1) has two possible communication partners, one is another deafblind person (deafblind 2) or a sighted and hearing person (see Fig. 4-1). In other words, the deafblind person can communicate independently with another deafblind person or with a sighted and hearing person. Communication with the former only requires tactile interface readable and usable by deafblind people, while in the latter, the sighted and hearing person can use either a mobile phone or any other audio/visual display device to interact with them either locally or remotely.

Local (or nearby) communication means that the deafblind person can independently communicate with a nearby person. The nearby person can either use a mobile phone or a custom-made handheld device. In both cases, the deafblind person only requires a tactile communication device (a glove in this case) equipped with a usable tactile interface for deafblind people and communication with a partner will be via Bluetooth. In this case the dotted red block (mobile phone) in Fig. 4-1 plays no role.

Remote (or long distant) communication on the other hand requires the deafblind person to have a means of transmitting information to a long-distant communication partner. In this case, a mobile communication interface is required and here a mobile phone (L-mobile for local mobile) is used for the description of the system. This means that the L-mobile will only be a gateway for the deafblind person to send information to long distances. Information sent by the deafblind person is received at the remote location by a remote mobile phone (R-mobile, for remote mobile).

A well-detailed flowchart that describes the entire communication system was developed and is presented in Appendix 2. It starts from the glove (equipped with touch sensors and actuators) worn by deafblind 1 who to choose either to communicate with a remote or nearby person (another deafblind or sighted and hearing person). The glove described is equipped with a means of choosing either to communicate with a "handheld" device or a mobile phone (held by sighted and hearing person).

So, the focus is on developing a tactile communication interface that is readable and usable by deafblind people based on the existing methods of deafblind communication. For POC purpose, two different interfaces were implemented by adopting two methods of communication (British deafblind manual alphabet, and Finger Braille method – See Chapter 2) by deafblind people. The reason for this choice is user-centred and will be seen in the results of the interview of deafblind people and staff of deafblind organisations discussed in the following section.

4.2 Development of the B-DMA Glove

B-DMA glove is a communication glove for deafblind people who use the British deafblind manual alphabet as explained in Chapter 2. This section presents the work done towards the development of this glove using commercially available components as a proof of concept and is based on the generic communication system presented in the previous section.

4.2.1 Methodology

The methodology employed in the development of the B-DMA glove is as follows:

- Examination of the existing devices
- End-user consultation
- Consultation with staff of deafblind organisations
- Interview of deafblind people
- Device design and development

- Establishment of design specifications
- Design and development of the hardware and software
- Cycles of laboratory testing and modifications

4.2.2 Examination of the Existing Deafblind Communication Devices

Literature survey of the existing communication devices for deafblind people were carried so as to have understanding of the communication by deafblind people as well as technologies employed in the development of solutions for them. The details of this survey were presented in Chapter 2. The devices examined were grouped into four different deafblind communication strategies namely: American Deafblind Manual Alphabet (A-DMA), British Deafblind Manual Alphabet (B-DMA), other Deafblind Manual Alphabets (O-DMA), and Braille.

4.2.3 Consultation with Staff of Deafblind Organisations

This is a very important stage before getting in contact with the real end-users particularly in this case where the end-users are hearing and vision impaired. This consultation opened door for the recruitment of the participants and provided insight on how best to work with this important group of people. First the Sense Scotland, deafblind Scotland, and Deafblind UK were contacted via email. The email sent to them contains a brief summary of the research and a request for a meeting to hear from them about deafblind people, devices used, and their opinion about the proposed device. Deafblind Scotland and Sense Scotland responded, and a meeting were scheduled to meet with their staff in their professional capacity.

The interaction with the staff of these organisations alongside the review of existing devices, led to a tentative qualitative feature requirement drawn up prior to interview of the deafblind people. A brief meeting of the research was then discussed in one of their quarterly meetings and also advertised in their monthly newsletter which is regularly accessed by deafblind people. This led to the recruitment of 9 participants. A questionnaire was then drafted, and ethical approval obtained in readiness for the interview.

4.2.4 Interview of Deafblind People

In order to get insight on the opinion of deafblind people regarding the proposed tactile interface, interview of nine deafblind people was carried out with the help of deafblind Scotland and Sense Scotland. Prior to obtaining ethical approval for interview of deafblind people, some features of the required device were drawn up by considering the objectives of

the research, examining the existing devices and interacting with staff of two deafblind organisations. Having obtained ethical approval, 9 deafblind people were interviewed in order to gather some requirement specifications which guide the modification of the ones initially drawn up. The method used for the interview including the result, analysis, and the established design specifications will be presented in subsequent sections.

Procedure

Before the interview, the following research questions were developed and the outcome of the interview is intended to answer some or all these questions. These include:

- What are the characteristics of deafblind people and what is the history and extent of their impairment?
- How many deafblind people are using or would want to use the deafblind manual alphabet?
- What other devices are in use?
- Do they want a wearable tactile communication device based on British deafblind manual alphabet?
- Do they have access to information and tactile communication device and how? (i.e. Do they use computer and mobile phones) and for those who don't, why, and would they want to use it?
- What are the features they would like in a future tactile communication device?

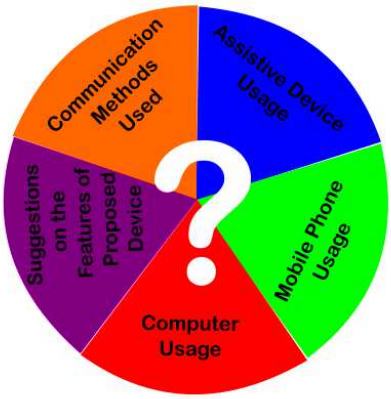

Fig. 4-2 Key focus of the questionnaire

Feedback from deafblind people is particularly important, as they are the main end-users of the proposed device to ensure that it meets their needs and preferences. Feedback from professionals, in this case staff of Deafblind Scotland and Sense UK, was obtained first via oral interviews, to provide preliminary information about some of the assistive devices used

by deafblind people, how best to work with them, before the interview of deafblind people. After obtaining the ethical approval, the questionnaire was prepared and distributed to the deafblind people with the assistance of Deafblind Scotland and Sense Scotland. I attended a quarterly meeting organised by both organisations differently. It was divided into four sections. The first section obtained data on gender, age, history of deafblindness and other demographic factors to ensure that the deafblind people surveyed covered the whole community and to see if there is any indication that requirements was influenced by demographic factors. However, this is possible with more number of participants.

The questions in the other three sections covered the following issues:

- Assistive device use: what devices, if any, were currently used, and what the respondent liked and disliked about them.
- Mobile or smart phone use: whether a phone was used and, if so, what for.
- Computer use: whether a computer was used and, if so, what for.
- British deafblind manual alphabet: current use of this alphabet and any plans to use it in the future, as well as the use of any other deafblind manual alphabets.
- Communication device to support the British deafblind manual alphabet: (i) interest in using the device; (ii) suggestions for the design, including features to include to support effective communication; (iii) whether the device should be wearable or carried in some other way; (iv) if wearable should the device be a glove, half glove or have some other form; (v) interest in time telling and other functions.

During the meeting, participants were coming to meet me one by one with their guide communicator. During the interview, questions were interpreted to the deafblind person by the guide communicator and the answer given. Some of the participants had residual hearing and could speak and listen independently. So every participant was attended to depending on their condition and effort was made to do it at their convenience.

4.2.5 Discussion

This section discusses some of the responses from those who were interview. This thesis does not claim that the result presented here is a justified representative of the majority of deafblind people. It is a guide for the establishment of the requirement specification for the work carried out. The interview analysis is based on how it was able to provide insight on

what might be the opinion of the majority of deafblind people to the research questions presented in Section.

(a) What are the characteristics of deafblind people and what is the history and extent of their impairment?

The responses of the participants from the section related to the history and degree of their impairment led to what is shown in Fig. 4-3. Regarding the profile of the people interviewd, those with no vision were more than those with low vision where as in terms of hearing impairment, those with no hearing were smaller than those with partial hearing. This means that any device being developed has to place no visual demand on the user and probably a little audio feature could be added. This means that the major focus in terms of user interaction with the device would be tactile. However, this is for only a small group in Scotland.

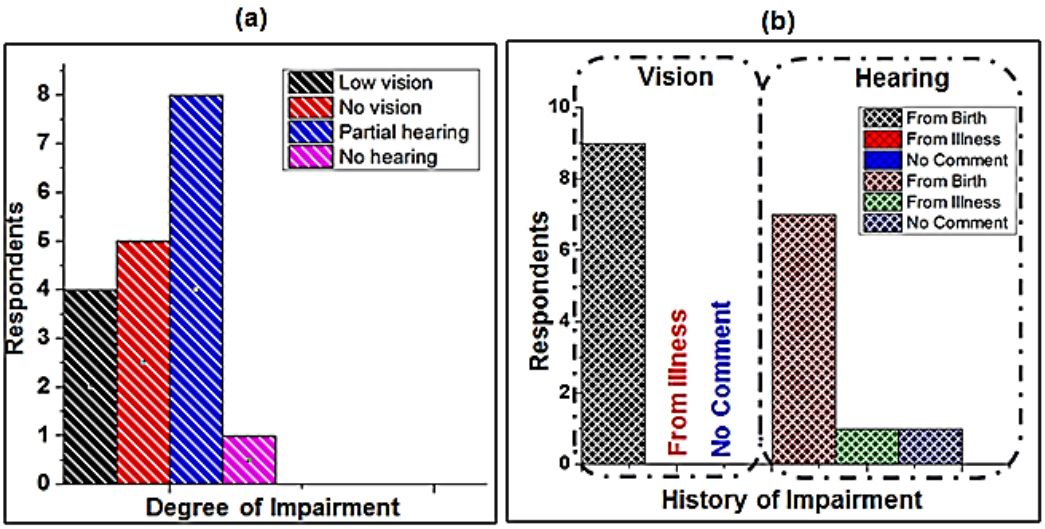

Fig. 4-3 (a) Degree of impairment (b) History of impairment: Analysis of participants' degree and history of impairment

(b) How many deafblind people are using or would want to use the deafblind manual alphabet?

Fig. 4-4 (a) shows that even though majority of the participants are not currently using the British deafblind manual alphabet as their main method of communication, majority are willing to use it in the future. Why some have heard about this method of communication before the interview and used at some point in their life, others have not. After explaining what this communication strategy is and how the proposed device would make it easier; majority agreed that they would be happy to use it in the future.

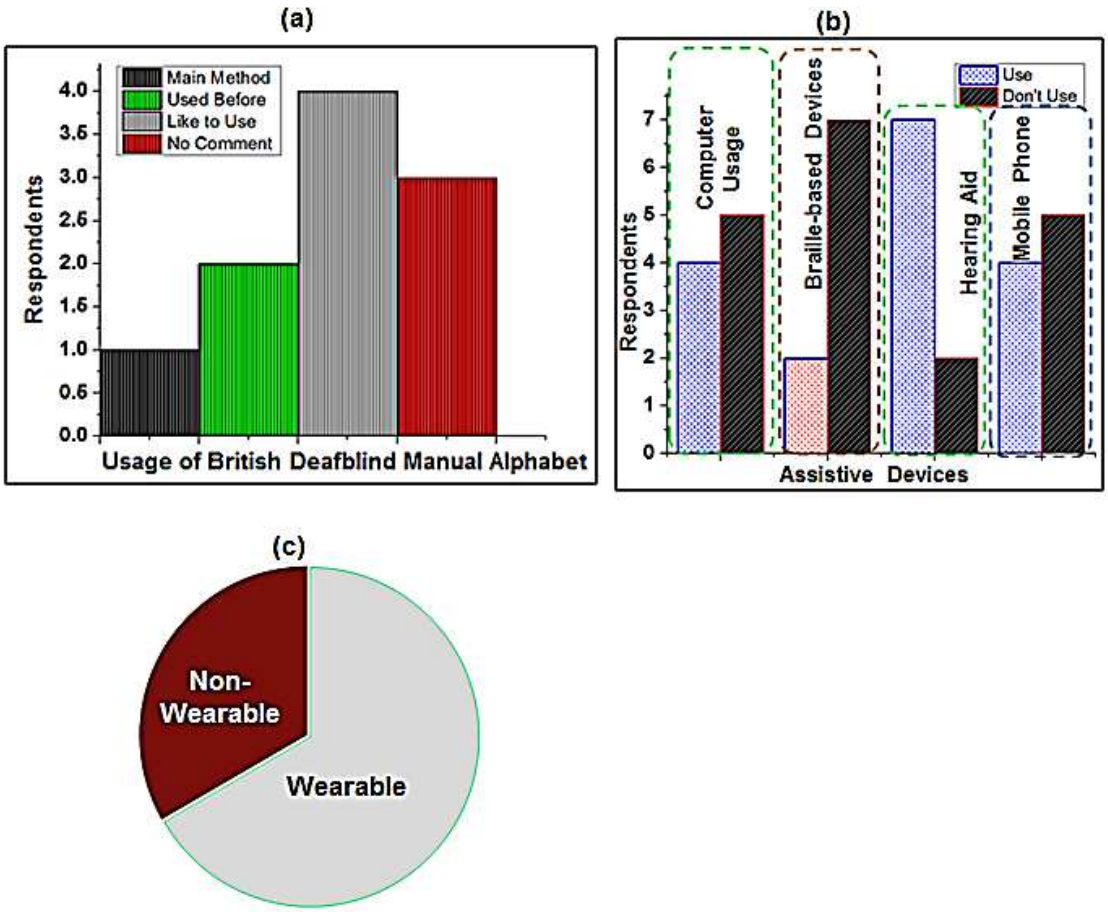

Fig. 4-4 (a) Analysis of the participants' use of Deafblind (DB) Manual alphabet (b) Usage of Assistive Devices (c) Desirability for wearable devices

(c) What other devices are in use?

Majority of the participants use hearing aid as shown in Fig. 4-4(b), and this is obvious from the fact that majority of them have partial hearing as discussed in section 6(a). Participants who use computer and mobile phones were seen to be the same. So, developing a device which would make the usage of computer and mobile phone more exciting will not only encourage those who have not used it before, but would make it more exciting for those who are already using it. From the few that were interviewed, majority were using or are interested in using a Braille-based device due to a common notion of difficulty in learning Braille.

(d) Do they want a wearable device that is based on British deafblind manual alphabet?

Fig. 4-4(c), shows that majority of the participants are interested in a wearable device. While some wanted a communication glove, others wanted a half glove due to breathability.

They equally suggested some other features for a future assistive tactile communication device. These include: Ability to give train and bus times, maps, social networking ability,

fashionable look, tactile buttons that are easy to distinguish, large screen texts that displays what the caller said and ability for user to call back with text, Braille watch, talking alarm, water proof, low cost, two-way communication, and speaking walking stick. While these are relevant features that would improve the life of deafblind people, not all can easily be implemented in one device. However, giving them access to computer and/or mobile phone through the proposed device would make it easy for them to enjoy most of the suggested feature. Hence, focus was now directed to developing a glove capable of making it possible for deafblind people who use deafblind manual alphabets/Braille to communicate face-to-face and remotely.

4.2.6 How the interview informed the design

Although the number of the participants interviewed are not statistically significant, the interview gave an insight on what they might require. Table 4-5 shows the features of the B-DMA glove, before and after the interview. Requirement before the interview were formed after examining the existing devices and having an initial meeting with the staff of Sense Scotland and Deafblind Scotland. Their opinion was based on their experience in working with this group of people.

Table 4-1: Requirement specification before and after the interview

Feature	Requirement Specification before interview	Requirement Specification after interview
Wearability	Wearable	Wearable
Input/Output Options	Deafblind manual alphabet & Braille input	Deafblind Manual Alphabet input only
Communication Distance	Face-to-Face and Remote	Face-to-Face and Remote
Access to other Bluetooth Devices?	Yes. Via Bluetooth	Yes. Via Bluetooth
Real time Clock?	Yes	No

4.3 Design of the B-DMA Glove

Fig. 4-5 (a) – (c) shows the concept of the B-DMA communication using the proposed device. It shows how deafblind people communicate without the glove as well as their communication using the glove. The deafblind person wears a glove having array of the

tactile sensor and actuator and signs on it to communicate with a sighted and hearing person who is using a custom-made QWERTY handheld device via Bluetooth.

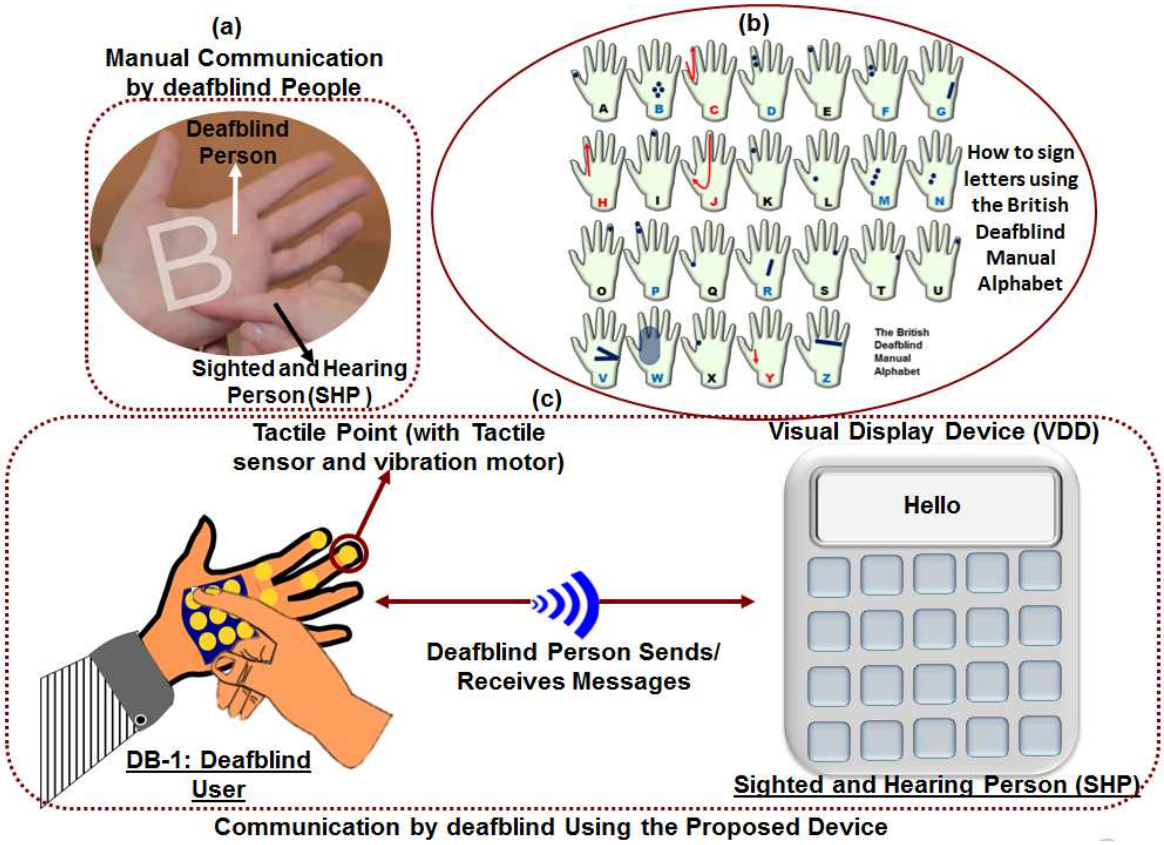

Fig. 4-5 (a) Communicatin by deafblind people without any device (b) How to sign different letters of the British deafblind manual alphabet (c) Communication concept of the B-DMA.

This prototype involves two main modules, a glove to be worn by the deafblind person and the QWERTY handheld device to be used by a nearby sighted and hearing person. Details of these different modules are shown in Fig. 4-6. It adopts the generic system presented in Section 4.1 without the mobile phone block. This is because communication here is between the deafblind person and a nearby sighted and hearing person.

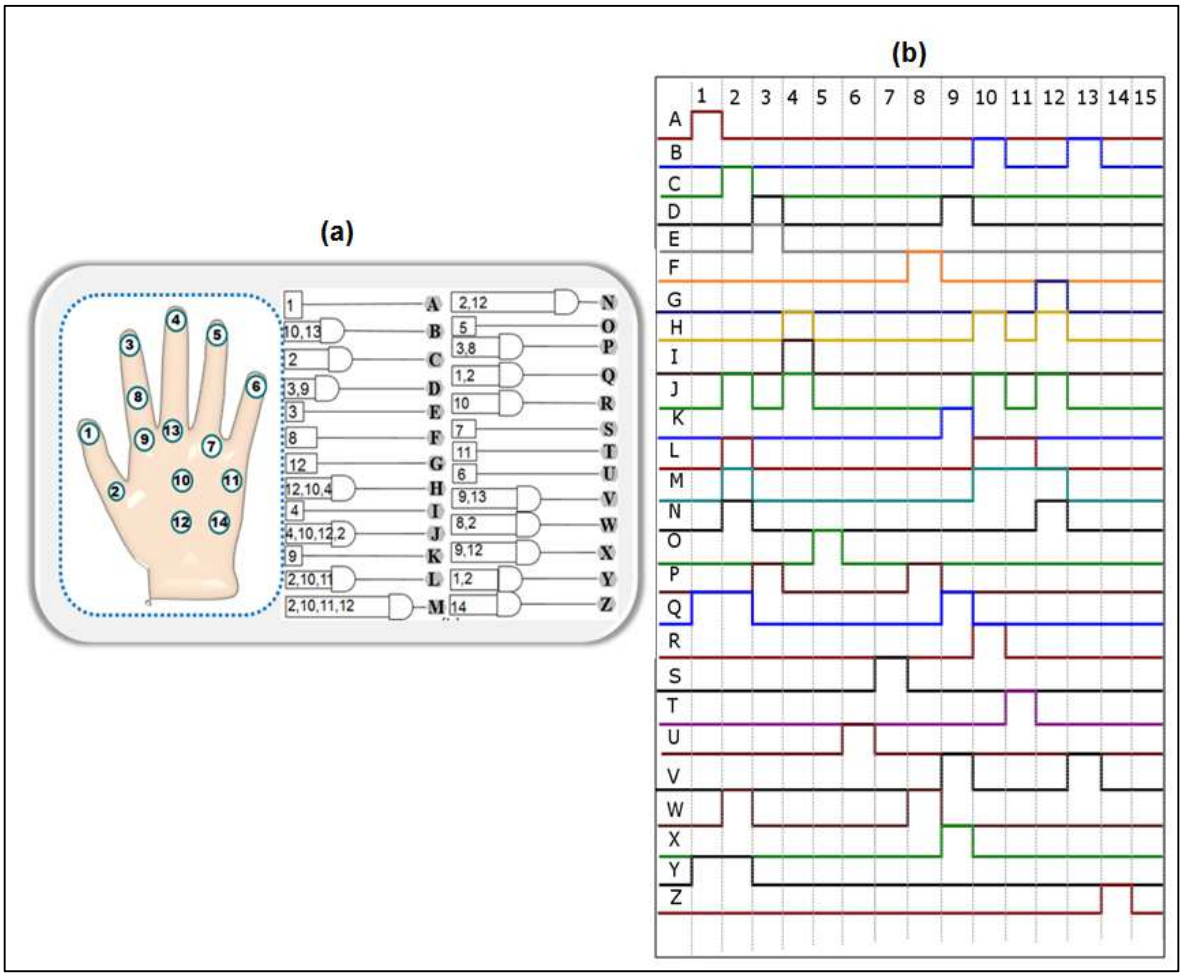

Fig. 4-6 Tactile Point to B-DMA Mapping for first prototype (a) Shows the different tactile points mapped on the hand of the user and the logic for each letter (b) Represents which switch is on when signing a particular letter

Fig. 4-6 (a) shows the tactile mapping for the glove based on the points touched by user of the British deafblind manual alphabet. The logic diagram shows the touch-points that are activated for each letter.. Fig. 4-6 (b) shows which switch is turned on during the signing of a particular letter. These were done based on the B-DMA communication method presented Chapter 2. The glove would be worn by the deafblind person and used for sending and receiving messages from the handheld device. It has two main units, the interface unit and the control unit.

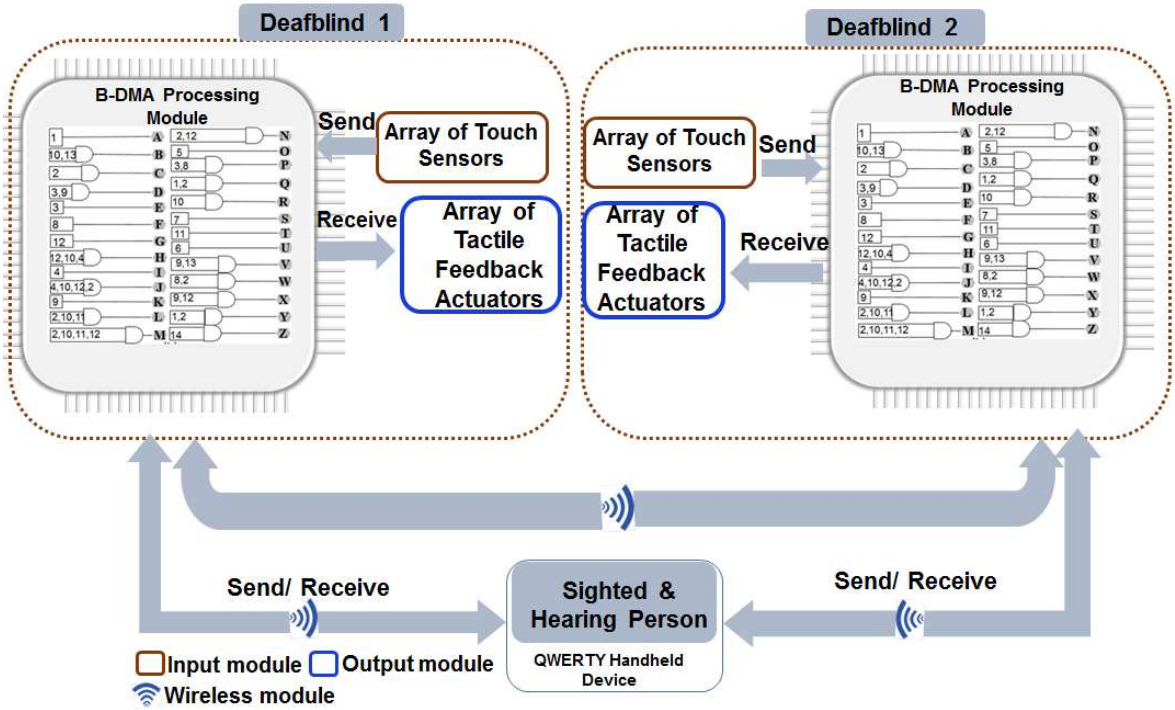

Fig. 4-7 Block diagram of the first B-DMA glove demonstrating the concept of deafblind-to-deafblind communication as well as communication of deafblind with sighted and hearing people

4.3.1 Interface Unit

The input unit is used by a deafblind person to compose messages and is compose of a matrix of touch-sensitive sensors chosen from low cost and commercially available tactile buttons. This is used by the deafblind person to compose messages by moving the fingers through the glove to activate the proper combination of these sensors as mapped in Fig. 4-6.

Fig. 4-6 shows the 2D mapping of the touch-points in the palm area according to the British deafblind manual alphabet method of communication described in Chapter 2. This mapping was designed in accordance with the B-DMA method of communication to represent touch-points corresponding to areas touched during communication. The English letter is properly represented by one or a combination of touch-sensitive sensors as shown in Fig. 4-6. In addition to a few other passive circuits not shown here, the different tactile switches were coupled to a microcontroller using a simple resistance ladder structured in Fig. 4-8 .

So, to determine the unique resistance values, the expected analog-to-digital converter (ADC) values were computed for different resistance values from 300Ω to 59.7KΩ in steps of 600Ω as to be able to choose resistors whose ADC values are at least 20 counts apart. This is to enable the individual sensors to be identified uniquely. Arduino micro board with ATmega32U4 was used and its ADC has a 10-bit resolution which is equal to N. Then, choosing R_B to be 10KΩ and knowing values of the selected R_x, the different ADC values

for each R_x were calculated. By randomly connecting different resistors on the switch and reading them through software, it was observed that resistors that give ADC values with differences less than 20 counts lead to touch-points being confused with others due to noise. Those that give values from 20 counts and above were quite distinguishable and were chosen. After selecting these resistors, the closest standard values for each were then chosen, and they were all connected as shown in Fig. 4-8. To see the practical values of the ADC, each switch was pressed, and the output of the ADC read from the Arduino serial monitor. The practical values were noted and recorded for use in the software algorithm.

The output unit is made from 3V, 8mm coin type ERM vibration motors from Precision Microdrives which serves as a feedback actuator with rated current of 70mA. Since the current required is more than what the Arduino microcontroller can supply, adequate transistors interface was used to drive all the motors.

4.3.2 Control Unit:

This unit basically controls the operation and communication of all the units in the glove and is made up of a processing unit and the wireless unit. The processing unit contains Atmel ATmega32U4 microcontroller which is in charge of all the processing in the glove, while the wireless unit was designed using HC-05 Bluetooth module. The HC-05 for the glove controller was configured as master using AT commands and coupled to the processing unit using a voltage divider interface.

4.3.3 Design and fabrication of the Handheld Device

A QWERTY type handheld device was designed for the purpose of nearby communication. The handheld device is primarily made up of a keypad and a liquid crystal display (LCD). The keypad is used to compose messages by the sighted and hearing communication partner while the LCD displays messages received from the glove via Bluetooth wireless communication.

The interface between the keypad and the MCU is as shown in Fig. 4-8 .The tactile buttons used were arranged in QWERTY fashion and each uniquely identified in software. See Appendix 7 to 9.

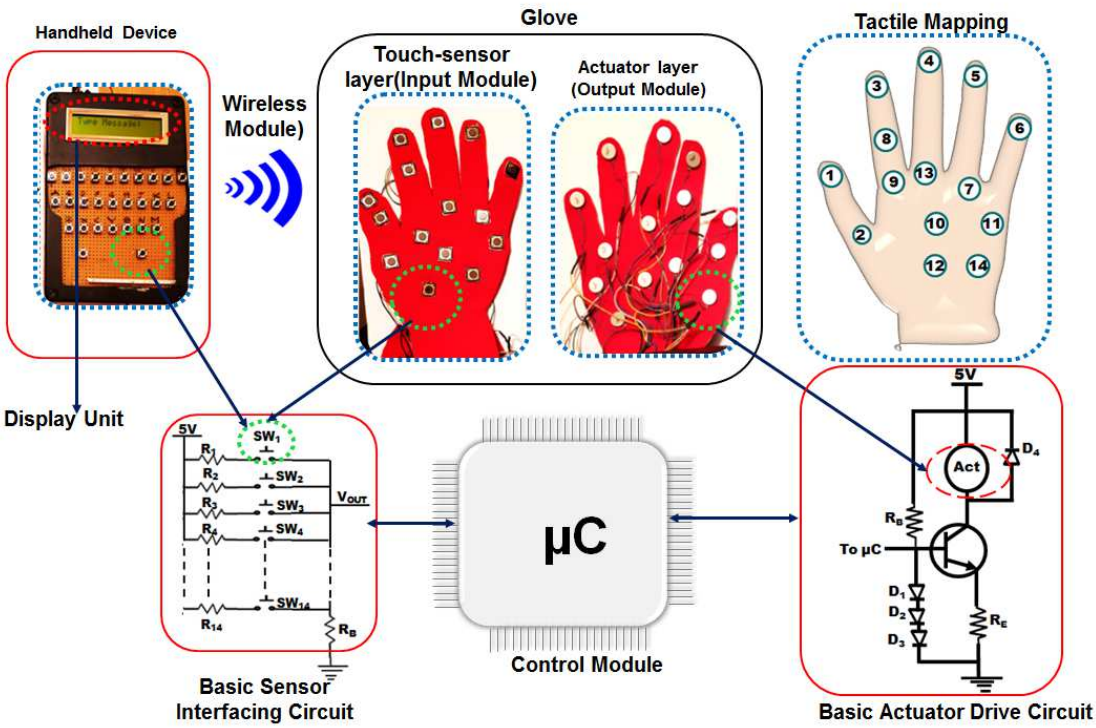

Fig. 4-8 Details of the Implemented Glove (First Prototype

The fabricated prototype including the glove and the handheld device and is as shown in Fig. 4-8 and each is powered by a rechargeable 3.7V lithium polymer (LiPo) battery. The current through the motor is approximately 60mA.

4.3.4 Testing of the Prototype

The different cycles of the prototype testing could be categorized into two - laboratory testing and user testing. The laboratory testing was done in a modular fashion to ensure that each module of the prototype is working. Details of the testing carried out so far are as follows:

The laboratory testing carried out here was to send and receive messages with both the glove and the handheld device. The glove was powered from a desk power supply to ensure low power does not affect the testing in any way, while the handheld was powered by its internal 3.7V lithium polymer battery and the Bluetooth was seen to connect automatically. The glove was used to send message to the handheld device by simply touching the touch-points that fall within the path of the letter being signed and the required letters were seen to display on the LCD of the handheld meaning that the glove was able to send the letter to the handheld via Bluetooth. The handheld was also used to send message the glove by pressing the required letter on the keypad. The corresponding motor(s) was seen to vibrate each time.

Both the glove and handheld were only able to send and receive messages one letter at a time.

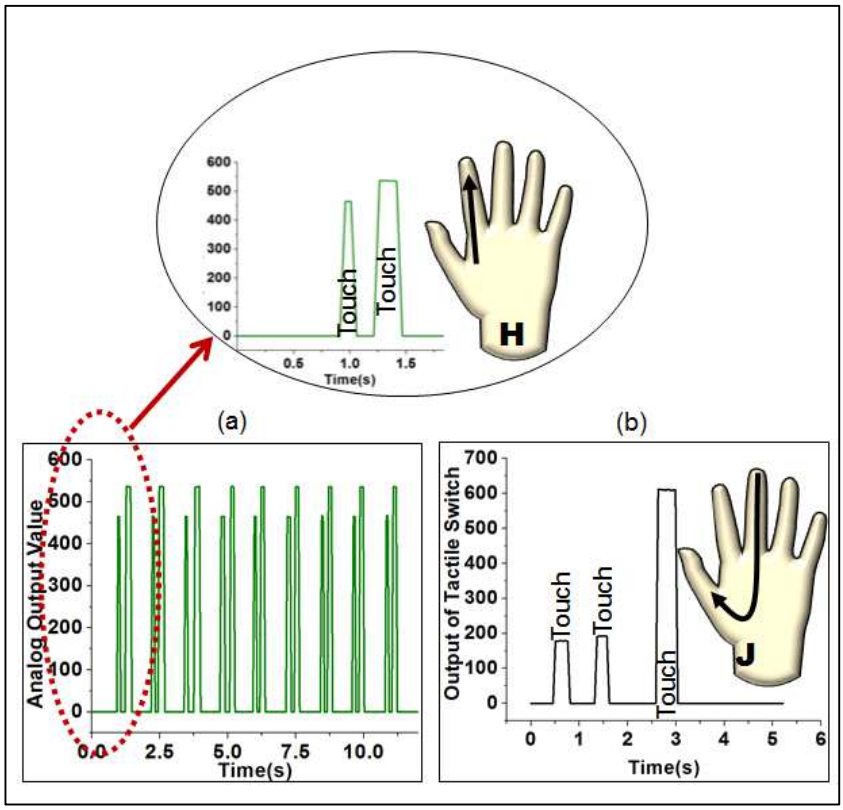

Fig. 4-9 Recorded output of different tactile switches when signing letter H and J as an example

Fig. 4-9 shows the response of some of the switches when signing the letter H and J. It shows the analog values read from the 10-bit microcontroller where 0 corresponds to 0V and 1024 corresponds to 5V.

4.3.5 Re-design of the Tactile Mapping of B-DMA

After testing the first prototype, it was observed that there is insufficient representation of the tactile points and hence the need to optimise the sensor/actuator mapping. Initially 14 tactile points (see Fig. 4-6) were considered and implemented but this was not sufficient. Hence, it was now modified to 27 tactile points (see Fig. 4-10) in order to sufficiently represent the tactile points of the B-DMA as described in Chapter 2.

Table 4-2 presents the different combinations of these points that are touched for the different letters of the English alphabet. This means that for a particular letter, there are different combinations of the points that could be activated. So, these are the main active area that the hand of the sender touches in order to communicate all the 26 letters of the

English alphabet. The tactile points could be regarded as major points, meaning there could be smaller points inside depending on the size of the tactile sensor/actuator used.

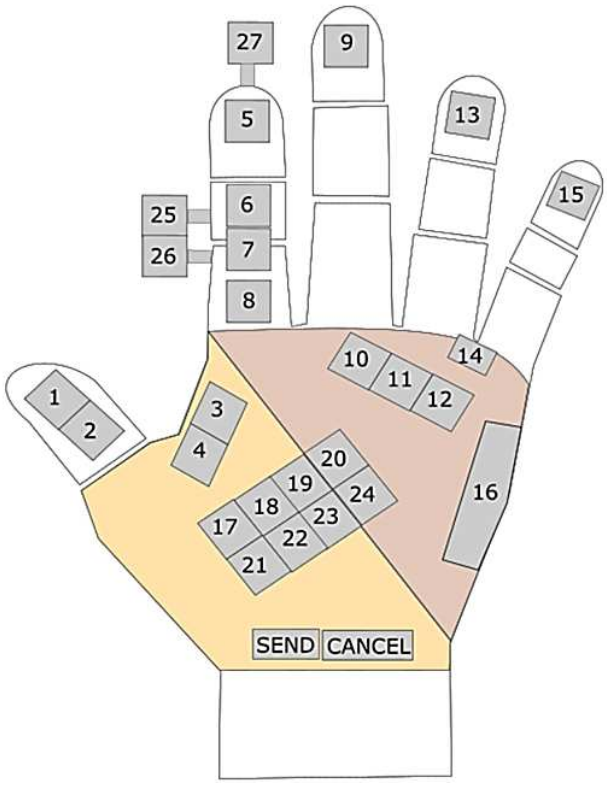

Fig. 4-10 Modified mapping of tactile points for B-DMA

Table 4-2 Tactile-points combination for B-DMA

Letter	Tactile-point Combination	Letter	Tactile Point Combination
A	1	**N**	(17&21&18&22)**OR**(18&22&19&23)**OR** (19&23&20&24)
B	17&18&19&20&21&22&23&24	**O**	13
C	1&2&25&26	**P**	5&27
D	5&6	**Q**	1&2
E	5	**R**	(17&18&19&20)**OR**(21&22&23&24)
F	7&8	**S**	14
G	10&11&12&17&18&19	**T**	16
H	5&6&7&8	**U**	15
I	9	**V**	(10&11&12&13)**OR**(17**OR**18 **OR** 19 **OR** 20 OR 21 **OR** 22 **OR** 23 OR 24)
J	9&10&20&1&2	**W**	1&2&3&4
K	7	**X**	8
L	(17&21)**OR**(18&22)OR(19&23) **OR**(20&24)	**Y**	3&4
M	17&18&19&20&21&22&23&24	**Z**	10&11&12

From Table 4-2, the logic of how these points are activated is represented with logic gates as shown in Fig. 4-11. Some letters were represented with no logic gate (example is letter "A") this means that only that tactile point is activated for the letter "A" some were represented with only AND gates, this means that all the points listed are meant to be activated for that letter. Others are represented by both AND and OR gates (see letters L, R, N, V in Fig. 4-11), this means that any of the combinations at could be activated to represent the letters. An example is the letter "N" which has N1, N2 and N3 as possible combination of the tactile points that produces the letter "N".

Corresponding truth table that represents these points are shown in Appendix 3. These tables are necessary for developing software algorithms that will represent these points.

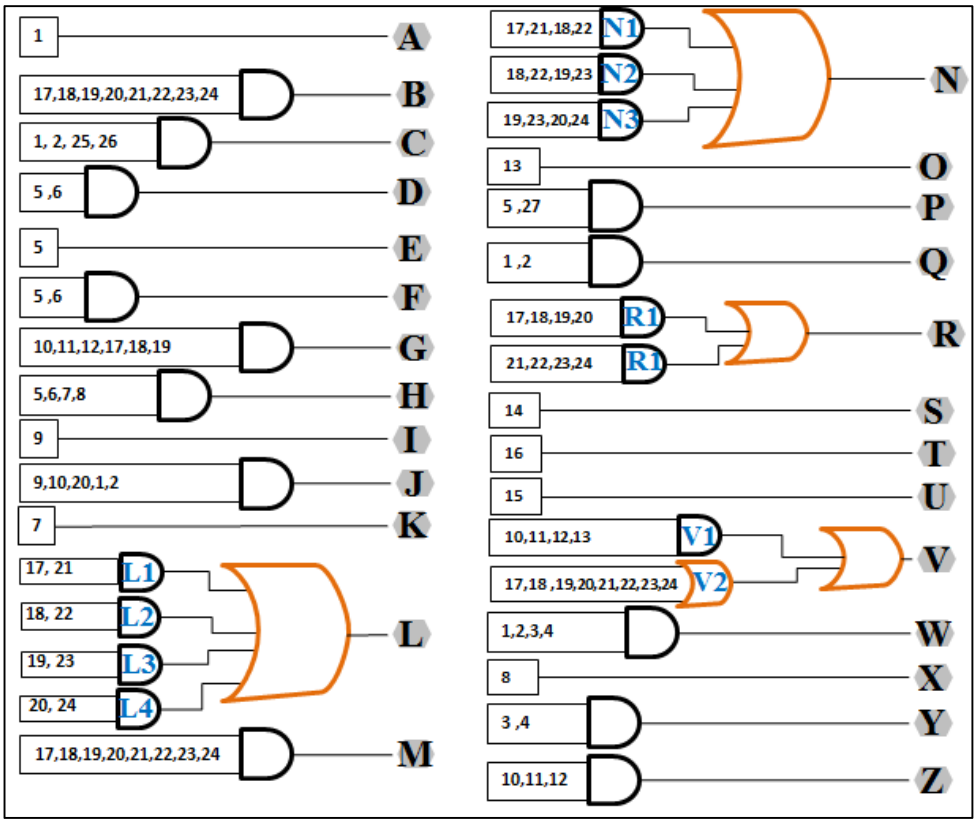

Fig. 4-11 Logical representation of the tactile mapping of the B-DMA

4.4 Design of the Smart Finger Braille

"SmartFinger" Braille is a smart communication glove based on the concept of finger Braille. It is a proposed facile method of using Braille which advances the state of the art through the simplification of the use of Braille and hence the tactile communication interfaces. Normal finger Braille communication requires the deafblind person to physically touch each other in order to communicate as described in Chapter 2. In this case, there is no physical contact between the communication partners, and so the deafblind person wears the

glove and can independently use it to send and receive messages from another deafblind person or from a sighted-and-hearing individual who uses a mobile phone. It equally adopts the generic communication system presented in Section 4.1. This is made up of a smart finger-glove that communicates with a mobile app via Bluetooth technology. Commercial tactile pressure sensors (Force Sensitive Resistor (FSR) from Interlink electronics) and actuators (coin-type vibration motors from Precision Microdrives) were used here to demonstrate this concept.

The concept of the smart finger Braille glove is as shown in Fig. 4-12. It comprises generally of six tactile pressure sensors and six tactile feedback actuator which represent the six dots of the Braille. The sensors are positioned at the tip of index, middle and ring fingers of both left and right hands, while the actuators are positioned at the back of these fingers correspondingly. So, each glove on the right and left hand contains three sensors and three actuators as shown in Fig. 4-12.

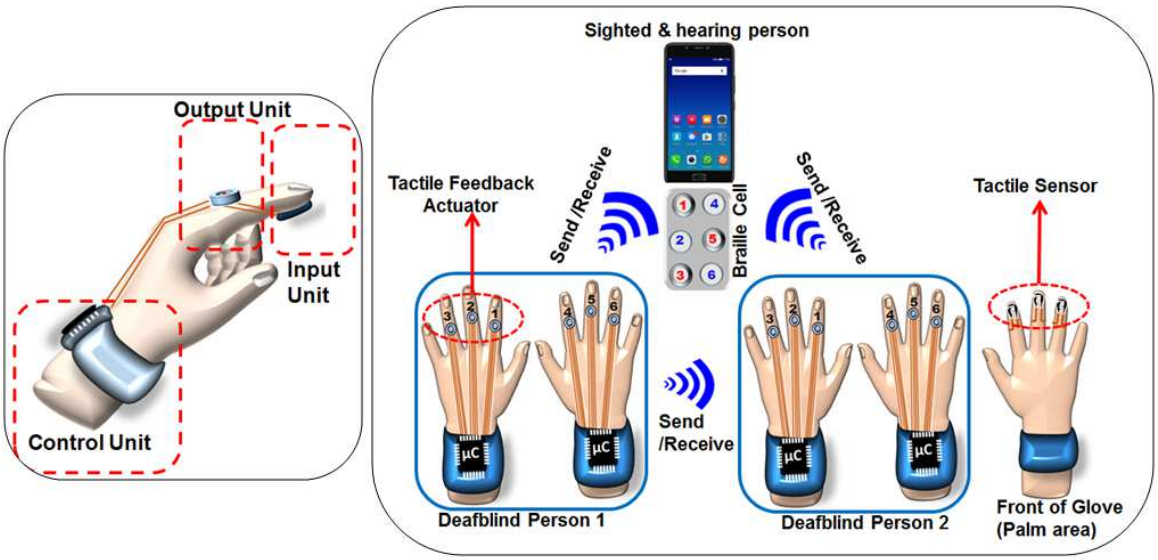

Fig. 4-12 The Concept of Smart Finger Braille Glove

The pressure sensors are used to compose and send messages to mobile devices by tapping the tip of the finger on any surface to compose messages based on Braille codes (described in Chapter 2). Deafblind person receives messages using the haptic actuators in the form of vibrations. This means that deafblind people can independently use this glove to communicate with a nearby or remote mobile phone user as well as a nearby or distant deafblind person that uses a similar glove. The glove-to-mobile communication is shown in Fig. 4-12 while the glove-to-glove communication is via the mobile phone and enables nearby and distant deafblind-to-deafblind as described in Section 4.1.

Fig. 4-13 shows the modular description of the smart finger Braille glove. The glove consists of four main modules the input, output, wireless and control Module (Fig. 4-12 and Fig. 4-13). The input module is made up of six Force Sensing Resistors (FSR) from Interlink Electronics – thickness 0.3mm, force range (0 to 20N)), the output module is made up of six actuators, the wireless unit is made up of HC-05 Bluetooth module and all the units are controlled by the control unit which is contains a microcontroller. Details of these modules are described in the following section.

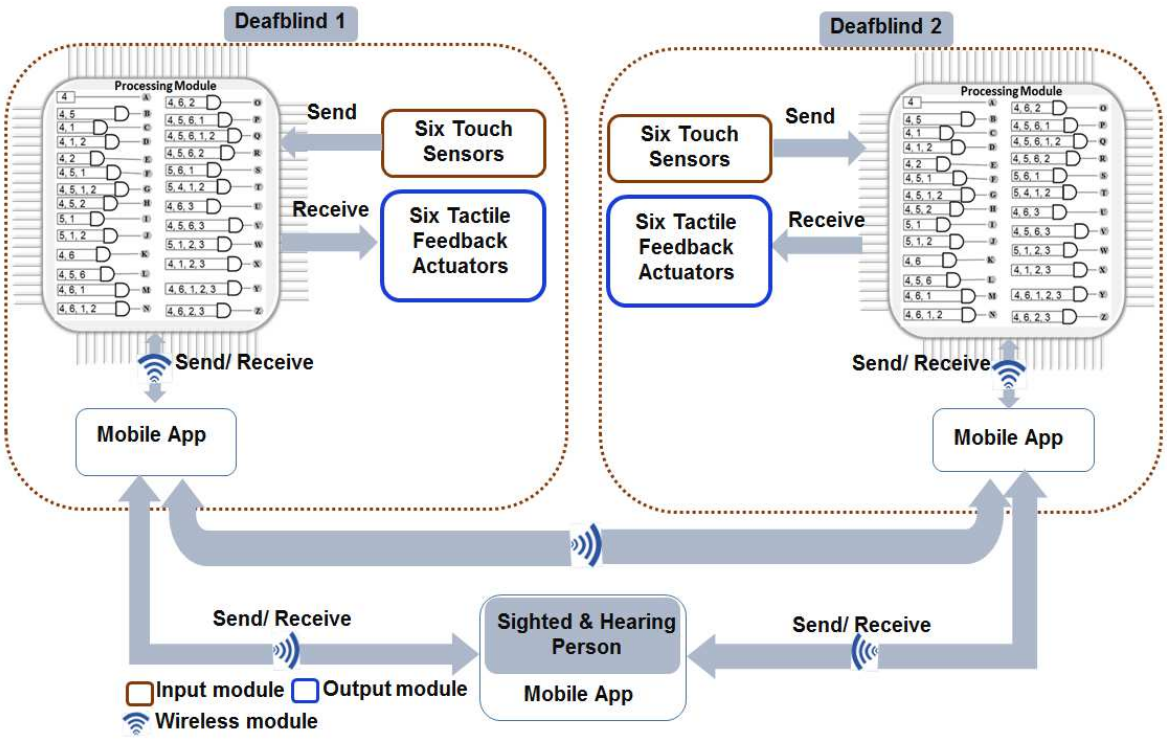

Fig. 4-13 Modular block diagram of the smart finger Braille glove

4.4.1 Input Module

The input unit receives user input from the glove wearer and comprises of six polymeric Force Sensing Resistors (FSR) placed at the tip of the ring, middle and index fingers of both left and right hands to represent the Braille codes. The FSR used is a polymeric thick film device whose resistance decreases with increase in applied force. It was chosen due to its low-cost and availability. The performance of the FSR was measured using different loads and Fig. 4-14 shows its response. It is clear from Fig. 3 that its sensing range falls within “gentle touch” which corresponds to a pressure of 5 - 90 kPa [203]. A digital filter was implemented in the program to compensate for any drift or noise in the measurement. A threshold was set during the design to effectively determine when a finger is pressed.

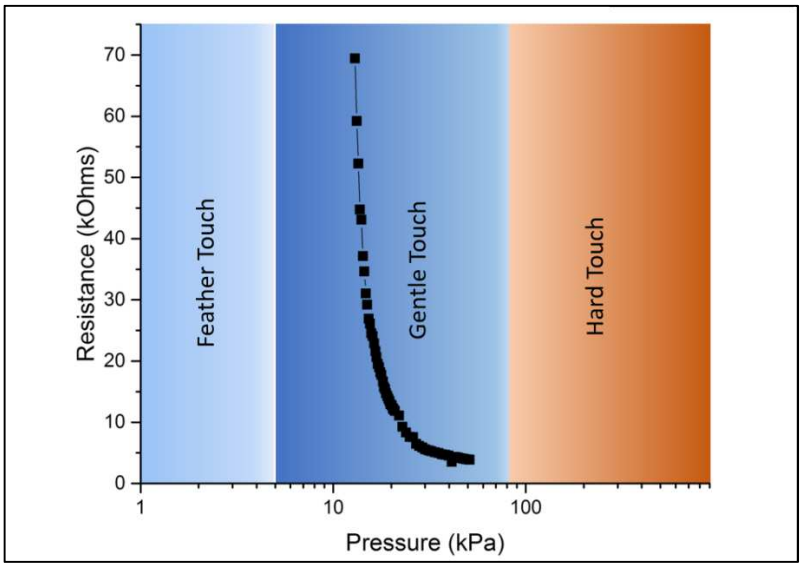

Fig. 4-14 Response of the FSR used in the glove implementation

Table 4-3 represents the logical table of finger Braille which was created from standard Braille codes and used for the implementation of Finger Braille in software.

Table 4-3 Logic Table for Finger Braille Communication

Letter	1	2	3	4	5	6
A	0	0	0	1	0	0
B	0	0	0	1	1	0
C	1	0	0	1	0	0
D	1	1	0	1	0	0
E	0	1	0	1	0	0
F	1	0	0	1	1	0
G	1	1	0	1	1	0
H	0	1	0	1	1	0
I	1	0	0	0	1	0
J	1	1	0	0	1	0
K	0	0	0	1	0	1
L	0	0	0	1	1	1
M	1	0	0	1	0	1
N	1	1	0	1	0	1
O	0	1	0	1	0	1
P	1	0	0	1	1	1
Q	1	1	0	1	1	1
R	0	1	0	1	1	1
S	1	0	0	0	1	1
T	1	1	0	1	1	0
U	0	0	1	1	0	1
V	0	0	1	1	1	1
W	1	1	1	0	1	0
X	1	1	0	1	0	0
Y	1	1	1	1	0	1
Z	0	1	1	1	0	1

4.4.2 Output Module

The output unit is primarily made of six 10mm Eccentric Rotation Mass (ERM) vibration motors (310-113.002 from Precision Microdrives) with rated current and voltage of 63mA and 3V. It has a rated vibration speed of 12,200rpm which is about 203Hz. In order to choose a suitable actuator capable of giving a suitable tactile stimulation to the finger of the deafblind user, some requirements specifications were formed and then parameters of different actuators compared based on these specifications. These specifications include: small size (about 10mm), vibration frequency of about 200Hz which is within the human-vibration detectable range of 20-1000Hz as cited in introduction, low power consumption, low cost, 3V DC input signal, simple drive mechanism, durable quality. Four different categories of actuators were considered, these are: Linear Resonant Actuator (LRA), piezoelectric and Electroactive polymer (EAP) actuators. Parameters considered include: Range of vibration frequency, type of drive signal, haptic performance, durability, cost and availability as shown in Table 4-4.

Table 4-4 Comparison of some common commercial actuators

Parameter	**Actuator type**				
	ERM	**LRA**	**Piezo-electric**	**Electro-active polymer**	**Choice for Smart Finger Braille**
Form factor	3mm-20mm	2mm-10mm	<3mm	<3mm	All
Vibration Freq. Range	47-280Hz	Fixed (typically 150 – 200Hz	About 150-300Hz usable	95-125Hz	All
Type of Drive Signal	DC	AC	DC	DC	ERM
Haptic performance	Good	Better	Very good	Very good	ALL
Durability	Dur-able	Very durable	Very durable	Excellent	All
Cost and avail-ability	Very cheap & available	Cheap and available	Expensive	Expensive	ERM

4.4.3 Control and Wireless Module

The control unit controls all the different modules in the smart glove and was built around an Atmega32U4 microcontroller. The control unit includes also the wireless unit and the power supply unit. The power supply was designed to give 3V to the vibration motors as per

motor specification and 5V to the rest of the circuit. Fig. 4-15 shows a simplified functional circuit diagram of the smart glove with some interfacing passive components. Details of the circuit schematics are show in the Appendix.

The wireless unit was realised using the HC-05 Bluetooth module because it is capable of being configured both as master and slave using ATtention (AT) commands, unlike the HC-06. Bluetooth wireless technology was chosen because it suits the following wireless communication requirements which were created for the implementation of the smart glove. These are: low power consumption, short range (10-100m), low data rate, small bandwidth, and ease of use with mobile phone, and cost. Bluetooth technology was selected with a major focus on range, cost and ease of use with mobile phone as shown in Table 4-5.

Table 4-5 Comparing four Wireless Protocols [204]

Parameter	**Wireless Communication Protocols**			
	Bluetooth	Ultra-wide band (UWB)	ZigBee	Choice for SmartFingerBraille
Frequency Band	2.4 GHz	3.1-10.6 GHz	868/915 MHz; 2.4 GHz	All
Max Signal Rate	1 Mb/s	1 10 Mb/s	250 Kb/s	Bluetooth, Zigbee
Nominal Range (m)	10-100	10	10 - 100	All
Nominal Transmitter Power	0 - 10 dBm	-41.3 dBm/MHz	(-25) - 0 dBm	ZigBee, Bluetooth
Channel Bandwidth	1 MHz	500 MHz - 7.5 GHz	0.3/0.6 MHz; 2 MHz	Bluetooth, ZigBee
Ease of Use with Mobile phone and PC	Very Easy to Configure	Not easy	Not easy	Bluetooth
Cost	Very cheap	Cheap	Very cheap	Bluetooth, ZibBee

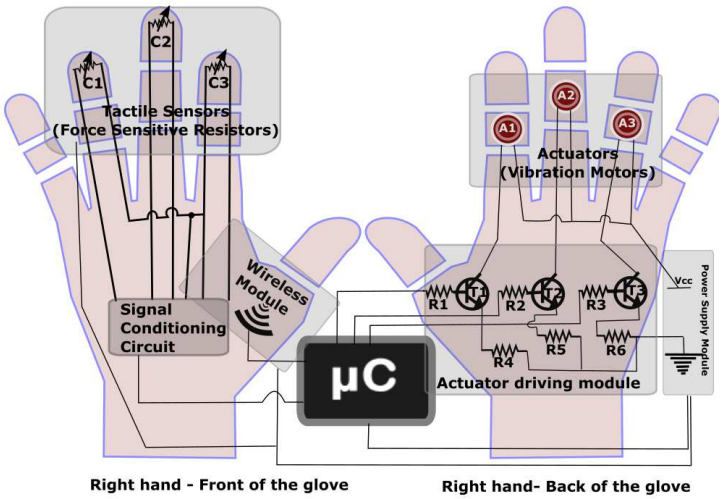

Fig. 4-15 Detailed functional Block diagram for the Finger Braille with basic interfacing circuits

4.4.4 Fabrication of the Smart Finger Braille Glove

Fig. 4-16 shows the fabricated smart finger Braille. The glove was fabricated using neoprene with the off-the-shelf touch sensors and actuators embedded in it. The input and output units were fabricated in two different segments. The input unit which has the FSR embedded was fabricated like a dome shape structure and sits on the finger like a finger cap.

The output unit which houses the vibration motor was made in ring shape and also worn like a ring. The front and back view of a single finger of the glove is shown in Fig. 4-16. The vibration motors were bonded to this neoprene using Iron-on fabric and the fabric sewn. The rectangular-shaped neoprene was then folded in the shape of a ring and sewn. The sewn neoprene was then turned inside-out to properly secured and position the embedded vibration motors. The input unit was fabricated by first cutting six different pieces of neoprene material into dome shapes. The input and output units of the glove were attached together using Velcro and all wires embedded in a stretchy cotton jersey fabric.

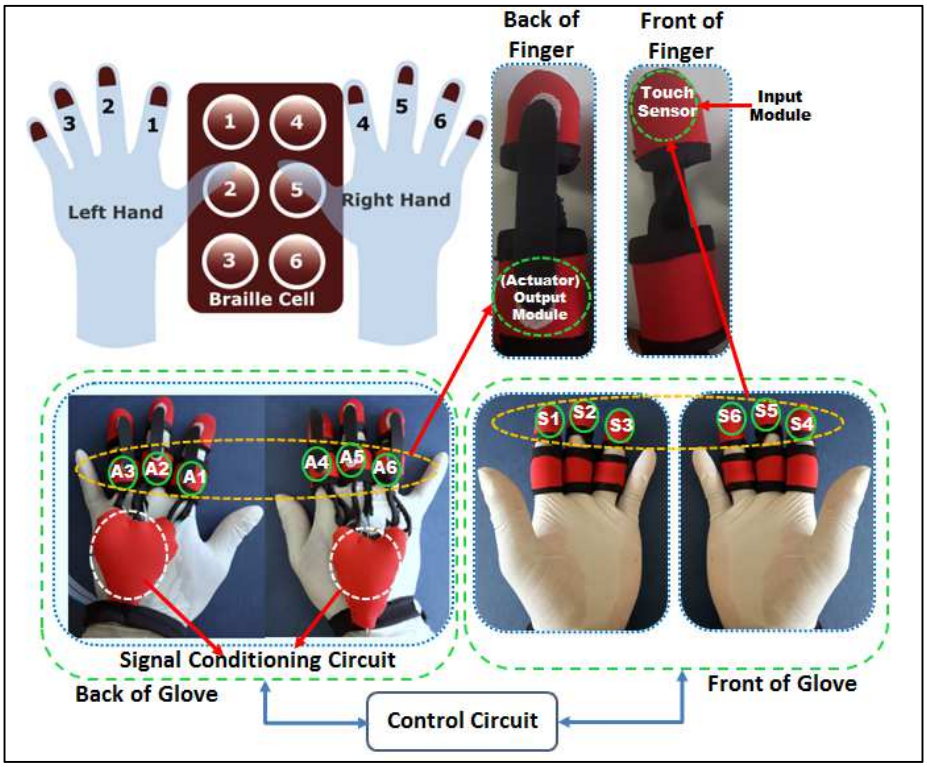

Fig. 4-16 Fabricated Smart Finger Braille Glove

4.4.5 Testing of Smart Finger Braille Glove

Two main testing stages are intended for this device: (1) Laboratory testing and (2) end-user testing. Only first stage testing was carried out which involved no real deafblind person. The testing involved three healthy male subjects. It involved verifying the correct transmission of the 26 letters of the English alphabet, short words, numbers and special characters. During the test, the glove was worn on the hand by one subject while the second subject holds the mobile phone and the third records the response and waits for a turn.

The Braille codes and the corresponding letters were visually presented to the subjects since they have no prior knowledge of Braille. The user wearing the glove taps the corresponding fingers on a desk to send messages to the mobile app. Each of the three subjects wore the glove and equally held the mobile phone in turn to have a feel of both sides and be able to give the necessary feedback. The Braille code of all the 26 letters of the English alphabets were first typed and sent one by one and then followed by numbers and special characters including space. Next was the typing and sending of different words e.g. “hi”, “touch of genius” etc. Both short and long phrases/words were able to be sent and received. Fig. 5b shows the smart finger-glove worn in the hand during testing. Fig. 6 shows the implemented smart phone app. Fig. 6a, shows the mobile app during the testing of the communication from mobile phone to the glove. The word “HI” was sent to the glove and the corresponding

fingers vibrated to translate the letters received to Braille codes. Fig. 4-5 shows the result of sending the Braille code for the letters “abcd” from the glove by gently tapping the corresponding fingers on a desk. All sent messages were properly displayed on the mobile app. However, it was occasionally observed that, the letters were not sent sometimes because of the user not tapping the fingers correctly.

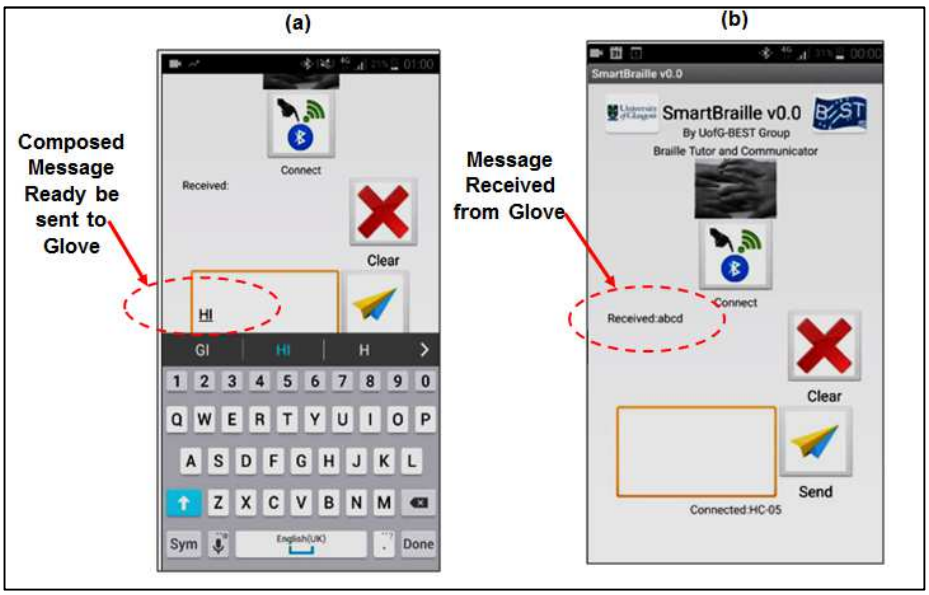

Fig. 4-17 Sending and Receiving message with the SmartBraille Mobile App

4.4.6 Summary

In this chapter, a generic tactile communication system for communication by deafblind people was presented. Two communication prototypes that make use of commercially available tactile sensors and actuators were developed using this system. This was done to understand the strengths and weaknesses of these using the rigid commercial sensors as well as try the proposed two-way communication system and simultaneously show the application of tactile communication interface for deafblind people.

Generally, a number of limitations were found and these include

- Difficulty in the integration of separately-made commercial touch sensor and actuator at the same point for the creation of localised tactile sensing and feedback
- Difficulty in miniaturisation due to the use of commercial sensors and actuators for the fabrication of an array of tactile points
- Rigidity of the actuators used and hence reduced wearability

- Inefficient representation of the tactile points due to little number of tactile sensors and actuators used

Considering these limitations, custom-made tactile sensors and actuators were developed as will be presented in Chapter 5 and 6. This involved the design and fabrication of a customised touch-sensitive flexible actuator, array or capacitive touch sensors for Block letter communication as well as possible application to B-DMA, and an inductance-based pressure sensor for application in finger Braille communication.

Chapter 5

5 Design and Fabrication: Tactile Feedback Actuators

This chapter presents the fabrication of flexible tactile feedback actuators capable of creating vibrotactile feedback for deafblind people and intended an alternative to the commercial vibration motor used in the POC described in Chapter 4. This will support customisation and development of array of actuators that can be effectively used to represent the tactile points. The nature of the deafblind communication methods described in Chapter 2 requires the positioning of tactile sensors and actuators at the same tactile points mapped on the hand of the user. Among the limitations found for using the commercial sensors and actuators presented in Chapter 4 are rigidity and the challenge of integrating both the sensor and actuator together at one point. Hence to remedy these, two different designs of novel flexible touch-sensitive electromagnetic actuators were fabricated in this work for two forms of tactile displays – (1) For the tactile display with exploration of surface (e.g. Braille display) and (2) for the tactile display for smart communication gloves (e.g. B-DMA glove) as presented in Chapter 4. To date, existing actuators used in conventional tactile displays (e.g. Braille displays and deafblind smart gloves) do not have integrated capability of both tactile sensing and feedback. So, developing a touch-sensitive actuator for tactile displays could be advantageous as it is a great opportunity to give it an inherent dual function of tactile sensing and feedback, a feature applicable for localised sending and receiving of information.

Fig. 5-1 shows the concept of the implemented touch-sensitive actuator. The two fabricated designs presented here can both fit in the finger and are based on the electromagnetic principle which has an inherent high speed, precision, force, and scalability (as explained in Chapter 2). Both can create localised vibrotactile feedback on the hand of the user. The major difference in the two designs is the location of the tactile sensor in each of them. In the first type (Type-1), the tactile sensor and the actuating point are positioned on opposite sides; this enables the skin contactor to be faced down directly on the body while the opposite side (which faces up) will be used for touch-sensing. In case of the second type (Type-2), the tactile sensor and actuating point were positioned on the same side – this is applicable in Braille Displays and other tactile displays that require surface exploration.

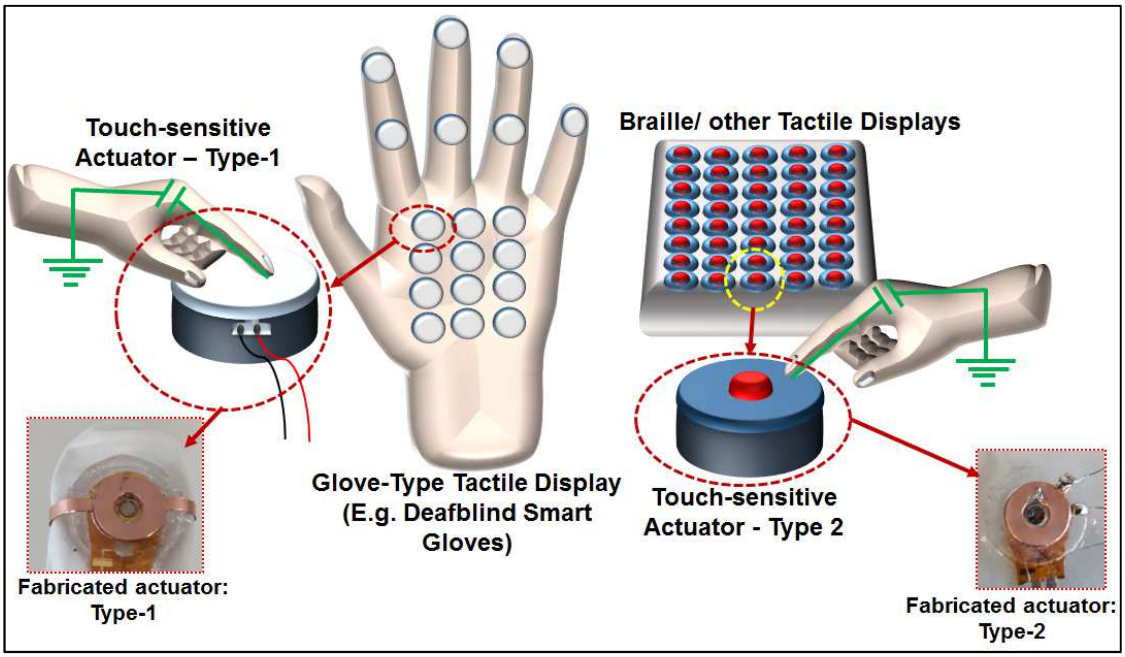

Fig. 5-1 The Concept of Touch-sensitive Actuator for deafblind communication

5.1 Design of the Spiral Coil

The actuator works through the electromagnetic interaction of a spiral coil and a permanent magnet. Hence the spiral coil is a major part of the actuator as it creates the necessary magnetic field for actuation. The higher the magnetic field the higher the interaction will be, and hence the more the actuation. Prior to the fabrication of the coil, simulations of various coil dimensions were carried out to determine the design with better performance, and the key consideration was the level of magnetic field produced as well as suitable dimension for the fingers.

5.1.1 Calculation of Spiral Coil parameters

This section presents the design and calculations of the spiral coil parameters which contributes to the level of the magnetic field it produces. Fig. 5-2 shows the 3D geometrical description, while Fig. 5-3 shows the 2D axisymmetric view of the fabricated spiral coil. The 2D axisymmetric model was used for the simulation of the coil using COMSOL Multiphysics software. So, the calculation was carried out based on the 2D axisymmetric geometry.

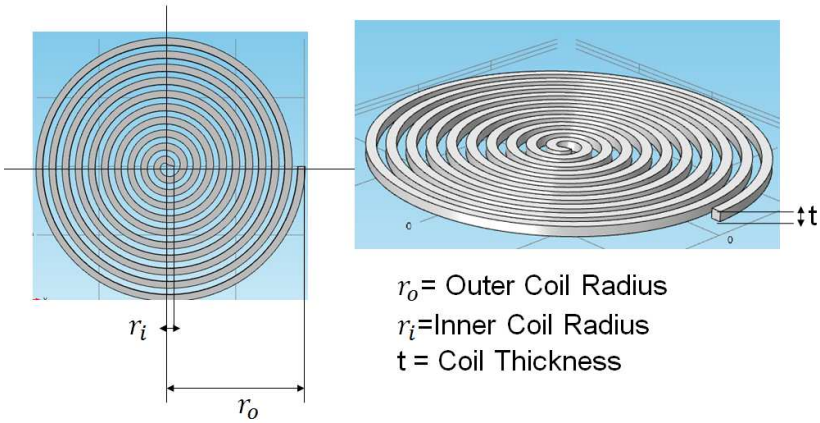

Fig. 5-2 3D Spiral Coil Geometry

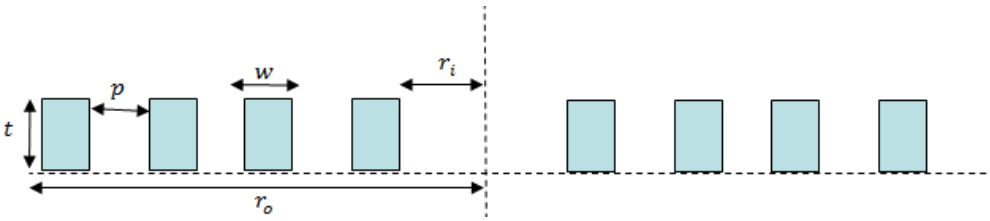

Fig. 5-3 2D Axisymmetric View of the Spiral Coil

Considering the 2D-axisymmetric model of the coil as shown in Fig. 5-3 which was adapted from [205], the relationship between the internal and external radii of the spiral coil is given as:

$$r_o - r_i = N(p + w) \tag{5-1}$$

Where p is the pitch of the coil, w is the width of the coil conductor, r_i and $r_o$is the inner and outer radius of the coil respectively.

The Coil Aspect Ratio (CAR) could be defined as:

$$\alpha = w/t \tag{5-2}$$

Combining Equation (5-1) and (5-2)

$$r_o - r_i = N(p + \alpha t) \tag{5-3}$$

And from Equation (5-3)

$$N = (r_o - r_i) / (p + \alpha t) \tag{5-4}$$

The length of the spiral coil is given by [205]

$$l = N2\pi r_o \tag{5-5}$$

Where, N = Number of turns, t = Thickness of the coil conductor

5.1.2 Calculation of the Magnetic Field Generated by the Spiral Coil

Any wire carrying current creates a magnetic field and the relationship between this current and the accompanying magnetic field is described by Biot Savart Law (see Appendix 5). For any coil, the magnetic field is directly proportional to the applied current.

So, if a spiral coil carrying current I is considered to be made up of n - number of circular loops with inner radius r_i, outer radius r_o and thickness t, then the magnetic field at the centre contributed by each n_{th} loop is given by:

If $n = N$, where N = number of turns of the spiral , then by combining Equation (5-3) and

$$B_{nth\ loop} = \frac{\mu_0 I}{2(r_o - r_i)} \ln\left(\frac{r_o}{r_i}\right) \tag{5-6}$$

(5-6), the magnetic field generated at the centre by the N-turns of spiral is given by:

And by considering the CAR (see Equation (5-2)), then Equation (5-7) now becomes:

$$B_{Center\ of\ Spiral} = \sum_1^N \frac{\mu_0 I}{2(N(w+p)} \ln\left(\frac{r_o}{r_o - N(w+p)}\right) \tag{5-7}$$

$$B_{Center\ of\ Spiral} = \sum_1^N \frac{\mu_0 I}{2(N(\alpha t+p)} \ln\left(\frac{r_o}{r_o - N(\alpha t+p)}\right) \tag{5-8}$$

5.1.3 Simulation of the Spiral Coil

The AC/DC module of the COMSOL Multiphysics was used to simulate different coil configurations before the fabrication of the coil in order to determine which one gives higher magnetic field. The diameter of the coil was set to 1cm so as to give it a form factor that will fit on average adult fingers. Using this, different groups having different conductor width and pitch were considered. The different groups considered are 100-50, 100-25, 90-50, 90-25, 80-50, 80-25, 75-50, 75-25 and for each group, the values correspond to conductor width and pitch. The aspect ratios of the different coil groups were calculated and through COMSOL simulation the magnetic field at the centre of each coil group was estimated.

Appendix 6 contains a table showing the parameter definitions used for the simulation. It contains the settings and parameters like thickness of coil, width of coil conductor, coil aspect ratio, current, area of the coil, inner and outer coil radius and other parameters. By automatically varying these parameters and, COMSOL creates different spiral coil geometries and by adding physics to the model it calculates the magnetic field generated by each.

5.1.3.1 Spiral Coil Geometry

The simulation geometry of the spiral coil was created using the real dimensions of the fabricated coil. Details of the parameters used for the design of the geometry is shown in Appendix 6, The thickness, coil conductor width, and thickness of the Polyimide substrate is 17µm, 75µm and 50µm respectively. Table 5-1 shows a summary of the properties of the coil geometry that was created.

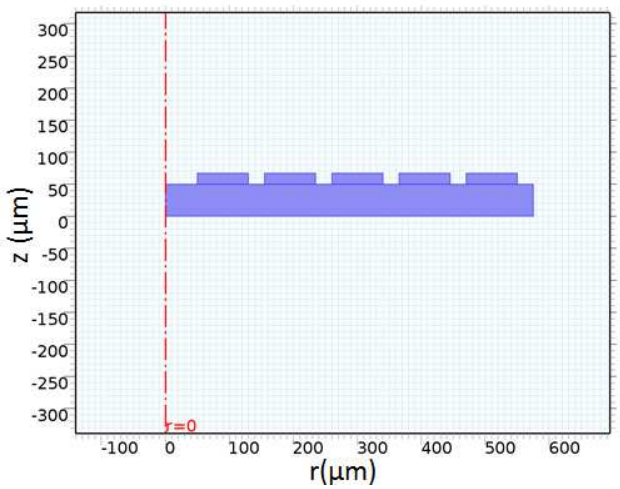

Table 5-1: Geometry Statistics

Property	Value
Space dimension	2
Number of domains	6
Number of boundaries	29
Number of vertices	24

5.1.3.2 Material

Two basic materials were selected for the coil - gold was selected as the material for the coil conductor while polyimide was chosen as the coil substrate.

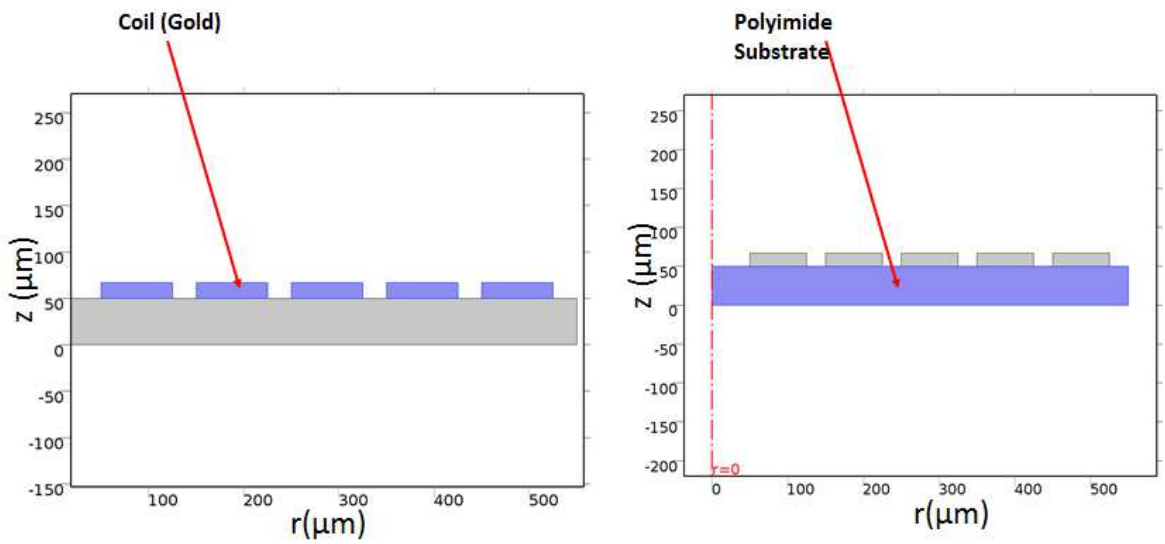

Fig. 5-4 Domains with Materials added

5.1.3.3 Addition of Physics to the Coil Model

The magnetic field node was added to domain 1 to 6 of the coil model, and hence Ampere's law was used by COMSOL to solve the model using Equation (5-9), (5-10), and (5-11) . Magnetic insulation was applied to the following boundaries: 2–4, 6–9, 11–14, 16–19, 21–24, and 26–29, and governed by Equation (5-12).

$$\nabla \times H = J \tag{5-9}$$

$$B = \nabla \times A \tag{5-10}$$

$$J = \sigma E \tag{5-11}$$

$$n \times A = 0 \tag{5-12}$$

Where

J = current density,
B = Magnetic flux density,
H = Magnetic field, A = Area,
E = Electric field,
σ = Electrical conductivity

5.1.3.4 Spiral Coil Parameters

The multi turn coil feature was chosen since the spiral coil has many turns. Under this condition, the conduction current is assumed to flow only through the conductor and the current excitation supplied is translated to current density and applied to the coil domain using Equation (5-13).

Where,

$$J_e = \frac{NI_{coil}}{A} \tag{5-13}$$

$$J_e = \text{current density}$$
$$I_{coil} = \text{coil current}$$
$$A = \text{area of coil}$$

5.1.3.5 Meshing of the Spiral Coil

The coil model was meshed using a physics-controlled mesh and the finer mesh element size chosen as shown in Fig. 5-5.

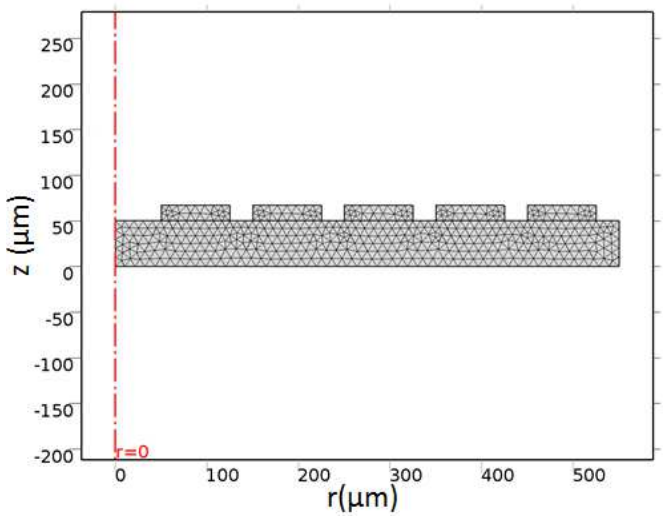

Fig. 5-5 The Mesh Structure used for the Coil Simulation

5.1.3.6 Study

In order to observe the response of the coil under different conditions, a stationary study was selected, and a parametric sweep used to see the performance of the coil under different conditions. These conditions include the variation of the coil diameter for different number of turns. This enabled the determination of the number of turns of coil required as well as which coil diameter would fit into the required 1cm for the finger.

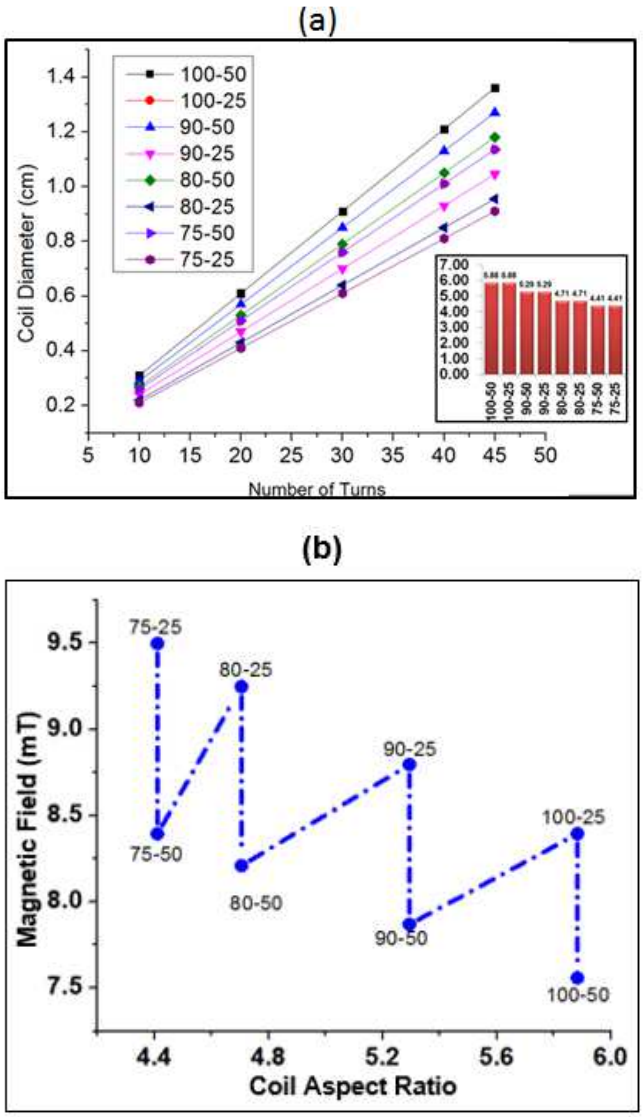

Fig. 5-6 (a) Possible coil diameters for different number of turns (b) Magnetic field at the centre of the coil for different coil aspect ratios

Fig. 5-6 shows that with different number of turns, the 75-25 group has the lowest coil aspect ratio (CAR) which gives it an advantage, while Fig. 2b also shows that the magnetic field at the centre of the coil is inversely proportional to the CAR which makes 75-25 coil group the right choice.

The magnetic field of at the centre of the coil was equally studied for the different coil groups, and the result of this study is shown in Fig. 5-6 (b). This was achieved using the parametric sweep feature by sweeping values of the CAR from minimum (4.4) to maximum (6.0) and COMSOL automatically computes the value of the magnetic field at the centre of the coil for each case.

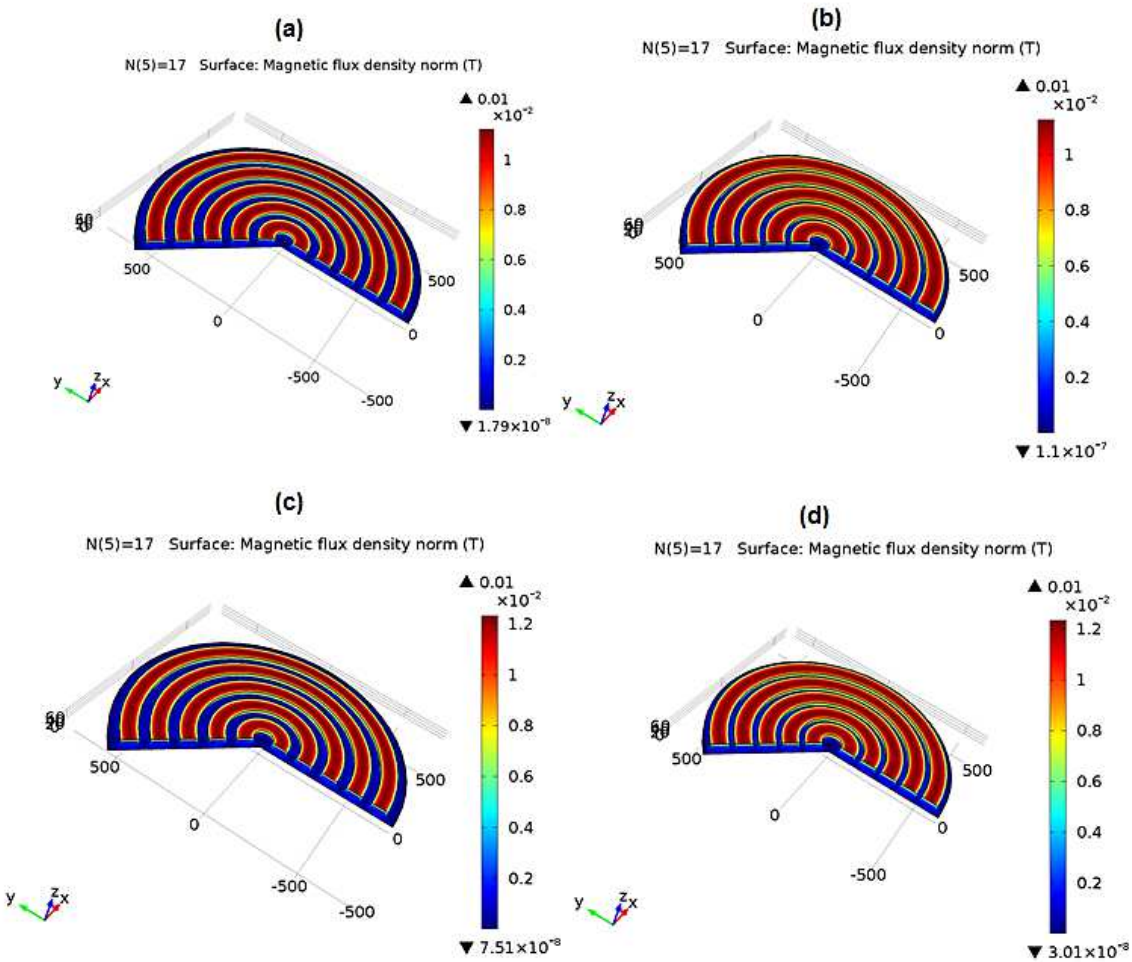

Fig. 5-7 shows the distribution of the magnetic flux density for all the simulated coils (a) 100-50 (b) 100-25 (c) 90-50 (d) 90-25

Fig. 5-7(a) – (d) and Fig. 5-8 (a) – (d) shows the distribution of magnetic flux density of the different coil group structures that were simulated. It shows maximum distribution over the coil conductor in each case and least on the polyimide substrate.

The magnetic flux distribution for the chosen and fabricated coil which has a pitch of 25µm and conductor width of 75µm is shown in Fig. 5-8 (d) The Maximum value of this magnetic flux from the simulation is about 14mT and was seen to be uniformly distributed around the coil conductor.

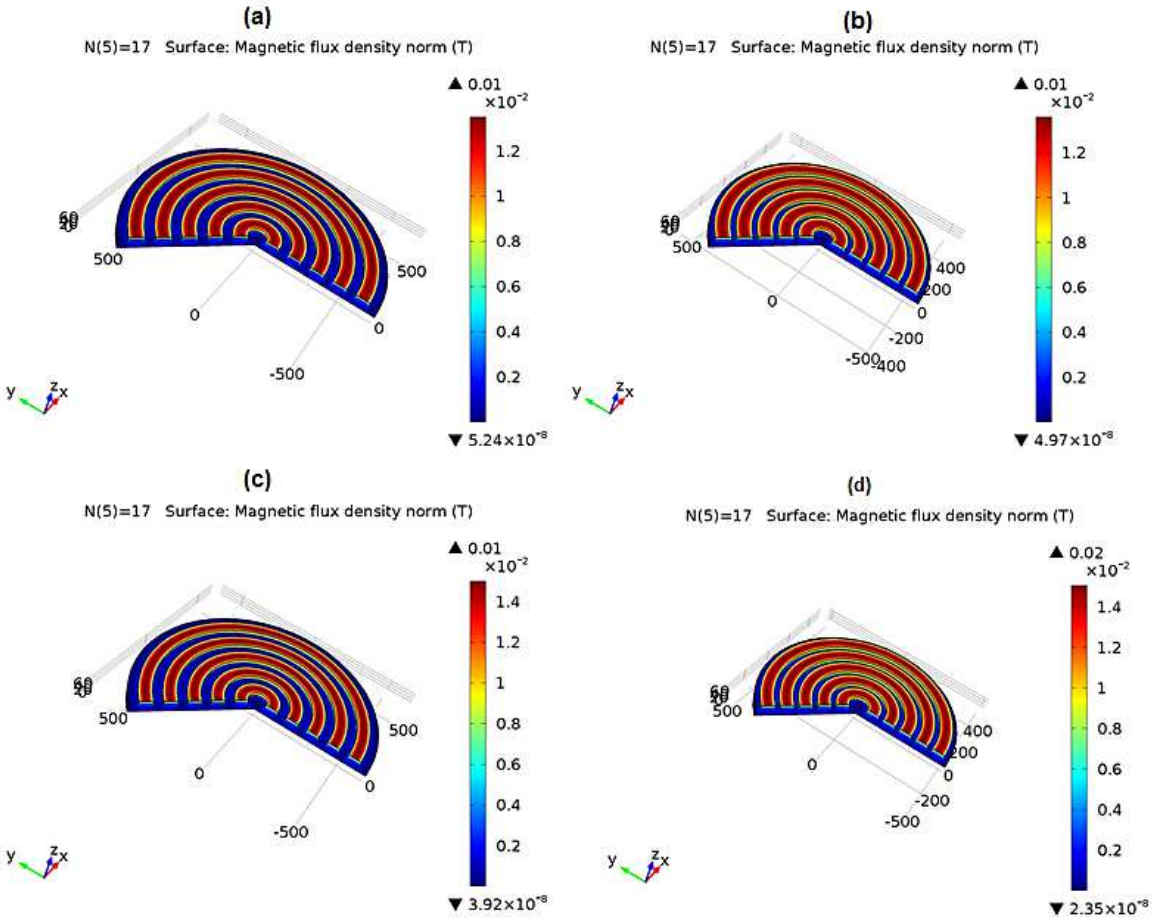

Fig. 5-8 Magnetic flux density (a) 80-5- (b) 80-25 (c) 70-50 (d) 70-25

5.2 Fabrication of the Spiral Coils

The steps for the fabrication of the coil are shown in Fig. 5-9. The coil was fabricated using the LIGA (Lithographie Galvanoformung Abformung) process as shown in Fig. 3. The motivation for using the LIGA is to increase the thickness of the coil using standard and low-cost electroplating method as described in Chapter 3. First, 20nm/50nm NiCr/Au was deposited on a flexible 50µm polyimide sheet using Plassys MEB 550S Electron Beam Evaporator system. An AZ4562 photoresist was then spun on the surface of the deposited metal at 2000rpm for 3 seconds. In order to avoid trapped bubbles, the sample was left at room temperature for 30 minutes to allow evaporation of some of the solvent before baking.

The sample was then baked with a hotplate at 100ºC for 10mins and again left for 30minutes before UV lithography. The baked sample was then exposed a through a dark-filled mask (designed as shown in Fig. 5-9(i)) for 60 minutes under a UV light using standard lithography technique (see Chapter 3). This was followed by the development of the exposed photoresist using AZ826 developer for 10minutes and washing using reverse osmosis water.

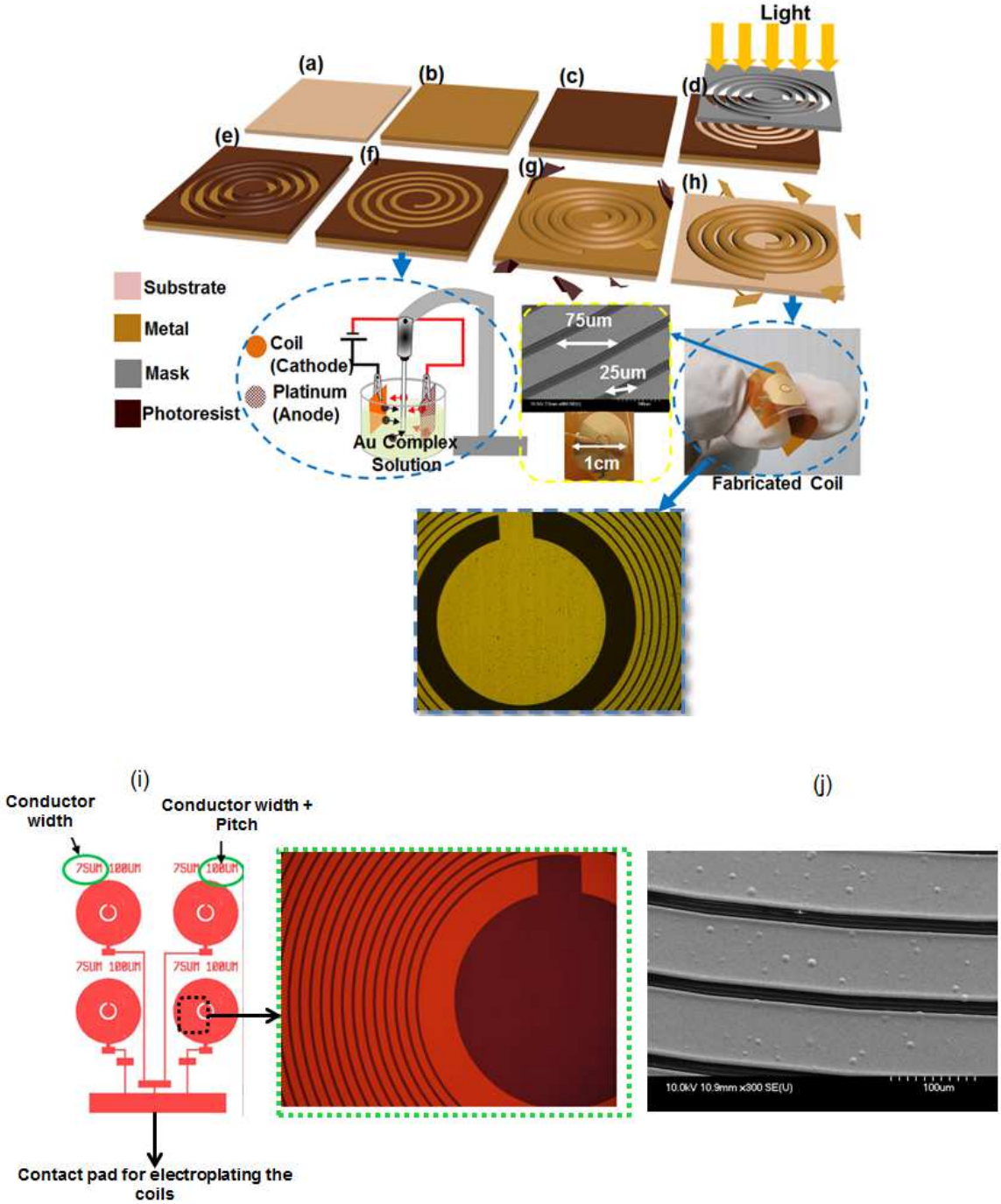

Fig. 5-9 Fabrication steps for coil (a) Initial flexible substrate (b) Deposit gold (c) Spin coat photoresist (d) Expose photoresist (e) Develop the photoresist (f) Electroplate the coil (g) lift-off the photoresist (h) Seed layer lift-off (i) Mask for the coils (j) SEM image of fabricated coil

The developed sample was then electroplated by connecting the sample to the cathode of a non-cyanide gold complex electroplating solution and plated for ~45minutes to realise a ~17µm thick coil with 45 turns. Non-cyanide gold plating solution was chosen because it is non-toxic, has high plating efficiency, very compatible with photoresists, and provides controllable residual stress of plated gold [206]. After the plating, unwanted gold layer was etched using a gold etchant for ~15 seconds and this removed part of the gold area that was

not plated exposing the NiCr seed layer. After gold etching, the sample was annealed at 350°C in a furnace for ~20 minutes under Nitrogen ambient. This is required to increase the strength of the electroplated metal before Nichrome etching, failure to do this will cause the entire coil pattern to lift off. Following this, the NiCr seed layer was then removed using Nichrome etchant exposing the flexible polyimide sheet with the required spiral coil pattern as shown in Fig. 5-9(h) and (j).

5.3 Fabrication of the Touch-Sensitive Layer

The touch-sensing module was fabricated using a facile planar capacitive structure realised by bonding two layers of low-cost flexible single-sided Printed Circuit Board (FPCB) with ~35µm of copper on a polyimide substrate. This was achieved by bonding non-conducting surface of one FPCB with the conducting copper surface of the other and so the polyimide of the one on top serves as the dielectric layer for capacitive sensing (see Fig. 5-10). FPCB was chosen due to its low-cost, ruggedness, flexibility as well as high conductivity of copper in comparison with other options like ITO or gold. The FPCB were cut using the Silhouette Cameo 2 blade cutter. The software of the Silhouette Cameo has a built-in library of different materials with options of editing their properties.

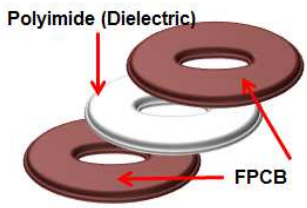

Fig. 5-10 Capacitive Touch-sensitive layer

The pattern to be cut was first designed in graphic software and transferred to the Silhouette Cameo 2 software for cutting. The non-conducting surface of the FPCB sheets was first bonded together with the PVC sheet using a double-sided tape. The bonded FPCB was then placed on a sticky 12 x 12in cutting mat for cutting. The Silhouette Cameo was set to be able to cut only the required portions of the sheet. To do this, the speed, force, and blade position of the blade cutter was set to 5cms-1, 20, and 10 respectively. After cutting, the unwanted parts were removed revealing only the pattern as shown in Fig. 5-10

5.4 Realisation of the Touch-Sensitive Actuator

The steps for the realisation of the touch-sensitive actuator are shown in Fig. 5-11 . Two different touch-sensitive actuators were realised, Type 1 and 2. The major difference between the two designs is the location of the touch-sensitive layer. The idea of having two

different types is to develop an actuator that could be used for the two different cases of tactile displays described in the introductory section. The main components of these actuators include the touch sensitive layer, the coil, a permanent magnet, skin contactor, and a Polydimethyl Siloxane (PDMS) packaging. The integration and packaging were carefully designed to reduce damping of the actuation/vibration.

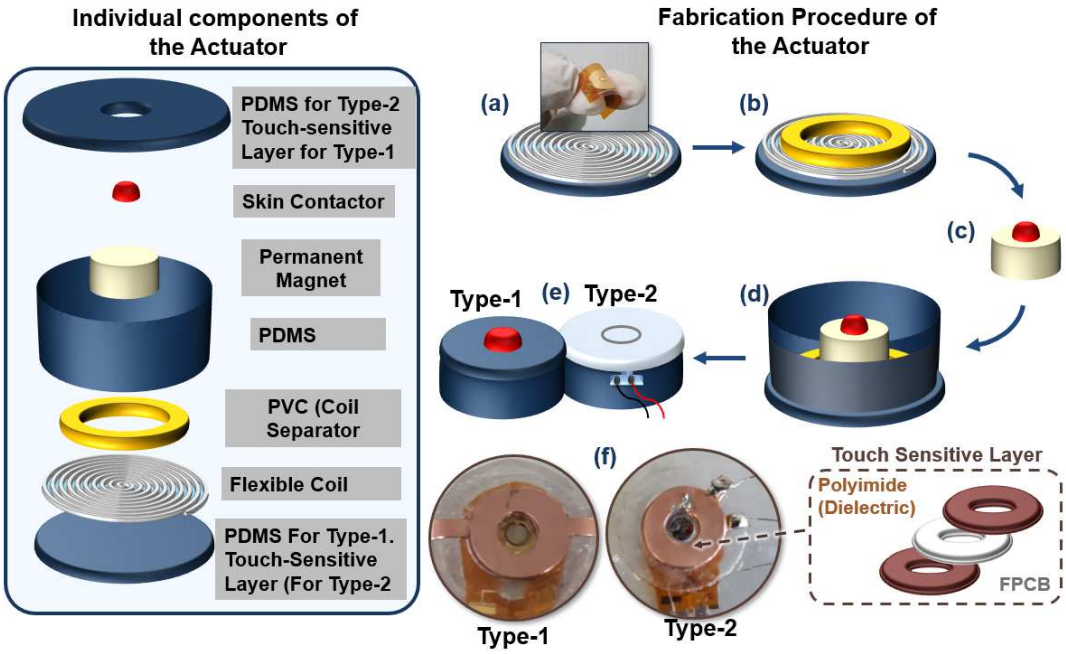

Fig. 5-11 Fabrication steps for the realisation of the touch-sensitive actuator

The actuator has a diameter of 15mm and was designed to fit appropriately into the finger. It was realised layer by layer as shown in Fig. 5-11 . A cylindrical mold with 15mm and 19mm inner and outer diameter respectively was designed and printed with 3D printer for the PDMS packaging. The mold is for the body of the actuator and meant to realise a PDMS packaging of diameter 15mm and height 3mm, with a hole of 1mm inner diameter for the movement of the skin contactor.

For the Type 1, PDMS (Sylgard 184) comprising of 10:1 mixture of pre-polymer base and crosslinking agent was prepared and poured into the mold and then cured at 80°C in the oven for 15 minutes. The same PDMS was also used to bond the touch-sensitive layer (described in previous Section), to the coil and cured for 10minutes (Fig. 5-11). The coil separator was then attached to the coil substrate (Fig. 5-11 (b)) using Loctite transparent adhesive. The permanent magnet used is a 2mm thick N42 grade Neodymium magnet from E-Magnets comprising of ~29%-32% Neodymium, 64.2% to 68.5% Iron and 1% to 1.2% E-Boron (NdFeB). A 1mm^2 skin contactor (made of Polylactic acid (PLA) plastic) was attached to

the permanent magnet using a Loctite transparent adhesive, and both placed on the coil separator. The actuator was then packaged with the cured PDMS described earlier in this section (Fig. 5-11).

The Type-2 actuator was realised in a similar way as Type 1, the major difference being the position of the touch-sensitive layer (Fig. 5-11). So, to realise the Type-2 touch-sensitive actuator, Sylgard 184 comprising of 10:1 mixture of pre-polymer base and crosslinking agent was spin coated on the coil at a spin speed of 200 RPM resulting in a thickness of (~110±10 µm) PDMS layer to protect the coil surface. The coil separator was then attached to the coil substrate (Fig. 5-11 (b)) using Loctite transparent adhesive. This was followed by placing the magnet with the attached skin contactor on the coil separator and then all were packaged using the cured PDMS. Finally, the touch-sensitive layer was attached to the surface of the structure having the skin contactor.

5.5 Characterisation of the Actuation Module

The two main modules (touch-sensing and actuating layer) that make up the touch-sensitive actuator was first characterised separately and then together. The displacement (actuation) characterization (the frequency and the amplitude characteristics) of the actuator in response to varying current pulse input has been carried out by employing optical lever technique. This optical lever method is a familiar and simple approach by which small static/dynamic displacements can be magnified and projected on a screen or recorded on a suitable media such as photographic plates, camera etc.

This magnified signal with proper calibration can be utilized to determine the original displacement accurately. During the experiment, a custom-made optical lever was used (Fig. 5-12) which consists of a pointed laser source, a reflective mirror on the top of the actuator, a white screen and a high speed camera which can record at 960 frames per second (fps). To drive the actuator, a signal generator, power supply and a simple constant current drive circuit was employed Fig. 5-12 . During the initial experimental setup, an adjustable stand was firmly secured to an optical table and the pointed laser source carefully attached to it. The actuator was equally attached on the optical table using double-sided tape with proper precautions to reduce damping effect. In order to be able to capture the reflected spot of laser light, a white screen was positioned accordingly and a high-speed camera mounted using a grip-tight camera adjustable tripod stand. Prior to measurements, the pointed laser was directed onto the reflective mirror on top of the actuator and adjusted properly to obtain a

sharp spot on the screen. The camera was equally adjusted to ensure it captures the spot properly and the setup was left undisturbed throughout the experiment.

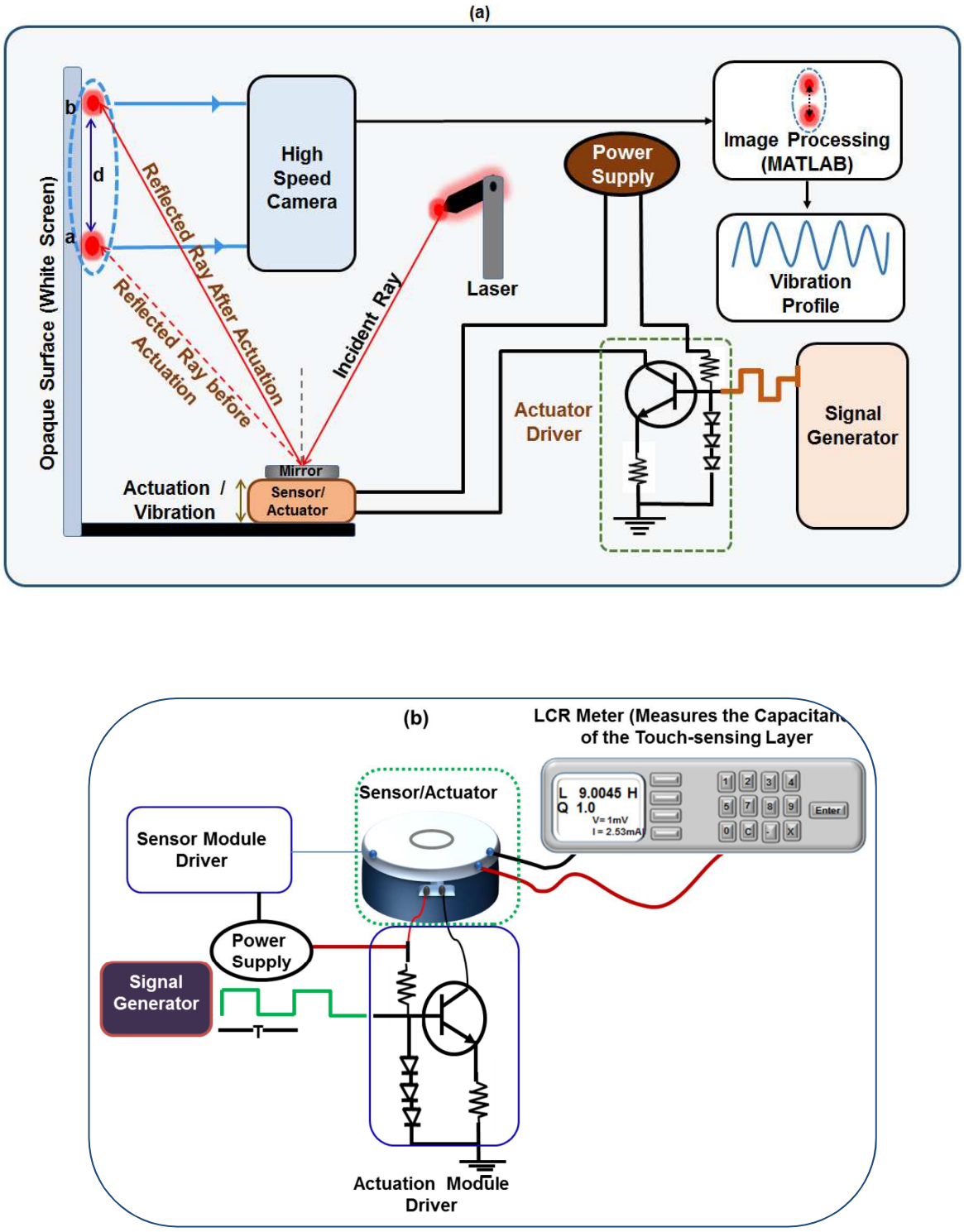

Fig. 5-12 Setup for the characterisation of sensing and actuating module (a) Setup for the characterisation of the sensor module (b) Setup for the characterisation of the actuating module

During the experiment, the actuator was driven using a uniform square pulse of current at different frequencies ranging from 10Hz to 200Hz. This produced a pulsating magnetic field

of corresponding frequency along the axis of the coil. The produced magnetic field exerts a periodic magnetic impulsive force on the tiny magnet of the actuator which causes a corresponding displacement and hence vibration of the actuator. The displacement was observed at a higher magnitude as an oscillatory displacement of the laser spot on the screen. The motion of the laser spot during the vibration of the actuator was recorded with the high-speed camera at a frame rate of 960fps. With proper calibration and using digital signal processing, the recorded video was processed by a MATLAB program (this was written outside work in this thesis by W.T.N) to obtain the dynamic response of the actuator.

Fig. 5-13 (a) and (b) shows the normalised displacement of the actuator at 30mA and 150mA repectively for frequency ranging from 10Hz to 200Hz. This significantly shows higher displacement for lower frequencies as compared to higher frequencies with maximum displacement (~ 191µm) observed at 40Hz.

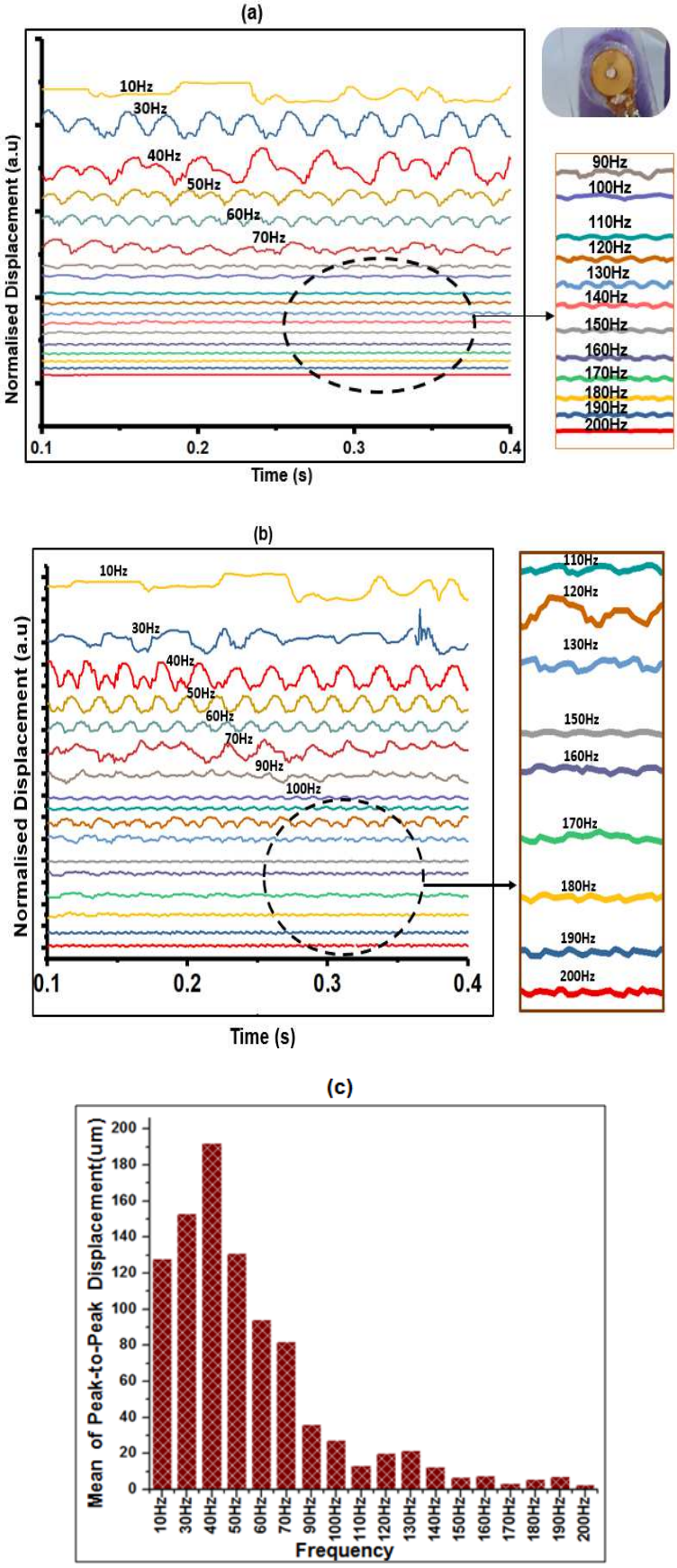

Fig. 5-13 Normalized displacement of the actuator at 30mA for frequencies ranging from 10 to 200Hz (b) Normalized displacement of the actuator at 150mA for frequencies ranging from 10 to 200Hz (c) Mean peak-to-peak displacement of the actuator

5.6 Characterisation of the Sensor Module

The response of the sensor layer characterisation is shown in Fig. 5-14. It was carried out using Keysight E4980AL precision LCR metre, and a LabVIEW program installed in a computer for automatic reading of the capacitance values. Capacitive values were read with the LabVIEW program for the case when actuator was touched and the vibration OFF and then ON. The same setup for the characterisation of the vibration was used to drive the actuator by making it vibrate at different frequencies 10Hz to 200Hz using a square wave of 5Vp-p, 50% duty cycle and zero offset. The results were similar, and so only the response of the actuator at frequency of 40Hz is presented as shown in Fig. 5-14 which is for Type-1 and 2 respectively. The mean of the relative change in capacitance ($\Delta C/C_0$) is (~ 0.33 and 0.34 for Type 1 touch plus no vibration and touch plus vibration respectively. For Type 2, the mean of the relative change in capacitance is ~0.43 for touch without vibration and ~0.31.

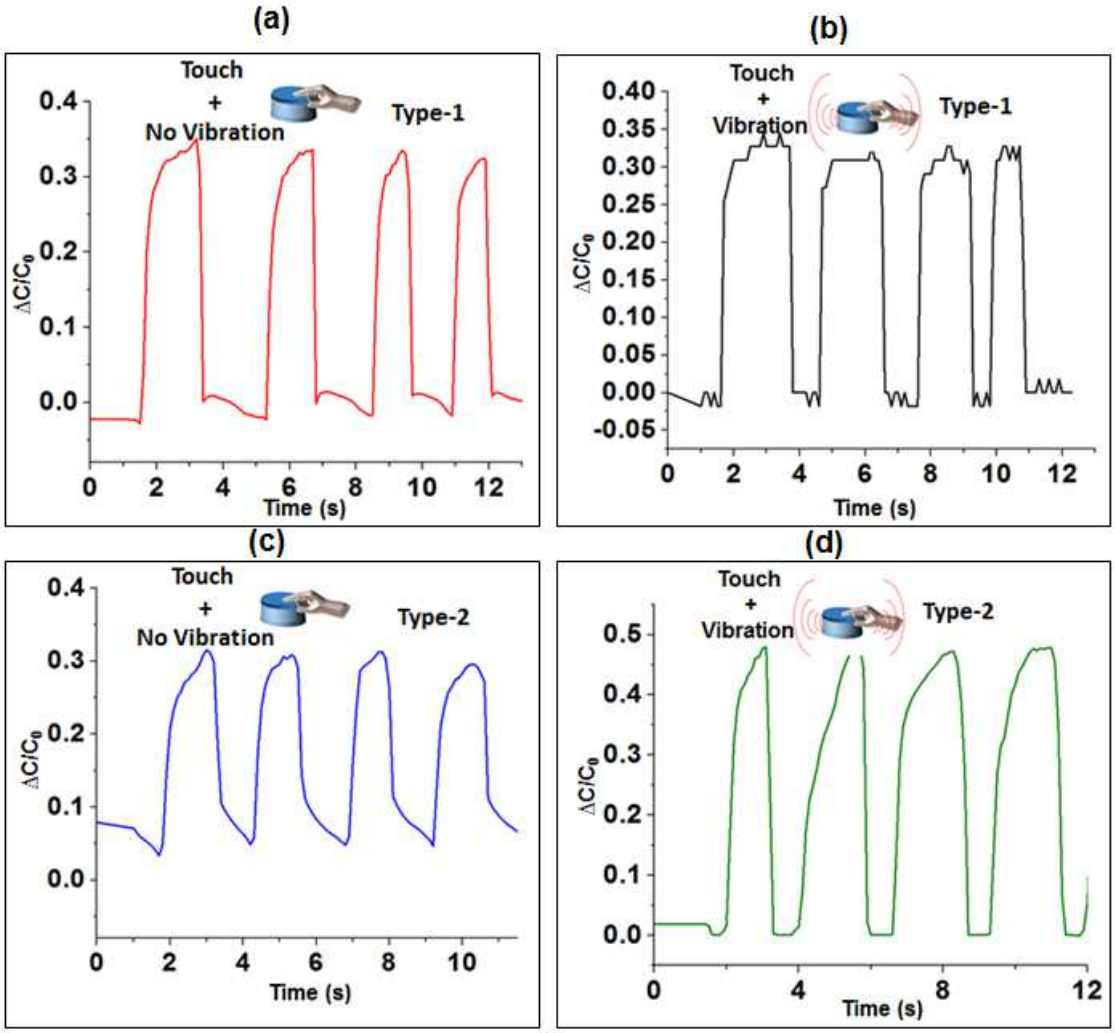

Fig. 5-14 Characterisation of the Touch Sensitive module

5.7 Application of Touch-sensitive Actuator

Fig. 5-15 shows the block diagram and result of testing the actuator with a mobile app developed in this work. This is to demonstrate one of the applications of the actuators which is wireless communication between either deafblind-to-deafblind or deafblind to hearing and sighted person, just as represented by the generic communication system presented in Chapter 4. The system comprises of four main modules (1) the fabricated touch-sensitive actuators (2) the control module including the drive and readout circuits (3) the wireless module (4) the mobile app. The actuator is used for sending and receiving information, the for deafblind- to -deafblind communication, each deafblind person wears the actuator, while for deafblind to hearing and sighted person, the deafblind uses the actuator to communicate with a mobile phone held by the sighted and hearing person. So, messages are sent by the deafblind using the touch-sensitive layer of the actuator and then received via the actuator in form of vibration.

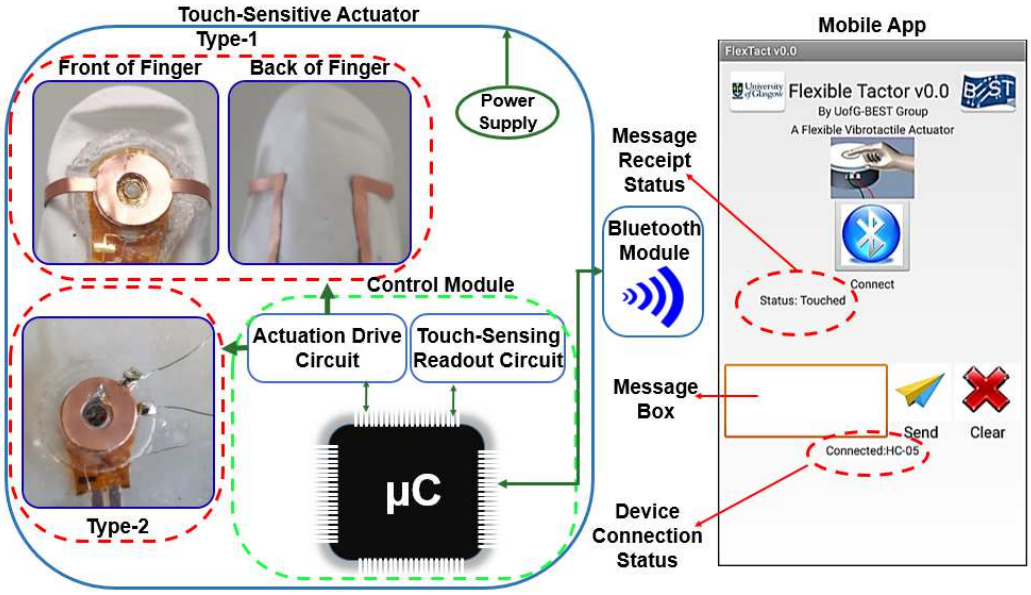

Fig. 5-15 Block Diagram of implemented wireless application using the actuator

Here, only the case of deafblind-to-hearing and sighted person is demonstrated with a single fabricated actuator. This demonstration was achieved using a mobile app which communicates with the actuator via Bluetooth. When the app is launched, the user presses the connect button to connect with the actuator and a connection status is displayed (see device connection status in Fig. 5-15). To communication from app to actuator, the user types a number in the message box of the app and sends it to the actuator via Bluetooth. When the actuator receives this information, it vibrates accordingly. When the number “1” is sent from app for instance, the actuator vibrates once, and when “2” is sent it vibrates

twice. To demonstrate the communication from actuator to the mobile app, the user of the actuator touches the actuator, this touch is then sensed, and the information sent to the mobile app via Bluetooth. When the mobile app receives this information, it displays the word "Touched" and "None" otherwise (see message receipt status in Fig. 5-15). Both type-1 and 2 actuators were tested; the app received data correctly while the actuators vibrated accordingly.

5.8 Summary

In this chapter, novel touch-sensitive actuators were fabricated and characterised as an alternative for the actuators used in the prototypes developed in Chapter 4. Particularly this is applicable for the British Deafblind Manual Alphabet (B-DMA) glove implemented in POC (Chapter 4) as well as other deafblind manual alphabets. One of the limitations pointed out in the literature review is that existing tactile displays do not have inherent capability for tactile sensing and feedback. So, the tandem combination of the sensor and actuator in one device give it an advantage and makes it a potential to be used in a tactile display for communication by deafblind people. An app developed for this purpose was used to send and receive message from the actuator demonstrating its application for communication between deafblind people and mobile phone users. The touch-sensitive actuator was able to overcome the limitations in the use of commercial sensors and actuators for deafblind communication- which include the inability to integrate localised tactile sensing vibrotactile feedback at the same point.

The following chapter presents the Fabrication of a novel inductance-based pressure sensor as well as capacitive tactile sensing array. The former is applicable in Finger Braille glove while the latter is for Block alphabet communication as well as for B-DMA and other deafblind manual alphabets (e.g. Lorm, and Malossi - described in Chapter 2).

Chapter 6

6 Design and Fabrication: Tactile Sensors

This chapter presents the design, fabrication and characterisation of a capacitive tactile sensing array as well as a single element inductance-based pressure sensor. As presented in Chapter 2, Block letter is one of the tactile communication methods used by deafblind people. This is a method in which a communicating partner manually writes the English block letters on the palm of the deafblind person who then intuitively interprets what was written. In this chapter, a tactile sensing array was fabricated, and a communication system was implemented enabling deafblind people to independently communicate with humans as well as robots using this method. It is particularly intended for deafblind people who have acquired a language (English) before they became deafblind. The motivation for developing a tactile interface applicable to this method is to provide an effective alternative to manual writing (by communication partner) of these letters on the palm of the deafblind person. So instead of a communication partner writing on the palm of the deafblind person, the deafblind person can wear a glove which is equipped with this array of tactile sensors and independently write the block letters on it. The information is then sent wirelessly to the communication partner. The system of using block letters is also applicable to sighted and hearing people who know the English alphabets. It could also be modified and used for B-DMA as well as other deafblind manual alphabets.

Also presented here is an inductance-based pressure sensor which is meant to be used as an alternative for the commercial sensors used in smart finger Braille. The fact that it uses a spiral coil means that it could also be adopted for the sensing layer of the actuator presented in Chapter 5. So, with an appropriate design, the same coil could be used for both sensing and feedback.

6.1 The Capacitive Tactile Sensing Array

The structure of the fabricated capacitive tactile sensing array is shown in Fig. 6-1 . It is made up of diamond-shaped row and column electrodes similar to that used for some touchscreens. By touching a particular point on the array, the mutual capacitance C_m (see Fig. 6-1 (b)) between nearby row and column electrodes changes and through quick scanning of the rows and columns, the particular touch point is determine.

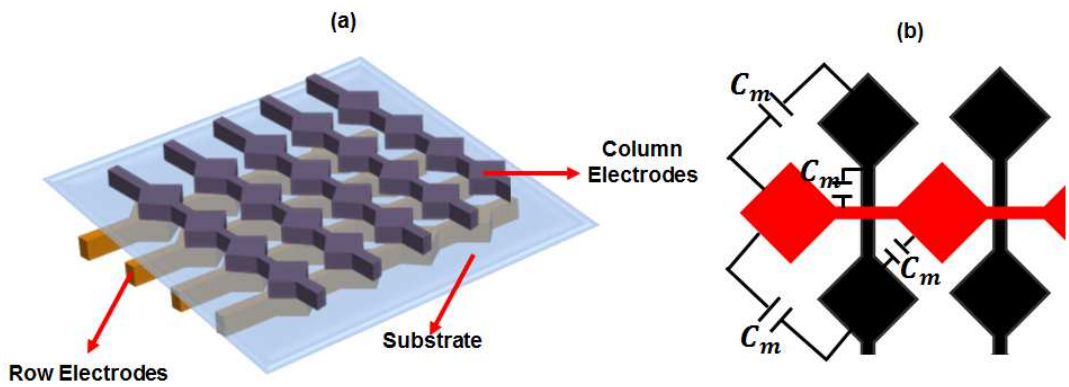

Fig. 6-1 Structure of the Capacitive Sensing Array

The touch-sensor array is based on the capacitive sensing similar to the implementation reported in [51] and details of how it works is presented in Chapter 2 (Section 2.4.2). The response of the touch sensors was converted from capacitive variation to a voltage through a circuit interface shown in Fig. 6-2 and this is based on Equation (6-1).

$$C = I_C(\Delta V/\Delta t)^{-1} \tag{6-1}$$

Where, C is the capacitance of the touch sensor, I_C is the constant current through the capacitor, ΔV is the change in voltage, and Δt is the change in time. The readout circuit is custom-made and built by William Taube for reading out the response of capacitive arrays. It uses a 18F45K22 PIC microcontroller to process the row and column capacitance values to determine the location of touch or contact on the array. For testing, these values were read into a LabVIEW program running on a computer via the serial port using MAX 232.

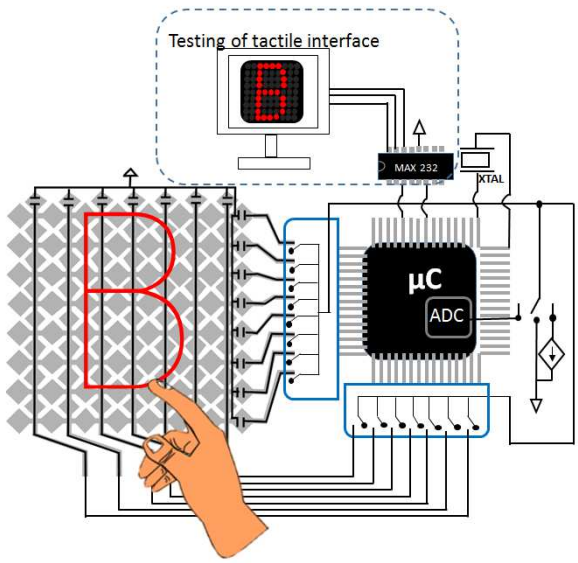

Fig. 6-2 Readout schematics for the capacitive tactile sensing array (Circuit used in [51] by W. T. Navaraj)

6.1.1 Fabrication of the Capacitive Tactile Sensing Array

The touch sensor array was fabricated on a flexible 80µm PVC substrate. The sensor has column electrodes deposited on one side of the PVC and row electrodes on the reverse side. A 90mm x 90mm shadow mask with a 1mm resolution between row and column electrodes was made using Polyvinyl Chloride (PVC) sheet and its design is shown in Fig. 6-3 (a) - (c). This was realised by correctly designing the pattern in graphics software as per dimensions shown in Fig. 6-3 (a) - (c) and then cutting this pattern on a laminated 80µm-thick PVC sheet using Silhouette Cameo 2 cutter. The dimensions were chosen to be able to fit into the palm area. The software of Silhouette Cameo 2 has a built-in library of different materials with options of editing their properties.

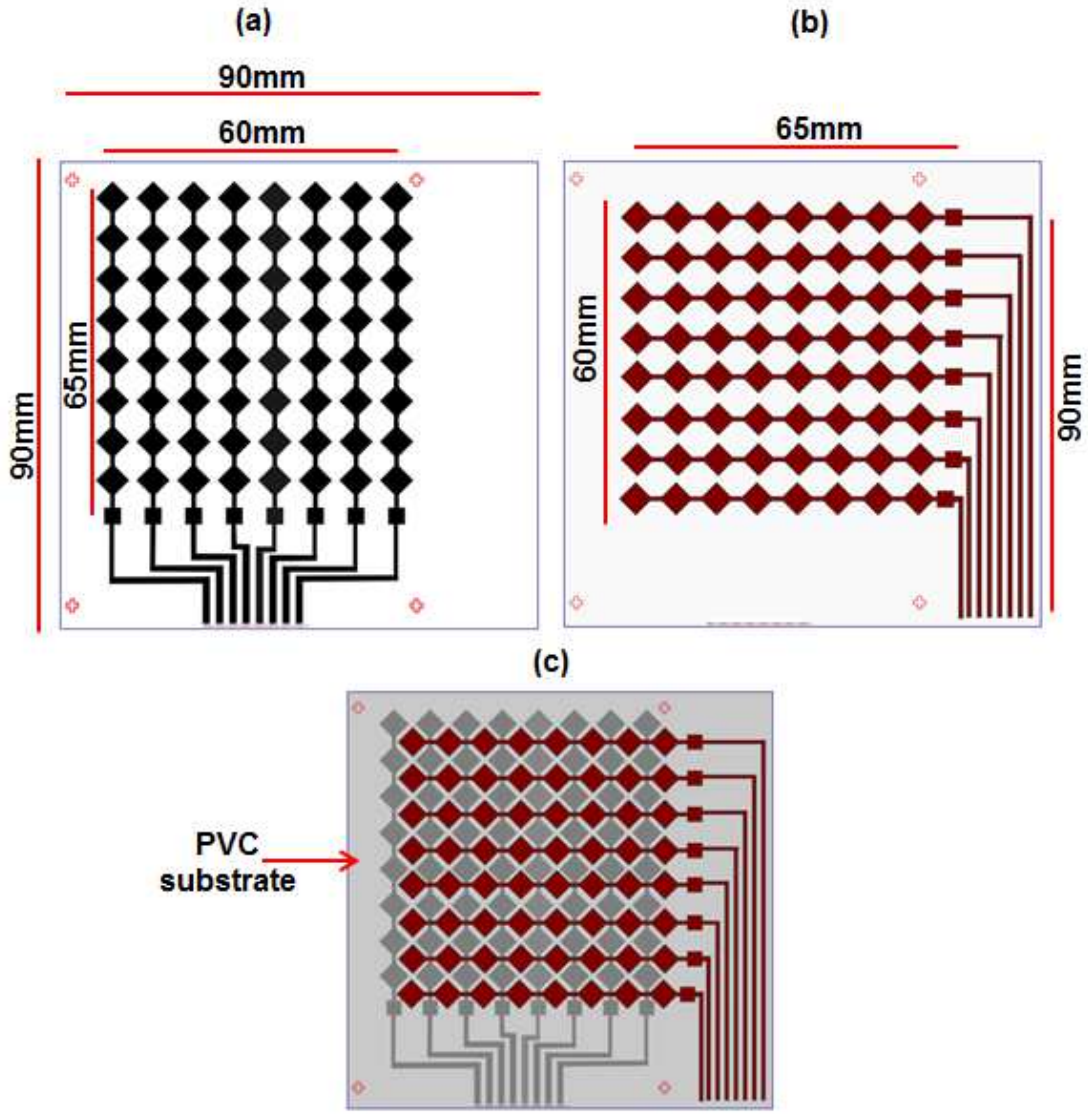

Fig. 6-3 Mask design for the deposition of column electrodes (b) Mask design for the deposition of row electrodes (c) Aligned row and column mask on the substrate

A PVC sheet was placed on a sticky cutting mat for improved accuracy and to avoid the overlapping of patterns. The blade of the cutter was set to position 10 and the mat with the PVC was loaded. Next the designed pattern was loaded on the Silhouette Cameo2 software, scaled, and then the cutting speed was set to 5cms-1 with a thickness of 33 and blade position of 10. Two masks were created, one for the column electrodes and the other for the row electrodes as shown in Fig. 6-3 (a) and Fig. 6-3 (b) respectively. The same settings were used in each case. After the cutting, the masks were aligned properly on the PVC substrate (one on each side) ready for metal deposition.

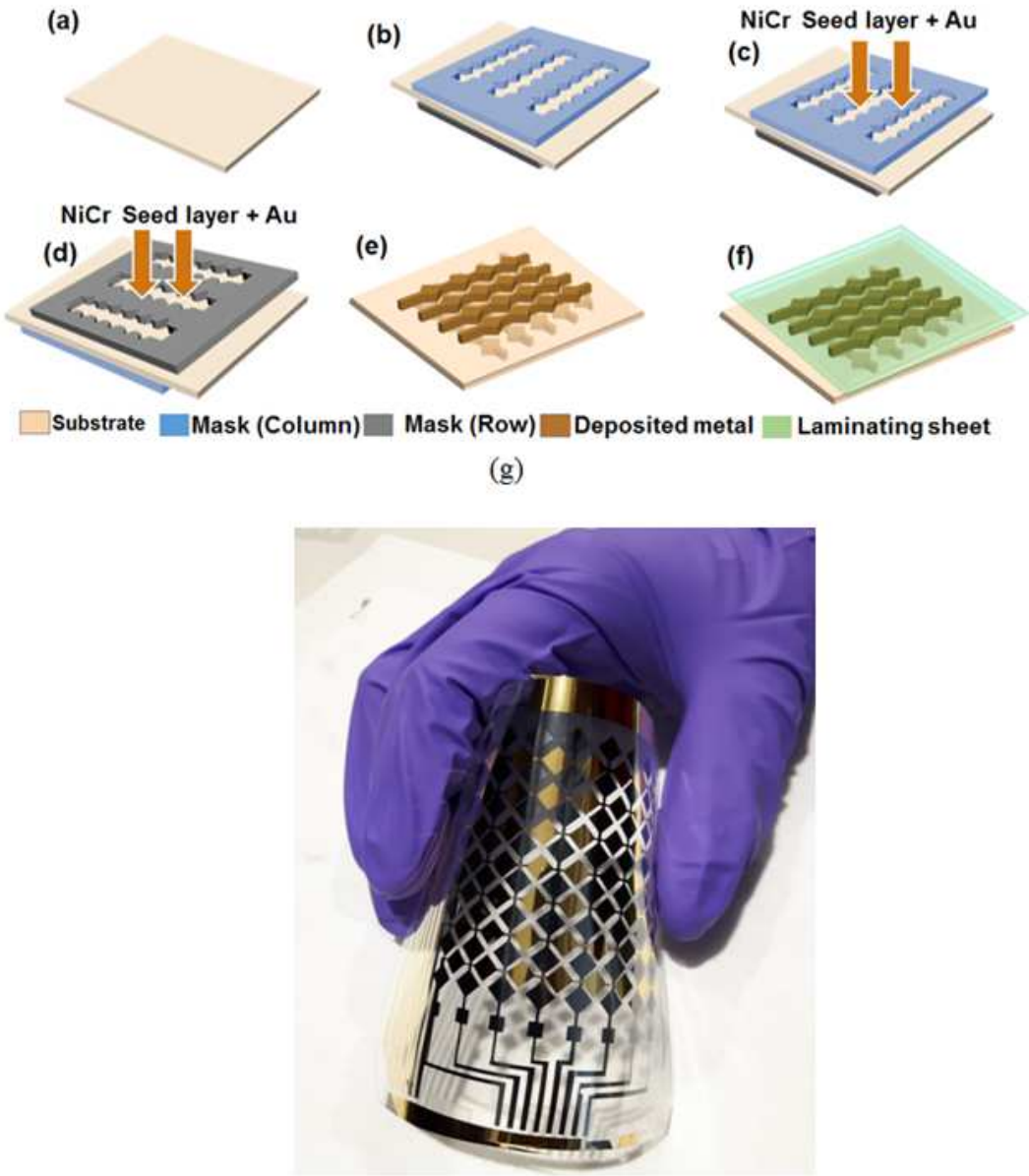

Fig. 6-4 The fabrication steps and the fabricated touch sensor array. (a) Initial flexible PVC substrate (b) Alignment of shadow-mask on the top and bottom of the PVC substrate (c) Deposition of column electrodes (20/120nm NiCr/Au) (d) Deposition of row electrodes (20/120nm NiCr/Au) (e) Removal of shadow mask (f) PVC lamination (g) Fabricated capacitive sensor array

The deposition of the row and column electrodes was carried out using the custom designed shadow masks. Plassys MEB 550S Electron Beam Evaporator system was used to deposit the electrodes (20/120nm NiCr/Au) on both sides of the substrate thereby resulting in the row and column electrode configuration. During metal deposition, the designed mask was attached to the sample holder of the E-beam evaporator. After the deposition of the electrodes, the hard mask was removed, and the surface of the sensor laminated with another piece of PVC sheet to protect the electrodes.

6.1.2 Characterisation of the Capactive Sensing Array

The performance of the implemented system was evaluated using four main tests: (1) Evaluation of the response of each pixel on the sensor array; (2) Evaluation of the feasibility of the system for Block letter communication; (3) Evaluation of the performance of the Convolution Neural Network (CNN); (4) Control of a simulated Baxter robot using the English block letters.

The tactile sensor array was interfaced to a LabVIEW program through a custom-developed hardware as shown in Fig. 6-5 . The program's user interface has two main windows: (a) an array of points that corresponds to locations on the sensor array, and (b) A decay graph. Both windows were used to show the sensor's response to a touch event. A touch event is represented in the LabVIEW program by: (i) A red dot in the in-pixel map; (ii) a white square in the decay graph which gradually turns blue upon the release event. The performance of the implemented system upon touch and release event at various taxels is shown in Fig. 6-5 (a) - (f).

Further, testing was carried out to analyse feasibility of the system for tactile communication. This was done by writing English alphabets on the touch sensor array. As a representation, the result of writing letter "I" on the array is depicted in Fig. 6-5 (g) – (l).

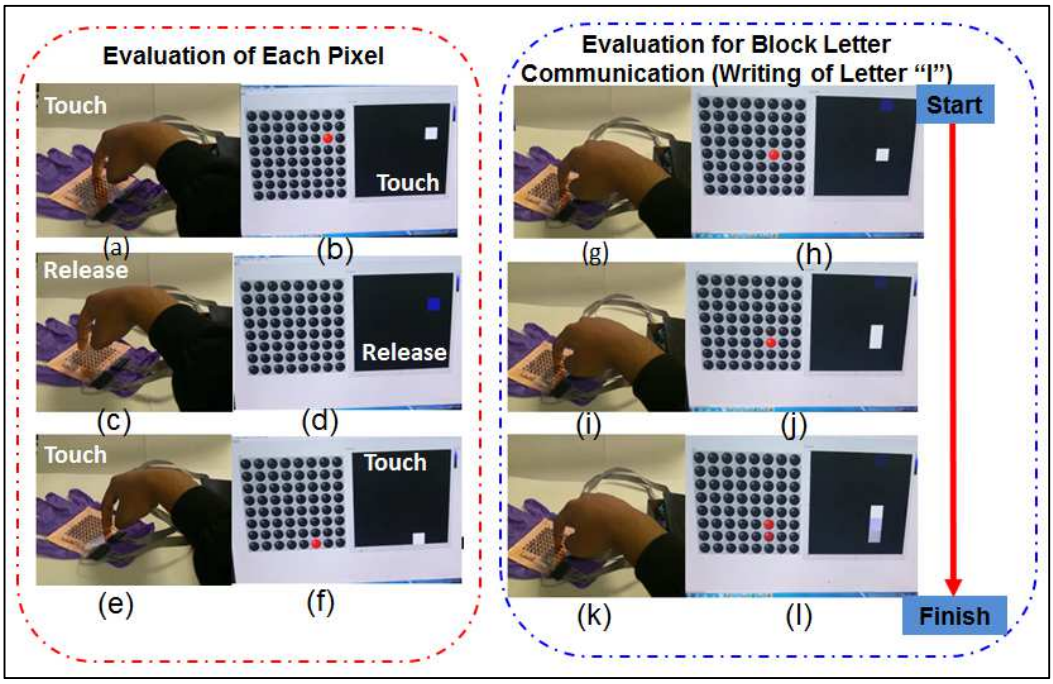

Fig. 6-5 Evaluation of the capacitive sensing array –(a)-(f) Evaluation of each pixel (g)-(l) Evaluation for writing Block letters (Letter "I")

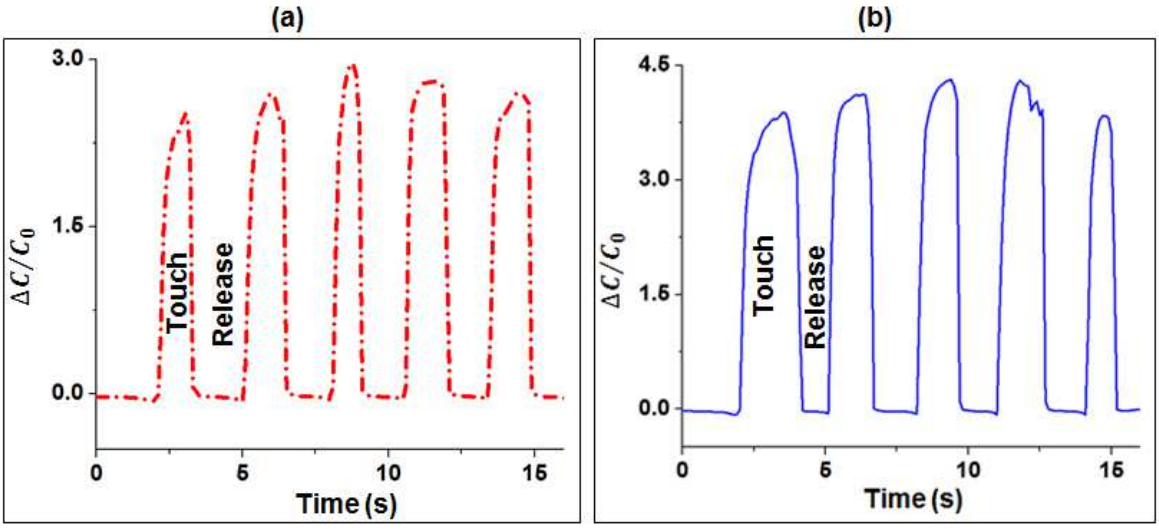

Fig. 6-6 Relative capacitive change for the pixels (a) Slight touch (b) Absolute touch

Fig. 6-6 shows the relative capacitance change as recoded using a Keysight E4980AL LCR meter connected to the array during the touch events. Fig. 6-5 (a) shows the capacitance change for five slight touch and release event on a single taxel while Fig. 6-5 (b) shows the capacitance change of an absolute touch on the taxel. The base value of the recorded capacitiance is 6.78pF at 10kHz frequency.

6.2 Flexible Inductance-based Pressure Sensor

This section presents the fabrication of a flexible inductance-based pressure sensor applicable as a tactile interface in assistive communication devices for deafblind people. The sensor has the potential to be used as a standalone/single element pressure sensor or developed in the form of an array for assistive communication by deafblind people. It can also be integrated in the touch-sensitive actuator presented in Chapter 5. Given that this sensor and the actuator use electromagnetic principles, then with adequate scaling, the same coil could be adopted for both sensing and feedback.

Here a single element inductance-based pressure sensor is presented as an alternative for the commercial tactile sensor used for the finger Braille communication glove presented in POC (Chapter 4). Eventually this will support the fabrication of flexible assistive communication gloves for the deafblind.

6.2.1 Design of the Inductance-based Pressure Sensor

The structure of the fabricated inductance-based pressure sensor is as shown in Fig. 6-7. The sensor has two main parts: (1) a spiral coil, and (2) a ferromagnetic elastomer made with a mixture of Ecoflex^{TM} (00-30) and Iron particles. The sensor works through a change in inductance which occurs when a force is applied on it. Every coil carrying current has a characteristic inductance and bringing a ferromagnetic material (like soft Iron) close to it changes this inductance. In this work, a flexible spiral coil was fabricated on a flexible polyimide substrate (using the same method described in Chapter 5) and an elastomer mixed with Iron particles was used to realise a ferromagnetic material.

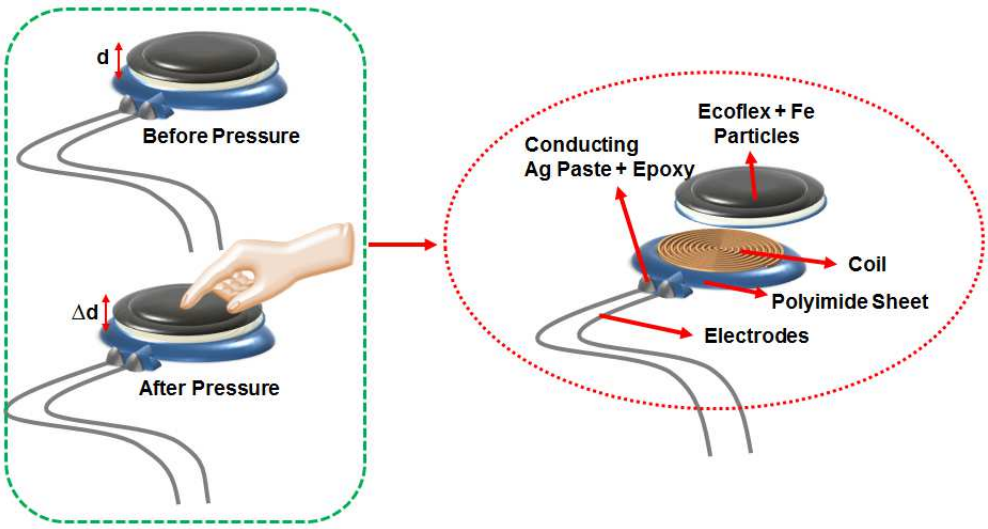

Fig. 6-7 Structure of the Inductance-based Pressuer Sensor

Although different polygonal-shaped spiral coils exist like square, octagonal, and hexagonal shaped coils, the same circular geometry used for the actuator coil presented in Chapter 5 was used. The inductance of the planar spiral coil is generally defined by the number of turns, the turn width, the turn spacing $, s$ and any one of the following: the outer diameter d_{out}, the inner diameter d_{in}, the average diameter d_{avg}, or the fill ratio ρ (See Fig. 6-8).

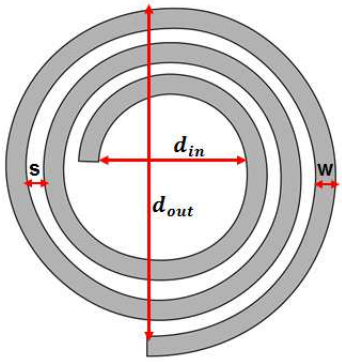

Fig. 6-8 Design of the spiral coil geometry

The inductance of the spiral coil for the sensor is defined by the modified Wheeler's formula [207] as:

$$L_{mw} = K_1 \mu_0 \frac{n^2 d_{avg}}{1 + K_2 \rho} \tag{6-2}$$

Where ρ is defined as:

$$\frac{d_{out} - d_{in}}{d_{out} + d_{in}} \tag{6-3}$$

And d_{avg} is given by:

$$0.5(d_{out} + d_{in}) \tag{6-4}$$

The thickness of the inductor has only a very small effect on the inductance and hence was not a major consideration in this work. However, increasing the thickness of the coil could lead to reduction in the coil resistance and a possible increase in the quality factor (see Equation 6-5). The quality factor of an inductor provides a measure of how much energy is lost each cycle due to resistive losses. An inductor with a higher quality factor will consume less energy per cycle, and so a good inductor needs to have minimal resistance. The quality factor (Q) can be expressed as:

$$Q = \frac{\omega L}{R} \tag{6-5}$$

Where $\omega =$ the angular frequency, L= the inductance and $R =$ the parasitic resistance of the inductor.

6.2.2 Fabrication of the Inductance-based Pressure Sensor

This involves two main processes (1) Fabrication spiral of coil (2) Fabrication of the Ferromagnetic elastomer. The same method used for the fabrication of the spiral coil for the touch-sensitive actuator was also used here and details of the steps are the same as presented in Chapter 5 (Section 5.2). This is one good advantage of the inductance-based pressure sensor as it adopts the same as the touch-sensitive actuator and hence could replace the capacitive sensing structure used. Each of the coils realised is ~17µm thick with 45 turns. Therefore, only the fabrication of the ferromagnetic elastomer is presented here along with how it was used to realise the sensor.

The ferromagnetic elastomer was realised using Ecoflex™ (00-30) silicone from Smooth-ON and Iron powder from First4magnets. Ecoflex was mixed with Iron powder in different ratios as shown in Fig. 6-9 . Different samples were prepared using Ecoflex to Iron ratio of 1:1, 2:1, 3:1, 5:1, 1:2, 1:3 and 1:5 respectively. These samples can be categorised into three:

- Those with equal Ecoflex and Iron by weight (1:1),
- Those with lower Iron particles by weight (2:1, 3:1, and 5:1)
- Those with higher Iron particles by weight (1:2, 1:3, 1:5)

Further increment in the weight of the Iron particles were not considered after 1:5 as it was observed that as from 1:6 onwards, it becomes very difficult to have sufficient Ecoflex that can mix the Iron powder correspondingly.

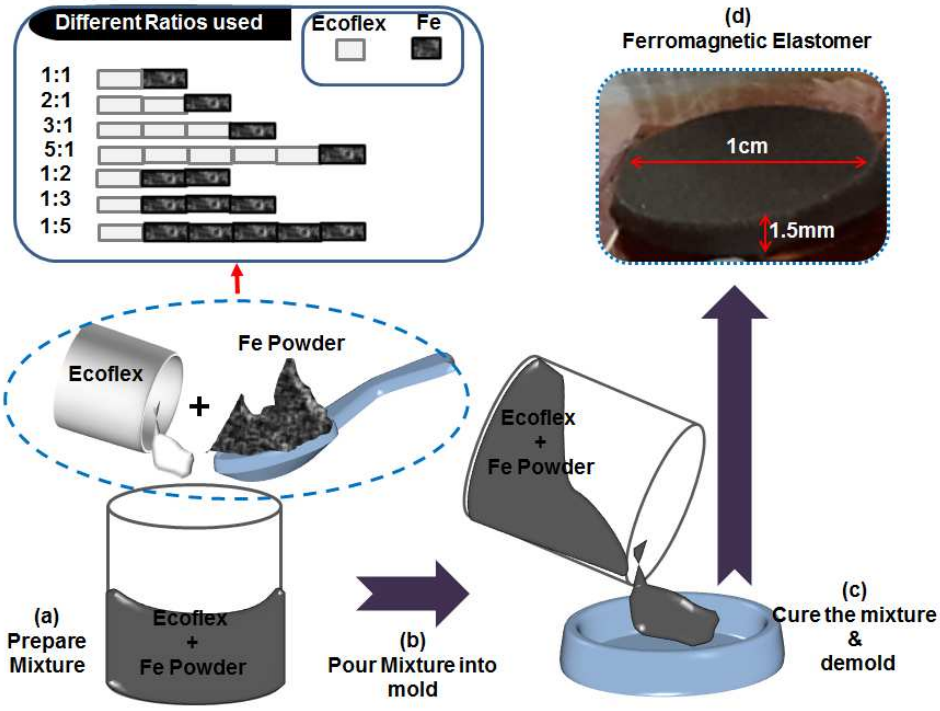

Fig. 6-9 Fabrication steps for the ferromagnetic elastomer

A cylindrical mold with an inner diameter of 10mm, 12mm outer diameter and a depth of 1.5mm was designed using the 3dsMax Computer Aided Design (CAD) software and printed with a 3D printer using Acrylonitrile Butadiene Styrene (ABS) filament. These dimensions were chosen so as to be able to realise an elastomer with 10mm diameter and 1.5mm height as shown in Fig. 6-9 . A diameter of 10mm was chosen as this can easily fit on an average adult finger. After mixing the composites, each of them was poured into its mold and allowed to cure at room temperature for at least 4 hours. After curing, each of the elastomers was demolded to realise a ferromagnetic elastomer. Plain Ecoflex (without Iron particles) was also prepared, poured into the mold and also left to cure for 4 hours before demolding. This is for the purpose of understanding the difference between using plain Ecoflex and a ferromagnetic elastomer. The fabricated sensor is shown in Fig. 6-13 (a).

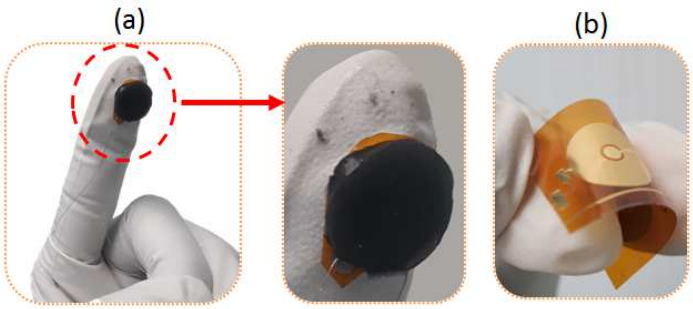

Fig. 6-10 Fabricated Inductance-based Pressure Sensor (b) Flexible coil used for the fabrication of the pressure sensor

Following the fabrication of the ferromagnetic elastomers is their integration with the spiral inductor coil to realise the pressure sensor. First, two contacts were made to the coil's contact pad using two different electrodes connected using a Silver conductive paint from RS-components (186-3600) and Araldite rapid tube epoxy adhesive. For the purpose of the experiment, each of the ferromagnetic elastomers was integrated temporarily on the spiral inductor using a transparent a Scotch tape in order to enable the detachability of the elastomers. In general, seven inductance-based pressure sensors were realised using each of the ferromagnetic elastomers and the characterisation and results are discussed in the following section.

6.2.3 Characterisation and Results

Generally, seven inductance-based pressure sensors were realised using each of the ferromagnetic elastomers. The following investigations were carried out to thoroughly understand the characteristics of each ferromagnetic elastomer and how it affects the performance of the pressure sensors:

- ***Scanning Electron Microscope (SEM) analysis:*** This was carried out to investigate how the iron particles are dispersed in Ecoflex for the different ratios
- ***Inductance and Q-factor at no load:*** This was done in order to investigate how the inductance of the spiral coil varies in the presence of these elastomers before loading, and also to establish their best orientation with respect to integration with the spiral coil
- ***Elasticity of the ferromagnetic elastomers:*** This was carried out to understand how the presence of the Iron particles affects the stiffness of the ferromagnetic elastomers used for the pressure sensor. To achieve this, the following were determined and compared in relation to plain (without Iron particles) Ecoflex.
    - Stress-Strain Relationship
    - Elastic modulus
    - Weight of the elastomers
- ***Sensor performance:*** This was done in order to understand the characteristic performance of the sensors under loading and unloading conditions, including their response time, recovery time as well as sensitivity. To achieve this, the following were determined for each sensor
    - Behaviour under cyclic loading
    - Response time

- Recovery time
- Calibration curve and hence sensitivity
- Response during loading and unloading conditions

6.2.3.1 SEM Analysis

First, SEM analysis of the ferromagnetic elastomers was carried out using a Hitachi S-4700, and SU-8240 Scanning Electron Microscope (SEM) and SEM images of a cross section of the samples are shown in Fig. 6-11 (a) - (g). It was observed that the elastomers do not have an even number of Iron particles dispersed within it and the particles have significantly settled down at the bottom of the mold creating a ferromagnetic elastomer with a gradient of Iron particles from the view of its cross section. For the purpose of analysis and discussion, part of the elastomer with more Iron particles will be called ***"Dense side"*** and its position *(Up or down)* with respect to the coil was varied to investigate the response of the sensor.

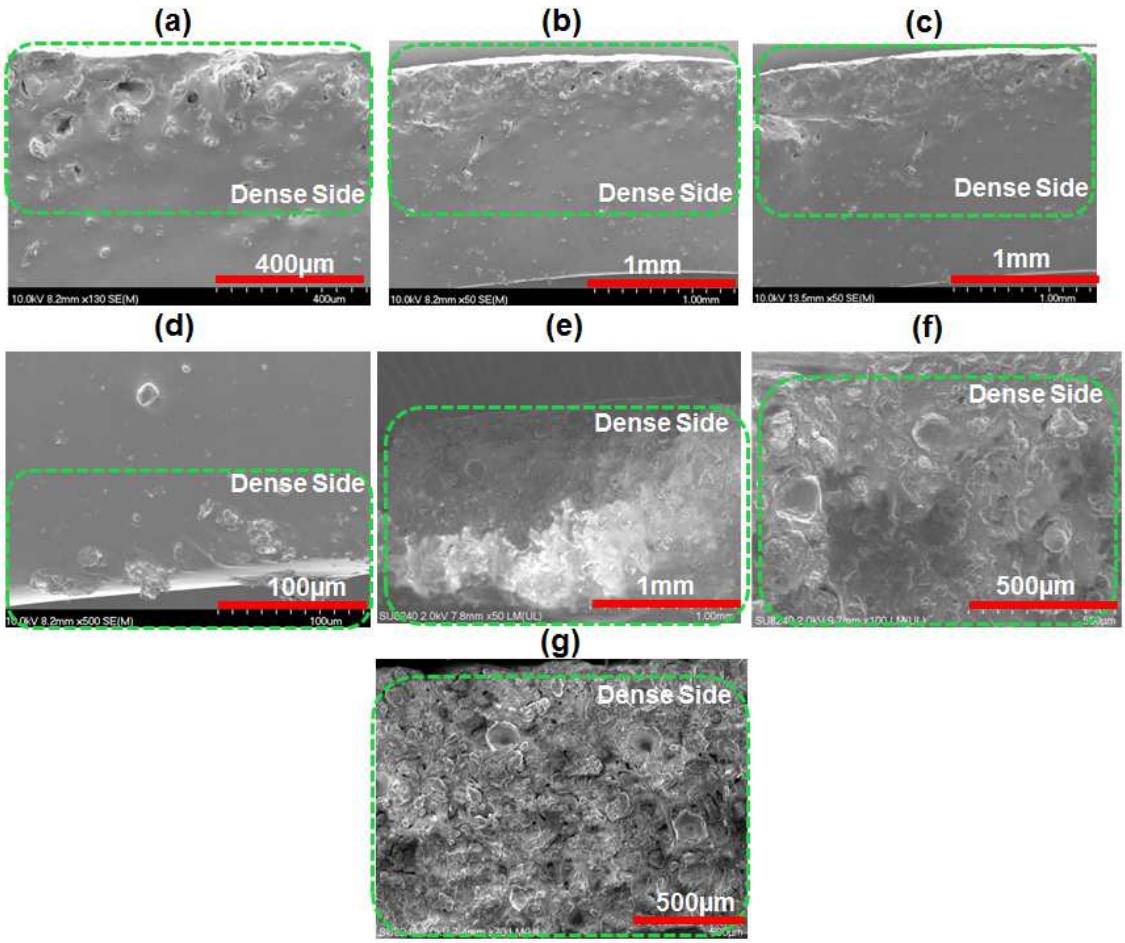

Fig. 6-11 SEM images of a cross section of the ferromagnetic elastomer showing the gradient of the Iron particles that settled after curing (a) 1:1 (b) 2:1 (c) 3:1 (d) 5:1(e) 1:2 (f) 1:3 (g) 1:5

It is important to study the behaviour of the sensor with different sides of the ferromagnetic elastomer integrated on the spiral inductor coil given that the elastomer does not have even

number of Iron particles dispersed within it. This is necessary considering the fact that the presence of the Iron particles in the elastomer is expected to lead to variation in the inductance of the coil and hence performance of the sensor.

To achieve this, the following two conditions were considered for all the characterisation of the corresponding sensors realised using different orientations of the seven ferromagnetic elastomers:

- ***"Dense side down" (DD) -*** When the part of the elastomer with more Iron particles is kept directly on the spiral coil to realise the sensor
- ***"Dense side up" (DU)*** –When the part of the elastomer with less particles are kept directly on the coil to realise the sensor

This means that there are seven sensors realised using the seven ferromagnetic elastomers. (1:1, 1:2, 1:3, 1:5, 2:1, 3:1 and 5:1). For each sensor, the performance was investigated for DD and DU to understand its behaviour and hence determine the best orientation of each ferromagnetic elastomer for each case. For instance, the sensor realised using the 1:1 elastomer will have results for 1:1DD and 1:1DU. This means the different sides (DD and DU) of the 1:1 elastomer were used and the same applies for all the ratios giving a total of 14 different samples (1:1DD, 1:1DU, 1:2DD, 1:2DU, 1:3DD, 1:3DU, 1:5DD, 1:5DU, 2:1DD, 2:1DU, 3:1DD, 3:1DU, 5:1DD, 5:1 DU) that were investigated.

The setup for the characterisation of the pressure sensor is shown in Fig. 6-12. The sensor characterisation was carried out using a vertical linear stage driven by a controllable linear motor with an attached square-shaped glass probe which applies the force on the sensor. A LabVIEW program was used to control the speed and position of the motor as well as to record the change in the inductance of the sensor as read by an Agilent E4980 LCR meter connected to a computer.

6.2.3.2 Inductance/Q -factor at no Load

The inductance and quality factor (Q-factor) of the 14 samples (sensors) were measured. This was carried out to find out the effect of the introduction of the Iron particles into Ecoflex as well as their orientation with respect to the spiral coil. To do this, the different samples were connected in turn to the Keysight E4980AL LCR meter and their inductance and Q-factor measured directly. The elastomer prepared with plain Ecoflex was also integrated to a spiral coil and also investigated. Fig. 6-13

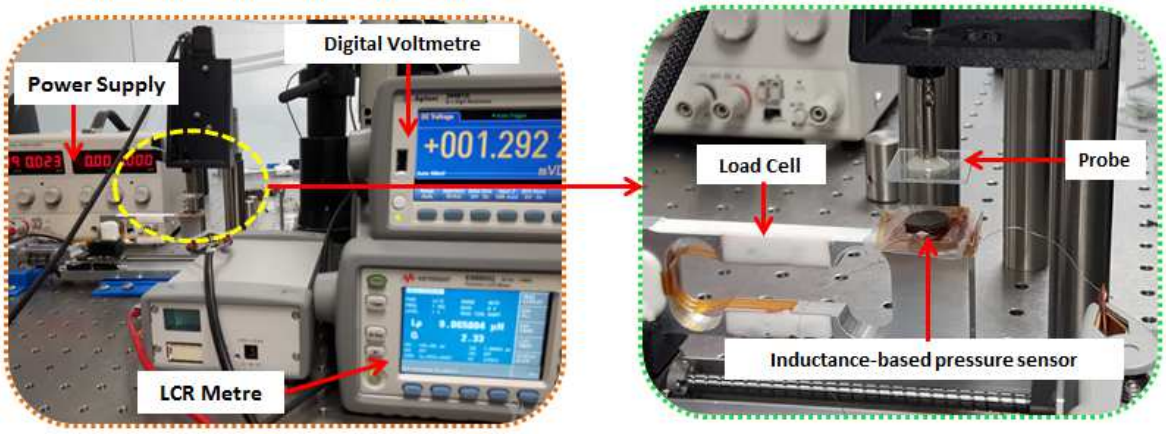

Fig. 6-12 Setup for the characterisation of the inductance pressure sensor

(a) and (b) demonstrates the variation of the inductance and Q-factor for the different elastomers respectively. As expected, an increase in the presence of the Iron particles increases the inductance of the sensor as well as the Q-factor. It equally shows that the pattern of the change in inductance is same for the quality factor and this agrees with Equation 6-5.

Considering the category with lower Iron particles by weight, the inductance of the spiral coil for dense side down and up was seen to be almost the same. This shows that for this category, there is a slight change in the inductance/Q-factor irrespective of the side of the elastomer on coil and then unlikely to affect the sensor's performance in this regard.

For the elastomer with higher Iron particles by weight (1:2, 1:3 and 1:5), significant variation in inductance was observed only for 1:2 and 1:3, while 1:5 showed an insignificant change. In the latter, it is likely that the Iron particles were significantly enough to be dispersed all over and hence both sides of the elastomer had relatively same amount of particles that made their inductance/Q-factor to have insignificant difference at no pressure.

For the elastomers with lower Iron particles by weight (2:1, 3:1 and 5:1), there was equally a change in inductance/Q-factor for both dense side down and dense side up. This shows that there could be a change in the response of the sensor when different sides are used. Furthermore, it shows that in comparison of the inductance of all the ferromagnetic elastomers with plain Ecoflex, a significant effect occurred due to the introduction of the Iron particles into the Ecoflex. It can also be clearly seen that in the case of using plain Ecoflex, the inductance of the spiral coil gave a lower value in comparison with the ferromagnetic elastomers.

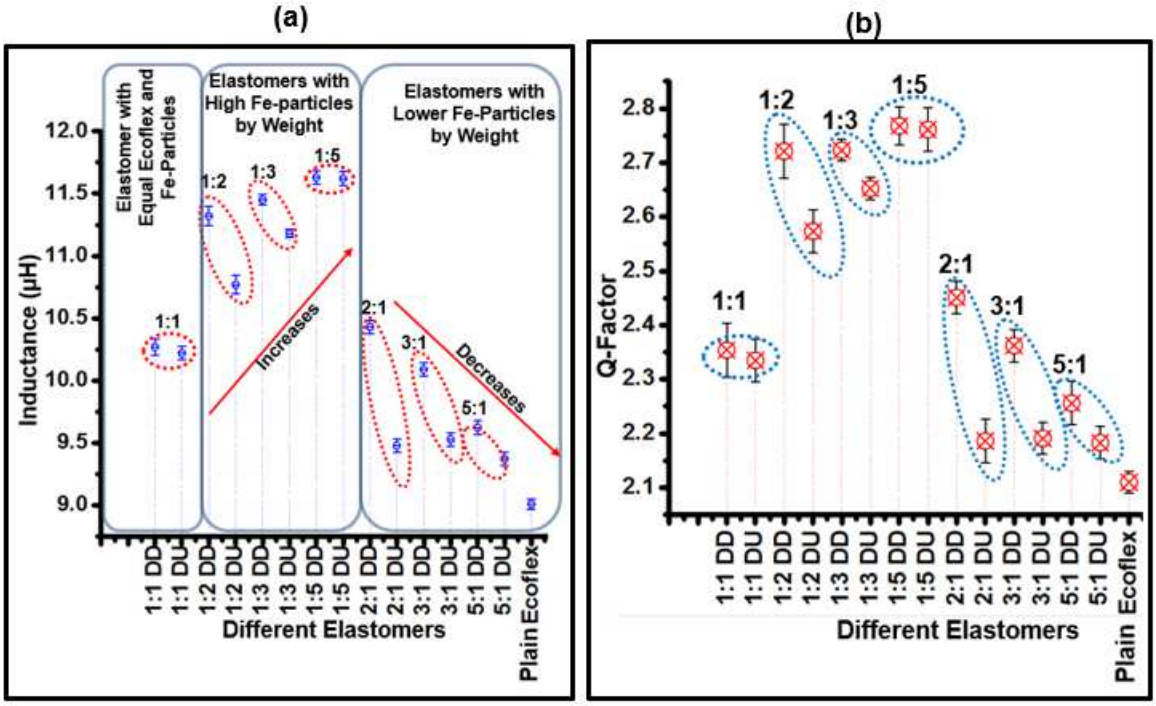

Fig. 6-13 (a) Variation of inductance of the sensor for the different elastomers with no applied pressure (b) Variation of the Q-factor of the sensor for the different elastomers with no applied pressure

This confirms that the presence of the Iron particles in the elastomer leads to a change in the inductance of the integrated spiral coil even before loading.

6.2.3.3 Elastic Characteristics of the Elastomers

Further characterisation of the different ferromagnetic elastomers was carried out to investigate the effect of the Iron particles on the elasticity of the ferromagnetic elastomer. This is important as it could affect the stiffness of these elastomers as well as the response of the sensor with different applied pressures.

In order to characterise the elasticity of the elastomers, each one was attached to a stable 1004 aluminium single point low-capacity load cell which measures the force applied on the elastomer via a square glass probe. The load cell was characterised using a voltmeter and according to its specification gives 1.5mV for every 1N of applied force (with a maximum of 6N). The sensor has an active area of 0.00031m^2, and to ensure even pressure distribution, the glass probe was made larger than the sensor's active area.

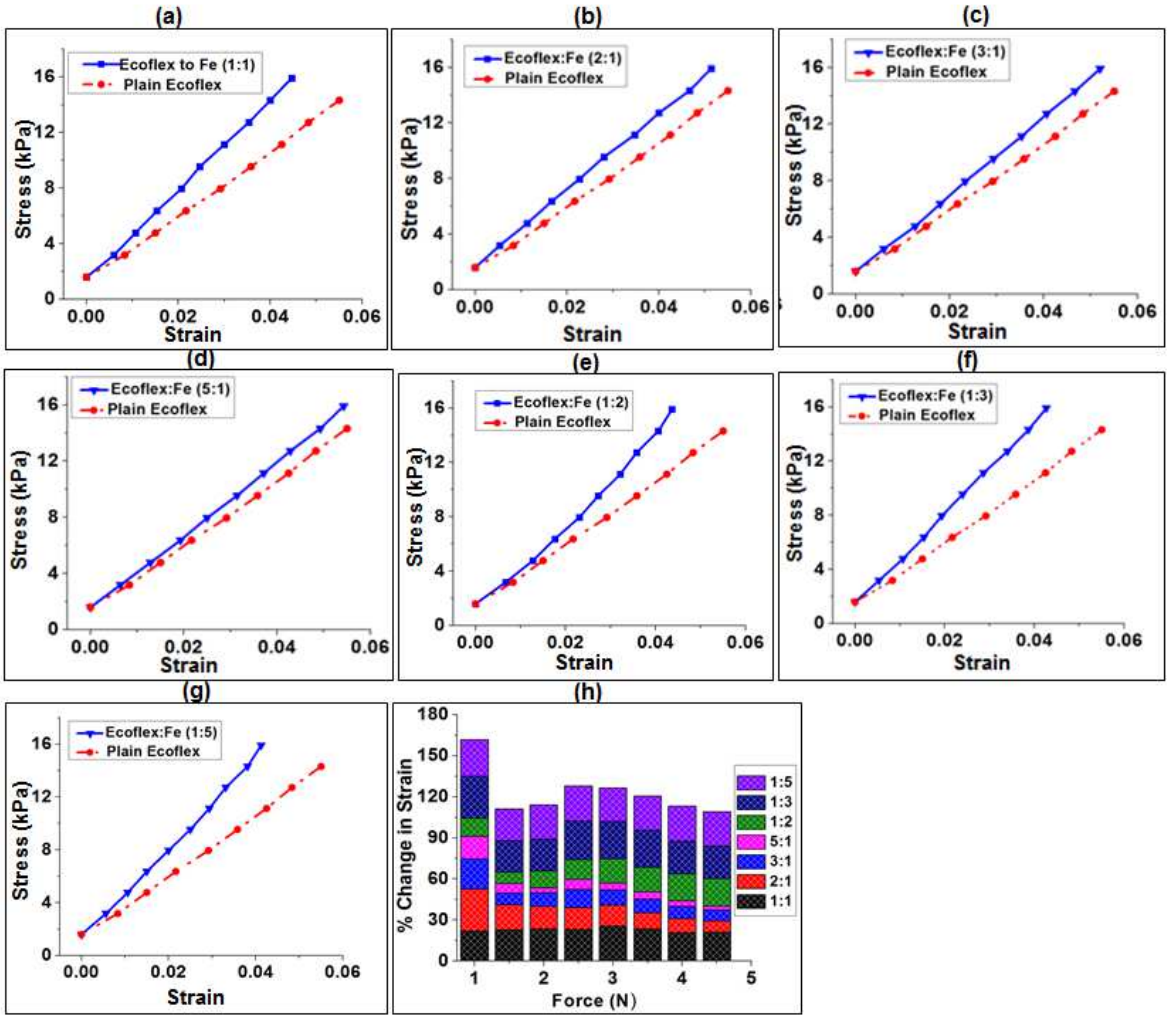

Fig. 6-14 (a) 1:1 (b) 2:1 (c) 3:1(d) 5:1 (e) 1:2 (f) 1:3 (g) 1:5 (h) Percentage change in compressive strain of the different elastomers relative to plain Ecoflex

Forces from 0N to 5N in steps of 0.5N were then applied on the sensors in turn and the motor position in each case was recorded. The motor position helps to determine the distance the elastomer was compressed. So, when force is applied on the elastomer, the initial and current motor positions are noted from the LabVIEW program. The strain was then computed in accordance with Equation 5-14 and the stress from Equation 5-15.

$$Strain = Change\ in\ length/original\ length \tag{5-14}$$

The stress-strain relationship of the different elastomers for different applied forces is shown

$$Stress = Force/Area \tag{5-15}$$

in Fig. 6-14 (a) – (g). It shows that for elastomers with higher Iron particles by weight, there is a gradual shift farther away from that of plain Ecoflex when moving from Fig. 6-14(a) – (g). For the elastomers with lower Iron particles by weight, there is a shift closer to the stress-

strain characteristics of plain Ecoflex when moving from Fig. 6-14 (a) – (g). Fig. 6-14(h) shows the percentage change in compressive strain for the ferromagnetic elastomers relative to plain Ecoflex. It shows that for all applied forces, the change is almost constant for the elastomers with higher Iron particles by weight and lower for the ones with lower Iron particles by weight. This change is relatively smaller for the elastomers with lower Iron particles (2:1, 3:1 and 5:1). This shows that increasing the amount of Iron particles increases the stiffness of the elastomer and hence reduces its compressibility.

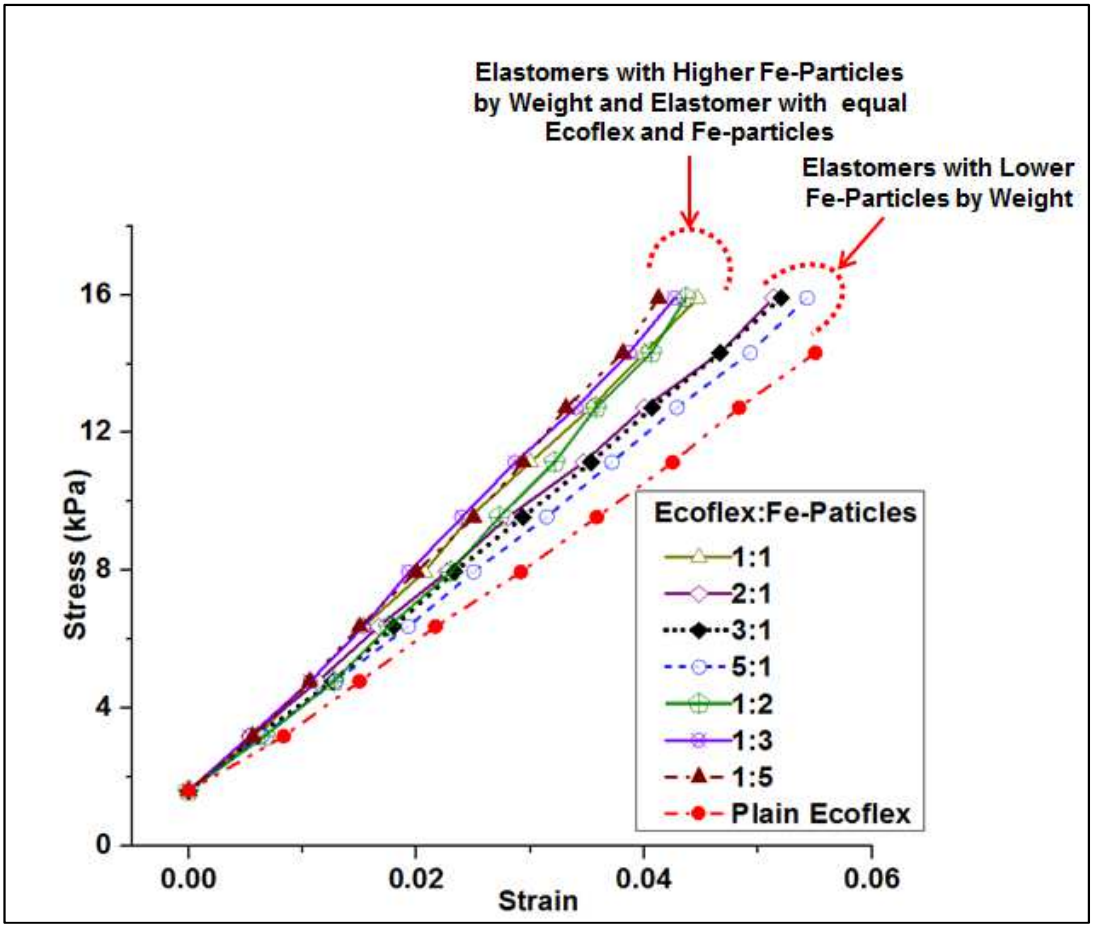

Fig. 6-15 Stress –Strain relationship for all the different elastomers. It shows a slight variation in the strain of the elastomers in the same group and a wider variation across groups

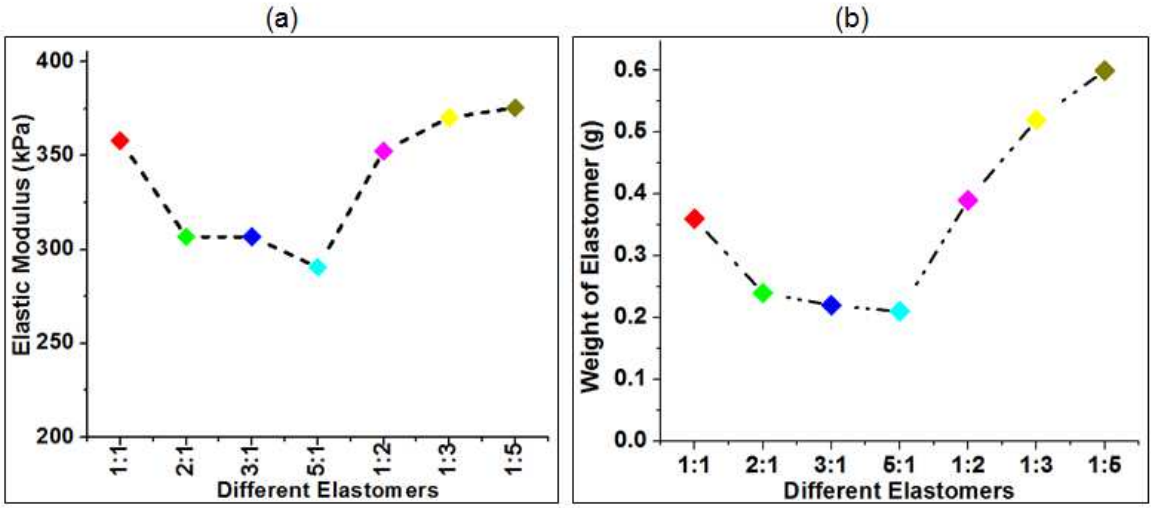

Fig. 6-16 (a) Elastic modulus of the different elastomers (b) Weight of the different elastomers

To further understand the effect of the Iron particles on the stiffness of the ferromagnetic elastomers, the elastic modulus of the different elastomers where computed and their weight measured (Fig. 6-16). The elastic modulus ($E = Stress/Strain$) was computed by determining the slope of the compressive stress-strain characteristic of the different ferromagnetic elastomers. The weights $W(g)$ were measured by placing each one on a weighing scale. Fig. 6-16 demonstrates a relationship between the weight of the elastomer and their elastic modulus. As shown, the 1:5 ratio elastomer which has the highest Iron particle by weight had the highest weight ($W \sim 0.6g$) and also the highest elastic modulus ($E \sim 375.5kPa$). The least weight and elastic modulus was obtained in the case of 5:1 ration elastomer with values of ~ $0.21g$ and $\sim 290.49kPa$ respectively. It can be seen that the elastomers with more Iron particles had higher weights as well as higher elastic modulus and hence stiffness.

6.2.3.4 Sensor Performance

In order to characterise the performance of the inductance-based pressure sensor, each of the elastomers were integrated with the spiral coil and the sensor response to cyclic loading was investigated for the 14 samples of the sensor. Each sensor was firmly attached to the load cell and connected to a Keysight E4980AL precision LCR meter (20Hz to 1MHz) which measures the inductance. It is expected that applying a force on each of the sensor will cause a corresponding change in the inductance of the sensor. The load cell was calibrated using an Agilent 34461A $6_{1/2}$ digital voltmeter in a similar to that used for the elasticity characterisation described in the previous section. The inductance measurement and motor control were automated via a computer running a LabVIEW program. Pulses of 0.5N

(~1.61kPa) force were then applied on the sensor using the square glass probe and the inductance automatically recorded via the LabVIEW program. The different categories of the sensors measured include:

- Sensors with ferromagnetic elastomer having equal Ecoflex and Iron by weight (1:1DD and 1:1DU)
- Sensors with ferromagnetic elastomer having higher Iron particles by weight (1:2DD, 1:2DU, 1:3DD, 1:3DU, 1:5DD, 1:5DU)
- Sensors with ferromagnetic elastomer having lower Iron particles by weight (2:1DD, 2:1DU, 3:1DD, 3:1DU, 5:1DD, 5:1DU)

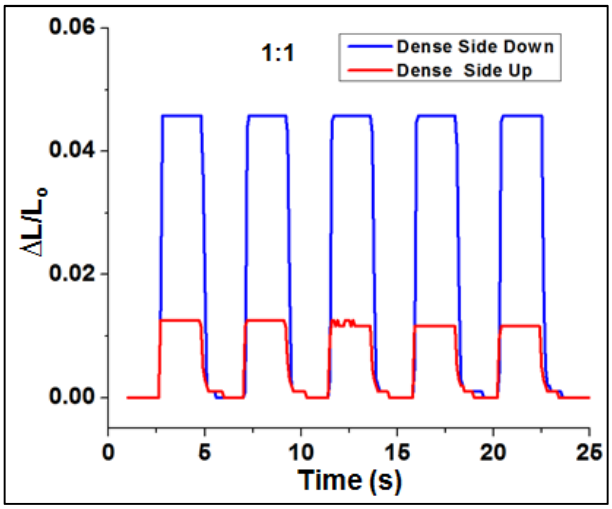

Fig. 6-17 Sensor's response on cyclic loading for the elastomer (1:1DD and1:1DU) with equal Ecoflex and Fe-particles by weight

Fig. 6-17 shows the result of five cycles of loading for the sensor realised with 1:1(DD and DU) elastomer. Calculating the mean of the cyclic measurement shows that the 1:1DD has a higher mean of $(\Delta L/L_0 = 0.0457)$ when compared to that of 1:1DU $(\Delta L/L_0 = 0.0125)$. In order to check the significance of the difference, t-test was carried out on the sample data for 1:1DD and 1:1DU, and the result gave a p-value of < 0.001. This shows that there is a significant variation in $\Delta L/L_0$ when different sides of the same elastomer are used for the realisation of the sensor.. This could be attributed to means that the Iron particles were closer to the spiral inductor and hence effected more change when pressed. This corresponds also to the test carried out for no load condition where the 1:1 ferromagnetic elastomer had a higher inductance value when the dense side is facing down. This means that the closer the Iron particles are to the coil, the higher the inductance. The results of the investigation of the other samples will confirm this as well.

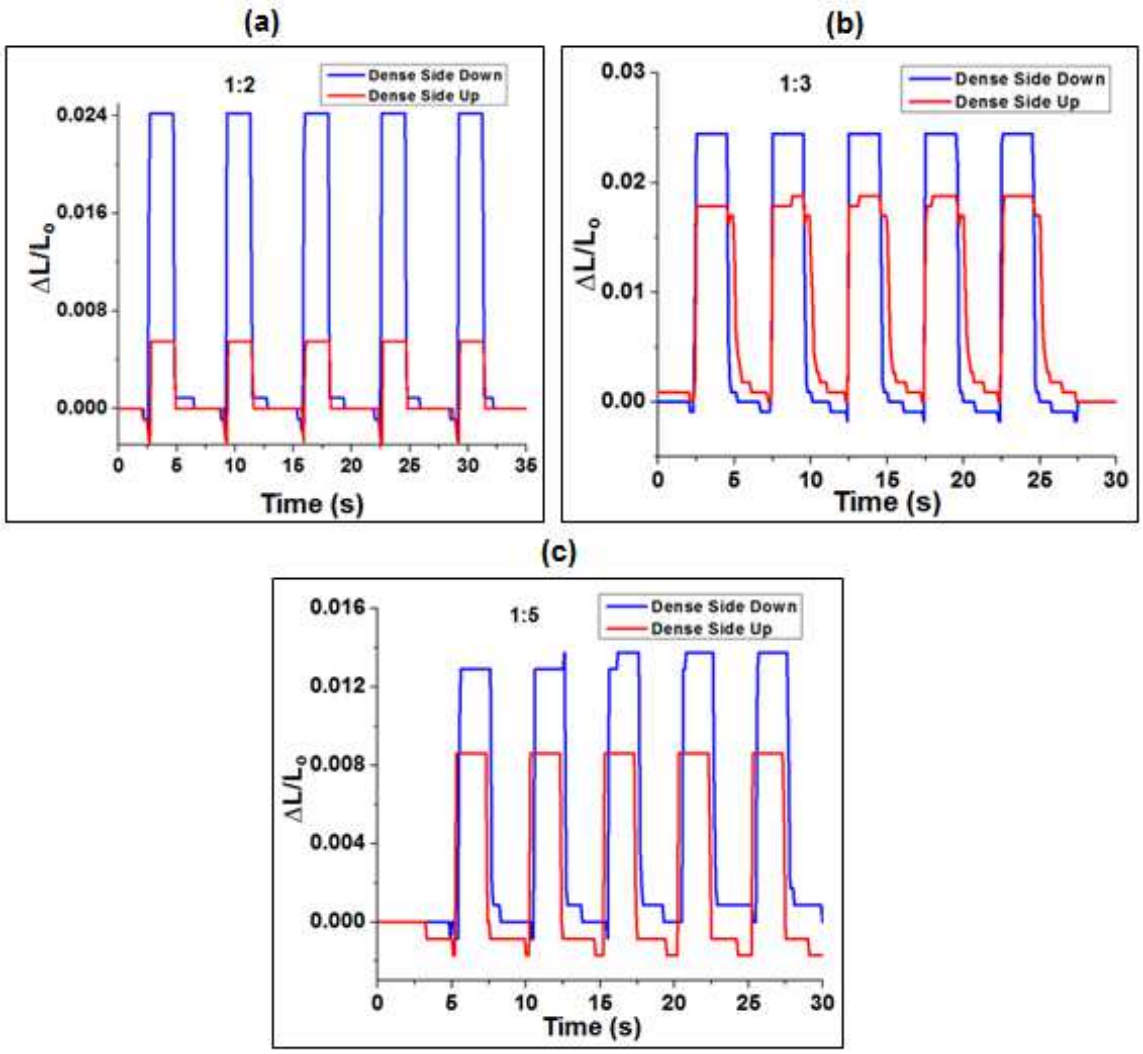

Fig. 6-18 Response of the sensor with the ferromagnetic elastomers that have higher Iron particles by weight (a) 1:2 Dense side down and dense side up (b) 1:3 Dense side down and dense side up (c) 1:5 Dense side down and dense side up

Fig. 6-18 shows the response of the sensor realised with ferromagnetic elastomers having higher Iron particles by weight (1:2DD, 1:2DU, 1:3DD, 1:3DU, 1:5DD, 1:5DU). In all, the sensors with the elastomer's dense side facing down had the highest change with values of $\Delta L/L_0 = 0.242$, $\Delta L/L_0 = 0.024$, $\Delta L/L_0 = 0.013$ for 1:2DD, 1:3DD and 1:5DD respectively. This gives ~9.9% difference between 1:2DD and 1:3DD and ~54.2% between 1:3DD and 1:5DD. Carrying out a t-test on each of the groups shows a p-value of less than < 0.001. This further confirms that the sensors having elastomers with their dense side down had the highest change in inductance. However this is not sufficient to show how much of the Iron particles will be mixed with Ecoflex to realise a particular desired change.

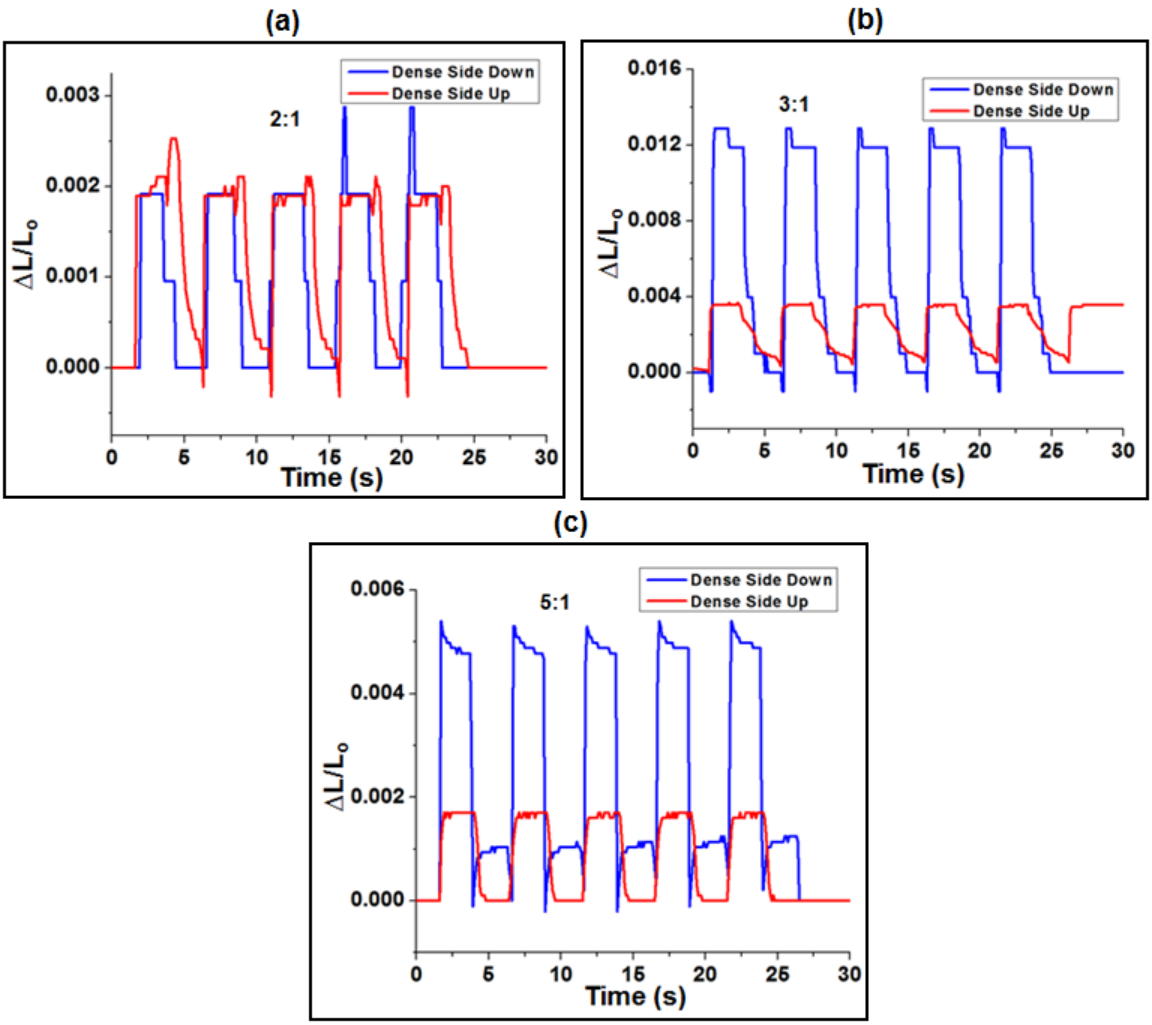

Fig. 6-19 Dynamic response of the sensor with the elastomers that have lower Iron particles by weight (a) 2:1 Dense side down and up (b) 3:1 Dense side down and up (c) 5:1 Dense side down and up

Fig. 6-19 shows the response for the sensors realised with lower Iron particles by weight (2:1DD, 2:1DU, 3:1DD, 3:1DU, 5:1DD. 5:1DU) during five cycles of loading. For all (Fig. 6-19 (a –c)), the sensors with the elastomer's dense side facing down were also found to give the highest change in inductance with values of $\Delta L/L_0 = 0.0029$ for 2:1DD, $\Delta L/L_0 = 0.129$ for 3:1DD and $\Delta L/L_0 = 0.0054$) and stastically all their p-values are less than 0.001. These values indicate ~ 2.2% difference between 2:1DD and 3:1DD, and then ~4.2% between 3:1DD and 5:1DD. This is a small change in comparison with the values obtained in the case of the sensors with the elastomers having higher Iron particles by weight as discussed in the previous section. However, the result also confirms that keeping the dense side of the elastomer down on the spiral coil gives greater change in inductance.

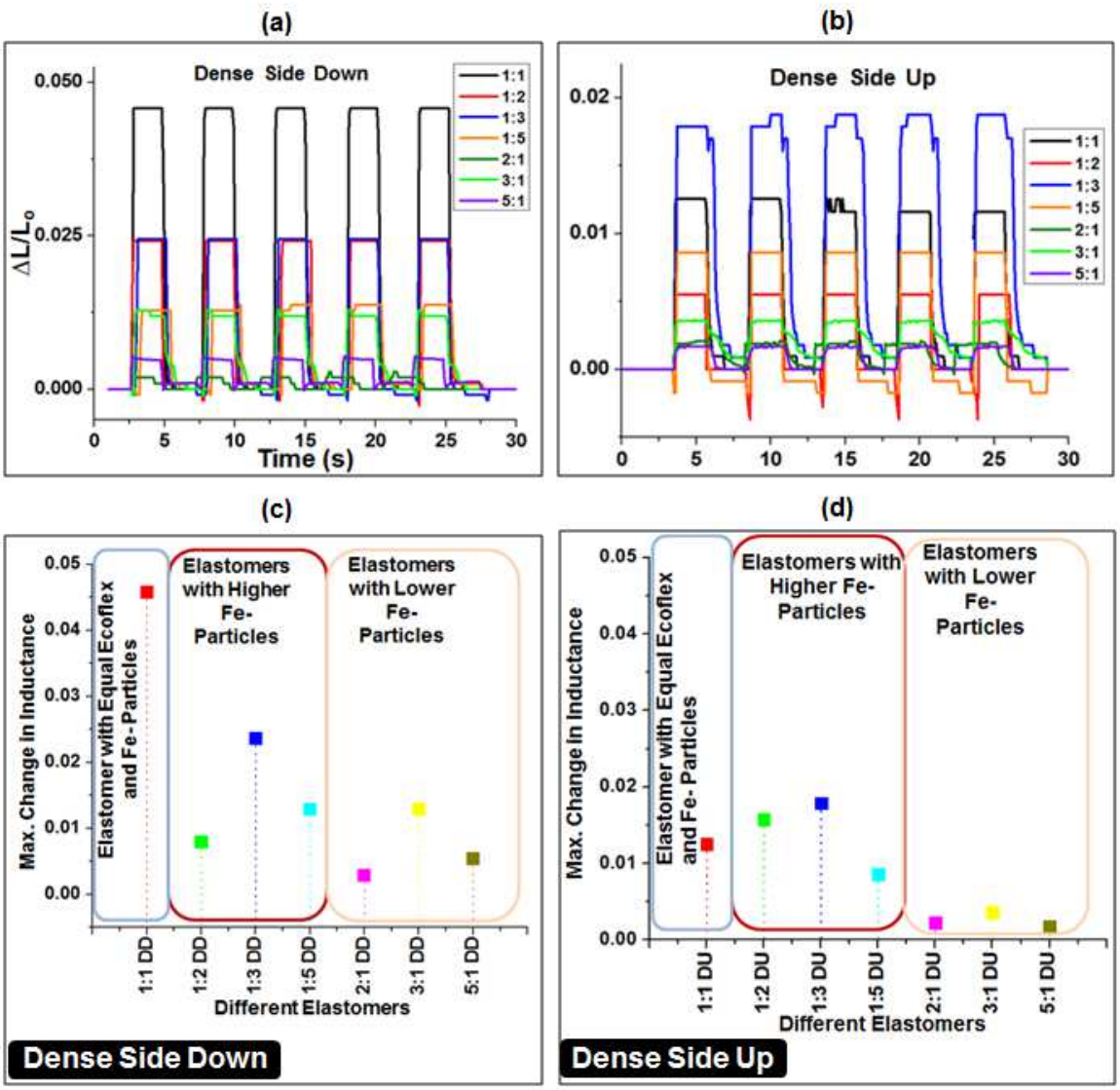

Fig. 6-20 Comparison of all the dynamic performance of all the ferromagnetic elastomers (a) Five cycles for all the sensors when dense side is down (b) Five cycles for all the sensors when dense side is up (c) Maximum change in inductance ($\Delta L/L_0$) for all sensors when dense side is down (d) Maximum change in inductance ($\Delta L/L_0$) for all sensors when dense side is up

The result in Fig. 6-20 (a) – (d) shows the comparison of all the ferromagnetic elastomer for the two cases (Dense side up and dense side down). It summarises and makes clear the effect of the orientation of the ferromagnetic elastomers on the sensor's performance in terms of the output level ($\Delta L/L_0$) for the same given input. Although in all cases, the elastomers having the highest Iron particles by weight had more change in the inductance for the same applied force of 0.5N, increasing the Iron particles does not necessarily mean a direct increase in the output level of the sensor. Surprisingly, the sensor with 1:1 ferromagnetic elastomer had the highest value of $\Delta L/L_0$ (0.045) for the case of the elastomers with higher Iron particles by weight, whereas the least value was shown for the sensor with 2:1 elastomer (0.002). However, in the case of the elastomers with lower Iron particles by weight, the

sensor with 1:3 elastomer had the highest relative change ($\Delta L/L_0 = 0.019$) and that with 5:1 elastomer had the least value ($\Delta L/L_0 = 0.002$). This equally confirms the fact that though more Iron particles in the elastomers lead to a higher change in the output of the sensor, there is no clear observation of the proportionality, but rather it was dependent on the ratio used and hence the orientation of the Iron particles within the elastomer. This is true for both dense side up and dense side down.

Furthermore, the ratios of Ecoflex to Iron particles, was chosen in such a way that each has a corresponding one with an opposite ratio composition. For instance there are 1:2 and 2:1, 1:3 and 3:1, 1:5 and 5:1. From this perspective also, it was observed in each case (see Fig. 6-20 (c) and (d)) that the elastomers with higher Iron particles by weight consistently gave a higher response. In particular, the maximum change in inductance for 1:2 is higher than 2:1, 1:3 is higher than 3:1, and 1:5 is higher than 5:1.

6.2.3.5 Calibration Curve and Sensitivity

One of the key parameters of a sensor is its sensitivity. It is the relative change of the output of the sensor to a corresponding change in the input of the sensor. In this case the sensitivity is given by ($\Delta L/\Delta p$) where L is the inductance and p is the applied pressure. The calibration curve helps to understand the sensor's linear range, dynamic range, and saturation point as well as its sensitivity. The calibration curves were obtained by taking readings of the sensor's output (L) for every corresponding pressure. This was achieved using the same setup shown in Fig. 6-12.

The sensors were in turn attached firmly to the load cell and connected to the Keysight E4890AL LCR meter which measures the inductance. A square glass probe controlled by the linear motor via a LabVIEW program was then used to apply different pressures on the sensor. The applied pressure ranges from 0 to 14.5kPa corresponding to ~0 to 4.5N applied force on sensor area of 0.00031m^2 in steps of 0.5N, and the inductance was recorded in each case. This measurement was carried out for all the 14 samples (1:1DD, 1:1DU, 1:2DD, 1:2DU, 1:3DD, 1:3DU. 1:5DD. 1:5DU, 2:1DD, 2:1DU, 3:1DD, 3:1DU, 5:1DD, 5:1DU) and the calibration curves plotted for elastomers with equal Ecoflex and Iron particles by weight, higher Iron particles by weight, and lower Iron particle by weight.

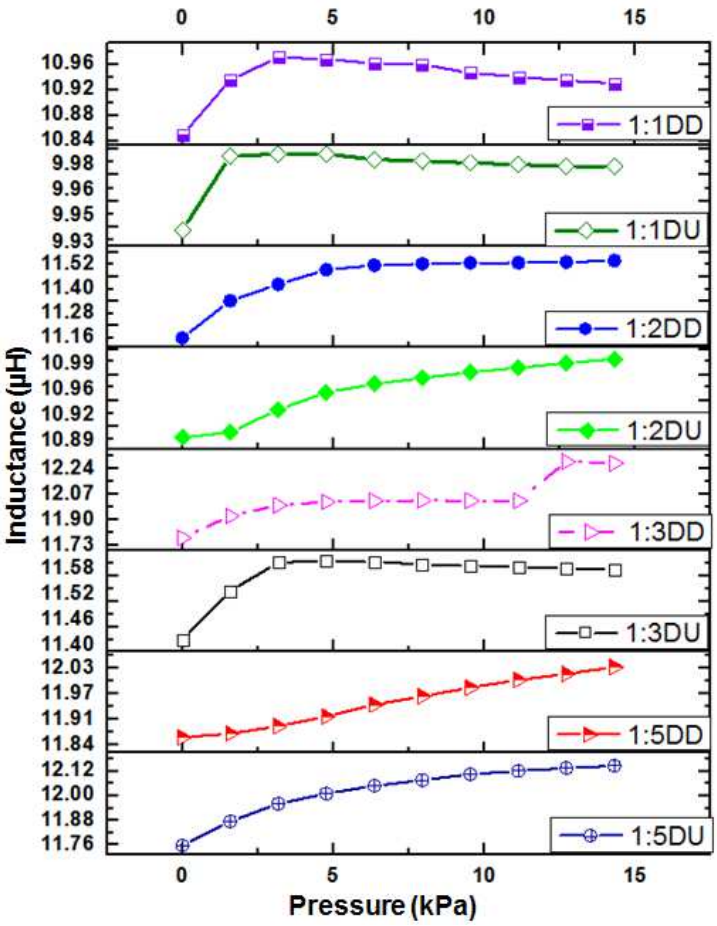

Fig. 6-21 Calibration curve for all sensors realised using elastomers with equal Ecoflex and Iron particles by weight (1:1DD and 1:1DU) and those with higher Iron particles by weight (2:1DD, 2:1DU, 3:1DD, 3:1DU, 5:1DD, 5:1DU).

Fig. 6-21 shows the calibration curve for all sensors realised using elastomers with equal Ecoflex and Iron particles by weight (1:1DD and 1:1DU) and those with higher Iron particles by weight (1:2DD, 1:2DU, 1:3DD, 1:3DU, 1:5DD, 1:5DU). In general, all the sensors in this category exhibited a positive change in inductance for every increase in pressure. In terms of the orientation of the elastomers with respect to the coil, those with elastomers having their dense side down (DD) had the highest dynamic range as well as higher inductance values in comparison with those with their dense side up (DU). This corresponds to the results obtained earlier about the elastomers with DD having more change in output for a given input. In terms of the linear range which is the linear area before saturation, it shows that increasing the iron particles seems to have increased the linear range in each case with 1:5DD having the most linear region and 1:1 the least.

Considering saturation of the output of the sensors, 1: 5DD also has a very good linear performance as it continues to be linear even up to 14.5kPa, while 1:1DD saturated just after 3kPa. This means that the composition is such that for every increase in pressure there is a

gradual increase in the inductance for 1:5DD as opposed to 1:1DD. Sensors in the DU category seem to also have noticeable saturation in comparison to those in DD category. This is because the presence of the Iron particles causes the resultant elastomer to be stiffer (as shown from the test of the elasticity of the elastomers discussed in Section 6.2.3.3). This slows down the variation of the inductance for a given applied pressure. But although higher pressure is required to reach same level of change for softer elastomers, there is more room for change for stiffer ones. Furthermore, the presence of the Iron particles in the elastomer increases the number of particles interacting with the coil in each case, and since the DD are closer to the coil they give higher responses.

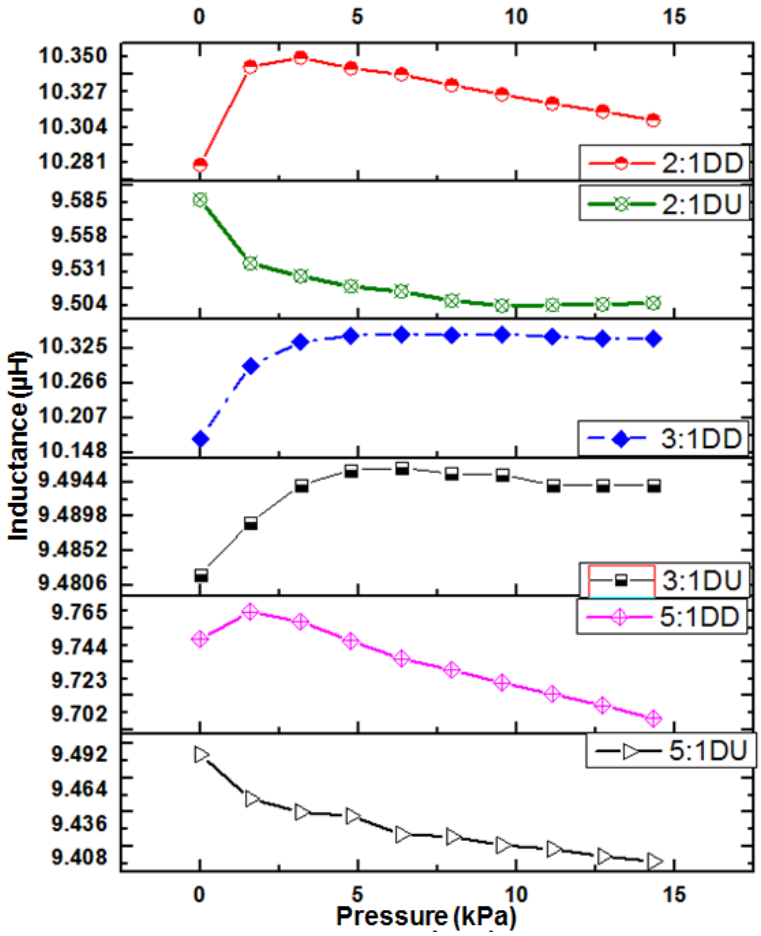

Fig. 6-22 Calibration curve for all sensors realised using elastomers with lower Iron particles by weight (2:1DD, 2:1DU, 3:1DD, 3:1DU, 5:1DD, 5:1DU)

The calibration curve for the sensors realised using the ferromagnetic elastomers with lower Iron particles by weight (2:1DD, 2:1DU, 3:1DD, 3:1DU, 5:1DD, 5:1DU) is shown in Fig. 6-22. In this case, sensors in the DD category show higher dynamic range. Apart from the 3:1DD and 3:1DU, the rest exhibited a negative slope which means that the inductance decreased at some point for an increase in the applied pressure. This is because of the low

content of Iron particles because bringing moving the Iron particles closer to the spiral coil is meant to increase the inductance and not decrease it. With the exception of 3:1DU, this decrease is particularly pronounced in the case where the dense side of the elastomer is up (Iron particles are quite far away from the spiral inductor). However, some sensors (2:1DD, 3:1DD, 3:1DU, and 5:1DD) experienced some increase in inductance for an increase in pressure. So, the main observation from this category is that a decrease in the inductance of the sensor was observed due to low Iron particles as compared to the sensors with higher Iron particles by weight which all exhibited positive change in inductance.

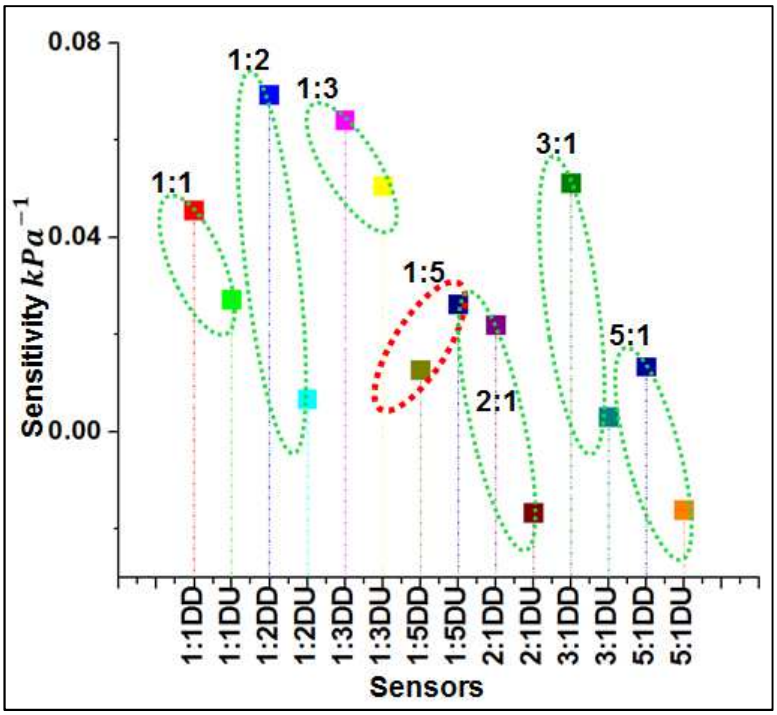

Fig. 6-23 Sensitivity of all the sensors

Fig. 6-23 shows the sensitivity of the different sensors which were determined from the calibration curve by taking the slope of the linear region. This means that the calibration curve was used to establish the unit change in the inductance for every change in pressure (0 up to 14.5kPa). Generally, for each category (DD and DU), the sensitivity also shows higher values for DD (except for the 5:1DD). The 1:2DD sensor had the highest sensitivity (0.07kPa^{-1}) while the lowest and negative values were observed for 2:1DU (-0.017kPa^{-1}) and 5:1DU (-0.016kPa^{-1}). Though there is no observed pattern of proportional relationship within groups (those with higher iron particles by weight and those with lower iron particles by weight), a statistical t-test carried out on the data using the one tail distribution shows a p -value < 0.05. So it is evident that higher Iron particles in the elastomer has some effect on the sensitivity of the sensor.

6.2.3.6 Response and Recovery Time

Response time is the time taken for the sensor to reach 90% of its steady state value. The response time was determined from the results of the cyclic loading of the sensor presented in Section 6.2.3.4 by finding the time it takes in each case for the sensor to reach 90% of its steady state value. The recovery time on the other hand is the time taken for the sensor to return to the base value of the measured variable. It is usually specified as the time to fall 10% of the final value. This was equally determined from Section 6.2.3.4.

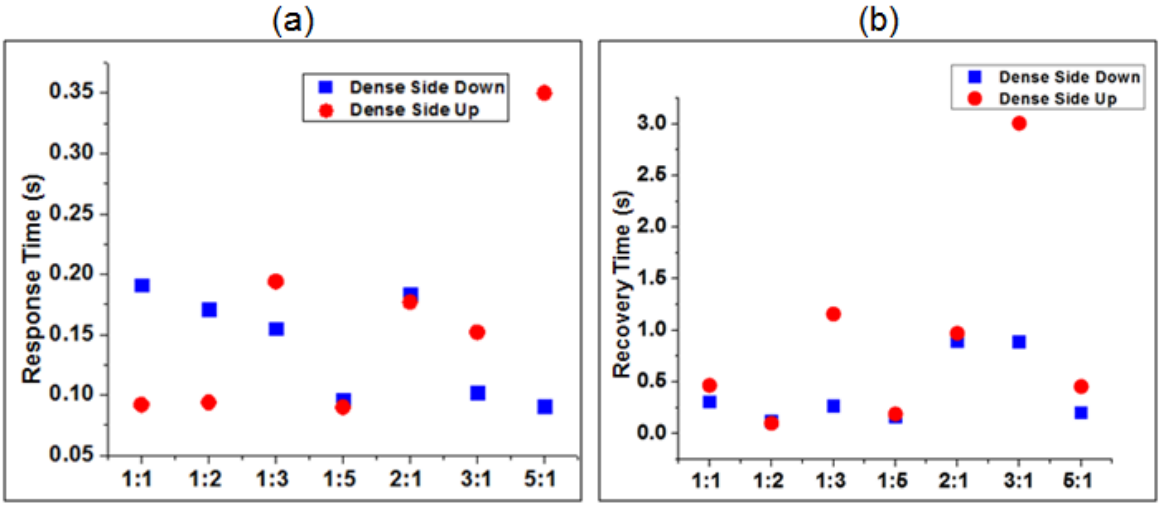

Fig. 6-24 (a) Response time for all the sensors - dense side up and dense side down (b) Recovery time for all the sensors -dense side up and dense side down

Fig. 6-24 demonstrates the response and recovery time of the different sensors both for the case where the elastomers have their dense side down as well as up. Considering the elastomers with their dense side down, it can be seen from Fig. 6-24 that the response time of the sensors decreases as the amount of Iron particles increases. The sensor realised with the 1:2 ferromagnetic elastomer has the largest (slowest) response time of $0.171s$ $(171ms)$ and 1:5 the smallest (fastest - $0.090s$ or $90ms$). Hence the sensor (1:5DD) realised using the 1:5 elastomer is the fastest in terms of response time. This could be attributed to the fact that this ferromagnetic elastomer contains more Iron particles than the rest. Therefore, there is a quicker interaction between these particles and the coil.

Except for the sensor with the 1:3 ferromagnetic elastomer, all the sensors having elastomers with higher Iron particles by weight (dense side down) (1:2 and 1:5) was observed to have faster response time than their opposite ratio with lower Iron particles by weight (2:1 and 5:1). In particular 1:2 $(response\ time = 0.094s)$ is faster than 2:1 $(response\ time = 0.177s)$, and 1:5 $(response\ time = 0.09s)$ is faster than 5:1 $(response\ time = 0.35s)$.

In terms of the recovery time, all the sensors realised using elastomers with higher Iron particles showed faster recovery time for all cases (dense side up and dense side down). This could be attributed to their stiffness and presence of more Iron particles. So, the presence of Iron particles in Ecoflex has significant effect on both response and recovery time of the sensors. While increasing the presence of the Iron particles lead to faster response time for the case when the dense side of the elastomers are facing up, the recovery time was generally faster for those with higher Iron particles.

6.2.3.7 Response under Loading and Unloading

The response of the sensors was also investigated for loading and unloading conditions. This was carried out particularly to determine how the sensors are able to return back to the base line during unloading and hence gain insight on how stable they are. This will also give idea of how much hysteresis exists in each case.

This was also carried out by using the same setup described in Section 6.2.3.4. The sensors were in turn attached to the load cell and then connected to a Keysight E4890AL LCR meter which records the inductance and Q-factor. A dynamic force is then applied on the sensor using the square glass probe controlled by a LabVIEW program. The load cell was calibrated using an Agilent 34461A $6_{1/2}$ digital voltmeter connected to its output in order to ensure a 1N load is not exceeded. Starting from no load, the sensor is loaded by moving the motor with a step of 0.05mm in order to apply force on the sensor. When a force of 1N is reached, as recorded by the corresponding output voltage on the voltmeter, the probe is released using the same step in order to return back to 0N.

Fig. 6-25 shows the result of loading and unloading for the sensor with equal Ecoflex and Iron particles by weight. It further confirms the fact that the sensors realised with the elastomers having their dense side down has higher inductance value. The Q-factor response was also seen to follow approximately the same shape as the inductance during loading and unloading curve. This agrees with $Q = \omega L/R$ as described in Section 6.2.1. The 1:1DD sensor was found to return to baseline much better than 1:1DU.

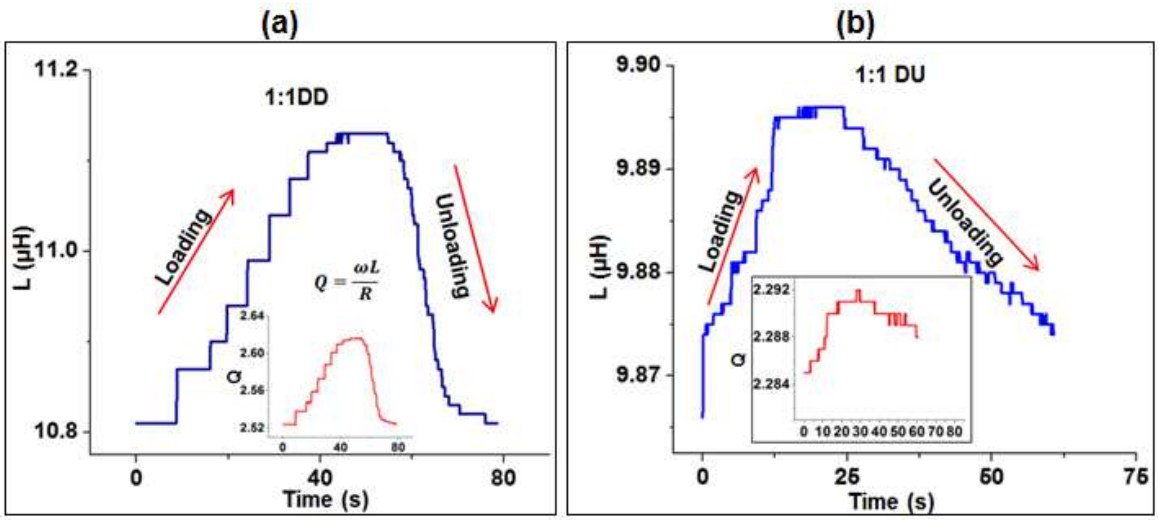

Fig. 6-25 Loading and unloading response for elastomer with equal Ecoflex and Iron particle by weight (a) 1:1DD (b)1:1DU

Fig. 6-26 and Fig. 6-27 show the result of loading and unloading the sensors for the elastomers with higher and lower Iron particles by weight respectively. Except for 2:1DD and 3:1DU, all the sensors relatively returned to base line. Major observation here is that 5:1DU behaved similar to the result of integrating plain Ecoflex with the spiral coil (see Fig. 6-27 (f) and Fig. 6-28). This shows that there is insignificant effect when the 5:1 ferromagnetic elastomer was used to realise a sensor (5:1DU).

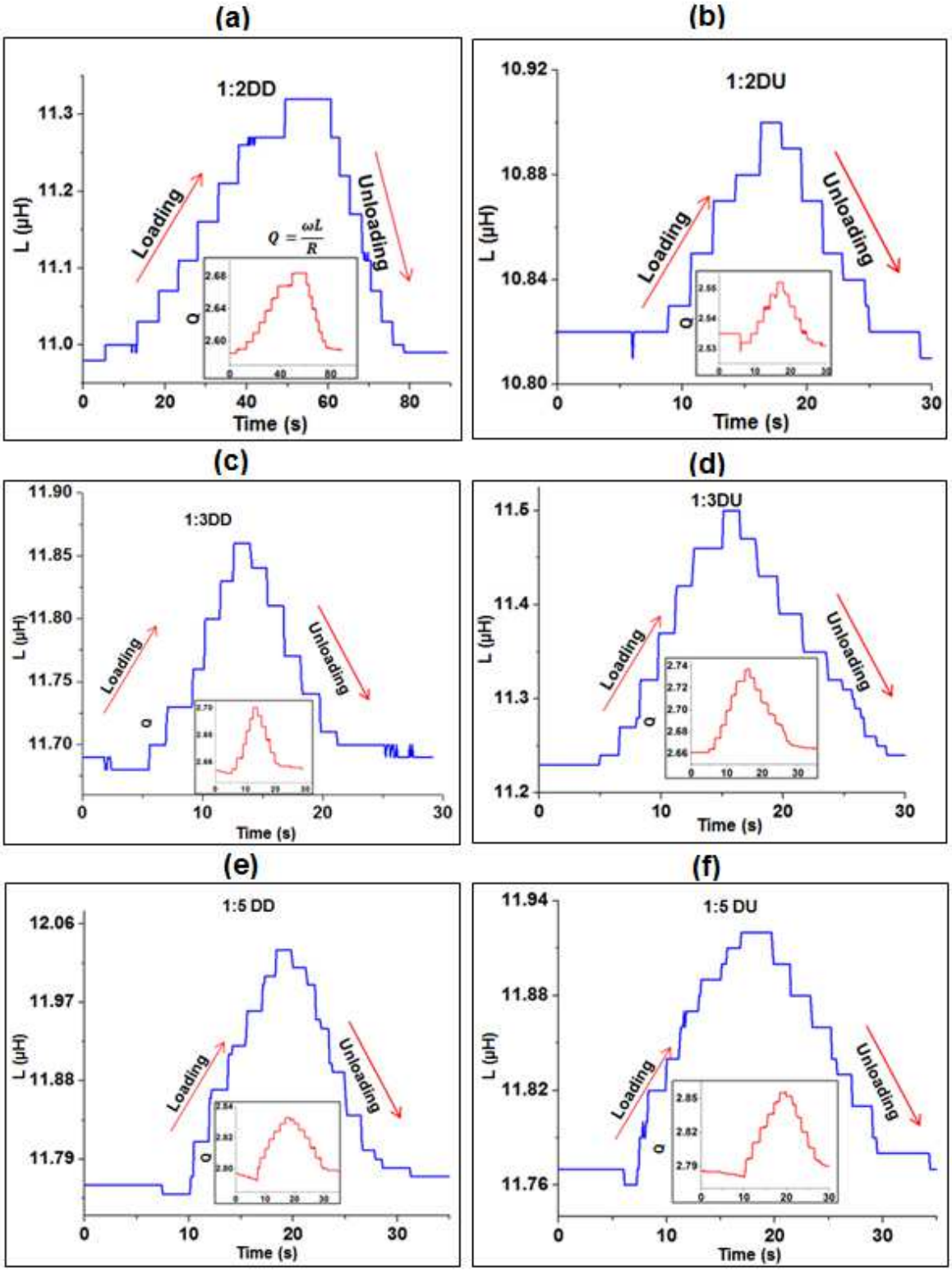

Fig. 6-26 Loading and unloading response for elastomer with higher Iron particles by weight (a) 1:2 DD (b) 1:2DU (c) 1:3DD (d) 1:3 DU (e) 1:5DD (f) 1:5 DU

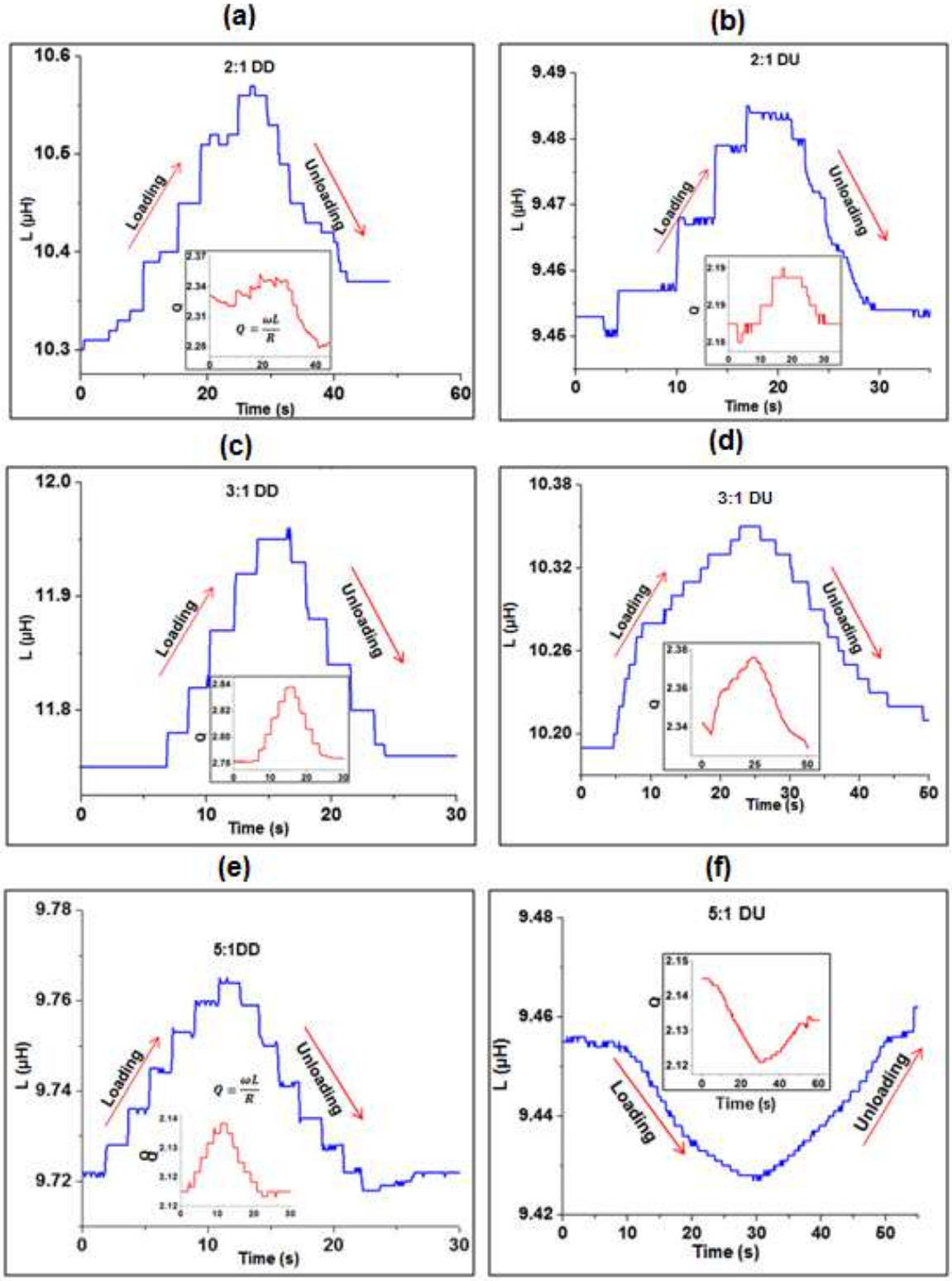

Fig. 6-27 Loading and unloading response for elastomer with lower Iron particles by weight (a) 2:1 DD (b) 2:1DU (c) 3:1DD (d) 3:1DU (e) 5:1DD (f) 5:1 DU

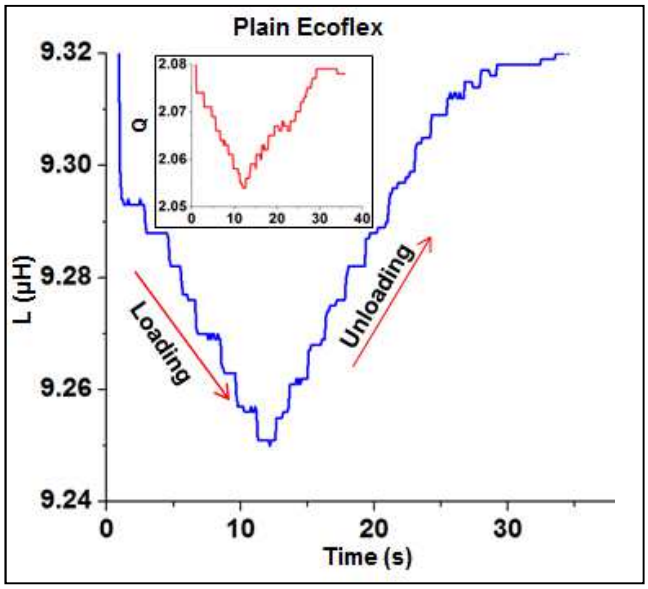

Fig. 6-28 Loading and unloading response of the sensor using plain Ecoflex

6.3 Summary

In this chapter, the fabrication and characterisation of a capacitive tactile sensing array and a single element flexible inductance-based pressure sensor were presented. The capacitive array is for the purpose of deafblind communication using the English block letters while the pressure sensor is mainly an option for replacement of the commercial sensor used for Finger Braille glove presented in Chapter 4.

The application of the tactile sensing array was demonstrated using a mobile app that has trained convolution neural network capable of recognising the English block letters written on the array. The performance of the system was demonstrated by controlling a virtual Baxter robot through the writing of English block letters on the array. This shows the performance of the sensor for potential use in the interaction of deafblind people with robot as well as sighted and hearing people.

Also presented in this chapter is the inductance-based pressure sensor. Seven different ferromagnetic elastomers were realised using different ratios of Ecoflex and Iron particles (1:1, 1:2, 1:3, 1:5, 2:1, 3:1, 5:1) and integrated with the spiral coil to realise the different sensors. These elastomers where categorised into three (1) Elastomer with equal Ecoflex and Iron particles (2) Elastomers with higher Iron particles by weight (3) Elastomers with lower Iron particles by weight. SEM analysis of the sensors shows a gradient of Iron particles for all the elastomers. The side with dense Iron particles were called ***"dense side"*** and the effect of its orientation (up or down) with respect to the spiral coil was investigated. Based on this,

14 different samples (two conditions - dense side up or dense side down for each sensor were investigated. The following summarises key parameters investigated and their results.

- ***SEM analysis of the fabricated ferromagnetic elastomers***: This revealed that Iron particles settled down at the bottom of the mold after curing, hence creating an elastomer with gradient of Iron particles
- ***Inductance and Q-factor at no load:*** This shows that the higher the amount of Iron particles, the higher the inductance as well as Q-factor. Elastomers with their dense side facing down on the coil were seen to have higher inductance and Q-factor at no load.
- ***Elasticity of the ferromagnetic elastomers:*** This confirms that the presence of the Iron particles increases the stiffness of the realised ferromagnetic elastomers. These were further confirmed by determining the stress-strain relationship, elastic modulus and weight of the different elastomers.
- ***Sensor performance:*** This was done in order to understand the characteristic performance of the sensors under loading and unloading conditions, including their response time, recovery time as well as sensitivity. The following are the key parameters and the results:
    - Cyclic loading: this shows that the sensors realised using elastomers with their dense side down had more change in inductance for a given load
    - Response time: This shows that the elastomers with higher Iron particles (dense side up) by weight has faster response time
    - Recovery time: Shows that the elastomers with higher Iron particles by weight has faster recovery time
    - Calibration curve/ sensitivity: This shows higher sensitivity for elastomers with higher Iron particles
    - Response during loading and unloading: most of the sensors were able to return to the baseline. A comparison with plain Ecoflex shows that the 5:1 (dense up) behaved almost like plain Ecoflex.

Chapter 7

7 Evaluation and User Feedback

This Chapter presents the evaluation of the tactile interfaces presented in this work (the capacitive sensing array presented in Section 6.1, the touch-sensitive electromagnetic actuator presented in Chapter 5, The SmartFinger Braille glove presented in Section 4.4. The evaluation was carried out to obtain user feedback regarding these interfaces and hence gather some useful user requirements useful for their improvement as well as for guide for future tactile interfaces for communication by deafblind people.

Prior to the test, ethical approval was obtained from University of Glasgow ethical committee and participants were given information sheet to understand what is involved in the test and how to participate. Both qualitative and quantitative data and analysis gathered in this process are presented here. Fig. 7-1 shows the evaluated devices and the key questions answered through this process.

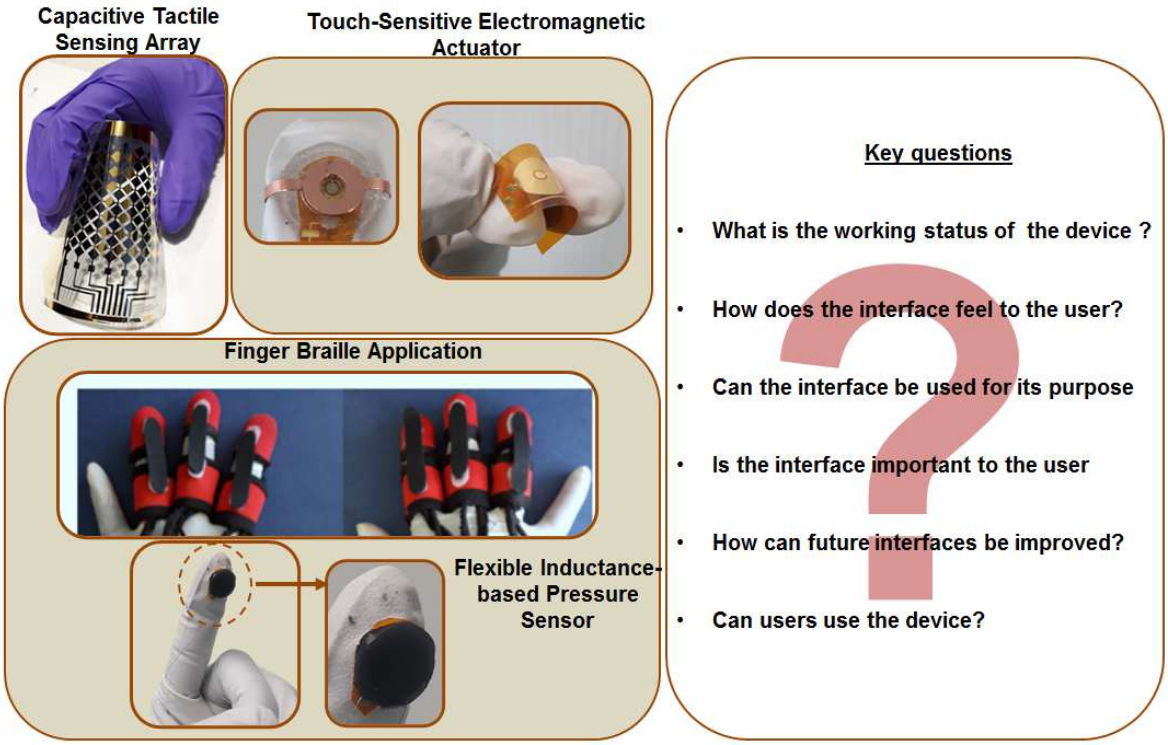

Fig. 7-1 Fabricated tactile interfaces and the key outcome measures

7.1 Evaluation of the Capacitive Sensing Array

7.1.1 Methodology

The capacitive sensing array presented in Chapter 6 is an array that enables deafblind people to communicate by writing block letters on it. Two main evaluations were carried out. (1) Laboratory evaluation, each of the pixels (2) Evaluation of writing block letters on the array (3) Semi-structured interview for general feedback. The primary aim of the evaluation is first to understand how the pixels of the array work, Secondly, is to understand if the 8 x 8 array is enough to represent the touch points for the block letters, thirdly is to understand how different users with different writing styles are able to successfully write using 8 x 8 tactile array. This was presented to 20 deafblind people and 20 sighted and hearing people to give a general evaluation on the device.

Prior to the evaluation, an application for ethical approval was submitted to the University of Glasgow ethical committee and this was approved. After the approval, different participants were recruited. 20 deafblind people and 20 sighted and hearing people were involved. The deafblind people were recruited with the help of Deafblind Scotland, Deafblind UK and Sense Scotland. The sighted and hearing people were recruited by advertisement through email with details of what is involved. After the recruitment, information sheet was handed over to the participants in the format they have chosen. Deafblind people were reached mainly through their interpreters who interpreted it to them. However, some of the deafblind participants have residual sight and hearing, and so were able to listen while I read out what is involved.

For the evaluation of how different deafblind people are able to write using an 8 x 8 tactile array, a custom mobile app (with the ability for character recognition) contributed by W.T. Navaraj as presented in [208] was used with same number of pixels as the capacitive tactile array for this demonstration. By signing on it, the probability of success and failure of recognising the handwritten English block was determined.

Table 7-1 Summary of Participants' Profile

Type Impairment	Gender
Completely Deafblind	1 Male
Residual Sight and/or Hearing	10 Males, 9 Females
Congenital Deafblind	None
Sigted and Hearing	10 Males, 10 Females
Total	40

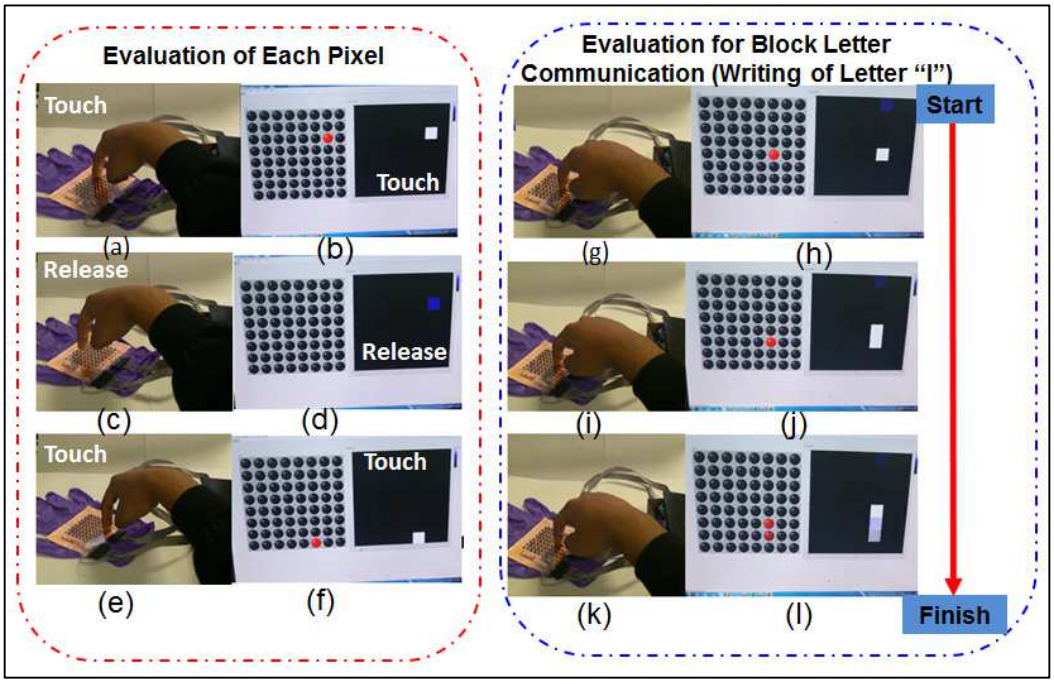

Fig. 7-2 Laboratory evaluation of the individual pixels of the capacitive tactile sensing array

7.1.2 Results

Fig. 7-2 shows the result of laboratory evaluation of each pixel of the capacitive tactile sensing array. The touch-points were touched individually and through a custom LabVIEW program with contribution by W.T. Navaraj as in [208, 209]. The red dots shows touch points as described earlier in Section 6.1.2.

After evaluation of the pixels, the users as shown in Table 7-1 also participated in evaluation of how letters are recognised on an 8 x 8 array. All the users have the knowledge of English language and during each time, they were told the random letters (A, B, C, D, E, F, G, J, S,

and Z) to write. Participants were informed to write block letters covering small area of the interface, and then block letters covering the large almost the entire area of the interface. Some of the deafblind participants are registered as deafblind but still have residual hearing and/or sight and with hearing aid some of them are able to communicate verbally.

Table 7-2 Probability of failure and success when writing small block letters using the 8 x 8 tactile array

Alphabet	Average No. Success	Average No. of Failure	Probability of Success	Probability of Failure
A	1	9	0.1	0.9
B	0	10	0	1
C	0	10	0	1
D	1	9	0	0.9
E	1	9	0.1	0.9
F	0	1	0	1
G	0	10	0	1
J	4	6	0.4	0.6
S	2	8	0.2	0.8
Z	7	3	0.7	0.3

Table 7-3 shows the Probability of failure and success when writing large block letters using the 8 x 8 tactile array. Table 7-3 shows the probability of failure and success for all the participants (20 deafblind and 20 sighted and hearing people) when small and large block letters were written on the array respectively. The letters were interpreted by the mobile app presented in [208] which has the ability for character recognition and made with an 8x8 array. When a character is written on the array, the app displays the interpreted letter. When the letter written is displayed correctly, success is recorded otherwise failure is recorded. From the result, letters written by covering most areas of the array was recognised more than letters written in small area of the array. This is an area on improvement as the array should be able to recognise letters written over large and small areas of the array. This is because different people have different styles of handwriting. There was also more difficulty in recognising letters with curves (e.g. S, G). All the mentioned failure is attributable to the size of the array. Increasing the size of the array will improve the recognition of letters.

From the semi-structured interview, participants provided useful general feedback about the device. Generally, users were happy with the flexibility of the material, but a few were not happy with the size of the array given that they were writing outside the sensitive area. There were also suggestions on including tactile cues on the array to aid users to independently recognise the touch points.

7.2 Evaluation of the Touch-sensitive Actuator

This Section presents the evaluation of the touch-sensitive electromagnetic actuator presented in Chapter 5. The primary goal of this test is to understand how the users are able to perceive the vibration produced by this device at different frequencies. Research shows there is a variation between the tactile sensitivity of deafblind people compared to sighted and hearing people due to their developed tactile sensitivity [210]. Hence there is need to test the vibration of the device with real end-user to understand their opinion on this. Given that they are the primary end user of the technology, they were involved in obtaining feedback on how it feels. In this experiment, 20 deafblind and 20 sighted and hearing people participated.

7.2.1 Methodology

During the experiment, participants were made to touch and feel the vibration produced by the device and give feedback as to whether it is sufficient, not enough or too strong. Sighted and hearing people participated by wearing ear plug and blind fold to minimize bias from vision and sound. The touch-sensitive actuator was excited at different frequencies ranging from 10Hz to 200Hz in steps of 10Hz using a pulsating current of 150mA and the response of each participant was recorded. The vibration was chosen to cover same range (10 – 200Hz) used in the characterisation of the actuator 5.5.

In addition to the vibration perception test, a semi-structured interview took place to understand the opinion of the participants regarding the device. Through this, data regarding the fabricated tactile interface was gathered and thematic analysis was used to analyse the result. The result is presented in the form of affinity diagram showing the themes and relationship between the responses of the participants. For the thematic analysis, the following steps were adopted:

- *Data familiarization:* Here, the interview data were reviewed and initial ideas for codes were generated.

- *Coding and categorization of*: Data collected from the interview was coded and categorized
- *Formation of Themes:* The codes from the data were generated, themes were formed to interpret the codes and data.

7.2.2 Results

Table 7-4 summarizes the result of vibration perception test. Although majority of the users acknowledged the vibrations at lower frequencies are more distinguishable, they felt more vibration at higher frequencies.

Table 7-4 Perception test for the fabricated touch-sensitive actuator carried out on 40 users (20 deafblind people and 20 sighted and hearing people)

Frequency Compared (Hz)	Most Recorded Perceived Frequency (Hz)		Comment	
10 and 20	20		TRUE	
20 and 30		50% = 30, 50% = ND		50% True
30 and 40	40		TRUE	
40 AND 50	50		TRUE	
50 and 60	60		TRUE	
60 and 70		60% = ND, 40% = 70		40% True
70 and 80	80		TRUE	
80 and 90	90		TRUE	
90 and 100	100		TRUE	
100 and 110		70% = 110, 30% = ND		70% TRUE
110 and 120		ND	FALSE	
120 and 130		ND	FALSE	
130 and 140		50% = 140, 50% = 130		50% TRUE
140 and 150		70% = ND, 30 = 150		30% TRUE
150 and 160		ND	FALSE	
160 and 170		50% = ND, 50% = 170		50% TRUE

170 and 180	80 = ND, 20% = 170	FALSE	
180 and 190	ND	FALSE	
190 and 200	50% = ND, 50% = 200		50% TRUE

7.3 Evaluation of the SmartFingerBraille glove

SmartFingerBraille glove was developed during the proof-of-concept phase and presented in Chapter 4. This is a communication method in which deafblind people who have the knowledge of Braille are able to communicate using the index, middle, and ring finger of both hands to represent the six dots of Braille as explained in Section 2.2.2. The purpose of this evaluation is to understand the opinion of the end users regarding this method of communication and requirements for developing such a tactile communication interface for deafblind people. As described in Chapter 6, the inductance-based pressure sensor fabricated in this work (Section 6.2), is proposed to be usable for the application of finger Braille communication and hence user feedback will aid future work in this direction.

For this experiment, semi-structured interview was used for the data collection and thematic analysis used for the analysis of the result. 20 deafblind and 20 sighted hearing people were also involved. The interview started with a general introduction about the glove and how it works with a presentation of the device to them. The device has touch sensors and actuator as described in Section 4.4. After this, thematic analysis was used to analyze the data as presented in Fig. 7-3. Generally, users preferred other colours to the red colour of the glove and advised for consideration of contrasting colours. The feel of the vibration from the device and the neoprene material was accepted by majority. Users also agree that finger Braille will be a useful method of communication especially for people without residual sight or hearing.

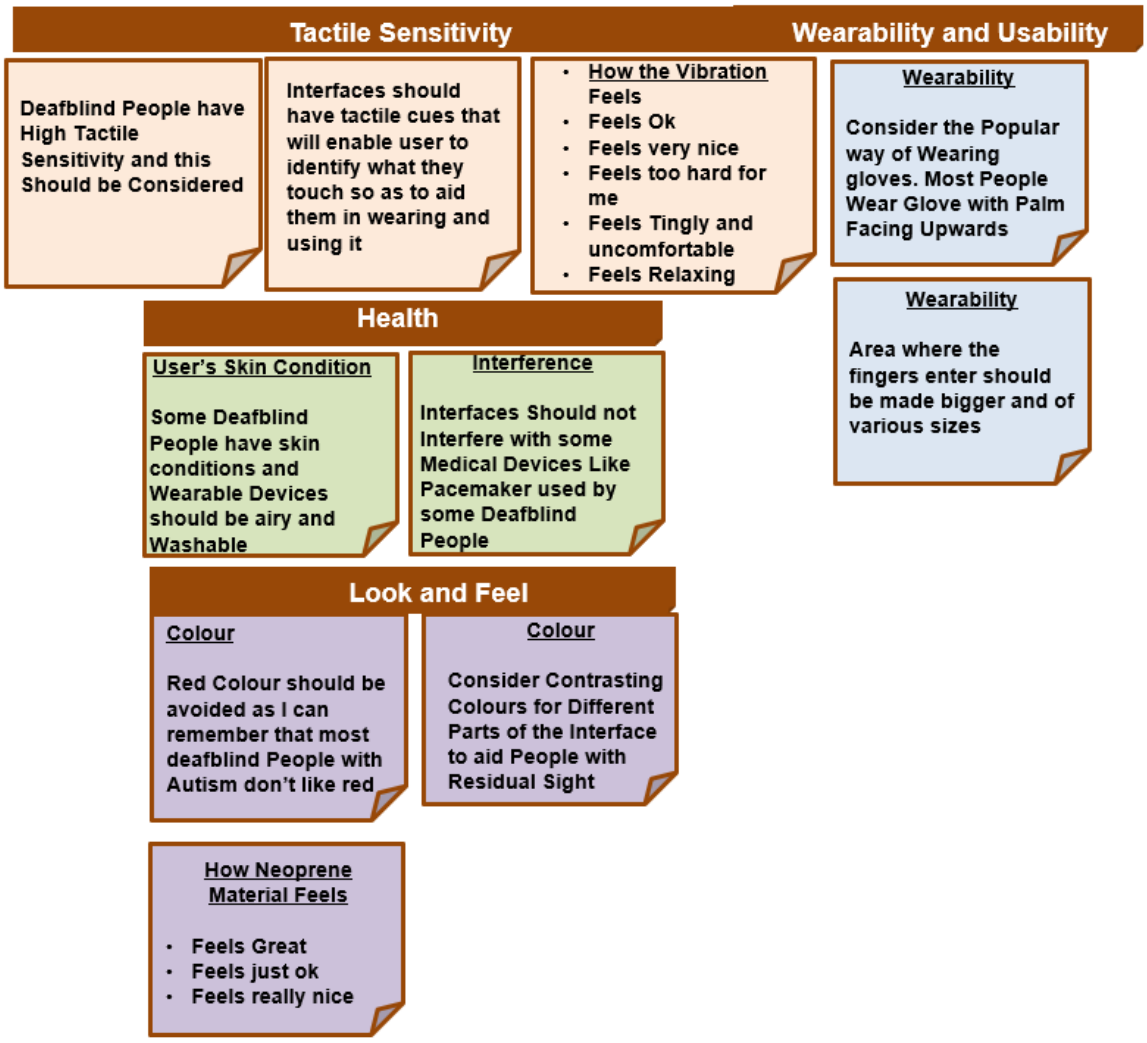

Fig. 7-3 Qualitative user feedback for the SmartFinger Braille Glove (presented in Section 4.4)

7.4 Chapter Summary

This chapter presented the evaluation of the tactile interfaces fabricated in this work. In particular, the capacitive array, touch-sensitive actuator and finger Braille evaluation were presented. The evaluation led to feedback from deafblind people, people who work with them as well as others who don't work with them, regarding the fabrication of tactile interfaces for communication by deafblind people. Fig. 7-2 shows a summary of the user responses. These were classified based on the relationship among them as determined using thematic data analysis. The result is a small pool of information regarding user requirement for anyone interested in developing tactile interfaces that will be used by deafblind people for communication.

General User Requirements

- Deafblind people have improved touch sensitivity and this should be considered in the design of Interfaces for them
- An interface on a glove is better since deafblind people are used to normal glove already
- Options for saving the tactile data for transfer to computer or the ability for the interface to be connected to computer
- Braille users are mainly older people and usability for this age group should be considered
- Tactile device for Braille should be worn on the fingers as small rings to represent dots of Braille
- Interference of tactile interface with some specialised health equipment like pacemakers should be considered and avoided

Ease of Learning

- Deafblind people have high mental demands due to vision and hearing impairment and complexity should be reduced in tactile interfaces.
- Communication devices involving the use of Block letters are easy to use by people who already know the English language
- It might be easier for people without residual vision or hearing to learn how to use the interfaces based on deafblind manual alphabets and Finger Braille as others are more accustomed to audio feedback devices and large prints.
- Finger Braille is a good way to teach Braille and this will be helpful for many deafblind people who want to learn Braille communication and for Braille Teachers as well.

Aesthetics and Wearability

- Red colour is generally not acceptable by many deafblind people
- Colour contrast is very key in interfaces, especially for the category of deafblind people who have residual sight. White and Black were suggested
- For glove type interfaces, the users are already used to normal glove and the method of wearing any glove-like tactile interface should take a cue from normal glove to reduce learning time
- Tactile interfaces should not be smooth and should have tactile cues to enable users identify what they are touching

Fig. 7-4 Summary of the user feedback for development of tactile interface for communication by deafblind people

Chapter 8

8 Discussion

This Chapter discusses the results of the work done in this thesis and identifies its position in the existing state of the art for development of tactile interface for communication by deafblind people. As described in Section 2.2, assistive devices developed to support deafblind communication are mainly inspired by two main tactile communication approaches (deafblind manual alphabets and Braille). This is done particularly to have a user-friendly interface that allows deafblind people to use these methods which they are already familiar with.

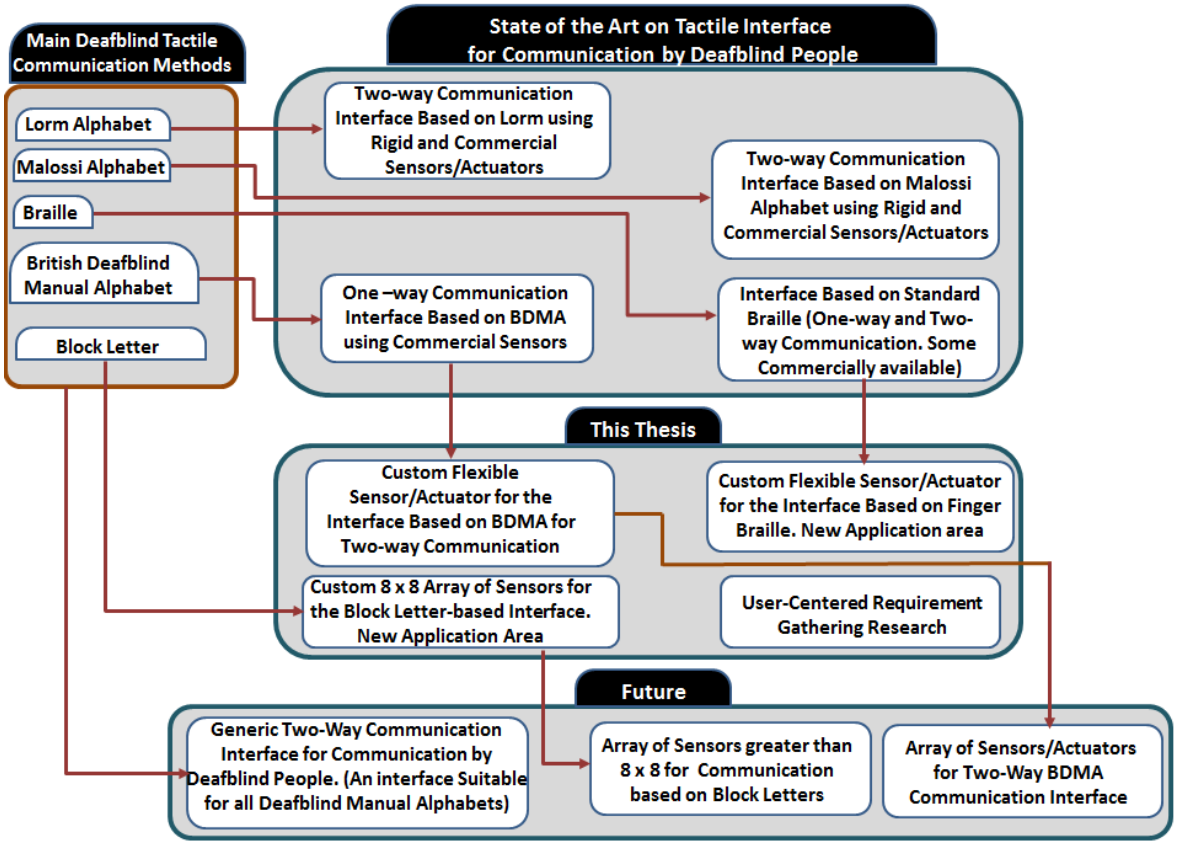

Fig. 8-1 State of the art on tactile communication interface for communication by deafblind people, the postion of the work done in this thesis and future direction

Fig. 8-2 summarizes (to date) the tactile interfaces developed for communication by deafblind people and clearly shows the position and contribution of this thesis in the state of the art and the doors it opens for future work in this direction.

Considering the main/popular tactile communication methods (Lorm, Malossi, Braille, deafblind manual alphabet, and Block letters) used by deafblind people, this thesis has contributed in the development of tactile interfaces that supports Braille, deafblind manual alphabets, as well as block letters. It opens new research areas particularly for the development of a generic interface that supports all types of deafblind manual alphabets.

8.1 Touch-sensitive Actuator

Examining the methods of communication used by deafblind people [120] as presented in Chapter 2 shows that the deafblind manual alphabets (Lorm, Malossi, and British deafblind manual alphabet) used in different parts of the world, requires same touch-points to be used for both sending and receiving of messages. Conventionally, to communicate with these methods, deafblind people bring out the palm of their hand and a touch or movement at specific locations means specific information for them (Section 2.2). So rather than people touching them manually for communication, developing a suitable tactile interface will enable a deafblind person to independently wear this interface on the hand and using the same communication approach s/he will interact with the interface to independently send message to mobile phone users and/or use computer.

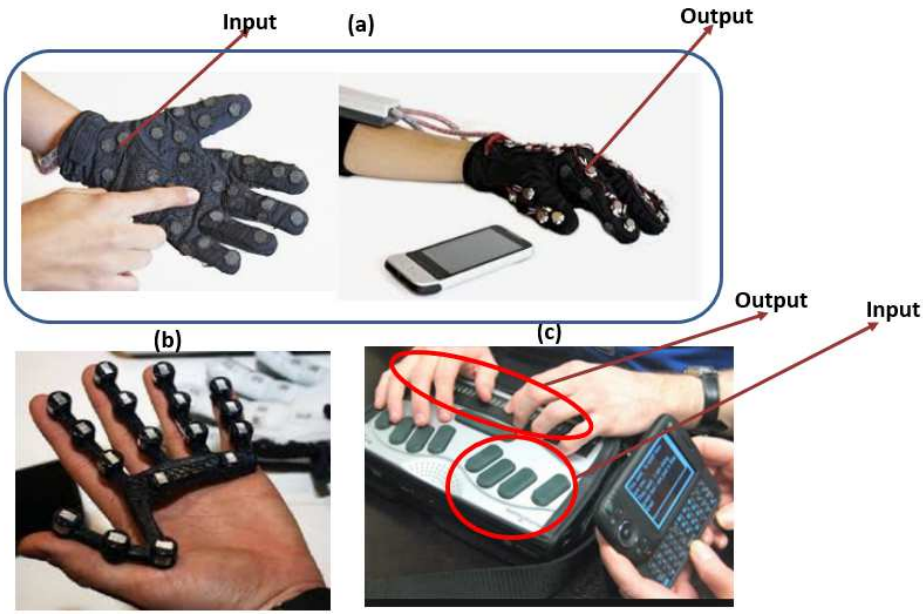

Fig. 8-2 (a) Tactile interface based on Lorm – sensors and actuators are located at different locations on the hand [31, 211] (b) Tactile interface based on Malossi deafblind manual alphabet – tactile sensors and actuators are located together on a rigid structure. Image from www.Medaarch.com (c) Brailler (image from https://www.perkinselearning.org

To date, most of the interfaces developed for deafblind people which supports the use of deafblind manual alphabets (Fig. 8-2) are all based on individual touch-sensor and actuators

(Section 2.2.1). This makes it challenging to represent the required touch-points. Previously, researchers have fabricated tactile communication interfaces with individual sensors and actuators placed at different locations [31] or stacked together at the touch points [32] for communication using deafblind manual alphabets. Since these are mainly separately fabricated commercial sensors and actuators for different purposes, integrating them together is often challenging. Sometimes it is difficult to find sensors and actuators with same size, compactible and with desired characteristics. So rather than having individual touch-sensors and actuators, integrating them together from design stage and at device fabrication level offers the option to develop a customisable tactile interface which makes it possible for users to use same touch point to send and receive messages. Messages are sent by touching at the touch-points and received exactly at the same location in the form of vibration.

Fig. 8-2(a) shows existing Lorm communication glove for deafblind people as described in Section 2.2.2. The glove is made up of fabric-based pressure sensors and vibration motor and it is meant for deafblind people who know how to use Lorm deafblind manual alphabet. By convention, most of the signing in Lorm alphabet is done on the palm area alone. But due to the inability to integrate both sensor and the feedback actuator at the same location inside the palm, the researchers in [211] separately positioned the sensors and actuators. This will be a challenge for the user as they will have to start learning how to understand cues at locations on the back of the hand. Alternatively, this thesis proposes a touch-sensitive actuator which is capable of both tactile sensing and feedback. This is advantageous as it will enable touch and vibrotactile feedback to be at the same location as opposed to what was done in Lorm glove. This will enable the fabrication of similar interfaces without changing the message decoding method for deafblind people. Similarly, Fig. 8-2 shows the Malossi glove in which the vibration motor and a capacitive layer are integrated together as one, but on a rigid material; hence the user will not be able to wear it and move their fingers. The same touch-sensitive vibrotactile actuator is a step towards a flexible solution as it uses flexible spiral coil as well as soft polymeric (Ecoflex) packaging as described in Section 5.1.

Additionally, Fig. 8-2 (c) shows the Perkins Brailler [212], it consists of Braille keys for sending messages and a pin array for reading the messages. The proposed finger Braille method (presented in Section 4.4) is a wearable version of the Perkins Braille with the index, middle and ring finger representing the six dots of Braille. Wearability is important in this case as it will provide opportunity for users to conveniently move about with the device. In

Perkins Brailler, the input is a set of keys on the device and the output is an array of pins which move up and down in accordance with the Braille code but in this thesis, the touch-sensitive actuator will support the development of a more efficient device using the concept of finger Braille. This will give feedback to users in the form of vibration instead of array of pins which is more difficult to read. The inductance-based pressure sensor presented in Section 6.2 is meant to support the fabrication of the Finger Braille concept and the motivation is that it uses a coil which can be harnessed for both sensing and actuation.

In terms of technology, tactile sensors and feedback actuators have been previously fabricated for assistive purpose with properties as summarised in Table 2-6 and Table 2-7 respectively. Amongst these (as described in Section 2.4 and Section 2.5), none has been reported to have both tactile sensor and actuator integrated together for tactile display. In this work, a single device (touch-sensitive actuator) with tandem tactile sensor and actuator is fabricated. This is advantageous as it inherently has both the sensor and the actuator as one device which opens door for a generic interface for all tactile deafblind communication methods summarised in Fig. 8-2. This is because all the deafblind manual alphabets have one thing in common, which is the fact that individual touch points and/or a combination of them are representative of different messages and are both used for sending and receiving messages. So, an array of touch-sensitive actuator could be developed to cover all areas of the hand and hence irrespective of the deafblind manual alphabet, the user can use the device. Further, the touch sensitive actuator also opens doors for applications like sensitive prosthetic hands where the same technology could be used for pressure sensing at the fingertip of the prosthetic hand and then the actuator at the stump of the amputee and both communicating wirelessly or wired. For wireless communication the coils could be used as antenna, the one at the fingertip will act as the sender while the one at the stump will be the receiver.

8.2 Inductance-based pressure sensor

This is proposed to be applicable to finger Braille communication interface. As at the time of writing this thesis, there is no reported finger Braille device for communication by deafblind people. Braille is reportedly difficult to learn and there are very few teachers [213]. Finger Braille provides a simplified way of learning and teaching Braille and developing touch-sensitive actuators for this purpose is a contribution towards achieving this.

So rather than having the vibration motor at the back of the finger and FSR at the tip of the finger as used in our work in [214], the exploration type design of touch-sensitive actuator

presented in Section 5.4 could be used for finger Braille application in which case the fingertip will contain both the touch sensor and the actuator integrated together. This offers the option of reduced space as well as to place the actuator at the tip of the finger which is one of the most tactile sensitive area of the body.

8.3 Capacitive tactile sensing array

The capacitive tactile sensing array presented in Section 6.1 is applicable for communication using block letters. A capacitive array that has the capability for writing of block letters will be advantageous as it will support the fabrication of wearable interfaces for deafblind people who already have the knowledge of reading and writing. The capacitive sensors used in the fabrication of the Lorm glove [31] for instance are individual sensors placed together in the hand. Having an array of these sensors will give more room for controllability and customisation as well as improved and defined resolution. The capacitive array is flexible and wearable and unlike mobile phone screen, will be dedicated for deafblind communication making it easier to adopt the method they are already familiar with.

Chapter Summary

This thesis advances the state of the art in three main ways and opens more doors and opportunities for further research. (1) To date, existing assistive tactile communication interface for communication by deafblind people uses separate single element sensor and/or actuator. In this thesis, a tactile feedback actuator was fabricated with an integrated sense of touch. Having the sensor and actuator integrated together as one device from fabrication stage will improve customisation and compatibility. It is advantageous for deafblind people because the communication methods they use require same touch-point for touch-sensing and tactile feedback. For the future, an array of this device will enable the realisation a generic tactile interface for people from different countries who use different types of deafblind manual alphabets; (2) It also opens opportunity for developing a means for deafblind people to communicate using block letters. This is where the fabricated capacitive array presented in this work comes into play (3) A soft and flexible inductance-based pressure sensor was fabricated for application in Finger Braille communication method which makes Braille teaching and learning easier. The idea is to create opportunity to enable same technology (electromagnetic) to be used for both sensing and actuation, and so it could further be customised in the future to also have sensor and actuator at the same location for effective sending and receiving of information.

Chapter 9

9 Conclusion and Future Work

9.1 Conclusion

The overall aim of this PhD research is to design and fabricate tactile sensing and feedback interface for assistive communication devices that support face-to-face as well as remote communication by deafblind people.

In this research, a requirement-gathering investigation was carried out by interviewing staff of three deafblind organisations (deafblind Scotland, deafblind UK and Sense Scotland) as well as 9 deafblind people based in Scotland to establish user-friendly requirements. These questions helped in the formulation of important qualitative requirements for the deafblind communication device as presented in Chapter 4. Based on the ideas from the interaction from the user, two proof-of-concept devices were developed – one for users of the British deafblind manual alphabet and the other for finger Braille users. These devices were realised using commercial sensors (Force Sensitive resistors from Interlink Electronics/Tactile switch from Digi-Key) and actuators (coin type vibration motors from Precision Microdrives UK) all of which were previously used by researchers for some existing deafblind communication devices. This was done to understand the merits/ limitations of some these commercial components as it applies to methods of deafblind communication. The limitations found in some cases include rigidity and difficulty in integrating them together given that they are differently made for other purposes and hence have various dimensions and properties. This equally makes it difficult in realising a good array of tactile points which effectively adopts the methods of deafblind communication.

To overcome some of these limitations inherent in the interface used, for deafblind communication devices, four flexible tactile interfaces were developed in this work. These include: two touch-sensitive electromagnetic actuators, one capacitive tactile sensing array, and a facile single element soft and flexible inductance-based pressure sensor. The interfaces fabricated in this work were evaluated by 40 participants (20 deafblind people and 20 sighted and hearing people).

The two fabricated touch-sensitive electromagnetic actuators (Type 1 and 2) are both based on electromagnetic principle and capable of simultaneous tactile sensing and feedback. Each

comprises of a tandem combination of two main modules - the touch-sensing module and the actuation module, both integrated as a single device. The result shows that the actuator could serve as a means of creating localised tactile sensing and feedback applicable for assistive tactile displays. The literature shows that existing assistive tactile displays do not have inherent touch capability and so this is a contribution in this direction. The results of characterisation carried out from a frequency of 10Hz to 200Hz with different pulsating current shows a maximum displacement (~ 190µm) at around 40Hz. This interface was evaluated by 40 participants (20 deafblind people and 20 sighted and hearing people). The result shows that they are able to feel vibrations in the range of 10Hz - 200Hz, and lower frequencies being more distinguishable.

Another tactile interface fabricated is an 8 x 8 capacitive tactile sensing array which was designed and fabricated using flexible polyimide sheet as substrate and diamond-shaped gold electrodes deposited on both sides in a row and column fashion (similar to the array for mobile phone screen). It is intended for use as an assistive tactile communication interface for deafblind people who communicate using deafblind manual alphabets as well as the English block letters. Testing of single pixels as well as drawing pattern on the array worked and shows that each pixel has good response to touch. This interface was evaluated by 40 participants (20 deafblind people and 20 sighted and hearing people) by writing block letters. Letters were not correctly interpreted all the time due to the limited effect of the 8 x 8 array.

A soft and flexible inductance-based pressure sensor was also designed, fabricated and characterised for use as an interface for finger Braille communication method. It was realised with a soft ferromagnetic elastomer and a 17µm-thick coil fabricated on a flexible 50 µm-thick polyimide sheet. The ferromagnetic elastomer acts as the core of the coil, which when pressed, sees the metal particles moving closer to each other, leading to changes in the inductance. The coil, with 75µm wide conductor and 25µm pitch, was also realised using LIGA (Lithographie Galvanoformung, Abformung) micromolding technique. Seven different sensors have been fabricated using different ratios (1:1, 1:2, 1:3, 1:5, 2:1, 3:1, and 5:1) of Ecoflex to Iron particles. SEM analysis of the ferromagnetic elastomers shows that the Iron particles settled at the bottom after curing and hence different sides of the elastomer (dense side down and dense side up) were used in each case to the test sensor's performance. Investigation of the effect of the presence of the Iron particles on the elasticity of the ferromagnetic elastomers was carried out by determining their weight, stress-strain relationship and hence Elastic Modulus. It was observed that the 1:5 ferromagnetic elastomer

which has the highest Iron particles by weight also has the highest weight (W=0.6g) as well as the highest elastic modulus. The least weight and elastic modulus was obtained in the case of 5:1 ratio elastomer with a value of 0.21g

Measurement of the inductance of the sensors before loading shows higher values of inductance and quality factor for those with more Iron particles by weight. In terms of the orientation of the elastomers, it was observed that sensors realised with the dense side of the elastomers facing down had more inductance as well as quality factor. This is expected given that the more the Iron particles closer to the coil, the more the inductance and hence quality factor. Performance of the sensors under cyclic loading shows that those realised using the dense side of the elastomer facing down also gave the highest change in inductance. To further understand the performance of the sensors, the calibration curve for all sensors was plotted. It was observed that sensors realised using ferromagnetic elastomers with equal Ecoflex and higher Iron particles by weight all showed positive change in inductance for every increase in pressure as opposed to those with lower iron particles by weight. Also, those with elastomers having their dense side down (DD) had the highest dynamic range as well as higher inductance values in comparison with those with their dense side up (DU). This means that increasing the iron particles relatively increased the sensor's linear range with 1:5DD having the most linear region and 1:1 the least.

In terms of sensitivity, higher values were observed for the case where the elastomer's dense side is down (except for the 5:1). The 1:2DD elastomer had the highest sensitivity (0.07kPa^{-1}) while the lowest and negative values were observed for sensors having 2:1DU (-0.017 kPa^{-1}) and 5:1DU (-0.016 kPa^{-1}). Considering the response and recovery time of the sensors, the presence of Iron particles in Ecoflex has significant effect on both response and recovery time of the sensors. While increasing the presence of the Iron particles lead to faster response time for the case when the dense side of the elastomers are facing up, the recovery time was generally faster for those with higher Iron particles.

Having carried out some statistical analysis with the t-test on the different data for various groups shows p-value < 0.05 in all cases considered, it can be concluded that the presence of Iron particles in the elastomer has positive influence on the overall performance of the sensors. However, relative to the coil design used in this work, there is a limit to what ratio can be used and as observed, ratios of Ecoflex to Iron particles higher than 5:1 will behave more like plain Ecoflex as there will be relatively few particles causing the change. Also, ratios lower than 1:5 are difficult to mix given that there will be insufficient Ecoflex to mix

the corresponding Iron particles. In general, sensors with higher Iron particles by weight gave better response with 1:5 having relatively good performance in all. It is therefore recommended for the intended application, especially for its fast response time, long linear and dynamic range.

In conclusion, four tactile interfaces were designed, fabricated and characterised for application in assistive tactile communication device for deafblind people. Each of the interfaces is uniquely targeted for a particular method of communication used by deafblind people.

However, this work is not without limitations. Although up to 40 participants (20 deafblind , and 20 sighted and hearing) participated in the evaluation of the devices, the user-requirement interview carried out before embarking on the development of the different devices involved only 9 deafblind people and so the opinion of majority of deafblind people has not been captured. Also, before the touch-sensitive actuator can be used for an array for the purpose of generic deafblind device, its size needs to be further scaled down and proper shielding done to avoid magnetic interference of neighbouring tactile points.

9.2 Future Work

The work carried out during this PhD provides a basis for the development of a wearable assistive two-way communication device for deafblind people. It opens doors for the possibilities of realising effective tactile communication devices for deafblind people.

Future work can extend this research in the following ways:

- Development of an array of the touch-sensitive actuators as an extension of both the capacitive tactile sensing array and the single element touch-sensitive actuator that was presented in this work. The capacitive tactile sensing array is only capable of touch sensing and has no tactile feedback, while the single element touch-sensitive actuator has both tactile sensing and feedback but is not designed as an array. The realisation of this will mean a complete realisation of a suitable generic tactile display capable of representing all the required tactile points for the different deafblind manual alphabets.
- The replacement of the capacitive layer of the single element touch-sensitive actuator with the inductance-based pressure sensor through the utilisation of same coil for tactile sensing and actuation.

- The adoption of the design proposed for the generic deafblind communication glove applicable for all deafblind manual alphabets used across countries: As presented in Chapter 2 of this thesis, deafblind people make use of different methods of communication amongst which the popular tactile method is deafblind manual alphabet and Braille. The latter is different for different countries and hence device developed so far are usually tailored to suit only a specific deafblind manual alphabet. However, all these methods have something in common which is that the same point used for sending message is also used for receiving. This thesis has leveraged this and developed a touch-sensitive actuator which has the inherent ability to sense touch and create vibration. This opens door for the development of a generic tactile interface usable for all deafblind manual alphabets for different countries. This is possible by developing an array of this touch-sensitive actuator with miniaturised taxels distributed all over the hand and programmed to activate based on the chosen deafblind manual alphabet.

Appendix

1. How to Sign Different Deafblind Manual Alphabets

How to sign the different types of deafblind manual alphabets (British Deafblind Manual Alphabet (B-DMA), Lorm, and Malossi)

English Letter	How to Sign on the Listener's Hand			
	B-DMA	**Lorm**	**Malossi**	**Comments (Similarities)**
A	Touch the tip of the thumb of the listener	Touch the tip of the thumb of the listener	Touch the tip of the thumb of the listener	Same for all
B	Touch in the middle of the listener's palm with all the tips of your fingers.	Move your finger continuously downwards along the index finger starting from the tip till just above the palm (don't touch the palm).	Touch the tip of the listener's index finger	Letter B and K have the same sign for Lorm and B-DMA.
C	Move your finger upwards starting from outside the thumb to the end of the index finger	Touch the middle point of the lowest part of the palm	Touch the tip of the listener's middle finger	N/A
D	Using the tip of your thumb and index finger, touch the middle of	Move your finger downwards along the middle finger	Touch the tip of the listener's ring finger	N/A

	the listener's index finger	starting from the tip till just above his palm (don't touch palm).		
English Letter	**B-DMA**	**Lorm**	**Malossi**	**Comments (Similarities)**
E	Touch the tip of the listener's index finger	Touch the tip of the index finger.	Touch the tip of the listener's little finger	Same for B-DMA and Lorm
F	With two tips of your fingers touch the side of the listener's index finger	Gently press together the tips of the index and middle finger.	Touch the centre of the listener's thumb	N/A
G	With the side of your fist touch the right part of the listener's palm	Move your finger downwards along the ring finger from the tip till just above his palm (don't touch palm).	Touch the centre of the listener's index finger	N/A
H	Move the tips of your index, middle and ring finger simultaneously along the listener's index finger starting from the base of the thumb	Move your finger downwards along the little finger starting from the tip till just above the palm (without touching palm).	Touch the centre of the listener's middle finger	N/A

I	Touch the tip of the middle finger of the listener	Touch the tip of the middle finger.	Touch the centre of the listener's ring finger	Same for B-DMA and Lorm
English Letter	**B-DMA**	**Lorm**	**Malossi**	**Comments (Similarities)**
J	Trace the shape of letter "J" starting from the tip of the middle finger to the base of the thumb	With the tip of your two fingers, gently press together the tip of the listener's middle finger.	Touch the centre of the listener's little finger	N/A
K	With your fist, touch the back of your middle finger at the centre of the listener's index finger	Touch in the middle of the listener's palm with all the tips of your fingers.	Touch the base of the listener's thumb	N/A
L	With the tip of your index finger, touch the centre of the listener's palm	Move your finger downwards with three tips along the index middle and ring finger starting from tip till just above his palm (don't touch palm).	Touch the base of the listener's index finger	N/A
M	With the tip of your index, middle and ring finger, touch	Touch with three tips of your finger the	Touch the base of the listener's middle finger	N/A

	simultaneously the centre of the listener's palm	higher part of the listener's palm in a horizontal way.		
English Letter	**B-DMA**	**Lorm**	**Malossi**	**Comments (Similarities)**
N	With the tip of your index and middle finger, touch simultaneously the centre of the listener's palm	Touch with the two tips of your finger the higher part of the palm of his hand in a horizontal way.	Touch the base of the listener's ring finger	N/A
O	Touch the tip of the listener's ring finger	Touch the tip of the ring finger	Touch the base of the listener's little finger	Same for B-DMA and Lorm
P	Press the tip (front and back together) of the listener's index finger	Move your finger upwards on the outside of the listener's index finger.	Pinch (press) the tip of the listener's thumb	N/A
Q	Grab the thumb of the listener with your hand wrapped round it	Move your finger upwards on the outside of his hand (on the side of the little finger).	Pinch (press) the tip of the listener's index finger	N/A
R	Using the back of your index finger touch the centre of the listener's palm	Drum slightly with several of your tips in the middle of the	Pinch (press) the tip of the listener's middle finger	N/A

		palm of the listener's hand.		
English Letter	**B-DMA**	**Lorm**	**Malossi**	**Comments (Similarities)**
S	With one tip of your finger touch between the listener's little and ring finger	Trace a circle in the middle of the palm of the listener's hand.	Pinch (press) the tip of the listener's ring finger	N/A
T	With one tip of your finger touch the right side of the listener's palm	You're your finger downwards on the outside of the listener's thumb.	Pinch (press) the tip of the listener's little finger	N/A
U	Touch the tip of his little finger	Touch the tip of his little finger	Pinch (press) the base of the listener's thumb	Same for B-DMA and Lorm
V	With your index and middle finger touch the centre of the listener's palm forming a V-shape	Touch with a tip of your finger on the palm (left side) between the meeting point of the thumb and the index finger.	Pinch (press) the base of the listener's index finger	N/A
W	Gently grab the listener's palm between the listener's thumb and index finger (with both palm facing each other	Touch with two tips (in a vertical way) in the palm (left side) between the meeting point of the thumb and the index finger.	Pinch (press) the below the base of the listener's index finger	N/A

X	With your index finger touch the listener's index finger between finger and palm	Move your finger horizontally (from left to right) over the wrist area (between wrist and palm)	Pinch (press) the base of the listener's middle finger	N/A
English Letter	**B-DMA**	**Lorm**	**Malossi**	**Comments (Similarities)**
Y	Move your finger from the base of the listener's thumb	Move your finger horizontal (from left to right) over the centre of all the fingers.	Pinch (press) the base of the listener's ring finger	N/A
Z	With the side of your palm touch the listener's palm between the fingers and palm	Move your finger diagonally (from left to right) over the centre of the palm of the listener's hand.	Pinch (press) the base of the listener's little finger	N/A

a. How to Sign the British Deafblind Manual Alphabet (B-DMA)

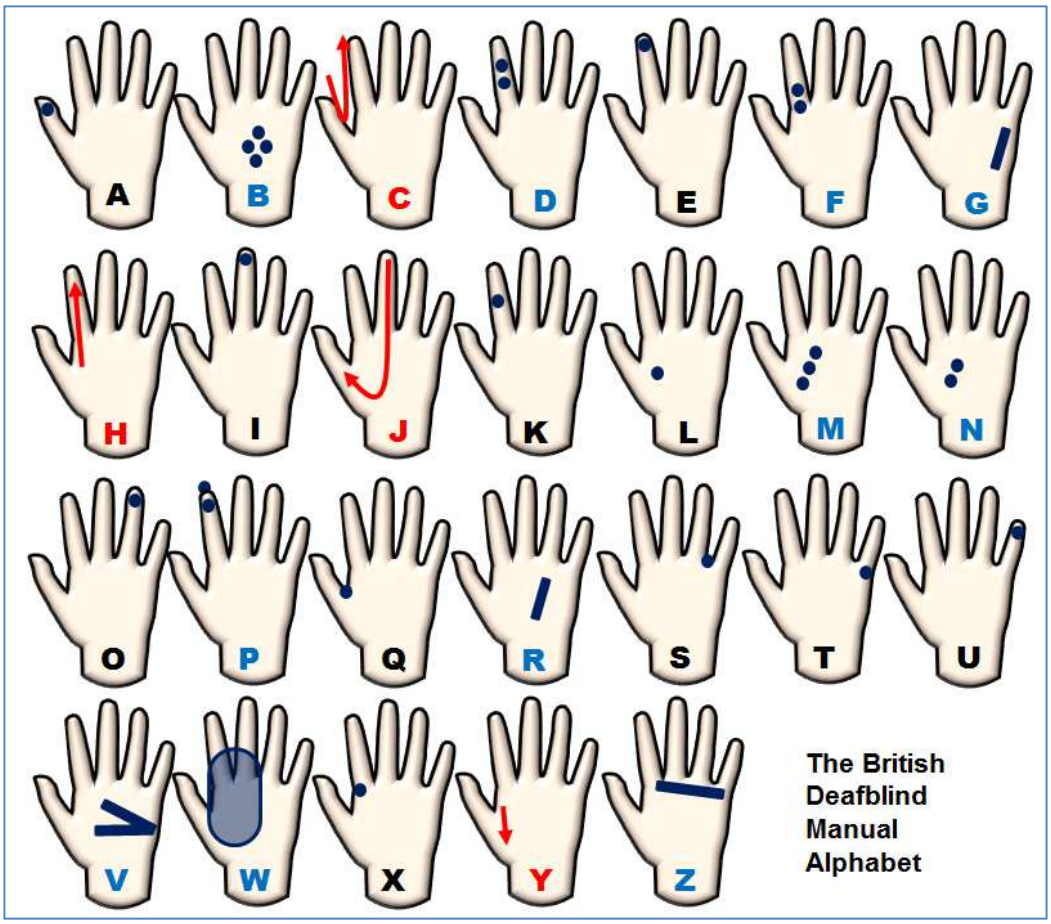

2. Flowchart of Proposed Generic Communication System for Deafblind People

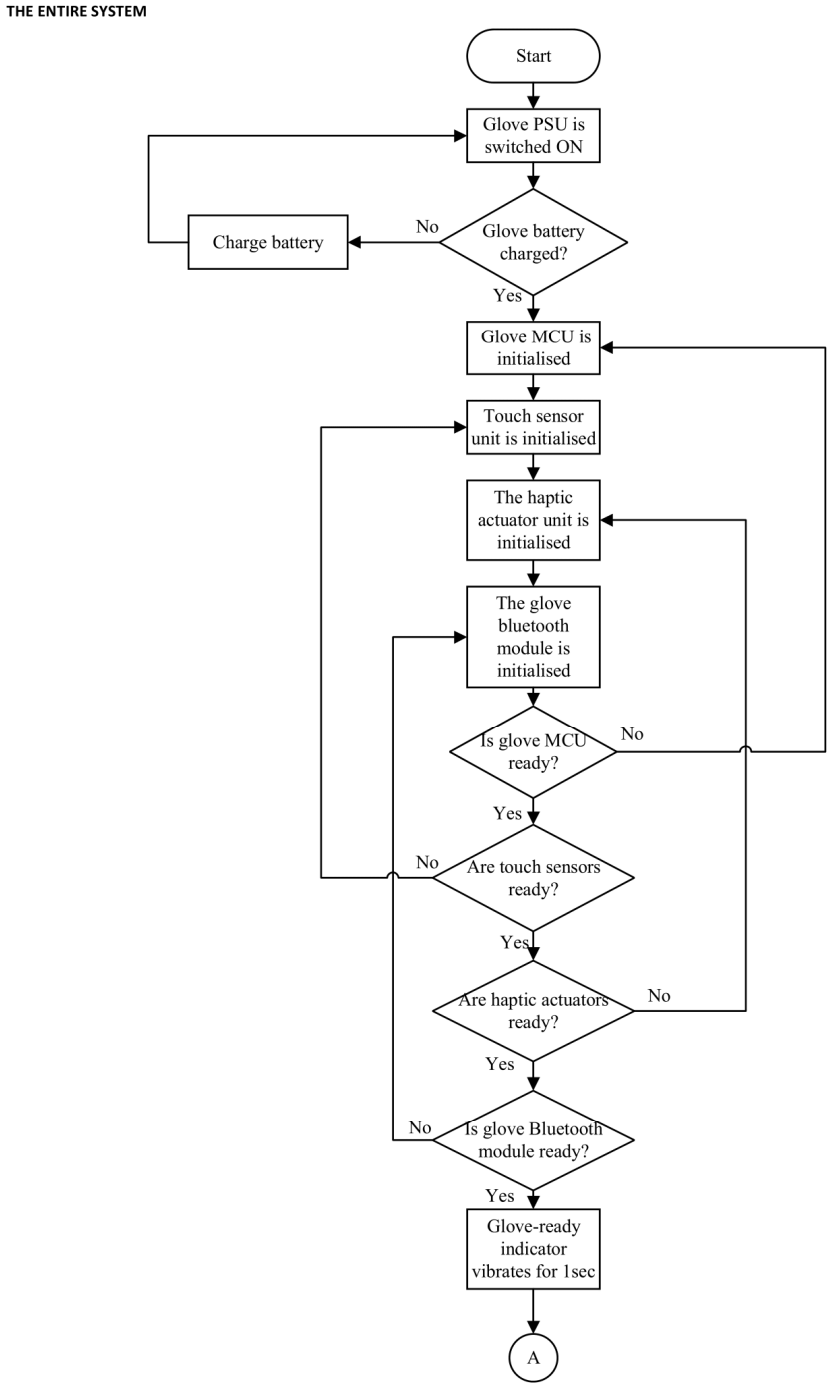

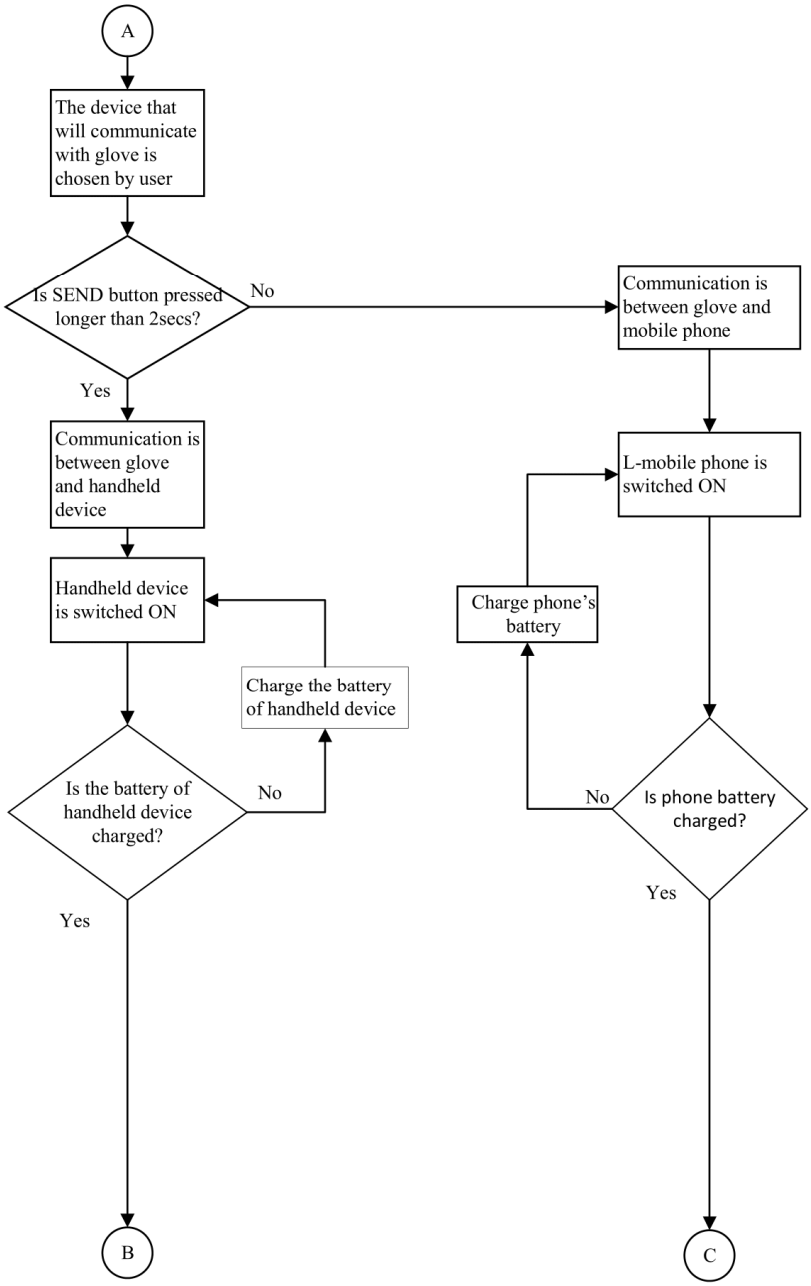
A
The device that will communicate with glove is chosen by user
Is SEND button pressed longer than 2secs?
No
Communication is between glove and mobile phone
Yes
Communication is between glove and handheld device
L-mobile phone is switched ON
Handheld device is switched ON
Charge phone's battery
Charge the battery of handheld device
Is the battery of handheld device charged?
No
No
Is phone battery charged?
Yes
Yes
B
C

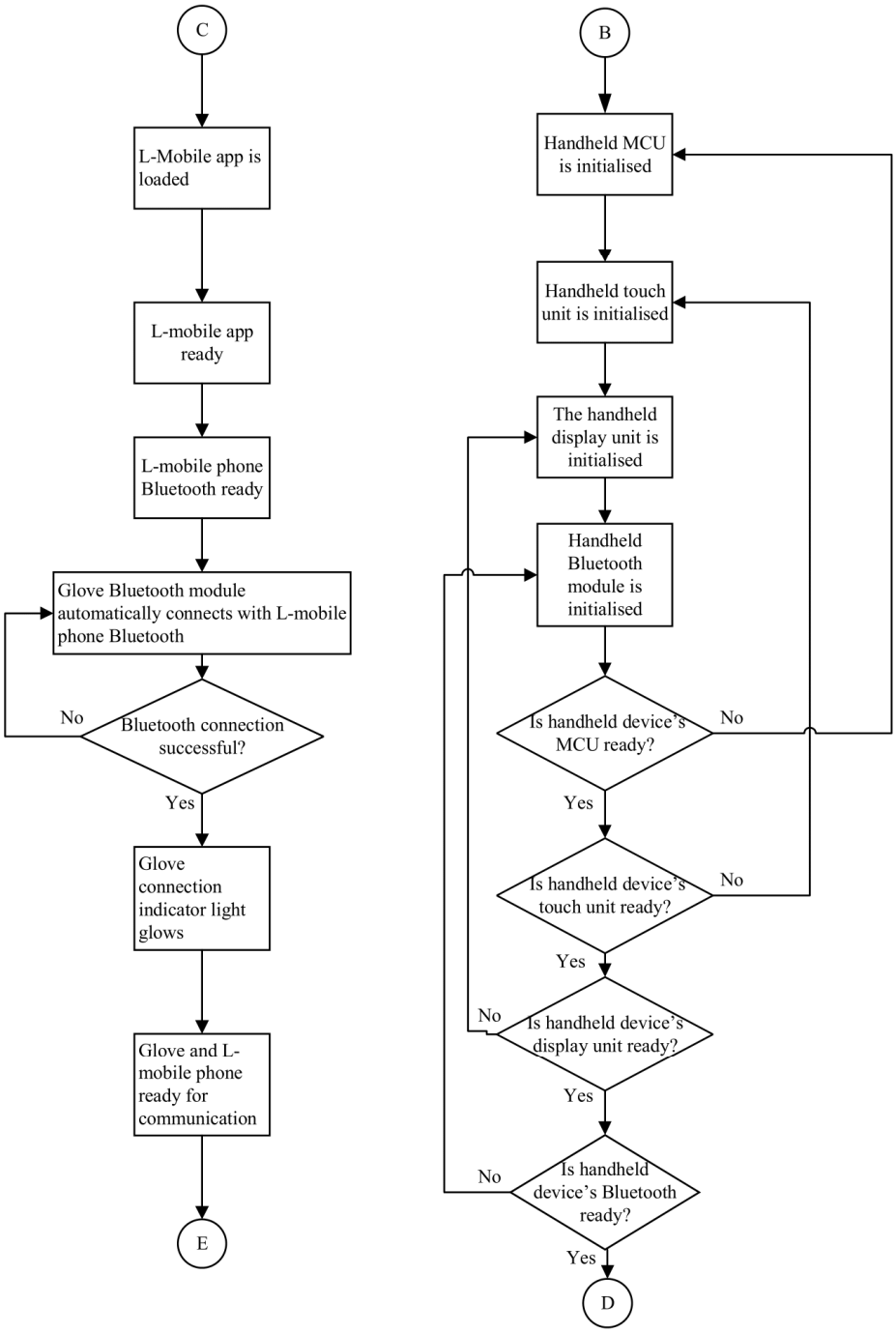
C
L-Mobile app is loaded
L-mobile app ready
L-mobile phone Bluetooth ready
Glove Bluetooth module automatically connects with L-mobile phone Bluetooth
Bluetooth connection successful?
No
Yes
Glove connection indicator light glows
Glove and L-mobile phone ready for communication
E
B
Handheld MCU is initialised
Handheld touch unit is initialised
The handheld display unit is initialised
Handheld Bluetooth module is initialised
Is handheld device's MCU ready?
No
Yes
Is handheld device's touch unit ready?
No
Yes
Is handheld device's display unit ready?
No
Yes
Is handheld device's Bluetooth ready?
No
Yes
D

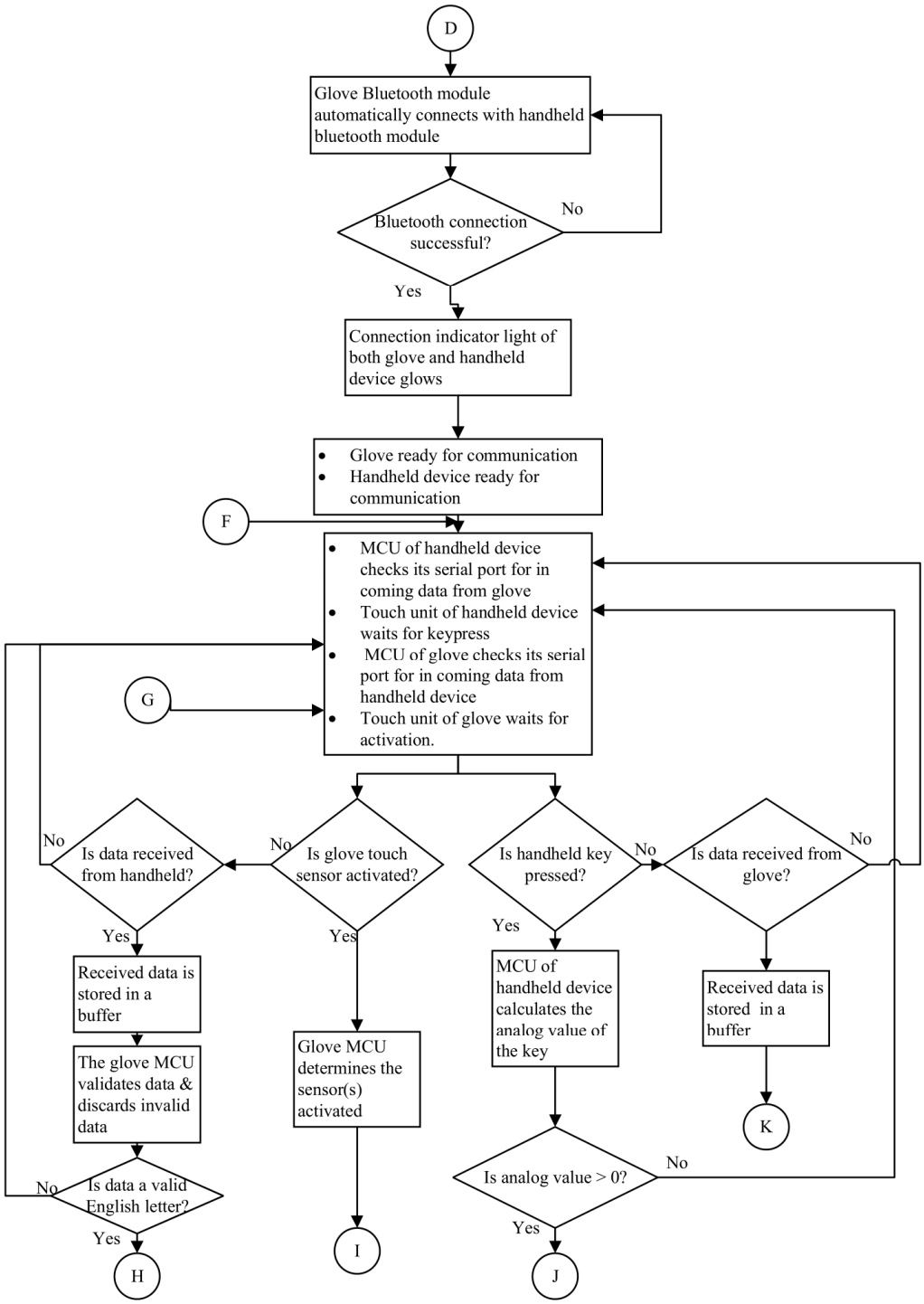
D
Glove Bluetooth module automatically connects with handheld bluetooth module
Bluetooth connection successful?
No
Yes
Connection indicator light of both glove and handheld device glows
Glove ready for communication
Handheld device ready for communication
F
MCU of handheld device checks its serial port for in coming data from glove
Touch unit of handheld device waits for keypress
MCU of glove checks its serial port for in coming data from handheld device
Touch unit of glove waits for activation.
G
Is data received from handheld?
Is glove touch sensor activated?
Is handheld key pressed?
Is data received from glove?
Received data is stored in a buffer
The glove MCU validates data & discards invalid data
Is data a valid English letter?
H
Glove MCU determines the sensor(s) activated
I
MCU of handheld device calculates the analog value of the key
Is analog value > 0?
J
Received data is stored in a buffer
K

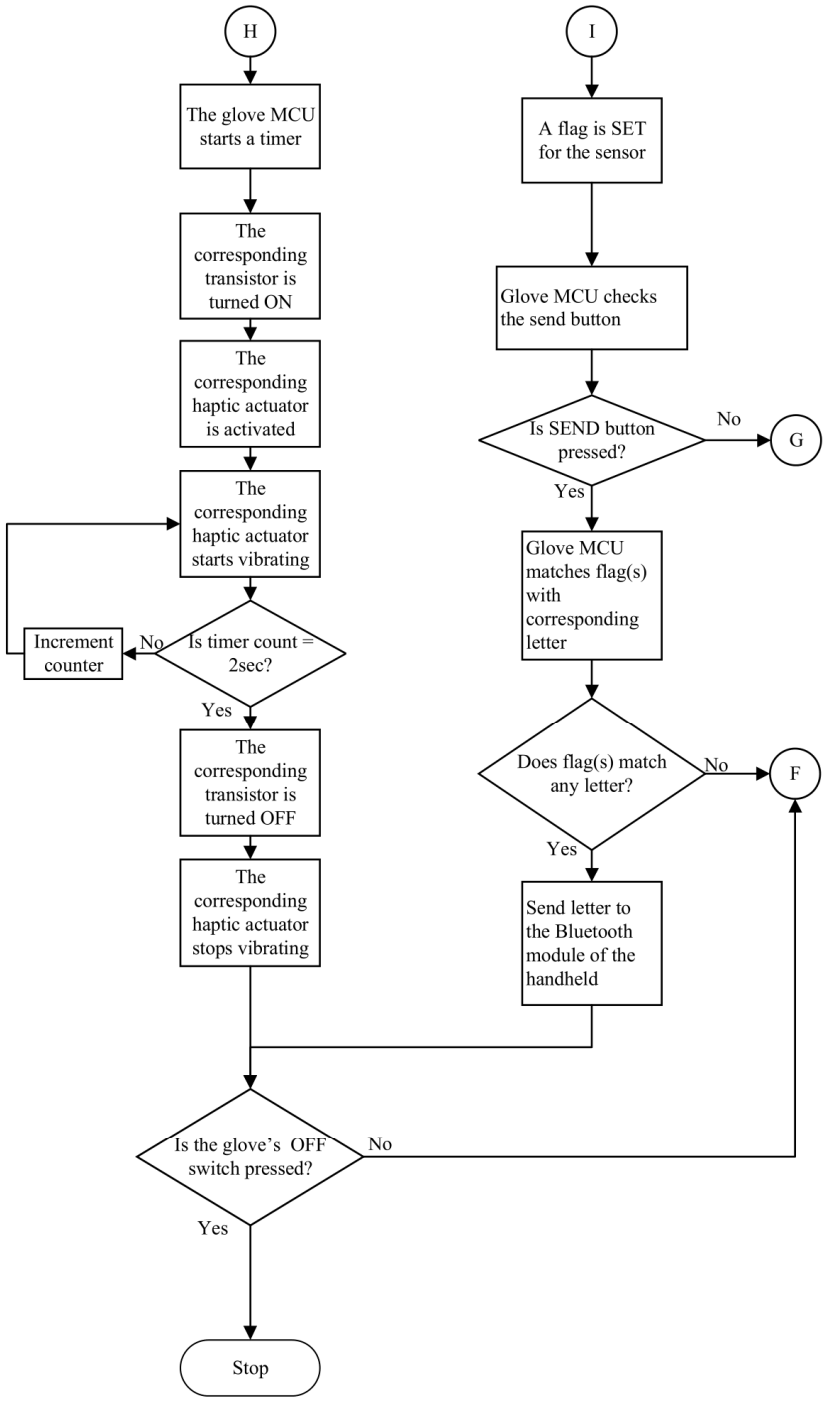
H
The glove MCU starts a timer
The corresponding transistor is turned ON
The corresponding haptic actuator is activated
The corresponding haptic actuator starts vibrating
Is timer count = 2sec?
No
Increment counter
Yes
The corresponding transistor is turned OFF
The corresponding haptic actuator stops vibrating
I
A flag is SET for the sensor
Glove MCU checks the send button
Is SEND button pressed?
No
G
Yes
Glove MCU matches flag(s) with corresponding letter
Does flag(s) match any letter?
No
F
Yes
Send letter to the Bluetooth module of the handheld
Is the glove's OFF switch pressed?
No
Yes
Stop

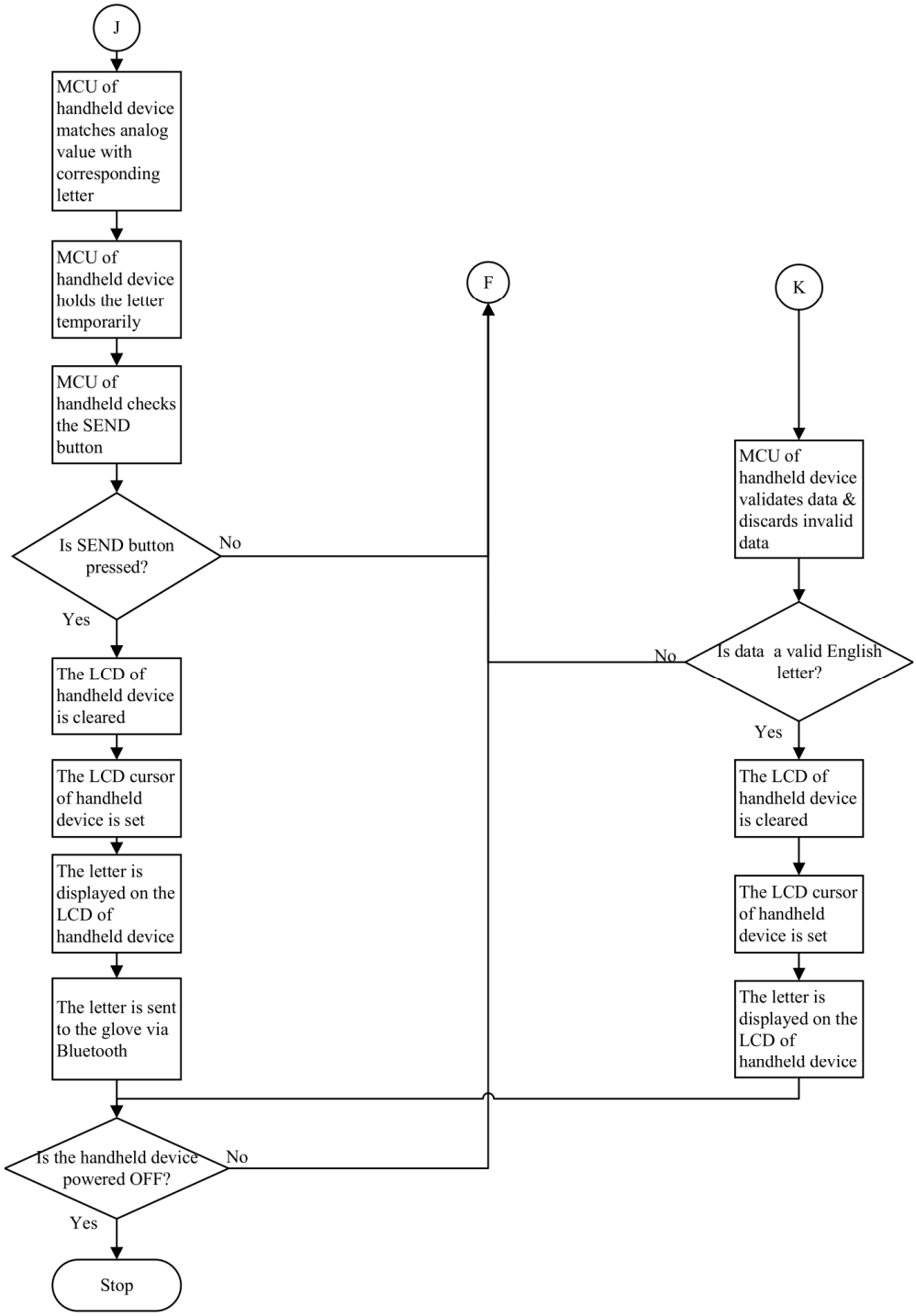
J
MCU of handheld device matches analog value with corresponding letter
MCU of handheld device holds the letter temporarily
MCU of handheld checks the SEND button
Is SEND button pressed?
No
Yes
The LCD of handheld device is cleared
The LCD cursor of handheld device is set
The letter is displayed on the LCD of handheld device
The letter is sent to the glove via Bluetooth
Is the handheld device powered OFF?
No
Yes
Stop
F
K
MCU of handheld device validates data & discards invalid data
Is data a valid English letter?
No
Yes
The LCD of handheld device is cleared
The LCD cursor of handheld device is set
The letter is displayed on the LCD of handheld device

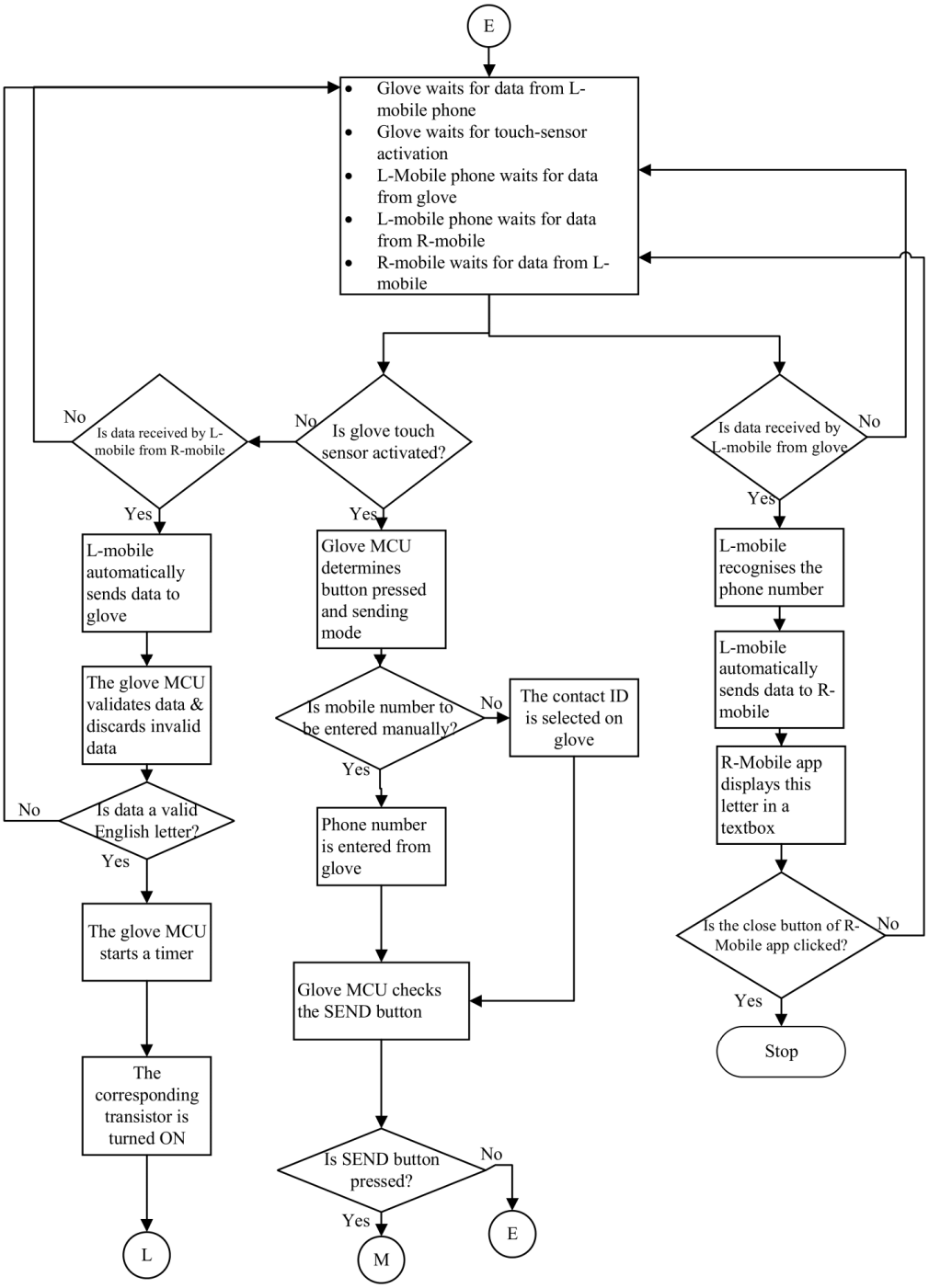
E
Glove waits for data from L-mobile phone
Glove waits for touch-sensor activation
L-Mobile phone waits for data from glove
L-mobile phone waits for data from R-mobile
R-mobile waits for data from L-mobile
Is data received by L-mobile from R-mobile
Is glove touch sensor activated?
Is data received by L-mobile from glove
No
Yes
L-mobile automatically sends data to glove
The glove MCU validates data & discards invalid data
Is data a valid English letter?
The glove MCU starts a timer
The corresponding transistor is turned ON
L
Glove MCU determines button pressed and sending mode
Is mobile number to be entered manually?
The contact ID is selected on glove
Phone number is entered from glove
Glove MCU checks the SEND button
Is SEND button pressed?
M
L-mobile recognises the phone number
L-mobile automatically sends data to R-mobile
R-Mobile app displays this letter in a textbox
Is the close button of R-Mobile app clicked?
Stop

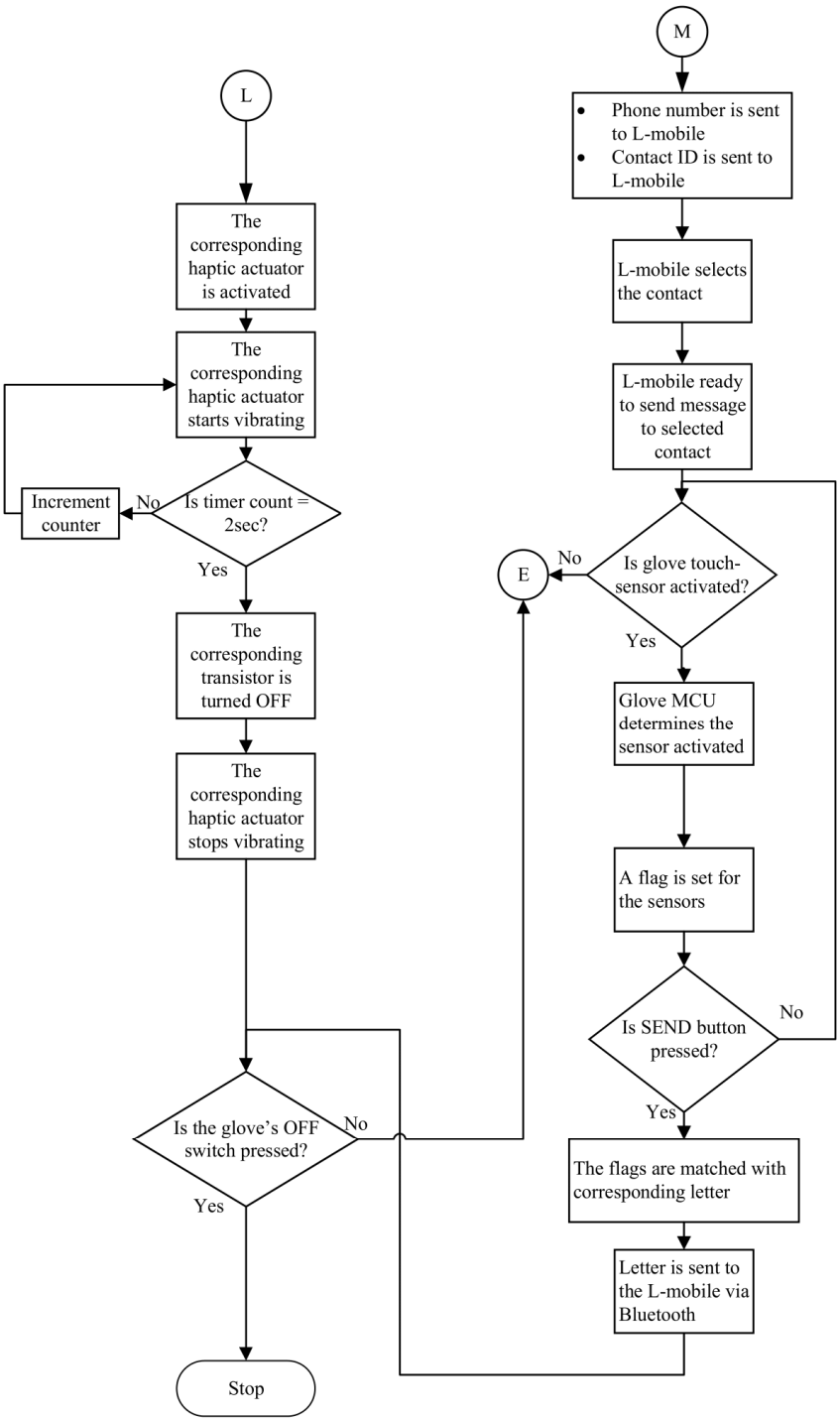
L
The corresponding haptic actuator is activated
The corresponding haptic actuator starts vibrating
Is timer count = 2sec?
No
Increment counter
Yes
The corresponding transistor is turned OFF
The corresponding haptic actuator stops vibrating
Is the glove's OFF switch pressed?
No
Yes
Stop
M
Phone number is sent to L-mobile
Contact ID is sent to L-mobile
L-mobile selects the contact
L-mobile ready to send message to selected contact
Is glove touch-sensor activated?
No
E
Yes
Glove MCU determines the sensor activated
A flag is set for the sensors
Is SEND button pressed?
No
Yes
The flags are matched with corresponding letter
Letter is sent to the L-mobile via Bluetooth

3. Truth Table of the B-DMA Logic

This table was derived from the tactile point mapping of B-DMA presented in Chapter 4 (represents all the tactile points for the 26 English alphabets using the British deafblind manual alphabets communication (See Fig. 4-10). For a particular letter, the number “1” means a tactile point is activated while “0” means it is not activated.

	Tactile Points																									
	1	**2**	**3**	**4**	**5**	**6**	**7**	**8**	**9**	**10**	**11**	**12**	**13**	**14**	**15**	**16**	**17**	**18**	**19**	**20**	**21**	**22**	**23**	**24**	**25**	**26**	**27**
A	1	0	0	0	0	0	0	0	0	0	0	0	0	0	0	0	0	0	0	0	0	0	0	0	0	0	0
B	0	0	0	0	0	0	0	0	0	0	0	0	0	0	0	0	1	1	1	1	1	1	1	1	0	0	0
C	1	1	0	0	0	0	0	0	0	0	0	0	0	0	0	0	0	0	0	0	0	0	0	0	1	1	0
D	0	0	0	0	1	1	0	0	0	0	0	0	0	0	0	0	0	0	0	0	0	0	0	0	0	0	0
E	0	0	0	0	1	0	0	0	0	0	0	0	0	0	0	0	0	0	0	0	0	0	0	0	0	0	0
F	0	0	0	0	0	0	1	1	0	0	0	0	0	0	0	0	0	0	0	0	0	0	0	0	0	0	0
G	0	0	0	0	0	0	0	0	0	1	1	1	0	0	0	0	1	1	1	0	0	0	0	0	0	0	0
H	0	0	0	0	1	1	1	1	0	0	0	0	0	0	0	0	0	0	0	0	0	0	0	0	0	0	0
I	0	0	0	0	0	0	0	0	1	0	0	0	0	0	0	0	0	0	0	0	0	0	0	0	0	0	0
J	1	1	0	0	0	0	0	0	1	1	0	0	0	0	0	0	0	0	0	1	0	0	0	0	0	0	0
K	0	0	0	0	0	0	1	0	0	0	0	0	0	0	0	0	0	0	0	0	0	0	0	0	0	0	0
L	See Table (b)																										
M	0	0	0	0	0	0	0	0	0	0	0	0	0	0	0	0	1	1	1	1	1	1	1	1	0	0	0
N	See Table (b)																										
O	0	0	0	0	0	0	0	0	0	0	0	0	1	0	0	0	0	0	0	0	0	0	0	0	0	0	0
P	0	0	0	0	1	0	0	0	0	0	0	0	0	0	0	0	0	0	0	0	0	0	0	0	0	0	1
Q	1	1	0	0	0	0	0	0	0	0	0	0	0	0	0	0	0	0	0	0	0	0	0	0	0	0	0
R	See Table (b)																										
S	0	0	0	0	0	0	0	0	0	0	0	0	0	1	0	0	0	0	0	0	0	0	0	0	0	0	0
T	0	0	0	0	0	0	0	0	0	0	0	0	0	0	0	1	0	0	0	0	0	0	0	0	0	0	0
U	0	0	0	0	0	0	0	0	0	0	0	0	0	0	1	0	0	0	0	0	0	0	0	0	0	0	0
V	See Table ©																										
W	1	1	1	1	0	0	0	0	0	0	0	0	0	0	0	0	0	0	0	0	0	0	0	0	0	0	0
X	0	0	0	0	0	0	0	1	0	0	0	0	0	0	0	0	0	0	0	0	0	0	0	0	0	0	0
Y	0	0	1	1	0	0	0	0	0	0	0	0	0	0	0	0	0	0	0	0	0	0	0	0	0	0	0

Z	0	0	0	0	0	0	0	0	0	1	1	1	0	0	0	0	0	0	0	0	0	0	0	0	0	0

a. Truth Table for letter that employ the "AND" and "OR"

INPUT											OUTPUT				
17	**18**	**19**	**20**	**21**	**22**	**23**	**24**	**L1**	**L2**	**L3**	**L4**	**N1**	**N2**	**N3**	**R1**	**R2**
1	0	0	0	1	0	0	0	1	0	0	0	0	0	0	0	0
0	1	0	0	0	1	0	0	0	1	0	0	0	0	0	0	0
0	0	1	0	0	0	1	0	0	0	1	0	0	0	0	0	0
0	0	0	1	0	0	0	1	0	0	0	1	0	0	0	0	0
1	1	0	0	1	1	0	0	0	0	0	0	1	0	0	0	0
0	1	1	0	0	1	1	0	0	0	0	0	0	1	0	0	0
0	0	1	1	0	0	1	1	0	0	0	0	0	0	1	0	0
1	1	1	1	0	0	0	0	0	0	0	0	0	0	0	1	0
0	0	0	0	1	1	1	1	0	0	0	0	0	0	0	0	1

b. Truth table for Letters L,N, and R

The truth table shows only the conditions in which letter L could be obtained (high) at other times the letter L is will not be obtained.

L1	L2	L3	L4	L
1	0	0	0	1
0	1	0	0	1
0	0	1	0	1
0	0	0	1	1

c. Truth table for V1

INPUT				OUTPUT
10	**11**	**12**	**13**	**V1**
1	1	1	1	1

d. Truth table for V2

The truth table shows only the conditions in which V2 is high and valid, any other condition V2 is 0 or not valid.

INPUT								OUTPUT
17	**18**	**19**	**20**	**21**	**22**	**23**	**24**	**V2**
1	0	0	0	0	0	0	0	1
0	1	0	0	0	0	0	0	1
0	0	1	0	0	0	0	0	1
0	0	0	1	0	0	0	0	1
0	0	0	0	1	0	0	0	1
0	0	0	0	0	1	0	0	1
0	0	0	0	0	0	1	0	1
0	0	0	0	0	0	0	1	1

The truth table shows only the conditions in which the letter V is high and obtained, any other condition V is 0 or will not be obtained.

e. Truth Table for V

V1	**V2**	**V**
1	0	1
0	1	1

4. Circuit Schematics

a. B-DMA: Output Module Drive Circuit

B-DMA GLOVE: Vibration Motor Drive Circuit

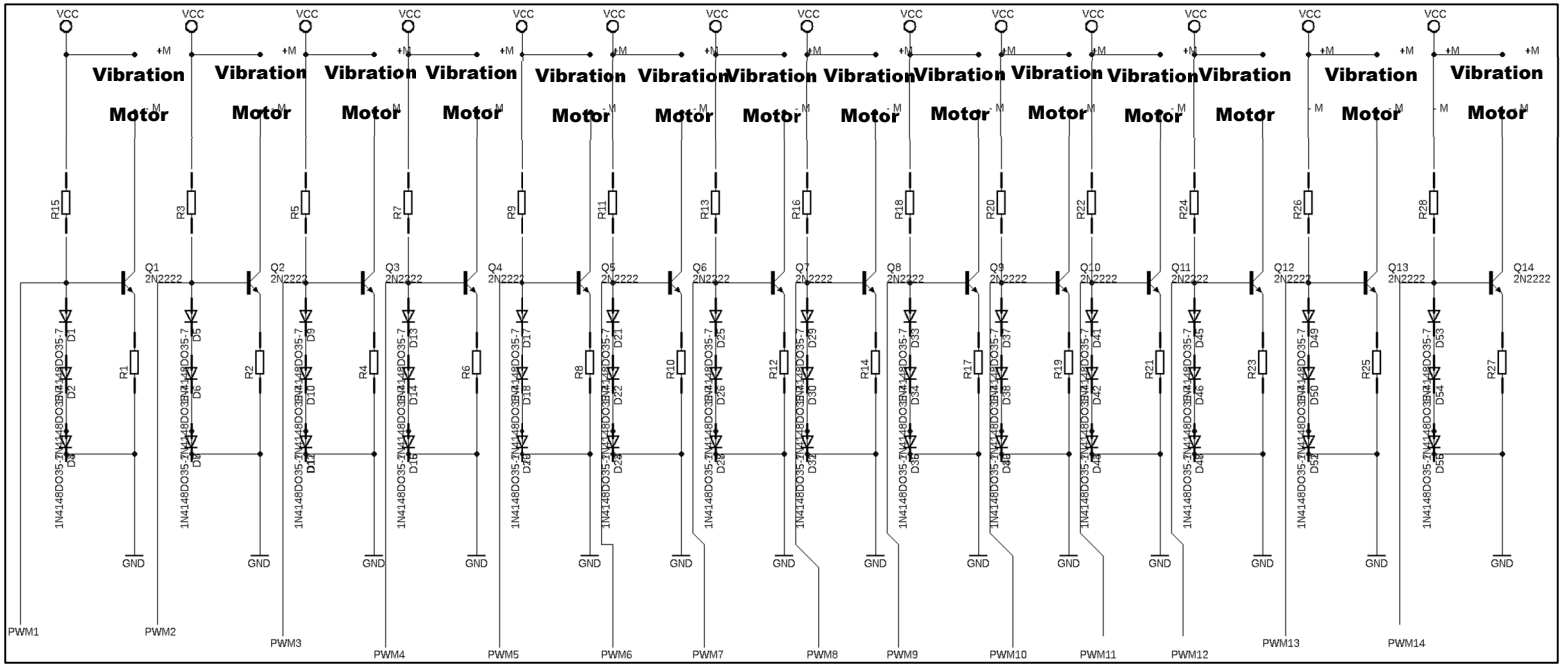

R1, R2, R4, R6, R8, R10, R12, R14, R17, R19, R21, R23, R25, R27 = 23Ω
R15, R3, R5, R7, R9, R11, R13, R16, R18, R20, R22, R24, R26, R28 = 3K

b. B-DMA: Input Module Drive Circuit

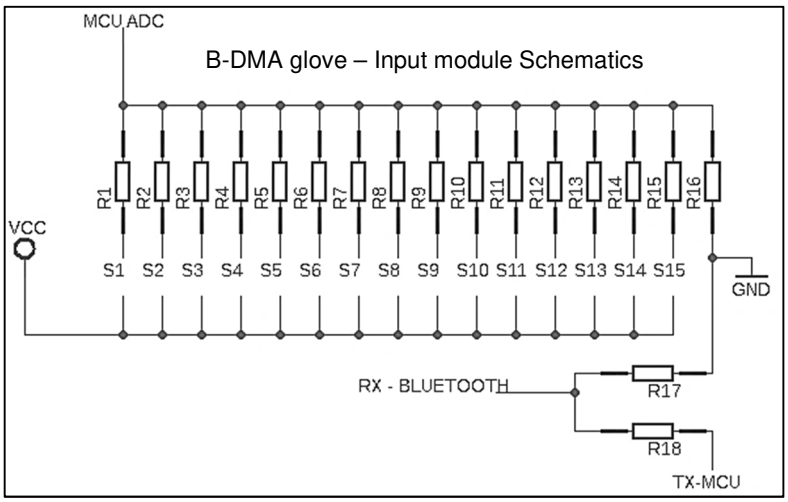

B-DMA glove – Input module Controller

R1 =47K, R2 = 43K, R3=30K, R4=22K, R5=18K, R6= 12K, R7=9.1K, R8=6.8K, R9=6.2K, R10=5.1K, R11=3.9K, R12=2.7K, R14=1.5K, R15= 300R, R16=10K, R17=10K, R18=20K

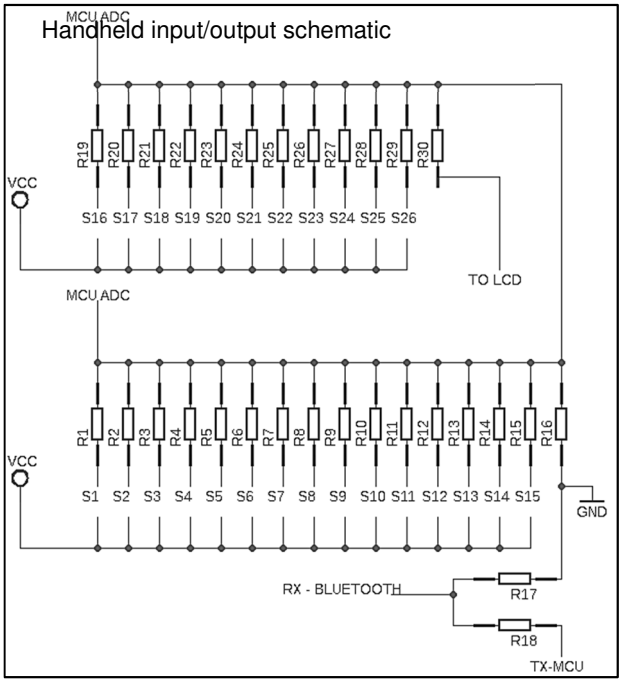

R1=47K,R2=43K, R3=36K, R4=33K, R5=30K,R6=27K, R7=22K, R8=20K, R9=18K, R10=15K, R11=12K, R12=11K, R13=9.1K, R14=8.2K, R15=6.8K, R16=6.2K, R19=5.6K, R20=5.1K, R21=4.7K, R22=3.9K, R23=3.3K, R24=2.7K, R25=2.2K, R26=1.5K, R25=910R, R26=330, R16=10K

a. B-DMA: Output Module Drive Circuit

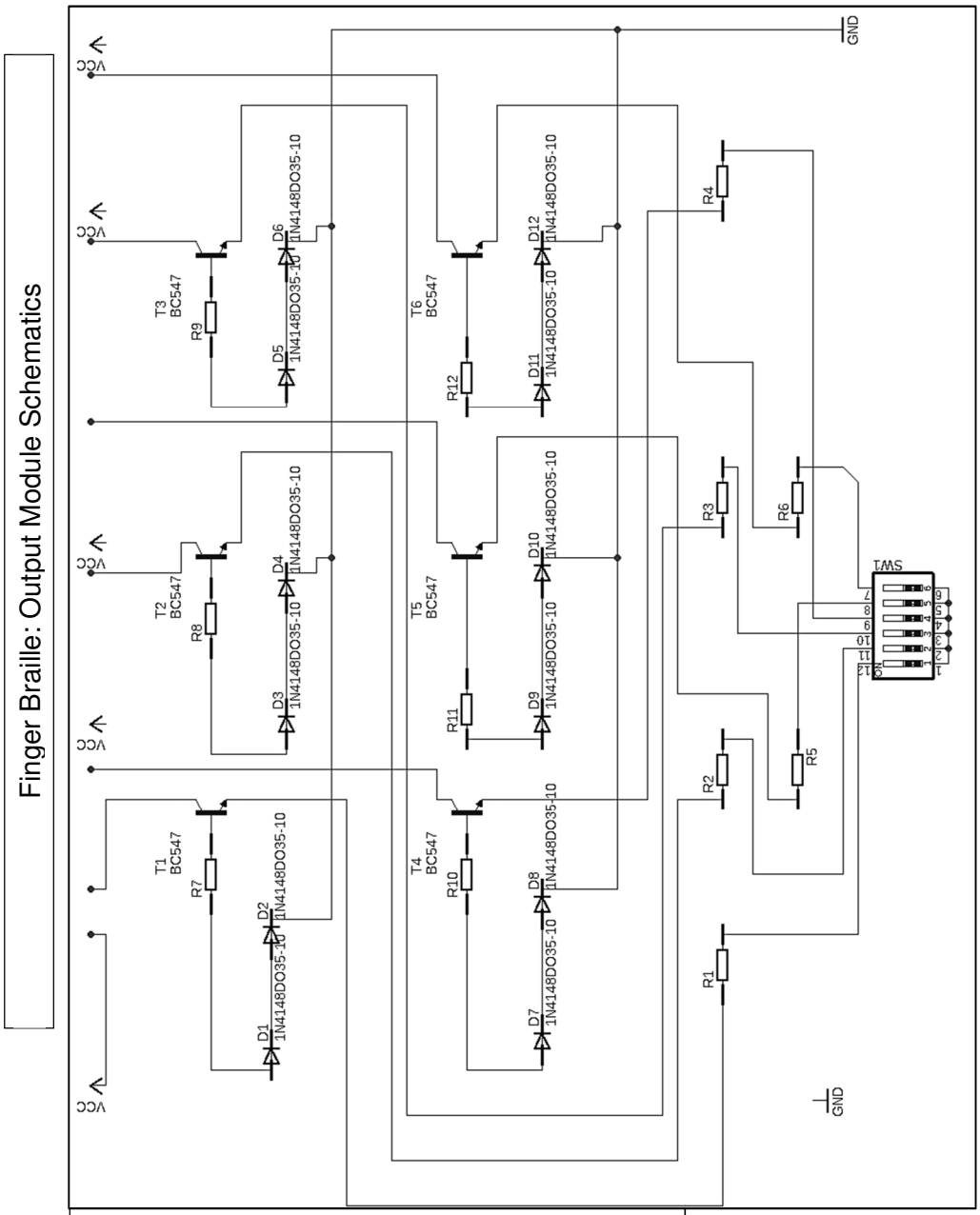

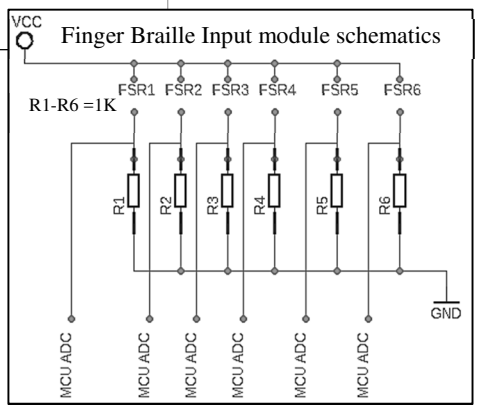

5. Biot Savart Law and Magnetic field due to current

Any wire carrying current creates a magnetic field and the relationship between this current and the accompanying magnetic field is described by Biot Savart Law. Consider a small current element of length $\overrightarrow{dl}$ which is infinitesimally small as shown in Fig. 1 . The small magnetic field $\overrightarrow{dB}$ due to the current I through this current element at a point P which is located at a distance r can be obtained using Biot Savart Law and is given by:

$$\overrightarrow{dB} = \frac{\mu_o}{4\pi}\frac{(I \times \overrightarrow{dl})}{r^2} \tag{1}$$

Considering the crossproduct, Equation (1) becomes:

$$dB = \frac{\mu_o}{4\pi}\frac{(I\ dl\ sin\theta)}{r^2} \tag{2}$$

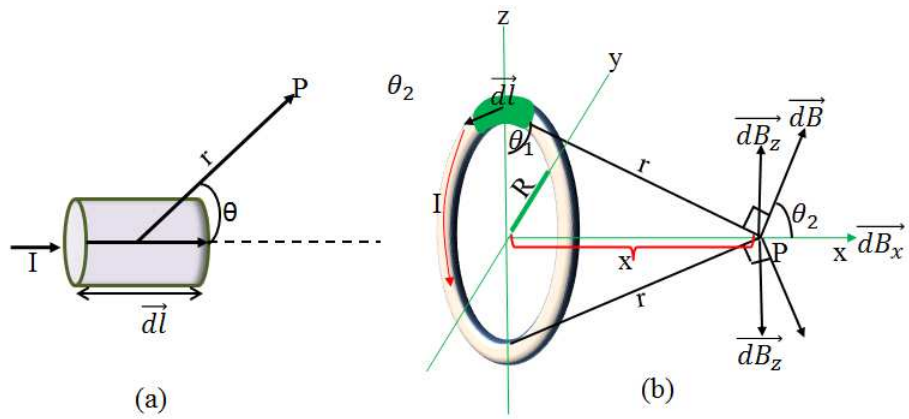

Fig. 1 Magnetic field strength: (a) Magnetic field at a point P due to a current element (b) magnetic field at the axis of a circular loop

So, to obtain the magnetic field due to a long wire, the value of the magnetic field $\overrightarrow{dB}$ due to the small current element is integrated over the entire length of the wire. This now becomes:

$$B = \int \frac{\mu_o}{4\pi}\frac{(I\ dl\ sin\theta)}{r^2} \tag{3}$$

a. Magnetic field on the axis of a circular loop

Consider a circular wire loop as shown in Fig. 1 , Biot Savart law can also be applied to analyse the magnetic field at a point P. To do this, the magnetic field due to a small current

element $\overrightarrow{dl}$ is first determined and then its value integrated over the length of the entire loop. Note that every small current element at any $\overrightarrow{dl}$ at any point in the loop has another $\overrightarrow{dl}$ on the opposite side of the loop that creates a z-component of the magnetic field dB_z which cancels out at the point P as shown in Fig. 1 . Therefore the only component of the magnetic field that exists at the point P is the x-component of the magnetic field dB_x given as:

$$dB_x = dB \cos\theta_2 \tag{4}$$

Substituting Equation (4) in (3)

$$dB_x = \frac{\mu_o}{4\pi}\frac{(I\ dl\ sin\theta_1)}{r^2}\ cos\theta_2 \tag{5}$$

$$Where\ \theta_1 = \ the\ angle\ between\ \overrightarrow{dl}\ and\ r,\ \ \theta_2 = the\ angle\ between\ \overrightarrow{dB}\ and\ \overrightarrow{dB_x}$$

But $\overrightarrow{dl}\ and\ r$ are at right angle and so Equation (5) now becomes

$$dB_x = \frac{\mu_o}{4\pi}\frac{(I\ dl\ cos\theta)}{r^2} \tag{6}$$

The magnetic field on the axis of a circular loop at the point P will now be the integral of Equation (6)

$$B = \frac{\mu_o \cos\theta}{4\pi r^2}\int dl \tag{7}$$

$$B = \frac{\mu_o \cos\theta\ 2\pi\ R}{4\pi r^2} \tag{8}$$

Substituting cos = R/r and $r = \sqrt{R^2 + x^2}$ in Equation 2-19,

$$B = \frac{\mu_o I}{2}\frac{R^2}{(R^2 + x^2)^{3/2}} \tag{9}$$

From this the magnetic field at the centre (x=0) of the circular loop is given by

$$B_{x=0} = \frac{\mu_o I}{2R} \tag{10}$$

b. Magnetic field due to a spiral coil

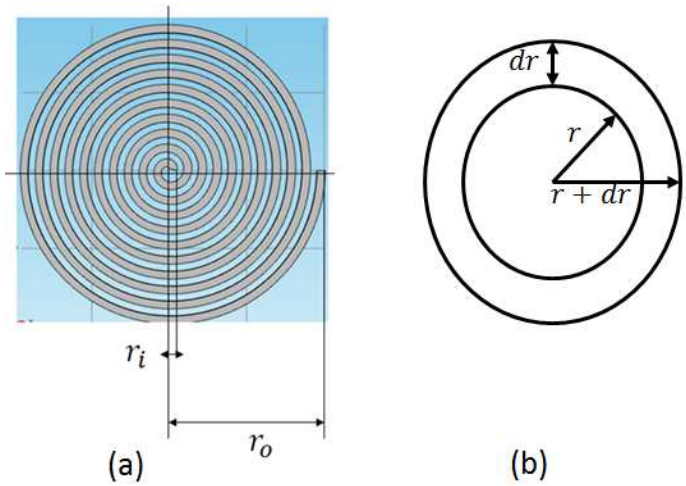

Fig. 2 Spiral Coil

Consider the spiral coil shown in Fig. 2 with inner radius r_i, outer radius r_0, and N number of turns. The number of turns per unit length is given by:

$$N_{per\ unit\ length} = \frac{N}{r_o - r_i} \tag{11}$$

Considering the spiral as being made of circles as shown in Fig. 2 b

The total number of turns in dr width is given by:

$$N_{dr} = \left(\frac{N}{r_o - r_i}\right) dr \tag{12}$$

Recall the magnetic field at the centre of a circular loop.

Using Equation (10) and (13), and also considering the case of the spiral (Fig. 2 b), the magnetic field at the centre due to the elemental width dr is

$$dB = \left(\frac{\mu_o I}{2r}\right) N_{dr} \tag{13}$$

Integrating Equation (13) gives B as:

$$B = \int_{r_i}^{r_o} \left(\frac{\mu_o I}{2r}\right)\left(\frac{N}{r_o - r_i}\right) dr \tag{14}$$

$$B = \frac{\mu_o IN}{2(r_o - r_i)} \int_{r_i}^{r_o} \frac{dr}{r} \tag{15}$$

Simplifying Equation (15) gives the total magnetic field at the centre of this spiral is as

$$B = \left(\frac{\mu_o IN}{2(r_o - r_i)}\right) ln \ \frac{r_o}{r_i} \tag{16}$$

6. COMSOL Simulation Parameters

This table show a list of the parameters defined for the simulation of the spiral coil as described in Chapter 5 (Section 5.1.3)

a. Table showing the parameters for the spiral coil simulation

Name	Expression	Value	Description
Thick_Coil	17[micrometer]	1.7000E-5 m	Thickness of Coil Conductor
Dia_Coil	75[micrometer]	7.5000E-5 m	Diameter of Coil Conductor
Pitch_Coil	25[micrometer]	2.5000E-5 m	Pitch of Coil
Ri	50[micrometer]	5.0000E-5 m	Inner Radius of Coil
Ro	Ri + (N*(Pitch_Coil + Dia_Coil))	5.5000E-4 m	Outer Radius of Coil
N	5	5.0000	Number of Turns
CAR	Dia_Coil/Thick_Coil	4.4118	Coil Aspect Ratio
L	2*pi*Ro*N	0.017279 m	Length of Coil
Hs	50[micrometer]	5.0000E-5 m	Thickness of Coil Substrate
A_Coil	(2*pi*Ro_Dia^2) + (2*pi*Ro_Dia*Thick_Coil)	9.2363E-7 m²	Area of Coil
S_Coil	pi*(N*Dia_Coil)^2	4.4179E-7 m²	Surface Area of Coil
Mu0	4*pi*exp(-7)[H/m]	0.011459 H/m	Permeability of Free Space
Current	0.07[A]	0.070000 A	Supply Current

7. Code for the B-DMA Glove implemented in Chapter Four

```
// Transmits and receives data using bluetooth & software serial

#include<SoftwareSerial.h>
const int rxPin = 10;              // RX pin
const int txPin = 11;              //TX pin
const int switchPin = A0;   // pin for all the glove switches
const int sendPin = 2;      //the send button is connected here

//declare the motor pins

const int mtOnePin = 3;    //mt means motor
const int mtTwoPin = 4;
const int mtThreePin = 5;
const int mtFourPin = 6;
const int mtFivePin = 7;
const int mtSixPin = 8;
const int mtSevenPin = 9;
const int mtEightPin = 12;
const int mtNinePin = 13;
const int mtTenPin = 15;
const int mtElevenPin = 16;
const int mtTwelvePin = 17;    //analog pins used as digital I/O pin
const int mtThirteenPin = 18;
const int mtFourteenPin = 19;

SoftwareSerial mySerial(rxPin,txPin);//RX,TX.

int flagOne = 0;        //initialise the flag variables that determines status of a switch
int flagTwo = 0;
int flagThree = 0;
int flagFour = 0;
int flagFive = 0;
int flagSix = 0;
int flagSeven = 0;
int flagEight = 0;
int flagNine = 0;
int flagTen = 0;
int flagEleven = 0;
int flagTwelve = 0;
int flagThirteen = 0;
int flagFourteen = 0;

int switchVal;                    //holds value read from the glove switches
int sensor;              //holds the unique values for each switch when pressed
int buttonSend;


//Function that clears the flags
void clearFlag(){
  flagOne = 0;
```

```
  flagTwo = 0;
  flagThree = 0;
  flagFour = 0;
  flagFive = 0;
  flagSix = 0;
  flagSeven = 0;
  flagEight = 0;
  flagNine = 0;
  flagTen = 0;
  flagEleven = 0;
  flagTwelve = 0;
  flagThirteen = 0;
  flagFourteen = 0;
}


void setup()
{

  pinMode(sendPin, INPUT);
  pinMode(mtOnePin, OUTPUT);
  pinMode(mtTwoPin, OUTPUT);
  pinMode(mtThreePin, OUTPUT);
   pinMode(mtFourPin, OUTPUT);
  pinMode(mtFivePin, OUTPUT);
  pinMode(mtSixPin, OUTPUT);
   pinMode(mtSevenPin, OUTPUT);
  pinMode(mtEightPin, OUTPUT);
  pinMode(mtNinePin, OUTPUT);
   pinMode(mtTenPin, OUTPUT);
  pinMode(mtElevenPin, OUTPUT);
  pinMode(mtTwelvePin, OUTPUT);
   pinMode(mtThirteenPin, OUTPUT);
  pinMode(mtFourteenPin, OUTPUT);


  Serial.begin(9600);              //start the serial monitor in case you need it
  mySerial.begin(9600);            //software serial data rate

}


void loop(){
  switchVal = analogRead(switchPin);      //reads and stores the analog value of a pressed switch
  buttonSend = digitalRead(sendPin);

  //check for incoming data


  if(mySerial.available() != 0){          //checks if incoming data is available

    int inData = mySerial.read();        //reads incoming data
    delay(3);
    if(inData !=13){                  //checks and removes the unwanted space transmitted with bluetooth
data
      if(inData !=10){
```

```
Serial.println(char(inData));
if(inData == 'A'){
 digitalWrite(mtOnePin, HIGH);
 digitalWrite(mtTwoPin, LOW);
 digitalWrite(mtThreePin, LOW);
 digitalWrite(mtFourPin, LOW);
 digitalWrite(mtFivePin, LOW);
 digitalWrite(mtSixPin, LOW);
 digitalWrite(mtSevenPin, LOW);
 digitalWrite(mtEightPin, LOW);
 digitalWrite(mtNinePin, LOW);
 digitalWrite(mtTenPin, LOW);
 digitalWrite(mtElevenPin, LOW);
 digitalWrite(mtTwelvePin, LOW);
 digitalWrite(mtThirteenPin, LOW);
 digitalWrite(mtFourteenPin, LOW);

}

else if(inData == 'B'){
 digitalWrite(mtOnePin, LOW);
 digitalWrite(mtTwoPin, LOW);
 digitalWrite(mtThreePin, LOW);
 digitalWrite(mtFourPin, LOW);
 digitalWrite(mtFivePin, LOW);
 digitalWrite(mtSixPin, LOW);
 digitalWrite(mtSevenPin, LOW);
 digitalWrite(mtEightPin, LOW);
 digitalWrite(mtNinePin, LOW);
 digitalWrite(mtTenPin, HIGH);
 digitalWrite(mtElevenPin, LOW);
 digitalWrite(mtTwelvePin, LOW);
 digitalWrite(mtThirteenPin, HIGH);
 digitalWrite(mtFourteenPin, LOW);
}

else if(inData == 'C'){
  digitalWrite(mtOnePin, LOW);
 digitalWrite(mtTwoPin, HIGH);
 digitalWrite(mtThreePin, LOW);
 digitalWrite(mtFourPin, LOW);
 digitalWrite(mtFivePin, LOW);
 digitalWrite(mtSixPin, LOW);
 digitalWrite(mtSevenPin, LOW);
 digitalWrite(mtEightPin, LOW);
 digitalWrite(mtNinePin, LOW);
 digitalWrite(mtTenPin, LOW);
 digitalWrite(mtElevenPin, LOW);
 digitalWrite(mtTwelvePin, LOW);
 digitalWrite(mtThirteenPin, LOW);
 digitalWrite(mtFourteenPin, LOW);

}

else if(inData == 'D'){
  digitalWrite(mtOnePin, LOW);
```

```
 digitalWrite(mtTwoPin, LOW);
 digitalWrite(mtThreePin, HIGH);
 digitalWrite(mtFourPin, LOW);
 digitalWrite(mtFivePin, LOW);
 digitalWrite(mtSixPin, LOW);
 digitalWrite(mtSevenPin, LOW);
 digitalWrite(mtEightPin, LOW);
 digitalWrite(mtNinePin, HIGH);
 digitalWrite(mtTenPin, LOW);
 digitalWrite(mtElevenPin, LOW);
 digitalWrite(mtTwelvePin, LOW);
 digitalWrite(mtThirteenPin, LOW);
 digitalWrite(mtFourteenPin, LOW);

}

else if(inData == 'E'){
 digitalWrite(mtOnePin, LOW);
 digitalWrite(mtTwoPin, LOW);
 digitalWrite(mtThreePin, HIGH);
 digitalWrite(mtFourPin, LOW);
 digitalWrite(mtFivePin, LOW);
 digitalWrite(mtSixPin, LOW);
 digitalWrite(mtSevenPin, LOW);
 digitalWrite(mtEightPin, LOW);
 digitalWrite(mtNinePin, LOW);
 digitalWrite(mtTenPin, LOW);
 digitalWrite(mtElevenPin, LOW);
 digitalWrite(mtTwelvePin, LOW);
 digitalWrite(mtThirteenPin, LOW);
 digitalWrite(mtFourteenPin, LOW);

}

else if(inData == 'F'){
  digitalWrite(mtOnePin, LOW);
 digitalWrite(mtTwoPin, LOW);
 digitalWrite(mtThreePin, LOW);
 digitalWrite(mtFourPin, LOW);
 digitalWrite(mtFivePin, LOW);
 digitalWrite(mtSixPin, LOW);
 digitalWrite(mtSevenPin, LOW);
 digitalWrite(mtEightPin, HIGH);
 digitalWrite(mtNinePin, LOW);
 digitalWrite(mtTenPin, LOW);
 digitalWrite(mtElevenPin, LOW);
 digitalWrite(mtTwelvePin, LOW);
 digitalWrite(mtThirteenPin, LOW);
 digitalWrite(mtFourteenPin, LOW);

}

else if(inData == 'G'){
  digitalWrite(mtOnePin, LOW);
 digitalWrite(mtTwoPin, LOW);
 digitalWrite(mtThreePin, LOW);
```

```
 digitalWrite(mtFourPin, LOW);
 digitalWrite(mtFivePin, LOW);
 digitalWrite(mtSixPin, LOW);
 digitalWrite(mtSevenPin, LOW);
 digitalWrite(mtEightPin, LOW);
 digitalWrite(mtNinePin, LOW);
 digitalWrite(mtTenPin, LOW);
 digitalWrite(mtElevenPin, LOW);
 digitalWrite(mtTwelvePin, HIGH);
 digitalWrite(mtThirteenPin, LOW);
 digitalWrite(mtFourteenPin, LOW);

}

else if(inData == 'H'){
  digitalWrite(mtOnePin, LOW);
 digitalWrite(mtTwoPin, LOW);
 digitalWrite(mtThreePin, LOW);
 digitalWrite(mtFourPin, HIGH);
 digitalWrite(mtFivePin, LOW);
 digitalWrite(mtSixPin, LOW);
 digitalWrite(mtSevenPin, LOW);
 digitalWrite(mtEightPin, LOW);
 digitalWrite(mtNinePin, LOW);
 digitalWrite(mtTenPin, HIGH);
 digitalWrite(mtElevenPin, LOW);
 digitalWrite(mtTwelvePin, HIGH);
 digitalWrite(mtThirteenPin, LOW);
 digitalWrite(mtFourteenPin, LOW);

}

else if(inData == 'I'){
  digitalWrite(mtOnePin, LOW);
 digitalWrite(mtTwoPin, LOW);
 digitalWrite(mtThreePin, LOW);
 digitalWrite(mtFourPin, HIGH);
 digitalWrite(mtFivePin, LOW);
 digitalWrite(mtSixPin, LOW);
 digitalWrite(mtSevenPin, LOW);
 digitalWrite(mtEightPin, LOW);
 digitalWrite(mtNinePin, LOW);
 digitalWrite(mtTenPin, LOW);
 digitalWrite(mtElevenPin, LOW);
 digitalWrite(mtTwelvePin, LOW);
 digitalWrite(mtThirteenPin, LOW);
 digitalWrite(mtFourteenPin, LOW);

}

else if(inData == 'J'){
  digitalWrite(mtOnePin, LOW);
 digitalWrite(mtTwoPin, HIGH);
 digitalWrite(mtThreePin, LOW);
 digitalWrite(mtFourPin, HIGH);
 digitalWrite(mtFivePin, LOW);
```

```
 digitalWrite(mtSixPin, LOW);
 digitalWrite(mtSevenPin, LOW);
 digitalWrite(mtEightPin, LOW);
 digitalWrite(mtNinePin, LOW);
 digitalWrite(mtTenPin, HIGH);
 digitalWrite(mtElevenPin, LOW);
 digitalWrite(mtTwelvePin, HIGH);
 digitalWrite(mtThirteenPin, LOW);
 digitalWrite(mtFourteenPin, LOW);

}

else if(inData == 'K'){
  digitalWrite(mtOnePin, LOW);
 digitalWrite(mtTwoPin, LOW);
 digitalWrite(mtThreePin, LOW);
 digitalWrite(mtFourPin, LOW);
 digitalWrite(mtFivePin, LOW);
 digitalWrite(mtSixPin, LOW);
 digitalWrite(mtSevenPin, LOW);
 digitalWrite(mtEightPin, LOW);
 digitalWrite(mtNinePin, HIGH);
 digitalWrite(mtTenPin, LOW);
 digitalWrite(mtElevenPin, LOW);
 digitalWrite(mtTwelvePin, LOW);
 digitalWrite(mtThirteenPin, LOW);
 digitalWrite(mtFourteenPin, LOW);

}

else if(inData == 'L'){
  digitalWrite(mtOnePin, LOW);
 digitalWrite(mtTwoPin, HIGH);
 digitalWrite(mtThreePin, LOW);
 digitalWrite(mtFourPin, LOW);
 digitalWrite(mtFivePin, LOW);
 digitalWrite(mtSixPin, LOW);
 digitalWrite(mtSevenPin, LOW);
 digitalWrite(mtEightPin, LOW);
 digitalWrite(mtNinePin, LOW);
 digitalWrite(mtTenPin, HIGH);
 digitalWrite(mtElevenPin, HIGH);
 digitalWrite(mtTwelvePin, LOW);
 digitalWrite(mtThirteenPin, LOW);
 digitalWrite(mtFourteenPin, LOW);

}

else if(inData == 'M'){
  digitalWrite(mtOnePin, LOW);
 digitalWrite(mtTwoPin, HIGH);
 digitalWrite(mtThreePin, LOW);
 digitalWrite(mtFourPin, LOW);
 digitalWrite(mtFivePin, LOW);
 digitalWrite(mtSixPin, LOW);
 digitalWrite(mtSevenPin, LOW);
```

```
 digitalWrite(mtEightPin, LOW);
 digitalWrite(mtNinePin, LOW);
 digitalWrite(mtTenPin, HIGH);
 digitalWrite(mtElevenPin, HIGH);
 digitalWrite(mtTwelvePin, HIGH);
 digitalWrite(mtThirteenPin, LOW);
 digitalWrite(mtFourteenPin, LOW);

}

else if(inData == 'N'){
  digitalWrite(mtOnePin, LOW);
 digitalWrite(mtTwoPin, HIGH);
 digitalWrite(mtThreePin, LOW);
 digitalWrite(mtFourPin, LOW);
 digitalWrite(mtFivePin, LOW);
 digitalWrite(mtSixPin, LOW);
 digitalWrite(mtSevenPin, LOW);
 digitalWrite(mtEightPin, LOW);
 digitalWrite(mtNinePin, LOW);
 digitalWrite(mtTenPin, LOW);
 digitalWrite(mtElevenPin, LOW);
 digitalWrite(mtTwelvePin, HIGH);
 digitalWrite(mtThirteenPin, LOW);
 digitalWrite(mtFourteenPin, LOW);

}

else if(inData == 'O'){
  digitalWrite(mtOnePin, LOW);
 digitalWrite(mtTwoPin, LOW);
 digitalWrite(mtThreePin, LOW);
 digitalWrite(mtFourPin, LOW);
 digitalWrite(mtFivePin, HIGH);
 digitalWrite(mtSixPin, LOW);
 digitalWrite(mtSevenPin, LOW);
 digitalWrite(mtEightPin, LOW);
 digitalWrite(mtNinePin, LOW);
 digitalWrite(mtTenPin, LOW);
 digitalWrite(mtElevenPin, LOW);
 digitalWrite(mtTwelvePin, LOW);
 digitalWrite(mtThirteenPin, LOW);
 digitalWrite(mtFourteenPin, LOW);

}

else if(inData == 'P'){
  digitalWrite(mtOnePin, LOW);
 digitalWrite(mtTwoPin, LOW);
 digitalWrite(mtThreePin, HIGH);
 digitalWrite(mtFourPin, LOW);
 digitalWrite(mtFivePin, LOW);
 digitalWrite(mtSixPin, LOW);
 digitalWrite(mtSevenPin, LOW);
 digitalWrite(mtEightPin, HIGH);
 digitalWrite(mtNinePin, LOW);
```

```
 digitalWrite(mtTenPin, LOW);
 digitalWrite(mtElevenPin, LOW);
 digitalWrite(mtTwelvePin, LOW);
 digitalWrite(mtThirteenPin, LOW);
 digitalWrite(mtFourteenPin, LOW);

}

else if(inData == 'Q'){
  digitalWrite(mtOnePin, HIGH);
 digitalWrite(mtTwoPin, HIGH);
 digitalWrite(mtThreePin, LOW);
 digitalWrite(mtFourPin, LOW);
 digitalWrite(mtFivePin, LOW);
 digitalWrite(mtSixPin, LOW);
 digitalWrite(mtSevenPin, LOW);
 digitalWrite(mtEightPin, LOW);
 digitalWrite(mtNinePin, LOW);
 digitalWrite(mtTenPin, LOW);
 digitalWrite(mtElevenPin, LOW);
 digitalWrite(mtTwelvePin, LOW);
 digitalWrite(mtThirteenPin, LOW);
 digitalWrite(mtFourteenPin, LOW);

}

else if(inData == 'R'){
  digitalWrite(mtOnePin, LOW);
 digitalWrite(mtTwoPin, LOW);
 digitalWrite(mtThreePin, LOW);
 digitalWrite(mtFourPin, LOW);
 digitalWrite(mtFivePin, LOW);
 digitalWrite(mtSixPin, LOW);
 digitalWrite(mtSevenPin, LOW);
 digitalWrite(mtEightPin, LOW);
 digitalWrite(mtNinePin, LOW);
 digitalWrite(mtTenPin, HIGH);
 digitalWrite(mtElevenPin, LOW);
 digitalWrite(mtTwelvePin, LOW);
 digitalWrite(mtThirteenPin, LOW);
 digitalWrite(mtFourteenPin, LOW);

}

else if(inData == 'S'){
  digitalWrite(mtOnePin, LOW);
 digitalWrite(mtTwoPin, LOW);
 digitalWrite(mtThreePin, LOW);
 digitalWrite(mtFourPin, LOW);
 digitalWrite(mtFivePin, LOW);
 digitalWrite(mtSixPin, LOW);
 digitalWrite(mtSevenPin, HIGH);
 digitalWrite(mtEightPin, LOW);
 digitalWrite(mtNinePin, LOW);
 digitalWrite(mtTenPin, LOW);
 digitalWrite(mtElevenPin, LOW);
```

```
 digitalWrite(mtTwelvePin, LOW);
 digitalWrite(mtThirteenPin, LOW);
 digitalWrite(mtFourteenPin, LOW);

}

else if(inData == 'T'){
  digitalWrite(mtOnePin, LOW);
 digitalWrite(mtTwoPin, LOW);
 digitalWrite(mtThreePin, LOW);
 digitalWrite(mtFourPin, LOW);
 digitalWrite(mtFivePin, LOW);
 digitalWrite(mtSixPin, LOW);
 digitalWrite(mtSevenPin, LOW);
 digitalWrite(mtEightPin, LOW);
 digitalWrite(mtNinePin, LOW);
 digitalWrite(mtTenPin, LOW);
 digitalWrite(mtElevenPin, HIGH);
 digitalWrite(mtTwelvePin, LOW);
 digitalWrite(mtThirteenPin, LOW);
 digitalWrite(mtFourteenPin, LOW);

}

else if(inData == 'U'){
  digitalWrite(mtOnePin, LOW);
 digitalWrite(mtTwoPin, LOW);
 digitalWrite(mtThreePin, LOW);
 digitalWrite(mtFourPin, LOW);
 digitalWrite(mtFivePin, LOW);
 digitalWrite(mtSixPin, HIGH);
 digitalWrite(mtSevenPin, LOW);
 digitalWrite(mtEightPin, LOW);
 digitalWrite(mtNinePin, LOW);
 digitalWrite(mtTenPin, LOW);
 digitalWrite(mtElevenPin, LOW);
 digitalWrite(mtTwelvePin, LOW);
 digitalWrite(mtThirteenPin, LOW);
 digitalWrite(mtFourteenPin, LOW);

}

else if(inData == 'V'){
  digitalWrite(mtOnePin, LOW);
 digitalWrite(mtTwoPin, LOW);
 digitalWrite(mtThreePin, LOW);
 digitalWrite(mtFourPin, LOW);
 digitalWrite(mtFivePin, LOW);
 digitalWrite(mtSixPin, LOW);
 digitalWrite(mtSevenPin, LOW);
 digitalWrite(mtEightPin, LOW);
 digitalWrite(mtNinePin, HIGH);
 digitalWrite(mtTenPin, LOW);
 digitalWrite(mtElevenPin, LOW);
 digitalWrite(mtTwelvePin, LOW);
 digitalWrite(mtThirteenPin, HIGH);
```

```
 digitalWrite(mtFourteenPin, LOW);

}

else if(inData == 'W'){
  digitalWrite(mtOnePin, LOW);
 digitalWrite(mtTwoPin, HIGH);
 digitalWrite(mtThreePin, LOW);
 digitalWrite(mtFourPin, LOW);
 digitalWrite(mtFivePin, LOW);
 digitalWrite(mtSixPin, LOW);
 digitalWrite(mtSevenPin, LOW);
 digitalWrite(mtEightPin, HIGH);
 digitalWrite(mtNinePin, LOW);
 digitalWrite(mtTenPin, LOW);
 digitalWrite(mtElevenPin, LOW);
 digitalWrite(mtTwelvePin, LOW);
 digitalWrite(mtThirteenPin, LOW);
 digitalWrite(mtFourteenPin, LOW);

}

else if(inData == 'X'){
  digitalWrite(mtOnePin, LOW);
 digitalWrite(mtTwoPin, LOW);
 digitalWrite(mtThreePin, LOW);
 digitalWrite(mtFourPin, LOW);
 digitalWrite(mtFivePin, LOW);
 digitalWrite(mtSixPin, LOW);
 digitalWrite(mtSevenPin, LOW);
 digitalWrite(mtEightPin, LOW);
 digitalWrite(mtNinePin, HIGH);
 digitalWrite(mtTenPin, LOW);
 digitalWrite(mtElevenPin, LOW);
 digitalWrite(mtTwelvePin, HIGH);
 digitalWrite(mtThirteenPin, LOW);
 digitalWrite(mtFourteenPin, LOW);

}

else if(inData == 'Y'){
  digitalWrite(mtOnePin, HIGH);
 digitalWrite(mtTwoPin, LOW);
 digitalWrite(mtThreePin, LOW);
 digitalWrite(mtFourPin, LOW);
 digitalWrite(mtFivePin, LOW);
 digitalWrite(mtSixPin, LOW);
 digitalWrite(mtSevenPin, LOW);
 digitalWrite(mtEightPin, LOW);
 digitalWrite(mtNinePin, LOW);
 digitalWrite(mtTenPin, LOW);
 digitalWrite(mtElevenPin, LOW);
 digitalWrite(mtTwelvePin, HIGH);
 digitalWrite(mtThirteenPin, LOW);
 digitalWrite(mtFourteenPin, LOW);
```

```
      }

      else if(inData == 'Z'){
        digitalWrite(mtOnePin, LOW);
       digitalWrite(mtTwoPin, LOW);
       digitalWrite(mtThreePin, LOW);
       digitalWrite(mtFourPin, LOW);
       digitalWrite(mtFivePin, LOW);
       digitalWrite(mtSixPin, LOW);
       digitalWrite(mtSevenPin, LOW);
       digitalWrite(mtEightPin, LOW);
       digitalWrite(mtNinePin, LOW);
       digitalWrite(mtTenPin, LOW);
       digitalWrite(mtElevenPin, LOW);
       digitalWrite(mtTwelvePin, LOW);
       digitalWrite(mtThirteenPin, LOW);
       digitalWrite(mtFourteenPin, HIGH);

      }
    }// inData not equal to 10
  }
 }//if serial is available


 //check if a switch is pressed and determine unique values

 if(switchVal>0){    //checks if a switch is pressed
  if(switchVal > 50 && switchVal <= 182){             //for analog value of 179
   flagOne = 1;
  }
 else if(switchVal > 182 && switchVal <= 199){        //for analog value of 193
  flagTwo = 1;
 }
  else if(switchVal > 199 && switchVal <= 260){      //for analog value of 255
  flagThree = 1;

  }
  else if(switchVal > 260 && switchVal <= 328){      //for analog value of 320
  flagFour = 1;

  }
  else if(switchVal > 328 && switchVal <= 370){      //for analog value of 366
  flagFive = 1;

  }
  else if(switchVal > 370 && switchVal <= 470){      //for analog value of 464
  flagSix = 1;

  }
    else if(switchVal > 470 && switchVal <= 540){   //for analog value of 535
  flagSeven = 1;

 }
  else if(switchVal > 540 && switchVal <= 615){      //for analog value of 609
  flagEight = 1;
```

```
    }
    else if(switchVal > 615 && switchVal <= 637){      //for analog value of 632
    flagNine = 1;

    }
    else if(switchVal > 637 && switchVal <= 685){      //for analog value of 679
    flagTen = 1;

    }
    else if(switchVal > 685 && switchVal <= 742){      //for analog value of 737
    flagEleven = 1;

    }
      else if(switchVal > 742 && switchVal <= 812){    //for analog value of 807
    flagTwelve = 1;

   }
    else if(switchVal > 812 && switchVal <= 845){      //for analog value of 839
    flagThirteen = 1;

    }
    else if(switchVal > 845 && switchVal <= 898){      //for analog value of 891
    flagFourteen = 1;

    }


  }//switchVal>0

  //check if the send pin is pressed

  if(buttonSend == HIGH){
    if(flagOne == 1 && flagTwo == 0 && flagThree == 0 && flagFour == 0 && flagFive == 0 &&
flagSix == 0 && flagSeven == 0
    && flagEight == 0 && flagNine == 0 && flagTen == 0 && flagEleven == 0 && flagTwelve ==
0 && flagThirteen == 0 && flagFourteen == 0){    //Sends A

      mySerial.print("A");
      clearFlag();
    }

    else if(flagOne == 0 && flagTwo == 0 && flagThree == 0 && flagFour == 0 && flagFive == 0
&& flagSix == 0 && flagSeven == 0
    && flagEight == 0 && flagNine == 0 && flagTen == 1 && flagEleven == 0 && flagTwelve ==
0 && flagThirteen == 1 && flagFourteen == 0){   //Sends B

      mySerial.print("B");
      clearFlag();
    }

    else if(flagOne == 0 && flagTwo == 2 && flagThree == 0 && flagFour == 0 && flagFive == 0
&& flagSix == 0 && flagSeven == 0
    && flagEight == 0 && flagNine == 0 && flagTen == 0 && flagEleven == 0 && flagTwelve ==
0 && flagThirteen == 0 && flagFourteen == 0){    //Send C

      mySerial.print("C");
```

```
    clearFlag();
  }

  else if(flagOne == 0 && flagTwo == 0 && flagThree == 1 && flagFour == 0 && flagFive == 0
&& flagSix == 0 && flagSeven == 0
  && flagEight == 0 && flagNine == 1 && flagTen == 0 && flagEleven == 0 && flagTwelve ==
0 && flagThirteen == 0 && flagFourteen == 0){  //send D

    mySerial.print("D");
    clearFlag();
  }

  else if(flagOne == 0 && flagTwo == 0 && flagThree == 1 && flagFour == 0 && flagFive == 0
&& flagSix == 0 && flagSeven == 0
  && flagEight == 0 && flagNine == 0 && flagTen == 0 && flagEleven == 0 && flagTwelve ==
0 && flagThirteen == 0 && flagFourteen == 0){ //send E

    mySerial.print("E");
    clearFlag();
  }

  else if(flagOne == 0 && flagTwo == 0 && flagThree == 0 && flagFour == 0 && flagFive == 0
&& flagSix == 0 && flagSeven == 0
  && flagEight == 1 && flagNine == 0 && flagTen == 0 && flagEleven == 0 && flagTwelve ==
0 && flagThirteen == 0 && flagFourteen == 0){    //sends F

    mySerial.print("F");
    clearFlag();
  }

  else if(flagOne == 0 && flagTwo == 0 && flagThree == 0 && flagFour == 0 && flagFive == 0
&& flagSix == 0 && flagSeven == 0
  && flagEight == 0 && flagNine == 0 && flagTen == 0 && flagEleven == 0 && flagTwelve ==
1 && flagThirteen == 0 && flagFourteen == 0){    //sends G

    mySerial.print("G");
    clearFlag();
  }

  else if(flagOne == 0 && flagTwo == 0 && flagThree == 0 && flagFour == 1 && flagFive == 0
&& flagSix == 0 && flagSeven == 0
  && flagEight == 0 && flagNine == 0 && flagTen == 1 && flagEleven == 0 && flagTwelve ==
1 && flagThirteen == 0 && flagFourteen == 0){    //sends H

    mySerial.print("H");
    clearFlag();
  }

  else if(flagOne == 0 && flagTwo == 0 && flagThree == 0 && flagFour == 1 && flagFive == 0
&& flagSix == 0 && flagSeven == 0
  && flagEight == 0 && flagNine == 0 && flagTen == 0 && flagEleven == 0 && flagTwelve ==
0 && flagThirteen == 0 && flagFourteen == 0){    //sends I

    mySerial.print("I");
    clearFlag();
  }
```

```
  else if(flagOne == 0 && flagTwo == 1 && flagThree == 0 && flagFour == 1 && flagFive == 0
&& flagSix == 0 && flagSeven == 0
  && flagEight == 0 && flagNine == 0 && flagTen == 1 && flagEleven == 0 && flagTwelve ==
1 && flagThirteen == 0 && flagFourteen == 0){    //sends J

    mySerial.print("J");
    clearFlag();
  }

  else if(flagOne == 0 && flagTwo == 0 && flagThree == 0 && flagFour == 0 && flagFive == 0
&& flagSix == 0 && flagSeven == 0
  && flagEight == 0 && flagNine == 1 && flagTen == 0 && flagEleven == 0 && flagTwelve ==
0 && flagThirteen == 0 && flagFourteen == 0){    //sends K

    mySerial.print("K");
    clearFlag();
  }

  else if(flagOne == 0 && flagTwo == 1 && flagThree == 0 && flagFour == 0 && flagFive == 0
&& flagSix == 0 && flagSeven == 0
  && flagEight == 0 && flagNine == 0 && flagTen == 1 && flagEleven == 1 && flagTwelve ==
0 && flagThirteen == 0 && flagFourteen == 0){    //sends L

    mySerial.print("L");
    clearFlag();
  }

  else if(flagOne == 0 && flagTwo == 1 && flagThree == 0 && flagFour == 0 && flagFive == 0
&& flagSix == 0 && flagSeven == 0
  && flagEight == 0 && flagNine == 0 && flagTen == 1 && flagEleven == 1 && flagTwelve ==
1 && flagThirteen == 0 && flagFourteen == 0){   //sends M

    mySerial.print("M");
    clearFlag();
  }

  else if(flagOne == 0 && flagTwo == 1 && flagThree == 0 && flagFour == 0 && flagFive == 0
&& flagSix == 0 && flagSeven == 0
  && flagEight == 0 && flagNine == 0 && flagTen == 0 && flagEleven == 0 && flagTwelve ==
1 && flagThirteen == 0 && flagFourteen == 0){  //sends N

    mySerial.print("N");
    clearFlag();
  }

  else if(flagOne == 0 && flagTwo == 0 && flagThree == 0 && flagFour == 0 && flagFive == 5
&& flagSix == 0 && flagSeven == 0
  && flagEight == 0 && flagNine == 0 && flagTen == 0 && flagEleven == 0 && flagTwelve ==
0 && flagThirteen == 0 && flagFourteen == 0){    //sends O

    mySerial.print("O");
    clearFlag();
  }
```

```
  else if(flagOne == 0 && flagTwo == 0 && flagThree == 1 && flagFour == 0 && flagFive == 0
&& flagSix == 0 && flagSeven == 0
  && flagEight == 1 && flagNine == 0 && flagTen == 0 && flagEleven == 0 && flagTwelve ==
0 && flagThirteen == 0 && flagFourteen == 0){  //sends P

    mySerial.print("P");
    clearFlag();
  }

  else if(flagOne == 1 && flagTwo == 1 && flagThree == 0 && flagFour == 0 && flagFive == 0
&& flagSix == 0 && flagSeven == 0
  && flagEight == 0 && flagNine == 0 && flagTen == 0 && flagEleven == 0 && flagTwelve ==
0 && flagThirteen == 0 && flagFourteen == 0){    //sends Q

    mySerial.print("Q");
    clearFlag();
  }

  else if(flagOne == 0 && flagTwo == 0 && flagThree == 0 && flagFour == 0 && flagFive == 0
&& flagSix == 0 && flagSeven == 0
  && flagEight == 0 && flagNine == 0 && flagTen == 1 && flagEleven == 0 && flagTwelve ==
0 && flagThirteen == 0 && flagFourteen == 0){    //sends R

    mySerial.print("R");
    clearFlag();
  }

  else if(flagOne == 0 && flagTwo == 0 && flagThree == 0 && flagFour == 0 && flagFive == 0
&& flagSix == 0 && flagSeven == 1
  && flagEight == 0 && flagNine == 0 && flagTen == 0 && flagEleven == 0 && flagTwelve ==
0 && flagThirteen == 0 && flagFourteen == 0){  //sends S

    mySerial.print("S");
    clearFlag();
  }

  else if(flagOne == 0 && flagTwo == 0 && flagThree == 0 && flagFour == 0 && flagFive == 0
&& flagSix == 0 && flagSeven == 0
  && flagEight == 0 && flagNine == 0 && flagTen == 0 && flagEleven == 1 && flagTwelve ==
0 && flagThirteen == 0 && flagFourteen == 0){  //sends T

    mySerial.print("T");
    clearFlag();
  }

  else if(flagOne == 0 && flagTwo == 0 && flagThree == 0 && flagFour == 0 && flagFive == 0
&& flagSix == 1 && flagSeven == 0
  && flagEight == 0 && flagNine == 0 && flagTen == 0 && flagEleven == 0 && flagTwelve ==
0 && flagThirteen == 0 && flagFourteen == 0){  //sends U

    mySerial.print("U");
    clearFlag();
  }

  else if(flagOne == 0 && flagTwo == 0 && flagThree == 0 && flagFour == 0 && flagFive == 0
&& flagSix == 0 && flagSeven == 0
```

```
   && flagEight == 0 && flagNine == 1 && flagTen == 0 && flagEleven == 0 && flagTwelve ==
0 && flagThirteen == 1 && flagFourteen == 0){    //sends V

     mySerial.print("V");
     clearFlag();
   }

   else if(flagOne == 0 && flagTwo == 1 && flagThree == 0 && flagFour == 0 && flagFive == 0
&& flagSix == 0 && flagSeven == 0
   && flagEight == 1 && flagNine == 0 && flagTen == 0 && flagEleven == 0 && flagTwelve ==
0 && flagThirteen == 0 && flagFourteen == 0){  //sends W

     mySerial.print("W");
     clearFlag();
   }

   else if(flagOne == 0 && flagTwo == 0 && flagThree == 0 && flagFour == 0 && flagFive == 0
&& flagSix == 0 && flagSeven == 0
   && flagEight == 0 && flagNine == 1 && flagTen == 0 && flagEleven == 0 && flagTwelve ==
1 && flagThirteen == 0 && flagFourteen == 0){    //sends X

     mySerial.print("X");
     clearFlag();
   }

   else if(flagOne == 1 && flagTwo == 0 && flagThree == 0 && flagFour == 0 && flagFive == 0
&& flagSix == 0 && flagSeven == 0
   && flagEight == 0 && flagNine == 0 && flagTen == 0 && flagEleven == 0 && flagTwelve ==
1 && flagThirteen == 0 && flagFourteen == 0){    //sends Y

     mySerial.print("Y");
     clearFlag();
   }

   else if(flagOne == 0 && flagTwo == 0 && flagThree == 0 && flagFour == 0 && flagFive == 0
&& flagSix == 0 && flagSeven == 0
   && flagEight == 0 && flagNine == 0 && flagTen == 0 && flagEleven == 0 && flagTwelve ==
0 && flagThirteen == 0 && flagFourteen == 1){    //sends Z

     mySerial.print("Z");
     clearFlag();
   }




  }//if buttonSend is HIGH




}
```

8. Code for the Handheld Device implemented in Chapter 4

```
#include <LiquidCrystal.h>
#include<SoftwareSerial.h>
const int rxPin = 10;
const int txPin = 11;
SoftwareSerial mySerial(rxPin,txPin);//RX,TX.
LiquidCrystal lcd(13, 12, 6, 5, 4, 3);

const int switchPin = A0;
int switchVal;

void setup() {
  // put your setup code here, to run once:
Serial.begin(9600);
mySerial.begin(9600);
lcd.begin(16,2);
lcd.print("Type Message:");
lcd.setCursor(0,1);
}
void loop() {
  switchVal = analogRead(switchPin);
//Serial.println(switchVal);
 if(mySerial.available() != 0){
    int inData = mySerial.read();
    delay(3);
    if(inData !=13){
      if(inData !=10){
        Serial.println(char(inData));
        lcd.clear();
        lcd.print(char(inData));
        lcd.setCursor(0,1);
      }
  }
  }
if(switchVal>0){
if(switchVal >50 && switchVal<=182){//analog Value of about 179
  mySerial.print('A');
  lcd.print("A");
  }
 if(switchVal>182 && switchVal <=200){//analog Value of about 193
  mySerial.print('B');
  lcd.print("B");
  }
  else if(switchVal>200 && switchVal <=228){//analog Value of about 222
  mySerial.print('C');
  lcd.print("C");
    }
  else if(switchVal>228 && switchVal <=242){//analog Value of about 238
  mySerial.print('D');
  lcd.print("D");
  }
  else if(switchVal>242 && switchVal <=258){//analog Value of about 256
```

```
mySerial.print('E');
lcd.print("E");
  }
else if(switchVal>258 && switchVal <=279){//analog Value of about 276
mySerial.print('F');
lcd.print("F");
  }
else if(switchVal>279 && switchVal <=325){//analog Value of about 321
mySerial.print('G');
lcd.print("G");
  }
else if(switchVal>325 && switchVal <=346){//analog Value of about 342
mySerial.print('H');
lcd.print("H");
  }
else if(switchVal>346 && switchVal <=368){//analog Value of about 365
mySerial.print('I');
lcd.print("I");
  }
else if(switchVal>368 && switchVal <=416){//analog Value of about 411
mySerial.print('J');
lcd.print("J");
}
else if(switchVal>416 && switchVal <=470){//analog Value of about 466
mySerial.print('K');
lcd.print("K");

}
else if(switchVal>470 && switchVal <=493){//analog Value of about 488
mySerial.print('L');
lcd.print("L");
}
else if(switchVal>493 && switchVal <=541){//analog Value of about 537
mySerial.print('M');
lcd.print("M");
}
else if(switchVal>541 && switchVal <=571){//analog Value of about 564
mySerial.print('N');
lcd.print("N");
}
else if(switchVal>571 && switchVal <=615){//analog Value of about 610
mySerial.print('O');
lcd.print("O");
}
else if(switchVal>615 && switchVal <=637){//analog Value of about 633
mySerial.print('P');
lcd.print("P");
}
else if(switchVal>637 && switchVal <=661){//analog Value of about 658
mySerial.print('Q');
lcd.print("Q");
}
else if(switchVal>661 && switchVal <=682){//analog Value of about 679
mySerial.print('R');
lcd.print("R");
}
```

```
  else if(switchVal>682 && switchVal <=702){//analog Value of about 698
  mySerial.print('S');
  lcd.print("S");
  }
  else if(switchVal>702 && switchVal <=742){//analog Value of about 738
  mySerial.print('T');
  lcd.print("T");
  }
  else if(switchVal>742 && switchVal <=776){//analog Value of about 771
  mySerial.print('U');
  lcd.print("U");
  }
  else if(switchVal>776 && switchVal <=812){//analog Value of about 807
  mySerial.print('V');
  lcd.print("V");
  }
  else if(switchVal>812 && switchVal <=844){//analog Value of about 840
  mySerial.print('W');
  lcd.print("W");
  }
  else if(switchVal>844 && switchVal <=896){//analog Value of about 891
  mySerial.print('X');
  lcd.print("X");
  }
  else if(switchVal>896 && switchVal <=942){//analog Value of about 938
  mySerial.print('Y');
  lcd.print("Y");
  }
  else if(switchVal>942 && switchVal <=999){//analog Value of about 994
  mySerial.print('Z');
  lcd.print("Z");
  }
    }
delay(200);
```

References

[1] G. H. Saunders and K. V. Echt, "An Overview of Dual Sensory Impairment in Older Adults: Perspectives for Rehabilitation," *Trends in Amplification,* vol. 11, pp. 243-258, 2007.

[2] F. A. Larsen and S. Damen, "Definitions of deafblindness and congenital deafblindness," *Research in Development Disabilities,* vol. 35, pp. 2568-2576, 2014.

[3] J. Dammeyer, "Deafblindness: A Review of the Literature," *Scandinavian Journal of Public Health, ,* pp. 554-562, 2014.

[4] *Written declaration for entry in the register pursuant to Rule 51 of the Rules of Procedure on the rights of deafblind people*, 2004.

[5] *Proposal for Constitution of the European Deafblind Union (EDBU) amended at the 3rd EDBU General Assembly*, 2013.

[6] A. Jaiswal, H. Aldersey, W. Wittich, M. Mirza, and M. Finlayson, "Participation experiences of people with deafblindness or dual sensory loss: A scoping review of global deafblind literature," *PloS one,* vol. 13, p. e0203772, 2018.

[7] "At risk of exclusion from CRPD and SDGs implementation: Inequality and Persons with Deafblindness," 2018.

[8] S. L. Smith, L. W. Bennett, and R. H. Wilson, "Prevalence and characteristics of dual sensory impairment (hearing and vision) in a veteran population," *Journal of Rehabilitation Research and Development,* vol. 45, pp. 597-610, 2008.

[9] J. Dammeyer, "Deafblindness and Dual Sensory Loss Research: Current Status and Future Direction," *World Journal of Otorhinolaryngology* vol. 5, pp. 37-40, May 28 2015.

[10] Senses-Australia, *Congenital Deafbliness*. Available from: http://www.deafblindinformation.org.au/congenital-deafblindness, 2015.

[11] L. Hyvarinen, L. Gimble, and M. Sorri, *Assessment of Vision and Hearing of Deaf-Blind Persons*. Australia: Royal Victorian Institute for the Blind, 1990.

[12] M. A. Hersh and M. A. Johnson, "Information Technology, Accessibility and Deafblind People," presented at the AAATE 2005, Lille, France, 2005.

[13] Sense-UK, *Information for Professionals working with older People*. Available: http://www.sense.org.uk/content/information-professionals-working-older-people, 2015.

[14] RNIB, "Older People and Sight Loss: Facts and Figures," RNIB2015.

[15] Age. *Hearing*. Available: http://www.ageuk.org.uk/northern-ireland/health--wellbeing/looking-after-your-body/hearing/, 2015.

[16] B. Dullard and G. H. .Saunders, "Documentation of Dual Sensory Impairment in Electronic Medical Records," *The Gerontologist,* pp. 1-5, 2014.

[17] H. L. Vreeken, G. H. v. Rens, S. E. Kramer, D. L. Knol, J. M. Festen, and R. M. v. Nispen, "Dual sensory loss: development of a dual sensory loss protocol and design of a randomized controlled trial," *BioMed Central Geriatrics,* vol. 13, pp. 1-12, 2013.

[18] M. Hersh, "Deafblind people, communication independence and isolation," *Journal of Deaf Studies and Deaf Education Advance Access* vol. 18, pp. 446-463, 2013.

[19] M. A. Hersh, K. Worrall, and M. A. Johnson, Eds., *A survey of AT for Deafblind People: State of the art and New Developments* (Assistive Technology: Shaping the future 11). IOS Press, 2003.

[20] A.Alfadhel, M. A. Khan, S. C. d. Freitas, and J.Kosel, "Magnetic tactile sensor for Braille reading," *IEEE Sensor Journal,* vol. 16, 2016.

[21] J. Gill and M. A. Hersh, "Dual sensory impairment: devices for deafblind people.," in *Assistive Technology for the Hearing Impaired, Deaf and Deafblind*, ed: Springer Verlag, 2003.

[22] M. A. Hersh and M. A. Johnson, Eds., *Assistive Technology for the Hearing-impaired, Deaf and Deafblind*. Springer-Verlag London, 2003.
[23] C. J. Laenger Sr, S. R. McFarland, and H. H. Peel, "Method and apparatus for communicating with people," ed: Google Patents, 1978.
[24] J. David L, "Evolution of mechanical fingerspelling hands for people who are deaf-blind," *Journal of Rehabilitation Research and Development,* vol. 31, pp. 236-244, 1994.
[25] M. Alexander, "Dexter - a finger-spelling hand for the deaf-blind," *IEEE,* pp. 1192-1195, 1987.
[26] D. L. Jaffe and W. S. Harwin, "The development of a third generation fingerspelling hand," *TITLE Engineering the ADA from Vision to Reality with Technology (16th, Las Vegas, Nevada, June 12-17, 1993). Volume 13. INSTITUTION RESNA: Association for the Advancement of Rehabilitation,* p. 175, 1993.
[27] M. David L Jaffe, "RALPH: a fourth generation fingerspelling hand," Rehabilitation R&D Center Progress Report.1994.
[28] J. P. Kramer, P. Lindener, and W. R. George, "Communication system for deaf, deaf-blind, or non-vocal individuals using instrumented glove," 5047952, 1988.
[29] L. O. Russo, G. A. Farulla, D. Pianu, A. R. Salgarella, M. Controzzi, C. Cipriani*, et al.*, "PARLOMA – A Novel Human-Robot Interaction System for Deaf-Blind Remote Communication," *International Journal of Advanced Robotic Systems,* vol. 12, p. 57, 2015.
[30] P. Grigson, N. Lofmark, and R. Giblin, "Hand-tapper III: a prototype communication device using finger-spelling," *British Journal of Visual Impairment,* vol. 9, pp. 13-15, 1991.
[31] U. Gollner, T. Bieling, and G. Joost, "Mobile Lorm Glove - Introducing a Communication Device for Deaf-Blind People," *TEI,* pp. 127 - 130, 2012.
[32] N. Caporusso, "A Wearable Malossi Alphabet Interface for Deafblind People," in *AVI '08 Proceedings of the working conference on Advanced visual interfaces*, Napoli Italy, pp. 445-448, 2008.
[33] R. H. Klein and R. Giblin, "A Pattern Decoding Glove for deafblind finger-spellers," *British Journal of Visual Impairment,* vol. 11, pp. 109-111, 1993.
[34] Sense, *Methods of Communicating with people who are deafblind*. Available: http://www.sense.org.uk/content/alphabet-based-communication, 2013.
[35] J. Rantala, R. Raisamo, J. Lylykangas, V. Surakka, J. Raisamo, K. Salminen*, et al.*, "Methods for Presenting Braille Characters on a Mobile Device with a Touchscreen and Tactile Feedback," *IEEE Transactions on Haptics,* vol. 2, pp. 28-39, 2009.
[36] GOV-UK. *Accessible communication formats*. Available: https://www.gov.uk/government/publications/inclusive-communication/accessible-communication-formats, 2018.
[37] RNIB, "Modern Day Braille," ed.
[38] M. Yasuhiro, I. Tsuneshi, S. Ichiro, E. Kobayashi, J. Yasuhiko, and A. Tatsuhiko, "Finger Braille Teaching System for People who Communicate with Deafblind People," in *Proceedings of the 2007 IEEE International Conference on Mechatronics and Automation*, Harbin, China, 2007.
[39] S. Mu-Chun, C.-Y. Chen, S. Shi-Yong, C. Chien-Hsing, H. Hsiang-Feng, and Y.-C. Wang, "Portable Communication aid for deaf-blind people," *Computer & Control Engineering Journal,* pp. 37-43, February 2001.
[40] O. Satoshi, H. Sadao, S. Nobuyuki, and H. Tetsumi, "The Introduction of Tele-Support System for Deaf-blind People using Body-Braille and a Mobile Phone," presented at the 5th IEEE Consumer Communication and Networking Conference, Las Vegas, Nevada, 2008.

[41] O. Satoshi, H. Sadao, S. Nobuyuki, and H. Tetsumi, "Hellen Keller Phone - a Communication System for Deaf-Blind People using Body-Braille and Skype.," presented at the 9th Annual IEEE Consumer Communication and Networking Conference, 2012.

[42] C. Tanay, K. Saurabh, and R. Pradyumna, "A Braille-Based Mobile Communication and Translation Glove for Deaf-blind People," presented at the 2015 International Conference on Pervasive Computing (ICPC), 2015.

[43] R. Sarkar, S. Das, and S. Roy, "SPARSHA: A Low Cost Refreshable Braille for Deaf-Blind People for Communication with Deaf-Blind and Non-disabled Persons," Berlin, Heidelberg, pp. 465-475, 2013.

[44] H. Nicolau, Jo, o. Guerreiro, T. Guerreiro, Lu*, et al.*, "UbiBraille: designing and evaluating a vibrotactile Braille-reading device," presented at the Proceedings of the 15th International ACM SIGACCESS Conference on Computers and Accessibility, Bellevue, Washington, 2013.

[45] R.-G. Fernando, M. O. Cesar, F. Alejandro, and C. H. Joel, "My Vox - Device for the Communication between People: Blind, Deaf, Deaf-blind, and Unimpaired," *IEEE* pp. 506-510, 2014.

[46] C. Jayant, C. Acuario, W. Johnson, J. Hollier, and R. Ladner, "V-braille: haptic braille perception using a touch-screen and vibration on mobile phones," presented at the Proceedings of the 12th international ACM SIGACCESS conference on Computers and accessibility, Orlando, Florida, USA, 2010.

[47] S. Ruman and S. D. Rudrapal, "A Low-Cost Microelectromechanical Braille for blind people to communicate with blind or deaf blind people through SMS subsystem.," presented at the 3rd IEEE International Advanced Computing Conference(IACC), Ghaziabad, 2013.

[48] H. Mitchitaka and A. Tomohiro, "Wearable finger-braille interface for navigation of deafblind in ubiquitous barrier free space", 2013.

[49] R. S. Dahiya and M. Valle, *Robotic Tactile Sensing: Technologies and System*: Springer Netherlands, 2013.

[50] Y. Gilaberte, L. Prieto-Torres, I. Pastushenko, and Á. Juarranz, "Chapter 1 - Anatomy and Function of the Skin A2 - Hamblin, Michael R," in *Nanoscience in Dermatology*, P. Avci and T. W. Prow, Eds., ed Boston: Academic Press, pp. 1-14, 2016.

[51] C. G. Núñez, W. T. Navaraj, E. O. Polat, and R. Dahiya, "Energy-Autonomous, Flexible, and Transparent Tactile Skin," *Advanced Functional Materials,* vol. 27, pp. 1606287, 2017.

[52] K. S. Hale and K. M. Stanney, "Deriving haptic design guidelines from human physiological, psychophysical, and neurological foundations," *IEEE Computer Graphics and Applications,* vol. 24, pp. 33-39, 2004.

[53] P. Goethals, "Tactile feedback for robot assisted minimally invasive surgery: an overview," *Department of Mechanical Engineering KU Leuven, Tech. Rep,* 2008.

[54] E. A. Lerner, "Pruriceptors," in *Pruritus*, L. Misery and S. Ständer, Eds., ed Cham: Springer International Publishing, pp. 13-20 2016.

[55] A. Zimmerman, L. Bai, and D. D. Ginty, "The gentle touch receptors of mammalian skin," *Science,* vol. 346, pp. 950-954, 2014.

[56] R. S. Johansson and Å. B. Vallbo, "Tactile sensory coding in the glabrous skin of the human hand," *Trends in Neurosciences,* vol. 6, pp. 27-32, 1983.

[57] P. S. Girão, P. M. P. Ramos, O. Postolache, and J. Miguel Dias Pereira, "Tactile sensors for robotic applications," *Measurement,* vol. 46, pp. 1257-1271, 2013.

[58] A. Chortos, J. Liu, and Z. Bao, "Pursuing prosthetic electronic skin," *Nat Mater,* vol. 15, pp. 937-950, 2016.

[59] R. S. Dahiya and M. Valle, *Robotic Tactile Sensing: Technologies and Systems*: Springer Dordrecht Heidelberg New York London, 2013.

[60] D. T. Blake, S. S. Hsiao, and K. O. Johnson, "Neural Coding Mechanisms in Tactile Pattern Recognition: The Relative Contributions of Slowly and Rapidly Adapting Mechanoreceptors to Perceived Roughness," *The Journal of Neuroscience,* vol. 17, pp. 7480-7489, 1997.

[61] W. H. Talbot, I. Darian-Smith, H. H. Kornhuber, and V. B. Mountcastle, "The sense of flutter-vibration: comparison of the human capacity with response patterns of mechanoreceptive afferents from the monkey hand," *Journal of Neurophysiology,* vol. 31, pp. 301-334, 1968.

[62] B. T. Nghiem, I. C. Sando, R. B. Gillespie, B. L. McLaughlin, G. J. Gerling, N. B. Langhals*, et al.*, "Providing a Sense of Touch to Prosthetic Hands," *Plastic and Reconstructive Surgery,* vol. 135, pp. 1652-1663, 2015.

[63] R. S. Johansson and A. B. Vallbo, "Detection of tactile stimuli. Thresholds of afferent units related to psychophysical thresholds in the human hand," *The Journal of Physiology,* vol. 297, pp. 405-422, 1979.

[64] G. A. Gescheider, R. T. Verrillo, J. T. Mccann, and E. M. Aldrich, "Effects of the menstrual cycle on vibrotactile sensitivity," *Perception & Psychophysics,* vol. 36, pp. 586-592, November 01 1984.

[65] R. T. Verrillo, "Effects of aging on the suprathreshold responses to vibration," *Perception & Psychophysics,* vol. 32, pp. 61-68, 1982.

[66] L. Venkatesan, S. M. Barlow, and D. Kieweg, "Age- and sex-related changes in vibrotactile sensitivity of hand and face in neurotypical adults," *Somatosensory & Motor Research,* vol. 32, pp. 44-50, 2015.

[67] Y. Wang, B. Millet, and J. L. Smith, "Designing wearable vibrotactile notifications for information communication," *International Journal of Human-Computer Studies,* vol. 89, pp. 24-34, 2016.

[68] L. A. Jones and S. J. Lederman, *Human Hand Function*: Oxford University Press, USA, 2006.

[69] S. J. Lederman and R. A. Browse, "The Physiology and Psychophysics of Touch," in *Sensors and Sensory Systems for Advanced Robots*, P. Dario, Ed., ed Berlin, Heidelberg: Springer Berlin Heidelberg, , pp. 71-91, 1988.

[70] L. A. Jones and S. J. Lederman, *Human hand function*. New York, NY, US: Oxford University Press, 2006.

[71] R.S.Johansson and A.B.Vallbo, "Detection of Tactile Stimuli. Thresholds of Afferent Units Related Psychophysical Thresholds in the Human Hand," *The Journal of Physiology,* vol. 297, pp. 405-422, 1979.

[72] J.Streque, T. Abdelkrim, P. Penod, and P. Vladimir, "New Magnetic Microactuator Design Based on PDMS Elastomer and MEMS Technologies for Tactile Display," *IEEE Transaction on Haptics,* vol. 3, pp. 88-97, 2010.

[73] M. Paré, H. Carnahan, and A. M. Smith, "Magnitude estimation of tangential force applied to the fingerpad," *Experimental Brain Research,* vol. 142, pp. 342-348, 2002.

[74] J. Biggs and M. A. Srinivasan, "Tangential versus normal displacements of skin: relative effectiveness for producing tactile sensations," in *Proceedings 10th Symposium on Haptic Interfaces for Virtual Environment and Teleoperator Systems. HAPTICS*, pp. 121-128, 2002.

[75] K.-U. Kyung, M. Ahn, D.-S. Kwon, and M. A. Srinivasan, "Perceptual and biomechanical frequency response of human skin: implication for design of tactile displays," in *Eurohaptics Conference, 2005 and Symposium on Haptic Interfaces for Virtual Environment and Teleoperator Systems, 2005. World Haptics 2005. First Joint*, pp. 96-101,2005.

[76] V. K. Nielsen, "The vibration stimulus. Effects of viscous-elastic resistance of skin on the amplitude of vibrations," *Electroencephalography and clinical neurophysiology,* vol. 38, pp. 647-652, 1975.
[77] S.-I. Lee, "Human sensitivity responses to vibrotactile stimulation on the hand: Measurement of differential thresholds," *Journal of the Ergonomics Society of Korea,* vol. 18, pp. 1-12, 1999.
[78] L. Spirkovska, "Summary of tactile user interfaces techniques and systems," 2005.
[79] K. A. Kaczmarek, J. G. Webster, P. Bach-y-Rita, and W. J. Tompkins, "Electrotactile and vibrotactile displays for sensory substitution systems," *IEEE Transactions on Biomedical Engineering,* vol. 38, pp. 1-16, 1991.
[80] G. A. Gescheider, S. J. Bolanowski, and R. T. Verrillo, "Some characteristics of tactile channels," *Behavioural Brain Research,* vol. 148, pp. 35-40, 2004/01/05/ 2004.
[81] R. W. Cholewiak and A. A. Collins, "Vibrotactile pattern discrimination and communality at several body sites," *Perception & Psychophysics,* vol. 57, pp. 724-737, July 01 1995.
[82] R. W. Cholewiak and A. A. Collins, "Vibrotactile localization on the arm: Effects of place, space, and age," *Perception & Psychophysics,* vol. 65, pp. 1058-1077, 2003.
[83] W. Schiff and E. Foulke, *Tactual Perception: A Sourcebook*: Cambridge University Press, 1982.
[84] C. E. Sherrick, "Basic and applied research on tactile aids for deaf people: Progress and prospects," *The Journal of the Acoustical Society of America,* vol. 75, pp. 1325-1342, 1984.
[85] M. I. Tiwana, S. J. Redmond, and N. H. Lovell, "A review of tactile sensing technologies with applications in biomedical engineering," *Sensors and Actuators A: Physical,* vol. 179, pp. 17-31, 2012.
[86] Y. Wan, Y. Wang, and C. F. Guo, "Recent progresses on flexible tactile sensors," *Materials Today Physics,* vol. 1, pp. 61-73, 2017.
[87] R. S. Dahiya, G. Metta, M. Valle, and G. Sandini, "Tactile Sensing; From Humans to Humanoids," *IEEE Transactions on Robotics,* vol. 26, pp. 1-20, 2010.
[88] H. Zhang and E. So, "Hybrid resistive tactile sensing," *IEEE Transactions on Systems, Man, and Cybernetics, Part B (Cybernetics),* vol. 32, pp. 57-65, 2002.
[89] S. Stassi, V. Cauda, G. Canavese, and C. F. Pirri, "Flexible tactile sensing based on piezoresistive composites: A review," *Sensors,* vol. 14, pp. 5296-5332, 2014.
[90] Y. Huang, Q. Jiang, Y. Li, C. Zhao, J. Wang, and P. Liang, "Research and design of a novel, low-cost and flexible tactile sensor array," *Measurement,* vol. 94, pp. 780-786, 2016.
[91] S.-J. Fang, S. Husson, C.-K. Fu, and C.-H. Lin, "Flexible tactile sensor array utilizing microstructured PDMS bumps with PEDOT: PSS conductive polymer," in *Micro Electro Mechanical Systems (MEMS), 2017 IEEE 30th International Conference on*, pp. 1029-1032, 2017
[92] S. Chun, Y. Choi, D. I. Suh, G. Y. Bae, S. Hyun, and W. Park, "A tactile sensor using single layer graphene for surface texture recognition," *Nanoscale,* vol. 9, pp. 10248-10255, 2017.
[93] M. Ahmed, M. M. Chitteboyina, D. P. Butler, and Z. Çelik-Butler, "MEMS force sensor in a flexible substrate using nichrome piezoresistors," *IEEE Sensors Journal,* vol. 13, pp. 4081-4089, 2013.
[94] J. C. Yeo, J. Yu, M. Shang, K. P. Loh, and C. T. Lim, "Highly Flexible Graphene Oxide Nanosuspension Liquid-Based Microfluidic Tactile Sensor," *Small,* vol. 12, pp. 1593-1604, 2016.

[95] H. K. Lee, S. I. Chang, and E. Yoon, "A Flexible Polymer Tactile Sensor: Fabrication and Modular Expandability for Large Area Deployment," *Journal of Microelectromechanical Systems,* vol. 15, pp. 1681-1686, 2006.
[96] H.-K. Kim, S. Lee, and K.-S. Yun, "Capacitive tactile sensor array for touch screen application," *Sensors and Actuators A: Physical,* vol. 165, pp. 2-7, 2011.
[97] H. B. Muhammad, C. Recchiuto, C. M. Oddo, L. Beccai, C. J. Anthony, M. J. Adams, *et al.*, "A capacitive tactile sensor array for surface texture discrimination," *Microelectronic Engineering,* vol. 88, pp. 1811-1813, 2011.
[98] M. Y. Cheng, X. H. Huang, C. W. Ma, and Y. J. Yang, "A flexible capacitive tactile sensing array with floating electrodes," *Journal of Micromechanics and Microengineering,* vol. 19, p. 115001, 2009.
[99] M.-Y. Cheng, C.-L. Lin, Y.-T. Lai, and Y.-J. Yang, "A Polymer-Based Capacitive Sensing Array for Normal and Shear Force Measurement," *Sensors,* vol. 10, p. 10211, 2010.
[100] F. Castelli, "An integrated tactile-thermal robot sensor with capacitive tactile array," *IEEE Transactions on Industry Applications,* vol. 38, pp. 85-90, 2002.
[101] P. Goethals, "Tactile feedback for robot assisted minimally invasive surgery: an overview," 2008.
[102] K. Kim, S. Zhang, J. Tian, P. Han, and X. Jiang, "Face-shear mode ultrasonic tactile sensor array," in *2012 IEEE International Ultrasonics Symposium*, pp. 1059-1062, 2012.
[103] C. H. Chuang, H. K. Weng, J. W. Cheng, and M. O. Shaikh, "Ultrasonic tactile sensor integrated with TFT array for contact force measurements," in *2017 19th International Conference on Solid-State Sensors, Actuators and Microsystems (TRANSDUCERS)*, pp. 512-515, 2017.
[104] S. Begej, "Planar and finger-shaped optical tactile sensors for robotic applications," *IEEE Journal on Robotics and Automation,* vol. 4, pp. 472-484, 1988.
[105] G. De Maria, C. Natale, and S. Pirozzi, "Force/tactile sensor for robotic applications," *Sensors and Actuators A: Physical,* vol. 175, pp. 60-72, 2012.
[106] J.-S. Heo, J.-H. Chung, and J.-J. Lee, "Tactile sensor arrays using fiber Bragg grating sensors," *Sensors and Actuators A: Physical,* vol. 126, pp. 312-327, 2006.
[107] T. Satoru, "A soft three-axis tactile sensor based on electromagnetic induction," in *2009 IEEE International Conference on Mechatronics*, , pp. 1-6, 2009
[108] A. Alfadhel, M. A. Khan, S. Cardoso, D. Leitao, and J. Kosel, "A Magnetoresistive Tactile Sensor for Harsh Environment Applications," *Sensors (Basel, Switzerland),* vol. 16, p. 650, 2016.
[109] M. Hakozaki, H. Oasa, and H. Shinoda, "Telemetric robot skin," in *Proceedings 1999 IEEE International Conference on Robotics and Automation*, pp. 957-961 vol.2. 1999.
[110] Z. Chi and K. Shida, "A new multifunctional tactile sensor for three-dimensional force measurement," *Sensors and Actuators A: Physical,* vol. 111, pp. 172-179, 2004.
[111] J. M. Vranish, *Magnetoresistive Skin for Robots*, 1984.
[112] P. Yu, W. Liu, C. Gu, X. Cheng, and X. Fu, "Flexible Piezoelectric Tactile Sensor Array for Dynamic Three-Axis Force Measurement," *Sensors,* vol. 16, p. 819, 2016.
[113] L. Seminara, L. Pinna, M. Valle, L. Basiricò, A. Loi, P. Cosseddu, *et al.*, "Piezoelectric Polymer Transducer Arrays for Flexible Tactile Sensors," *IEEE Sensors Journal,* vol. 13, pp. 4022-4029, 2013.
[114] K.-H. Yu, T.-G. Kwon, M.-J. Yun, and S.-C. Lee, "Development of a tactile sensor array with flexible structure using piezoelectric film," *KSME International Journal,* vol. 16, p. 1222, 2002.

[115] R. S. Dahiya, M. Valle, G. Metta, and L. Lorenzelli, "POSFET Based Tactile Sensor Arrays," in *2007 14th IEEE International Conference on Electronics, Circuits and Systems*, pp. 1075-1078, 2007

[116] M. A. Srinivasan and C. Basdogan, "Haptics in virtual environments: Taxonomy, research status, and challenges," *Computers & Graphics,* vol. 21, pp. 393-404, 1997.

[117] M. Sreelakshmi and T. D. Subash, "Haptic Technology: A comprehensive review on its applications and future prospects," *Materials Today: Proceedings,* vol. 4, pp. 4182-4187, 2017.

[118] M. Srinivasan, "Human and Machine Haptics", 1999.

[119] A. M. Okamura, "Haptic Feedback in Robot-Assisted Minimally Invasive Surgery," *Current opinion in urology,* vol. 19, pp. 102-107, 2009.

[120] F. Sorgini, R. Caliò, M. C. Carrozza, and C. M. Oddo, "Haptic-assistive technologies for audition and vision sensory disabilities," *Disability and Rehabilitation: Assistive Technology,* pp. 1-28, 2017.

[121] O. Gomis-Bellmunt and L. F. Campanile, *Design Rules for Actuators in Active Mechanical Systems*: Springer London, 2009.

[122] C.-W. Song and S.-Y. Lee, "Design of a solenoid actuator with a magnetic plunger for miniaturized segment robots," *Applied Sciences,* vol. 5, pp. 595-607, 2015.

[123] D. De Bhailís, C. Murray, M. Duffy, J. Alderman, G. Kelly, and S. Ó. Mathúna, "Modelling and analysis of a magnetic microactuator," *Sensors and Actuators A: Physical,* vol. 81, pp. 285-289, 2000.

[124] J. R. Claycomb, *Applied Electromagnetics Using QuickFieldTM & MATLAB*: Jones & Bartlett Learning, 2010.

[125] B. Di Bartolo, *Classical Theory of Electromagnetism*: World Scientific, 2004.

[126] J.Streque, A Talbi, P. Pernod, and V. Preobrazhensky, "Pulse-driven magnetostatic micro-actuator array based on ultrasoft elastomeric membranes for active surface applications," *Journal of Micromechanics and Microengineering,* vol. 22, pp. 1-10, 2012.

[127] A.Talbi, O. Ducloux, N. Tiercelin, Y. Deblock, P. Pernod, and V.Preobrazhensky, "Vibrotactile using micromachined electromagnetic actuators array," presented at the International MEMS Conference 2006.

[128] F.Tsumori and J.Brunne, "Magnetic Actuator using Interaction between Micro Magnetic Elements," presented at the Micro Electro Mechanical Systems (MEMS), 2011 IEEE 24th International Conference, Cancun, Mexico, 2011.

[129] H.Yin, Y.Huang, W.Fang, and J.Hsieh, "A novel electromagnetic elastomer membrane actuator with a semi-embedded coil," *Sensors and Actuators A, Elsevier,* vol. 139, pp. 194-202, 2007.

[130] M.M.Said, J.Yunas, R. E. Pawinanto, B. Y. Majlis, and B.Bais, "PDMS based electromagnetic actuator membrane with embedded magnetic particles in polymer composite," *Sensors and Actuators A, Elsevier,* vol. 245, pp. 85-96, 2016.

[131] M.Khoo and C.Liu, "Micro magnetic silicone elastomer membrane actuator," *Sensors and Actuators A, Elsevier,* vol. 89, pp. 259-266, 2001.

[132] C.-Y. Lee, Z.-HChen, H.-T. Chang, C.-YWen, and C.-HCheng. Design and fabrication of novel micro electromagnetic actuator, Microsystem Tech. Vol. 15, Issue 8, pp.1171-1177, 2008.

[133] M.Benali-Khoudja, M. H. a, and A.Kheddar, "VITAL: An electromagnetic integrated tactile display," *Displays- Elsevier,* vol. 28, pp. 133-144, 2007.

[134] L.Lagorce and O.Brand, "Magnetic Microactuators Based on Polymer Magnets," *IEEE Journal of Microelectromechanical Systems,* vol. 8, pp. 2-9, 1999.

[135] K.H.Kim, H.J.Yoon, O.C.Jeong, and S.S.Yang, "Fabrication and test of a micro electromagnetic actuator," *Sensors and Actuators A, Elsevier,* vol. 117, pp. 8-16, 2005.

[136] T. Fukuda, H. Morita, F. Arai, H. Ishihara, and H. Matsuura, "Micro Resonator Using Electromagnetic Actuator for Tactile Display," in *1997 International Symposium on Micromechanics and Human Science*, 1997.

[137] T. Noguchi, S. Nagai, and A. Kawamura, "Electromagnetic Linear Actuator providing High Force Density per Unit Area without Position Sensor as a Tactile Cell," *IEEJ Journal of Industry Applications,* vol. 7, pp. 259-265, 2018.

[138] D. Leonardis, L. Claudio, and A. Frisoli, "A Survey on Innovative Refreshable Braille Display Technologies," Cham, pp. 488-498, 2018.

[139] K. J. Kim and S. Tadokoro, "Electroactive polymers for robotic applications," *Artificial Muscles and Sensors,* vol. 23, p. 291, 2007.

[140] L. Qu, Q. Peng, L. Dai, G. M. Spinks, G. G. Wallace, and R. H. Baughman, "Carbon nanotube electroactive polymer materials: Opportunities and challenges," *MRS bulletin,* vol. 33, pp. 215-224, 2008.

[141] G.-H. Feng and S.-Y. Hou, "Investigation of tactile bump array actuated with ionic polymer–metal composite cantilever beams for refreshable braille display application," *Sensors and Actuators A: Physical,* vol. 275, pp. 137-147, 2018.

[142] J. J. Pak, J. Kim, S. W. Oh, J. H. Son, S. H. Cho, S.-K. Lee*, et al.*, "Fabrication of ionic-polymer-metal-composite (IPMC) micropump using a commercial Nafion," in *Smart Structures and Materials*, p. 9, 2004.

[143] K. Ki-Uk, M. Ahn, K. Dong-Soo, and M. A. Srinivasan, "A compact broadband tactile display and its effectiveness in the display of tactile form," in *First Joint Eurohaptics Conference and Symposium on Haptic Interfaces for Virtual Environment and Teleoperator Systems. World Haptics Conference*, pp. 600-601, 2005.

[144] Y. Ikei, K. Wakamatsu, and S. Fukuda, "Texture presentation by vibratory tactile display-image based presentation of a tactile texture," in *Proceedings of IEEE 1997 Annual International Symposium on Virtual Reality*, pp. 199-205, 219 1997.

[145] T. Maucher, K. Meier, and J. Schemmel, "An interactive tactile graphics display," in *Proceedings of the Sixth International Symposium on Signal Processing and its Applications*, pp. 190-193 vol., 2001.

[146] F. Yao, C. H. Erol, K. G. Muralidhar, and M. S. Geoff, "Design, fabrication and testing of piezoelectric polymer PVDF microactuators," *Smart Materials and Structures,* vol. 15, p. S141, 2006.

[147] M. Jungmann and H. F. Schlaak, "Miniaturised electrostatic tactile display with high structural compliance," in *Proceedings of the Conference" Eurohaptics*, 2002.

[148] T. Hui and D. J. Beebe, "A microfabricated electrostatic haptic display for persons with visual impairments," *IEEE Transactions on Rehabilitation Engineering,* vol. 6, pp. 241-248, 1998.

[149] R. M. Strong and D. E. Troxel, "An Electrotactile Display," *IEEE Transactions on Man-Machine Systems,* vol. 11, pp. 72-79, 1970.

[150] H. S. Lee, H. Phung, D.-H. Lee, U. K. Kim, C. T. Nguyen, H. Moon*, et al.*, "Design analysis and fabrication of arrayed tactile display based on dielectric elastomer actuator," *Sensors and Actuators A: Physical,* vol. 205, pp. 191-198, 2014.

[151] J. D. Grade, H. Jerman, and T. W. Kenny, "Design of large deflection electrostatic actuators," *Journal of Microelectromechanical Systems,* vol. 12, pp. 335-343, 2003.

[152] H. Conrad, H. Schenk, B. Kaiser, S. Langa, M. Gaudet, K. Schimmanz*, et al.*, "A small-gap electrostatic micro-actuator for large deflections," vol. 6, p. 10078, 2015.

[153] A. Yamamoto, S. Nagasawa, H. Yamamoto, and T. Higuchi, "Electrostatic tactile display with thin film slider and its application to tactile telepresentation systems," *IEEE Transactions on Visualization and Computer Graphics,* vol. 12, pp. 168-177, 2006.

[154] E. Mallinckrodt, A. L. Hughes, and W. Sleator, "Perception by the Skin of Electrically Induced Vibrations," *Science,* vol. 118, pp. 277-278, 1953.

[155] J. Mohd Jani, M. Leary, A. Subic, and M. A. Gibson, "A review of shape memory alloy research, applications and opportunities," *Materials & Design (1980-2015),* vol. 56, pp. 1078-1113, 2014.

[156] L. Sun and W. M. Huang, "Nature of the multistage transformation in shape memory alloys upon heating," *Metal Science and Heat Treatment,* vol. 51, pp. 573-578, 2009.

[157] P. S. Lobo, J. Almeida, and L. Guerreiro, "Shape Memory Alloys Behaviour: A Review," *Procedia Engineering,* vol. 114, pp. 776-783, 2015.

[158] T. Matsunaga, K. Totsu, M. Esashi, and Y. Haga, "Tactile display using shape memory alloy micro-coil actuator and magnetic latch mechanism," *Displays,* vol. 34, pp. 89-94, 2013.

[159] P. S. Wellman, W. J. Peine, G. Favalora, and R. D. Howe, "Mechanical design and control of a high-bandwidth shape memory alloy tactile display," in *Experimental Robotics V: The Fifth International Symposium Barcelona, Catalonia, June 15–18, 1997*, A. Casals and A. T. de Almeida, Eds., ed Berlin, Heidelberg: Springer Berlin Heidelberg, pp. 56-66, 1998.

[160] P. M. Taylor, A. Moser, and A. Creed, "A sixty-four element tactile display using shape memory alloy wires," *Displays,* vol. 18, pp. 163-168, 1998.

[161] R. Velazquez, E. E. Pissaloux, and M. Wiertlewski, "A compact tactile display for the blind with shape memory alloys," in *Proceedings 2006 IEEE International Conference on Robotics and Automation, ICRA* pp. 3905-3910, *2006.*

[162] X.Wu, S.H.Kim, H.Zhu, C. Ji, and M.G.Allen, "A Refreshable Braille Cell Based on Pneumatic Microbubble Actuators," *IEEE Journal of Microelectromechanical Systems,* vol. 21, pp. 908-916, 2012.

[163] M. B. Cohn, M. Lam, and R. S. Fearing, "Tactile feedback for teleoperation,"pp. 240-254, 1993.

[164] D. G. Caldwell, N. Tsagarakis, and C. Giesler, "An integrated tactile/shear feedback array for stimulation of finger mechanoreceptor," in *Proceedings 1999 IEEE International Conference on Robotics and Automation*, pp. 287-292 vol.1, 1999.

[165] Y. Tanaka, H. Yamauchi, and K. AMEMIYA, "Wearable haptic display for immersive virtual environment," in *Proceedings of the jfps international symposium on fluid power*, pp. 309-314, 2002.

[166] G. Moy, C. Wagner, and R. S. Fearing, "A compliant tactile display for teletaction," in *Proceedings 2000 ICRA. Millennium Conference. IEEE International Conference on Robotics and Automation. Symposia Proceedings (Cat. No.00CH37065)*, pp. 3409-3415 vol.4, 2000.

[167] Y. Makino, N. Asamura, and H. Shinoda, "A whole palm tactile display using suction pressure," in *Robotics and Automation, 2004. Proceedings. ICRA'04. 2004 IEEE International Conference on*, pp. 1524-1529, 2004.

[168] N. Kitamura, J. Chim, and N. Miki, "Electrotactile display using microfabricated micro-needle array," *Journal of Micromechanics and Microengineering,* vol. 25, p. 025016, 2015.

[169] M. Tezuka, K. Ishimaru, and N. Miki, "Electrotactile display composed of two-dimensionally and densely distributed microneedle electrodes," *Sensors and Actuators A: Physical,* vol. 258, pp. 32-38, 2017.

[170] H. Kajimoto, N. Kawakami, S. Tachi, and M. Inami, "SmartTouch: electric skin to touch the untouchable," *IEEE Computer Graphics and Applications,* vol. 24, pp. 36-43, 2004.
[171] J.-S. Oh and S.-B. Choi, "State of the art of medical devices featuring smart electro-rheological and magneto-rheological fluids," *Journal of King Saud University - Science,* 2017.
[172] C.-H. Lee and M.-G. Jang, "Virtual surface characteristics of a tactile display using magneto-rheological fluids," *Sensors,* vol. 11, pp. 2845-2856, 2011.
[173] V. G. Chouvardas, A. N. Miliou, and M. K. Hatalis, "Tactile displays: Overview and recent advances," *Displays,* vol. 29, pp. 185-194, 2008.
[174] A. Muhammad, X.-l. Yao, and Z.-c. Deng, "Review of magnetorheological (MR) fluids and its applications in vibration control," *Journal of Marine Science and Application,* vol. 5, pp. 17-29, September 01 2006.
[175] J. Rabinow, "The Magnetic Fluid Clutch," *Transactions of the American Institute of Electrical Engineers,* vol. 67, pp. 1308-1315, 1948.
[176] R. Jacob, "Magnetic fluid torque and force transmitting device," ed: Google Patents, 1951.
[177] W.M.Winslow, "Induced Fibrillation of Suspensions," *J.Appl.Phys.,* vol. 22, 1949.
[178] T.-H. Yang, J.-H. Koo, S.-Y. Kim, and D.-S. Kwon, "A miniature magneto-rheological actuator with an impedance sensing mechanism for haptic applications," *Journal of Intelligent Material Systems and Structures,* vol. 25, pp. 1054-1061, 2014.
[179] P. M. Taylor, A. Hosseini-Sianaki, and C. J. Varley, "An electrorheological fluid-based tactile array for virtual environments," in *Proceedings of IEEE International Conference on Robotics and Automation*, , pp. 18-23 vol.1, 1996
[180] R. Bansevicius and J. A. Virbalis, "Two-dimensional Braille readers based on electrorheological fluid valves controlled by electric field," *Mechatronics,* vol. 17, pp. 570-577, 2007.
[181] Y. Liu, R. Davidson, P. Taylor, J. Ngu, and J. Zarraga, "Single cell magnetorheological fluid based tactile display," *Displays,* vol. 26, pp. 29-35, 2005.
[182] J. Voldman, M. L. Gray, and M. A. Schmidt, "Microfabrication in Biology and Medicine," *Annu. Rev. Biomed. Eng,* vol. 1, pp. 401-425, 1999.
[183] A. Hierlemann, O. Brand, C. Hagleitner, and H. Baltes, "Microfabrication techniques for chemical/biosensors," *Proceedings of the IEEE,* vol. 91, pp. 839-863, 2003.
[184] H. Li, "Microfabrication techniques for producing freestanding multi-dimensional microstructures," *Microsystem Technologies,* vol. 22, pp. 223-237, 2016.
[185] W. J. Jack, "Microelectromechanical systems (MEMS): fabrication, design and applications," *Smart Materials and Structures,* vol. 10, p. 1115, 2001.
[186] S. Kota, G. K. Ananthasuresh, S. B. Crary, and K. D. Wise, "Design and Fabrication of Microelectromechanical Systems," *Journal of Mechanical Design,* vol. 116, pp. 1081-1088, 1994.
[187] M. Gad-el-Hak, *The MEMS Handbook*: CRC Press, 2001.
[188] S. Lee, S. Park, and D.-I. Cho, "The surface/bulk micromachining (SBM) process: a new method for fabricating released MEMS in single crystal silicon," *Journal of Microelectromechanical Systems,* vol. 8, pp. 409-416, 1999.
[189] T. Masuzawa, "State of the Art of Micromachining," *CIRP Annals,* vol. 49, pp. 473-488, 2000.
[190] G. T. Kovacs, N. I. Maluf, and K. E. Petersen, "Bulk micromachining of silicon," *Proceedings of the IEEE,* vol. 86, pp. 1536-1551, 1998.
[191] K. Biswas and S. Kal, "Etch characteristics of KOH, TMAH and dual doped TMAH for bulk micromachining of silicon," *Microelectronics Journal,* vol. 37, pp. 519-525, 2006.

[192] K. Biswas, S. Das, D. K. Maurya, S. Kal, and S. K. Lahiri, "Bulk micromachining of silicon in TMAH-based etchants for aluminum passivation and smooth surface," *Microelectronics Journal,* vol. 37, pp. 321-327, 2006.

[193] R. T. Howe, R. S. Muller, K. J. Gabriel, and W. S. Trimmer, "Silicon micromechanics: sensors and actuators on a chip," *IEEE spectrum,* vol. 27, pp. 29-31, 1990.

[194] P. Verma, K. Z. Khan, S. Khonina, R. Skidanov, N. Kazanskiy, and R. Gopal, "UV-LIGA FABRICATION PROCESS FOR REALIZATION OF METAL BASED MEMS GYROSCOPE," , pp. 279-282, 2016.

[195] H.-K. Chang and Y.-K. Kim, "UV-LIGA process for high aspect ratio structure using stress barrier and C-shaped etch hole," *Sensors and Actuators A: Physical,* vol. 84, pp. 342-350, 2000.

[196] C.-H. Ho, K.-P. Chin, C.-R. Yang, H.-M. Wu, and S.-L. Chen, "Ultrathick SU-8 mold formation and removal, and its application to the fabrication of LIGA-like micromotors with embedded roots," *Sensors and Actuators A: Physical,* vol. 102, pp. 130-138, 2002.

[197] M. S. Mahmood, Z. Celik-Butler, and D. P. Butler, "Design, fabrication and characterization of flexible MEMS accelerometer using multi-Level UV-LIGA," *Sensors and Actuators A: Physical,* vol. 263, pp. 530-541, 2017.

[198] S. D. Minteer, *Microfluidic techniques: reviews and protocols* vol. 321: Springer Science & Business Media, 2006.

[199] R. Luttge, "Chapter 3 - Advanced Microfabrication Methods," in *Microfabrication for Industrial Applications*, ed Boston: William Andrew Publishing, 2011, pp. 55-89.

[200] H. H. Lou and Y. Huang, "Electroplating," 2006.

[201] M. Schlesinger and M. Paunovic, *Modern Electroplating*: Wiley, 2011.

[202] S. Dimitrijević, M. Rajčić-Vujasinović, and V. Trujić, "Non-cyanide electrolytes for gold plating–a review," *Int. J. Electrochem. Sci,* vol. 8, pp. 6620-6646, 2013.

[203] W. T. Navaraj, H. Heidari, A. Polishchuk, D. Shakthivel, D. Bhatia, and R. Dahiya, "Upper limb prosthetic control using toe gesture sensors," in *2015 IEEE Sensors*, pp. 1-4, 2015.

[204] J.-S. Lee, Y.-W. Su, and C.-C. Shen, "A Comparative Study ofWireless Protocols: Bluetooth, UWB, ZigBee, and Wi-Fi," presented at the The 33rd Annual Conference ofthe IEEE Industrial Electronics Society (IECON), Taipei, Taiwan, 2007.

[205] I. J. Busch-Vishniac, "The case for magnetically driven microactuators," *Sensors and Actuators A: Physical,* vol. 33, pp. 207-220, 1992.

[206] M. Schlesinger and M. Paunovic, *Modern electroplating* vol. 55: John Wiley & Sons, 2011.

[207] S. S. Mohan, M. del Mar Hershenson, S. P. Boyd, and T. H. Lee, "Simple accurate expressions for planar spiral inductances," *IEEE Journal of solid-state circuits,* vol. 34, pp. 1419-1424, 1999.

[208] O. Ozioko, W. T. Navaraj, N. Yogeswaran, M. Hersh, and R. Dahiya, "Tactile Communication system for the Interaction between Deafblind and Robots," in *2018 27th IEEE International Symposium on Robot and Human Interactive Communication (RO-MAN)*, pp. 416-421, 2018.

[209] O. Ozioko, M. Hersh, and R. Dahiya, "Inductance-Based Flexible Pressure Sensor for Assistive Gloves," in *2018 IEEE SENSORS*, 2018, pp. 1-4.

[210] R. W. Van Boven, R. H. Hamilton, T. Kauffman, J. P. Keenan, and A. Pascual–Leone, "Tactile spatial resolution in blind Braille readers," *Neurology,* vol. 54, pp. 2230-2236, 2000.

[211] U. Gollner, T. Bieling, and G. Joost, "Mobile Lorm Glove: introducing a communication device for deaf-blind people," in *Proceedings of the sixth international conference on tangible, embedded and embodied interaction*, pp. 127-130, 2012.

[212] J. Seymour-Ford, "History of the Perkins Brailler," Perkins School for the blind, Watertown2009 2009.

[213] S. Woodin and J. Heilbrunn, "Braille Teaching and Literacy A Report for the European Blind Union and European Commission," 2018.

[214] O. Ozioko, W. Taube, M. Hersh, and R. Dahiya, "SmartFingerBraille: A tactile sensing and actuation based communication glove for deafblind people," in *2017 IEEE 26th International Symposium on Industrial Electronics (ISIE)*, pp. 2014-2018. 2017.